# The Role of PP2A in VE-cadherin Modulation in Human Cerebral Microvascular Endothelial Cells

A thesis submitted to Trinity College Dublin,
The University of Dublin

In the fulfilment of the requirement
For the degree of
Doctor of Philosophy
2026

By

**Fawza Alenazi**

**Supervisor: Professor Paul Spiers**

Discipline of Pharmacology and Therapeutics, School of Medicine
Trinity College Dublin

# Declaration

I declare that this thesis has not been submitted as an exercise for a degree at this or any other university and it is entirely my own work. I agree to deposit this thesis in the University's open access institutional repository or allow the library to do so on my behalf, subject to Irish Copyright Legislation and Trinity College Library conditions of use and acknowledgement.

_____

**Fawza Alenazi**

# Dedication

To my beloved parents,
Your love and support have been the roots of all my achievements.

To my dear father, may your soul rest in peace
You dreamed of this moment long before I could see it for myself.
Though you are no longer here to witness it, I carry your memory in my heart every step of the way.
I miss you deeply and love you more than words can ever express.
This doctorate is, and always will be, for you.

To my loving husband, Mohammed,
Thank you for standing beside me with endless patience, love, and encouragement.
Your belief in me gave me strength when I needed it most.

To my precious children, Hala, Halla, Abdulrahman and Ola
You are my joy, my light, and my greatest motivation.
This accomplishment is as much yours as it is mine.

# Acknowledgments

After completing my master's degree in Germany, I intended to continue with a PhD in the same lab. However, life had other plans. When I became pregnant with my son, Abdulrahman, I returned home to give birth and decided to pause my academic journey to focus on raising him. I resumed my position as a university lecturer, but the dream of pursuing a PhD remained alive. Over the next two years, while teaching and welcoming another child, I actively searched for PhD opportunities in English-speaking countries. Although I received an offer to begin my PhD in Germany, I hoped to continue in an English-speaking environment. Unfortunately, due to student limitations from my region, UK universities were not an option at the time. It was a discouraging period, and I questioned my luck.

Then came a turning point: I was accepted into the PhD program under the supervision of Professor Paul Spiers in Ireland. I was overjoyed at the opportunity to pursue my academic goals in an English-speaking country, gain new knowledge, and eventually return home to contribute to the scientific community there. I still remember the first day I met Professor Spiers, November 4th, 2020, in the seminar room where we spoke about the project, expectations, and working hours. His warm smile and my excitement that day remain vivid in my memory. From the beginning, the lab provided a welcoming and supportive environment. In my first year, Professor Spiers patiently guided me through experimental work. I am deeply grateful to all the lab members, Pierce, Ken, Margaret, Manos, Teresa, Ismail, and Bashir, for being there whenever I needed help.

Professor Paul Spiers supported me through every stage of my project. His insightful feedback and encouragement enriched every discussion and helped shape my research. Our meetings were always engaging and full of meaningful discussions mixed with laughter that made even the most stressful times enjoyable. His light-hearted personality helped ease the challenges of scientific work. Under his mentorship, I grew not only as a researcher but also as a person. For that, I am sincerely thankful; words cannot fully capture how much your support and kindness have meant to me. A special thank you to Pierce for standing by me throughout the journey. Your calm presence, encouragement, and patience, especially when I needed to talk, made a tremendous difference. Beyond the logistics of lab work, your intelligence and willingness to help were invaluable. I often told both you and Ken, "You're like brothers to me," and though Ken used to laugh and say, "You say that to everyone," I truly meant it. My PhD journey was more than just research; it was a meaningful chapter of my life. Last year was especially difficult, as we experienced the heartbreaking loss of Ken, a dear friend and true supporter.

Ken, may God bless you always. I appreciate your kindness, for treating me like family, for staying late with me in the lab, and for your thoughtful gestures, from snacks to smiles. Your presence is deeply missed.

Thank you, Teresa, for our coffee breaks and warm conversations. I may have gained weight from all the chocolate you shared, but those moments brought joy. I often wish we could have those times again after your retirement. To Dr. Ismail, thank you for being a patient trainer, a generous teacher, and a supportive friend. The time and laughter we shared helped me learn with confidence. To Dr. Manos and Dr. Bashir, thank you for your collaboration, encouragement, and positive energy. I also want to express my sincere thanks to the team at SCOMIC, Ronny Schmidt, Christoph Schroder, Ramy Girgis, Marco Klein, and Katrin Hufnagel, for your support and expertise in microarray analysis. Your contribution played a key role in the success of my project. Thank you to Dr. Margaret and Sakshi for the open conversations, support, and light moments. Your honesty and warmth helped me through difficult days. I also thank everyone in the Pharmacology and Therapeutics Department for their support and kindness throughout my time there.

To my family, thank you from the depths of my heart. To my parents, especially my father, my first teacher and greatest supporter, your belief in me never wavered. Even though you passed away last year, your love and guidance continue to inspire me. To my beloved husband, your unwavering support, especially with our children, made this journey possible. You carried me through the toughest moments, and I am forever grateful. To my children, Hala, Halla, Abdulrahaman and Ola, your laughter, tiny hands, and joyful energy gave me strength and peace after long workdays. You were my motivation and my light. To my sisters and brothers, thank you for your encouragement and love. Your support helped me stay grounded and strong.

Finally, I extend my heartfelt thanks to all my colleagues in other labs for their collaboration, kindness, and for creating a positive and supportive research environment. I am also deeply grateful to every person who taught, advised, or guided me along the way. Each piece of advice, no matter how small, made a difference in my journey and helped shape the researcher and person I have become. Thank you.

# Thesis abstract:


## Introduction:

The blood–brain barrier (BBB) is a highly specialised and dynamic interface that protects the central nervous system (CNS) by tightly regulating the passage of molecules between the circulation and neural tissue. This barrier is primarily maintained by brain microvascular endothelial cells interconnected through tight and adherens junctions. Among the components of adherens junctions, vascular endothelial (VE)-cadherin plays a pivotal role in maintaining endothelial cell–cell adhesion, vascular stability, and BBB integrity. Disruption or internalisation of VE-cadherin has been implicated in numerous neurological and systemic disorders, including stroke, inflammation, and Alzheimer's disease.

The function and stability of VE-cadherin at the plasma membrane are critically influenced by its phosphorylation status. Protein phosphatase 2A (PP2A), a major serine/threonine phosphatase, is recognised as a regulator of junctional protein dephosphorylation and endothelial barrier function. Notably, PP2A has been identified as part of the VE-cadherin interactome, and previous studies suggest that it contributes to the formation of epithelial tight junctions and the maintenance of barrier integrity. However, the specific role of PP2A in regulating adherens junction components, particularly VE-cadherin, at the BBB remains unclear.

## Aims:

This thesis aimed to investigate the role of PP2A in regulating VE-cadherin abundance and the functional integrity of the BBB using *in vitro* models of human brain microvascular endothelial cells. Specifically, the objectives were to (1) determine how PP2A inhibition affects VE-cadherin abundance and BBB integrity, (2) determine the broader proteomic changes associated with PP2A inhibition, and (3) determine whether metformin, a PP2A activator, can counteract these effects.

## Methods:

Human brain endothelial cells (hCMEC/D3) were treated with the PP2A inhibitor okadaic acid (OA). VE-cadherin protein and mRNA abundance, subcellular distribution, and junctional localisation were analysed using Western blotting, RT-PCR, subcellular fractionation, and immunofluorescence. Barrier function was assessed by transwell permeability assays. PP2A activity was quantified with a phosphatase assay, and the involvement of proteasomal or

lysosomal pathways was tested using MG132 and chloroquine. Proteomic alterations following OA exposure were examined using microarray analysis and bioinformatic pathway/network tools. The roles of Rab11A and Rab5A were assessed using siRNA knockdown. The impact of metformin on PP2A activity and VE-cadherin regulation was evaluated by cytotoxicity testing, PP2A activity measurement, and time-course analysis of VE-cadherin abundance.

## Results:

OA produced a concentration-dependent reduction in VE-cadherin protein (50–70%), accompanied by its loss from endothelial junctions and a marked increase in paracellular permeability. These effects occurred without cytotoxicity and coincided with a ~60% decrease in PP2A activity. VE-cadherin reduction was prevented by proteasomal inhibition and associated with increased ubiquitination, indicating that OA promotes proteasomal degradation of VE-cadherin. Proteomic profiling identified 104 proteins altered by OA, highlighting pathways related to ubiquitination, membrane trafficking, tight junction regulation, and neurodegeneration. Rab11A upregulation was detected; however, Rab11A and Rab5A knockdown did not prevent OA-induced VE-cadherin loss. Metformin did not restore PP2A activity or reverse VE-cadherin reduction at 24 hours, although early time-course data suggested a partial transient attenuation of OA's effect at 10 hours.

## Conclusions:

PP2A plays a critical role in maintaining VE-cadherin stability and BBB integrity. Inhibition of PP2A disrupts endothelial junctions by promoting proteasomal degradation of VE-cadherin, leading to increased barrier permeability. These findings reveal a mechanism through which PP2A dysfunction contributes to BBB impairment. Although metformin showed limited restorative capacity, early temporal effects suggest that modulating PP2A signalling may offer therapeutic potential for preserving BBB integrity under pathological conditions.

# Publications and Presentations

## Papers in preparation

Mechanism of VE-cadherin Breakdown in the Blood-Brain Barrier following Protein Phosphatase Inhibition by Okadaic acid

Differential Protein Expression in Okadaic Acid-Treated hCMEC/D3 Cells Identified by Proteomic Microarray Analysis

VE-cadherin Phosphorylation, Internalisation, and its Ability to be Recycled in Endothelial Cells

## Oral Presentation

**Fawza Alenazi**, Ronny Schmidt, Christoph Schroder, Ramy Girgis, Marco Klein, Katrin Hufnagel, Paul Spiers. VE-cadherin degradation and ubiquitination upon pharmacological inhibition of PP2A and the ability to recycle by Rab11a – Annual meeting of the Irish association of Pharmacologists, Ireland 2023.

### Poster Presentation

**Fawza Alenazi**, Ronny Schmidt, Christoph Schroder, Ramy Girgis, Marco Klein, Katrin Hufnagel, Paul Spiers. Metformin does not reverse the effect of pharmacological inhibition of Protein Phosphatase 2A on VE-cadherin in human microvascular endothelial cells - Scottish Cardiovascular Forum**,** Aberdeen, Scotland 2023.v Published in Heart, 2023, 109, Suppl 2, A1-A7

**Fawza Alenazi**, Ronny Schmidt, Christoph Schroder, Ramy Girgis, Marco Klein, Katrin Hufnagel, Paul Spiers. Rab5a and Rab11a are not involved in VE-cadherin trafficking, internalisation or recycling in human cerebral microvascular endothelial cell (hCMEC/D3) – 10$^{th}$ Mediterranean Neuroscience Society Conference, Chania, Greece 2025.

# List of Abbreviations

| | |
|---|---|
| α– cat | α–catenin |
| ACC | Acetyl-CoA carboxylase |
| AD | Alzheimer disease |
| AJ | Adherent junctions |
| ALI | Acute lung injury |
| AML | Acute myeloid leukaemia |
| AMPK | AMP-activated protein kinase |
| ARDS | Acute Respiratory Distress Syndrome |
| AURKB | Aurora kinase B |
| β/γ–cat | β/γ–catenin |
| β2AP | Beta-2 Adrenergic Receptor |
| BaF | Bafilomycin |
| BBB | Blood Brain Barrier |
| BCA | Bicinchoninic acid |
| BDNF | Brain-derived neurotrophic factor |
| BMP6 | Bone morphogenetic protein |
| cAMP | Cyclin AMP |
| CAMs | Cell adhesion molecule |
| CAR | Coxsackie and adenovirus |
| CATH | Cathepsin |
| CBP | CREB-binding protein |
| CCM1 | Cerebral cavernous malformation protein 1 |
| CCNB1 | Cyclin B1 |
| CDC42 | Cell division control protein 42 |
| CDH1 | Cadherin 1 |
| CDK1 | Cyclin-dependent kinase 1 |
| CIE | Clathrin -independent endocytosis |
| CKII | Casein kinase II |
| CME | Clathrin-mediated endocytosis |
| CMTM4 | CKLF-like Marvel transmembrane domain 4 |
| CNS | Central nervous system |
| CQ | Chloroquine |
| CSF | Cerebrospinal Fluid |

| | |
|---|---|
| DAPI | 4,6-diamidino-2-phenylindole |
| Dep1 | Density enhanced protein tyrosine phosphatase 1 |
| DMSO | Dimethyl sulphoxide |
| DTX | Dinophysistoxin |
| eB3 | End binding protein 3 |
| ECs | Endothelial cells |
| EGFR | Epidermal growth factor receptor |
| EMT | Epithelial-mesenchymal transition |
| ERC | Endosomal recycling compartment |
| ESAM | Endothelial cell-selective adhesion molecule |
| EXO | Exocyst |
| FAK | Focal adhesion kinase |
| FBP | Fructose-1,6-biphosphate |
| FBS | Foetal bovine serum |
| FGFR | Fibroblast growth factor receptor |
| GAP | GTPase-activating protein |
| GAPDH | Glyceraldehyde-3-phosphate dehydrogenase |
| GDI | GDP dissociation inhibitors |
| GEF | Guanine nucleotide exchange factor |
| GK | Gunayly1-kinase domain |
| GPCRs | G protein-coupled receptors |
| GPI | Glucose phosphate isomerase |
| GSIE3 | Glycogen synthase kinase 3 |
| GSTP1 | Glutathione s-transferase Pi 1 |
| HCQ | Hydroxychloroquine |
| HMVEC | Human microvascular endothelial cells |
| HPMVECs | Human pulmonary microvascular endothelial cells |
| HUVECs | Human Umbilical vein endothelial cells |
| IFT20 | Intraflagellar transport proteins |
| IGFBP3 | Insulin growth factor binding protein 3 |
| IR | Insulin receptors |
| JAK2 | Janus kinase 2 |
| JAM | Junctional adhesion molecules |
| LMVECs | Lung microvascular endothelial cells |

| | |
|---|---|
| LPS | Lipopolysaccharide |
| MAPK | Mitogen -activated protein kinase |
| MAPT | Microtubule-associated protein Tau |
| MCL | Markow cluster analysis |
| Met | Metformin |
| MS | Multiple sclerosis |
| mTORC1 | Mechanistic target of rapamycin complex 1 |
| NCE | Nonlathering endocytosis |
| OA | Okadaic acid |
| OCT | Organic cation transporters |
| OSBP | Oxysterol binding protein |
| PA | Phosphatidic acid |
| PAR3/6 | Partition defect protein 3/6 |
| PBS | Phosphate buffered saline |
| PCNA | Proliferating cell nuclear antigen |
| PI3K | Phosphoinositide 3 kinase |
| PIs | Proteosome Inhibitor |
| PKC | Protein kinase |
| PP2A | Protein phosphatase 2A |
| PTP-1b | Protein tyrosine phosphatase 1b |
| PVDF | Polyvinylidene fluoride |
| qPCR | Semi-quantitative PCR |
| Rag | Rag family GTPases |
| RBD | Rab binding |
| rCBF | Regional cerebral blood flow |
| S1P | Sphinosine-1-phospate receptor |
| S3A | Semaphorin 3A |
| SDS-PAGE | Sodium dodecyl sulphate-polyacrylamide gel |
| SEC | Secretion |
| Shp2 | Src homology protein tyrosine phosphatase 2 |
| SNX1 | Sortin Nexin |
| T2DM | Type 2 diabetes mellitus |
| Tiam | T-cell lymphoma invasion and metastasis |
| TJS | Tight junctions |

| | |
|---|---|
| TNFα | Tumour necrosis factor alpha |
| UB | Ubiquitin |
| UBB | Ubiquitin +1 |
| UBP4 | Ubiquitin carboxyl-terminal hydrolase 4 |
| UPP | Ubiquitin proteosome pathway |
| UPS | Ubiquitin proteosome system |
| VE-CAD | VE-cadherin |
| VE-PTP | Vascular endothelial protein tyrosine phosphatase |
| VEGF | Vascular endothelial growth factor |
| VEGFR2 | Vascular endothelial growth factor receptor 2 |
| Vim | Vimentin |
| Vinc | Vinculin |
| ZO | Zonula occludens |

# List of Figures

# List of Tables:

# Table of Contents

# Chapter 1

# Introduction

## 1.1The Central Nervous System

The central nervous system (CNS) is regarded as one of the most sensitive systems in the human body and includes the brain and spinal cord [10]. It is crucial for the regulation and management of physiological functions, including reception, processing, and reaction to sensory information [11]. The CNS is enclosed by the axial skeletal bones, with the brain being protected within the cranial cavity of the skull, and the spinal cord being housed in the vertebral (spinal) canal [12].

### 1.1.1 The Brain

The brain is an organ of nervous tissue responsible for sensation, movement, emotion and communication, thought processing, and memory. It is made up of four primary components: the right and left cerebral hemispheres, the diencephalon, the cerebellum, and the brainstem. Pathological lesions in the brain can lead to localised neurological impairments as well as disconnection syndromes, highlighting that the brain operates both as a complex network of distributed processing and as a set of distinct functionally specialised areas [12].

### 1.1.2 The Spinal Cord

The spinal cord is located inside the vertebral column and transmits motor signals from the brain to the peripheral body and conveys sensory data from the sensory organs back to the brain. The adult spinal cord, also known as the spinal medulla, measures around 45 cm in length. The spinal cord itself runs from the foramen magnum at the base of the skull down to the first or second lumbar vertebrae. It functions as a bidirectional pathway connecting the brain and the rest of the body and is divided into four regions: cervical, thoracic, lumbar, and sacral. These regions comprise 31 segments, each associated with a pair of spinal nerves. There are 8 cervical nerves, 12 thoracic nerves, 5 lumbar nerves, 5 sacral nerves, and a single coccygeal nerve. Each nerve exits the vertebral column through the intervertebral foramina to reach its specific destination in the body. The spinal cord concludes in a cone-shaped structure known as the conus medullaris, which is anchored to the coccyx by the filum terminal. Ligaments are present throughout the spinal column to provide stability from the top to the bottom [12].

The CNS is an extremely sensitive microenvironment, requiring strict homeostatic regulation to maintain neuronal signalling. In order to do this, physical separation of the CNS from the rest of the body is required [13]. The CNS is surrounded by three cellular barriers: the blood–brain barrier (BBB), which separates the blood from the brain interstitial fluid; the choroid plexus (CP), which is between the blood and the ventricular cerebrospinal fluid (CSF); and the

arachnoid epithelium (meningeal barrier), which separates the blood from the subarachnoid CSF (Figure 1.1) [13]. These three cellular barriers regulate compound and nutrient exchange at the interfaces between the blood and the brain or its fluid spaces. The BBB is the most important of the three and has received extensive attention as a pharmacological target [13].

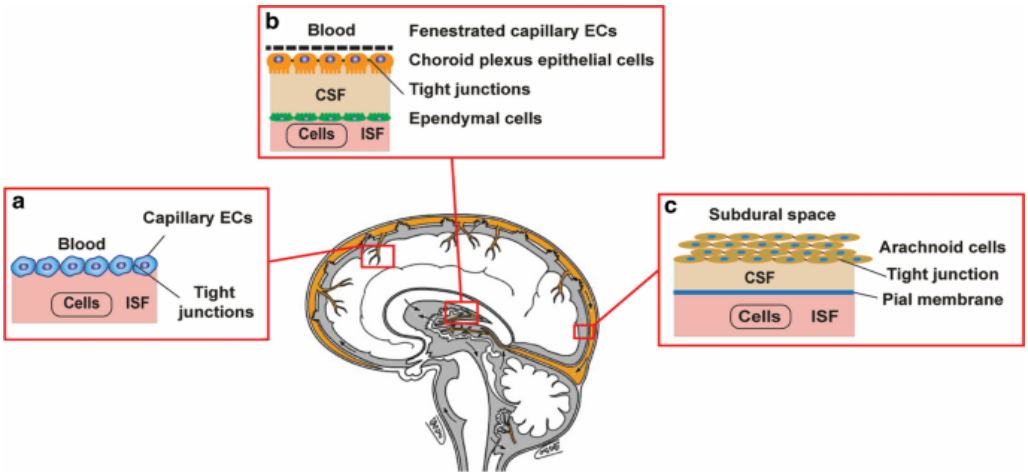


**Figure 1.1: A diagrammatic representation of the three cellular barriers that protect the central nervous system.** a) blood-brain barrier, b) choroid plexus and c) meningeal barrier [14].

Over a century ago, Paul Ehrlich (1885) noted that certain active molecules and dyes, when injected into the bloodstream, quickly spread to various organs, but did not penetrate the central nervous system, which includes the brain, spinal cord, and retina, due to its high impermeability to most small molecules. Ehrlich suggested that the CNS environment had unique characteristics that limited the entry of only a select few circulating substances. These observations contributed to the development of the blood-brain barrier (BBB) concept [15]. Consequently, the idea of a vascular BBB, serving also as a brain-blood barrier, emerged [16].

## 1.2 Blood-Brain Barrier

The BBB is a diffusion barrier that is required for normal CNS function [17]. It is a highly specialised structural and biochemical barrier that controls the entry of blood-borne molecules into the brain and maintains ionic homeostasis within the brain microenvironment [18]. It is composed of an endothelial cell membrane that, while semipermeable to $O_2$, $CO_2$, water, and small molecules, prevents pathogens and most macromolecules from entering [19]. Permeability of the BBB is a critical factor requiring consideration when developing new drugs for CNS diseases [20].

The mechanisms for penetrating the BBB are classified as passive or active. Passive diffusion allows small, lipophilic molecules to cross the BBB [18] and enter the brain from the luminal and abluminal membranes. Many unwanted molecules are returned to the circulatory system by efflux pumps, which regulate passive transport into the brain, while large, hydrophilic, and highly charged molecules such as proteins and peptides are transported across the BBB via active routes, including receptor-mediated endocytic transport [21]. In some studies, the latter was used for efficient drug delivery to target cells. For example, the transferrin receptor (TfR) and insulin receptor (IR) have been targeted to deliver therapeutic proteins as IgG fusion proteins via endocytosis [22].

### 1.2.1 Cells Forming the Blood-Brain Barrier

The blood-brain barrier is made up of blood vessels formed by specialised endothelial cells (ECs), astrocytes, pericytes, and neurons (Figure 1.2) [20].

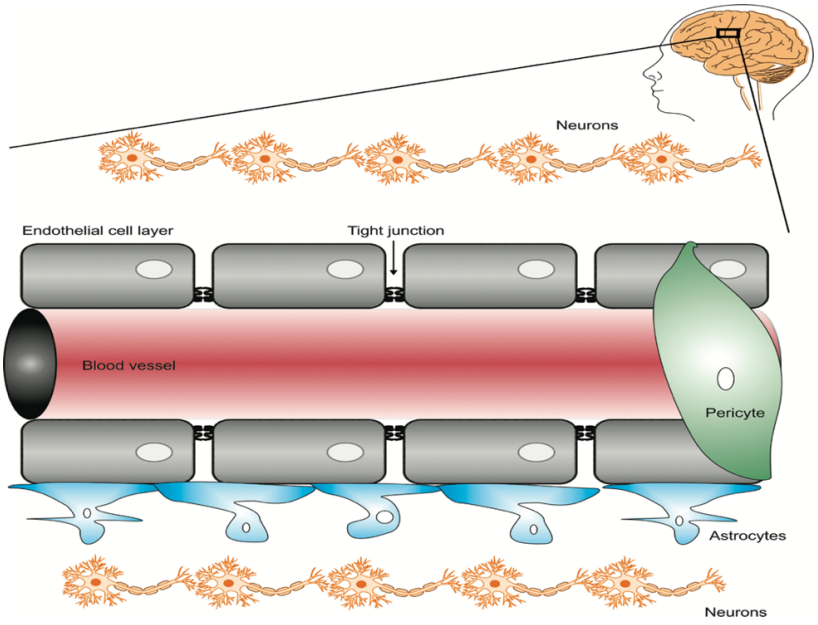


**Figure 1.2: A diagrammatic representation of the structure of the blood-brain barrier showing key cellular components and the location of tight junctions [13].**

#### 1.2.1.1 Brain Endothelial Cells (Endothelium)

The endothelium is the first line of defence between the circulatory system and the brain [23]. Endothelial cells arise from the mesoderm. They are modified simple squamous epithelial cells that line the surfaces of capillaries [24]. Endothelial cells of the CNS have unique properties compared with endothelial cells in other tissues that allow them to form tight junctions (TJs), which greatly limit the paracellular flux of solutes [2, 3, 25]. BBB endothelial cells are

distinguished from peripheral endothelial cells by the absence of fenestrations, low pinocytotic activity, and the presence of tight junctions [10]. The CNS microvascular endothelial cells are approximately 39% thinner than endothelial cells from muscle, resulting in a luminal/parenchymal separation of less than a quarter of a micron [24]. Historically, these characteristics have been used to define the endothelium as the primary barrier for drug transport into the brain. Furthermore, brain endothelial cells have an increase in mitochondrial content, which drives the multiple energy-dependent processes involved in nutrient support and brain protection [26]. Endothelial monolayers maintain their barrier properties via cell-cell contacts such as adherents and tight junctions [27].

#### 1.2.1.2 Astrocytes

Astrocytic glial cells represent the most abundant cell type within the brain and are characterised by their star-like morphology. They reside between neurons, pericytes, and endothelial cells, and communicate through a network of foot processes. Astrocytes originate from radial glia and standard brain precursor cells during the late stages of gestation, suggesting that astrocytes cannot regulate early processes that induce the blood-brain barrier [28]. There are two types of astrocytes in the brain. Protoplasmic cells are found in grey matter, whereas fibrillary cells are found in white matter. Astrocytes play a fundamental role in guiding the migration of developing neurons and in maintaining homeostasis by regulating extracellular potassium ($K^+$) concentrations and neurotransmitter levels [29]. Following injury to the central nervous system, astrocytes engage in dynamic communication with adjacent neuronal and vascular networks, contributing to the clearance of pathological protein aggregates, including β-amyloid and α-synuclein. During neuronal activity, the generation of action potentials results in the release of $K^+$ into the extracellular milieu. Astrocytes, which express a high density of potassium channels, function as spatial buffers to mitigate fluctuations in extracellular $K^+$ concentrations [30]. Astrocytes are essential regulators of the BBB, contributing to its formation and maturation. They enhance tight junctions, modulate transporter expression and polarity, and support enzymatic activity necessary for BBB function [31-41]. Furthermore, astrocytes have been shown to induce barrier properties in peripheral blood vessels in transplantation models and to enhance endothelial barrier integrity in *in vitro* coculture systems [38, 41]. Additionally, astrocyte end-feet regulate regional cerebral blood flow through the release of vasoactive substances in response to neuronal activity [26].

### 1.2.1.3 Pericytes

Pericytes are multifunctional mural cells found in capillaries, venules, and arterioles that wrap around endothelial cells [42]. They cover a significant portion of the abluminal endothelial surface in the CNS [43]. Structurally, they support the microvasculature and provide vaso-dynamic capacity [44]. Pericytes are distributed throughout the vascular endothelium in microvascular networks, approximately one for every 5 to 6 brain endothelial cells, and they establish gap junctions with brain endothelial cells, indicating a close functional connection [45]. Their strong connection with endothelial cells facilitates the transfer of ions, metabolites, second messengers, and ribonucleic acids between the two types of cells [46]. Pericytes in the brain influence the behaviour of endothelial cells, manage inflammation, and oversee the formation and size of capillaries. Pericytes are essential and multifunctional cells that play a pivotal role in preserving the integrity of the BBB and maintaining cerebral homeostasis [47]. They contribute to angiogenesis, microvascular stability, and BBB maintenance by secreting signalling molecules that regulate tight junction formation between endothelial cells and influence the alignment of astrocytic end-feet [43, 46, 48]. A reduction in pericyte coverage has been linked to the disruption of endothelial tight junctions, resulting in increased BBB permeability [47].

### 1.2.1.4 Neurons

Neurons reside close to the capillaries and form connections with astrocytic end feet near the BBB. Neurons in the brain are rarely more than 8–20 μm away from a capillary [49]. Every neuron has its capillary system. They regulate blood flow and microvascular permeability, interact with the extracellular matrix, and have the ability to release angiogenesis-stimulating factors [50]. They also help to maintain the integrity of the endothelial cell monolayer by assisting in the synthesis and localisation of tight junction proteins [51].

## 1.3 Blood-Brain Barrier (BBB) Junctional Complex

The BBB junction complex is made up of tight junctions and adherent junctions (Figure 4) [18].

### 1.3.1 Tight Junctions

Tight junctions at the BBB are protein complexes that create extensive rows of overlapping junctions between brain microvascular endothelial cells. Tight junctions are located at the points where the outer surfaces of the plasma membranes of adjacent endothelial cells or the

same cells come together [52]. Tight junctions begin to form early during the development of the blood-brain barrier, establishing a barrier that restricts the movement of proteins and macromolecules during the initial stages of brain development [53].

Tight junctions are composed of three integral membrane proteins, claudin, occludin, and junction adhesion molecules (JAMS), as well as several cytoplasmic accessory proteins, including Zonula occludens-1, -2, -3 (ZO-1, ZO-2, ZO-3), cingulin, and others (Figure 1.3). The cytoplasmic proteins connect membrane proteins to actin, the primary cytoskeleton protein responsible for the structural and functional integrity of the endothelium [14]. Tight junctions are primarily made up of claudins [54]. Tight junctions significantly limit the paracellular diffusion pathway between endothelial cells for ions and other polar solutes, and they effectively prevent the passage of macromolecules through this pathway [53]. The regulation of tight junction protein is based upon protein–protein interactions, post-translational modification, and cellular localization [26].

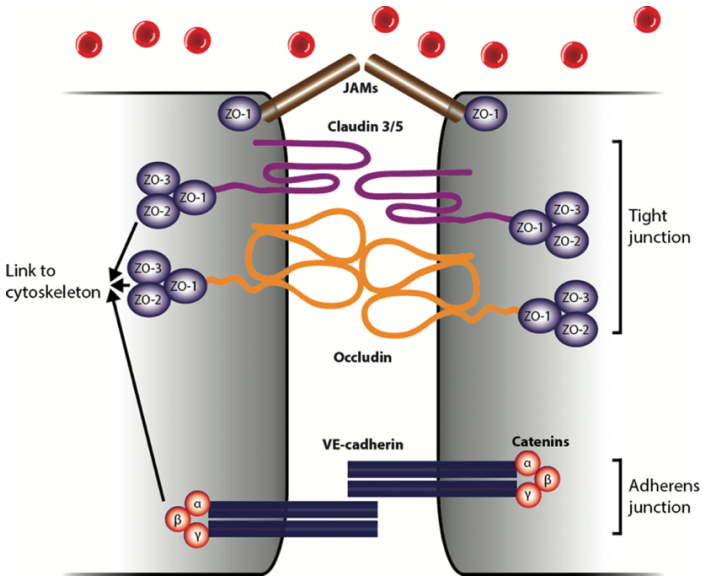


**Figure 1.3: A schematic representation of the structural components of adherens and Tight junctions.** Abbreviations: ZO, Zonula occludens; JAMs, junctional adhesion molecules [13].

### 1.3.1.1 Claudin

Claudins were first identified by Furuse *et al* [55]. Claudins are integral membrane proteins that regulate the function of the tight junctions. In mice and humans, a total of 24 claudin family members have been identified [47]. They are 22 kDa phosphoproteins with four transmembrane

domains. To form the tight junction seal, claudins bind in a homotypic manner to claudins on adjacent endothelial cells [56]. In addition, the carboxy terminal of claudins binds to cytoplasmic proteins such as ZO-1, ZO-2, and ZO-3 [47]. Claudin-5 is a vital transmembrane protein within tight junctions between brain endothelial cells, playing a central role in regulating the selective permeability of the blood-brain barrier [57, 58]. Claudin-5 is also involved in modulating endothelial and epithelial permeability during various pathological conditions, including inflammation, oedema, trauma, and tumour progression [59]. Furthermore, it is critically expressed during early angiogenic processes in the central nervous system, highlighting its importance in both BBB formation and maintenance [60].

#### 1.3.1.2 Occludin

Occludin was discovered in 1993 as the first integral protein found at tight junctions [61] using immunogold freeze fracture microscopy in chickens [59], and subsequently in mammals [61]. Occludin is a larger phosphoprotein than claudin [62], with a molecular weight of approximately 60–65 kDa [26]. The expression of occludin is greater in endothelial cells of the brain than in non-neural tissues [63].

Occludin has four transmembrane regions, two extracellular loops, a short N-terminal and a long C-terminal cytoplasmic domain. Both the N- and C-termini are located intracellularly [18]. Occludin has a regulatory function and may influence paracellular transport. Occludin and claudins form heteropolymers and transcellular tracts with selective ion and hydrophilic molecular transport channels. It may also play a role in maintaining BBB electrical resistance and in the formation of aqueous pores [47]. As such, occludin acts as a regulatory protein capable of modifying paracellular permeability [63].

#### 1.3.1.3 Junctional Adhesion Molecules (JAMs)

JAMs are members of the immunoglobulin subfamily with a molecular weight of 40 kDa. JAMs have the following structural domains: an extracellular domain with two immunoglobulin-like loops, a single transmembrane domain, and a short intracellular domain. The JAM family of proteins is divided into two groups based on sequence similarities: First is the closely related JAM-A, -B, and -C, and second is the more distantly related coxsackie and adenovirus (CAR)-like membrane protein, endothelial cell-selective adhesion molecule (ESAM), and JAM-4. Because JAMs are expressed on endothelial cells, epithelial cells, and/or blood cells, they act as cell-cell adhesion molecules not only between the same types of cells but also between different types of cells (e.g., leukocytes, platelets, and/or endothelial cells) via homophilic and

heterophilic interactions [64]. Both JAM-A and JAM-C maintain the stability of tight junctions, while JAM-B maintain the stability of tight junctions by interacting with JAM-C [65]. ESAM is involved in endothelial cell-cell interactions that are necessary for vascular development and neutrophil extravasation during the early stages of inflammation [18].

#### 1.3.1.4 Cytoplasmic Accessory Proteins

Cytoplasmic accessory proteins include Zonula occludin proteins (ZO-1, ZO-2, and ZO-3), as well as cingulin [47]. ZO belongs to the membrane-associated guanylate kinase family and is made up of three PDZ domains, one SH3 domain, and a guanylyl-kinase domain (GK). ZO proteins interact directly with many transmembrane proteins, including occludin, claudins, and JAM. ZO proteins are involved in both signal transduction and transcriptional modulation. ZO-1 is a 220 kDa phosphoprotein that associates with the C-terminus of claudins via its PDZ-1 domain and connects to JAM via PDZ-2 and -3 domains, and occludin via the GK domain. ZO-1 binds to the actin cytoskeleton via its C-terminus. This interaction is critical for tight junction stability and function; dissociation of ZO-1 from the junctional complex frequently results in increased BBB permeability. ZO-2 is a 160 kDa phosphoprotein that shares sequence homology with ZO-1. Because ZO-2 is redundant with ZO-1, it can be used to replace ZO-1 in the formation of a morphologically competent tight junction. ZO-3 is a 130 kDa phosphoprotein with a sequence and domain organisation like ZO-2 [65].

### 1.3.2 Adherens Junction

Adherens junctions (AJs) are complexes that facilitate adhesion between cells, playing crucial roles in both embryonic development and the maintenance of tissue integrity [66-68]. It is a family of transmembrane cadherin proteins (epithelial (E), neuronal (N), placental (P), vascular endothelial (VE), and others, named after the tissue where they were first described) that interact in the extracellular space in a homophilic, calcium-dependent manner to physically link cells together [69]. Adherens junctions are responsible for a variety of functions, including cell-cell adhesion initiation and stabilization, actin cytoskeleton regulation, intracellular signalling, and transcriptional regulation. Interactions between transmembrane glycoproteins of the classical cadherin superfamily, such as E-cadherin, and catenin family members such as p120-catenin, β -catenin, and α-catenin, form the core of the adherens junction. These proteins collaborate to control the formation, maintenance, and function of adherens junctions**.** The major adhesive protein of the adherens junction, vascular endothelial cadherin (VE-cadherin), is specific for vascular endothelial cells [70] and is discussed in more detail below.

### 1.3.2.1 Cadherins

Vascular endothelial (VE)-cadherin also known as cadherin 5 or CD144, is a structural component for brain vascular integrity, and therefore is the primary target of BBB breakdown signalling events [71]. It is an endothelial adhesion molecule found exclusively at endothelial cell junctions [72] that acts as an endothelial cell adhesion zipper. VE-cadherin is made up of five extracellular domains, a transmembrane domain, and a cytoplasmic domain (Figure 4). Each domain is constructed from a seven-stranded beta barrel fold. One such strand is the A strand, which allows two VE-cadherins from adjacent endothelial cells to connect via the extracellular domain 1. In addition to maintaining endothelial to endothelial cell contact, VE-cadherin also regulates cell proliferation and apoptosis, and modulates the function of vascular endothelial growth factor receptors [73]. VE-cadherin plays a crucial role in regulating the permeability of the endothelial monolayer and in the process of angiogenesis [74]. It also facilitates the initial stages of vascular linking and fusion [75, 76].

The VE-cadherin multimers connect to the actin cytoskeleton through several accessory molecules (primarily β- and p120-catenins), which in turn interact with the actin-binding proteins α-catenin, vinculin, and eplin (Figure 1.4). The dephosphorylation of β-catenin and the mobility of VE-cadherin aid in the stabilisation of endothelial cell–cell junctions. γ-Catenin (also known as plakoglobin) is another accessory protein that can directly interact with VE-cadherin. With regard to p120-catenin, the juxtamembrane domain, which interacts with VE-cadherin, is a key regulator of VE-cadherin expression, trafficking, and stability at the plasma membrane [72].

Interestingly, several serine/threonine and tyrosine phosphatases are part of the VE-cadherin interactome. Vascular endothelial protein tyrosine phosphatase (VE-PTP), src homology protein tyrosine phosphatase 2 (shp2), protein phosphatase 2A (PP2A), density enhanced protein tyrosine phosphatase 1 (DEP-1/CD148), and protein tyrosine phosphatase 1B (PTP1B) appear to directly stabilize VE-cadherin based adhesion. These enzymes dephosphorylate VE-cadherin and associated catenin which strengthens cell-cell adhesion [72].

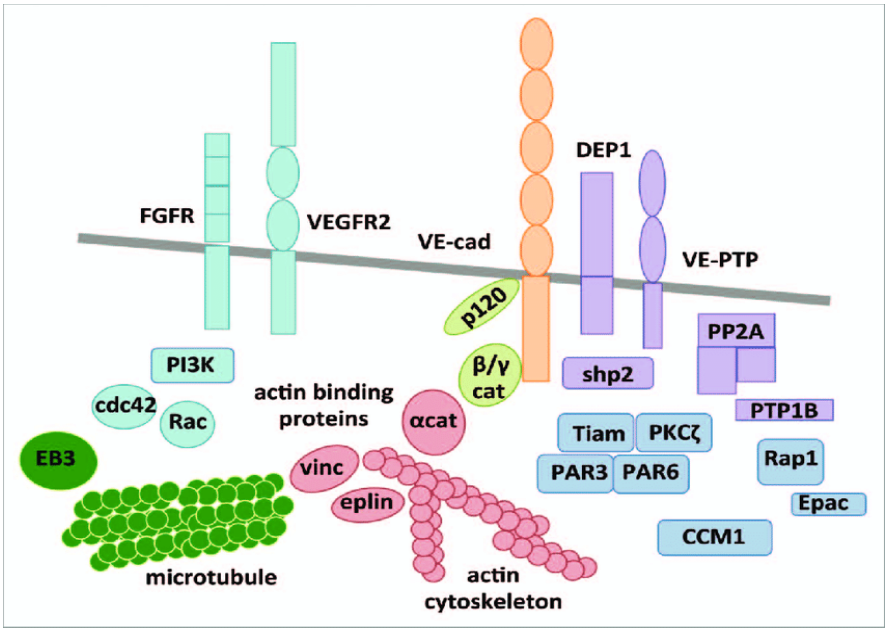


**Figure 1.4: A schematic representation of key proteins interacting with VE-cadherin.** Abbreviations: PP2A, protein phosphatase 2A; VE-cad, VE-cadherin; VE-PTP, Vascular endothelial protein tyrosine phosphatase; PTP1B, protein tyrosine phosphatase 1B; shp2, src homology protein tyrosine phosphatase 2, α-cat, α- catenin; β/γ -cat, β/γ -catenin; Vinc, vinculin; cdc42, cell division control protein 42 homolog; CCM1, cerebral cavernous malformation protein 1; DeP1, density enhanced protein tyrosine phosphatase 1; eB3, end binding protein 3; FGFR, fibroblast growth factor receptor; PAR3/6, partition defect protein 3/6; Pi3K, phosphoinositide 3 kinase; PKC, protein kinase C; PTP1B, protein tyrosine phosphatase 1B; Tiam, T-cell lymphoma invasion and metastasis; veGFR2, vascular endothelial growth factor receptor 2 [72].

### 1.3.2.2 Catenin Family Members

#### 1.3.2.2.1 P120-Catenin

p120-Catenin was initially discovered as a substrate for Src-tyrosine receptor kinase and was later identified as a member of the catenin family based on sequence homology to an armadillo domain of β-catenin. There exist four isoforms of p120 that arise from post-translational modifications or various internal translation initiation sites. p120-catenin contains eight tyrosine phosphorylation sites [77] and eight serine/threonine phosphorylation sites [78]. Within the juxtamembrane domain, p120-catenin binds VE-cadherin via a highly conserved octapeptide sequence (YDEEGGGE). The association of p120-catenin with the juxtamembrane domain of VE-cadherin stabilizes VE-cadherin at the plasma membrane during cell-cell contact

formation [79]. p120-catenin also regulates the turnover of cadherin at the cell surface, thereby controlling the amount of cadherin available for cell–cell adhesions [78]. p120 plays a crucial role in the immune response and inflammatory reactions of organisms [80, 81]. p120 also plays various physiological roles, including the preservation of epidermal physiological function [82], regulation of signal transduction [83, 84], embryonic development [85-87] and mitigation of pulmonary fibrosis [88]. p120-catenin also acts as a modulator of cell movement via the actin cytoskeleton by engaging with Rho family GTPases [89].

#### 1.3.2.2.2 β-Catenin

β-catenin, referred to as Armadillo in Drosophila, is an essential structural component of cadherin-mediated adherens junctions and functions as the main nuclear effector in the canonical Wnt signalling pathway inside the nucleus [90]. β-catenin was first discovered in Drosophila as the segment polarity protein armadillo, which has 13 repeats of a 42 amino acid armadillo domain that forms a triple helix. The β-catenin protein, composed of 781 amino acid residues in humans, features a central region (residues 141–664) containing 12 imperfect Armadillo repeats (R1–12), which are bordered by distinct N- and C-terminal domains, referred to as NTD and CTD, respectively. Near the CTD, there is a specific conserved helix (Helix-C) situated close to the final Armadillo repeat (residues 667–683) [91]. The N-terminal domain and the C-terminal domain exhibit structural flexibility, while the central section maintains a more stable scaffold. This scaffold acts as a site for interaction with numerous β-catenin binding partners, both at the membrane, in the cytoplasm, and within the nucleus [92]. β-Catenin can move back and forth between the nucleus and the cytoplasm [93, 94].

β-Catenin functions as a protein in adherens junctions, connecting adherens to the actin cytoskeleton [95] and a transcription factor that is crucial to the Wnt signalling pathway [90, 96]. The function of β-catenin is modulated through phosphorylation events under the control of various kinases. For instance, when E-cadherin is phosphorylated, it gains a negative charge that enhances its interaction with the positively charged central cavity of β-catenin. This phosphorylation-dependent interaction also enables β-catenin to associate with the C-terminal cytoplasmic domain of VE-cadherin [97-99]. Phosphorylation of β-catenin often causes a weakening of the cadherin-β-catenin interaction, directing β-catenin into signalling mode. Casein kinase II (CKII) and glycogen synthase kinase-3 (GSK-3) phosphorylate three serine residues in the cadherin cytoplasmic domain ($Ser^{684}$, $Ser^{686}$, $Ser^{692}$), resulting in additional interactions between β-catenin and VE-cadherin and a significant increase in the affinity of the interaction [79].

β-catenin, a key component of the canonical Wnt signalling pathway, plays a crucial role in regulating angiogenesis within the central nervous system and maintaining the integrity of the blood-brain and blood-retina barriers [99]. This signalling pathway is essential for BBB development, primarily by promoting the expression of tight junction proteins and transporters in brain capillaries. Dysregulation of Wnt/β-catenin signalling has been associated with BBB disruption in various neurological disorders, including multiple sclerosis, stroke, Alzheimer's disease, Huntington's disease, bipolar affective disorder and brain tumours [100].

#### 1.3.2.2.3 α-Catenin

α-Catenin is a key mechanosensitive scaffold protein that connects the cadherin–catenin complex to the cortical actin cytoskeleton at adherens junctions [101, 102]. α-Cat was identified in 1984 by Vestweber and Kemler as a 102 kDa protein linked with the adhesive molecule E-cadherin, which was initially called uvomorulin [103, 104]. α-Catenin can exist as a monomeric or homo-dimeric protein. α-Catenin binds monomeric β-catenin but not actin. Homo-dimeric α-catenin, on the other hand, binds actin filaments but not β-catenin [79]. The α-catenin family includes four members, αE-catenin, αN-catenin, αT-catenin, and α-cat, all of which play crucial roles in cell development and differentiation. α-cat engages with proteins like Ajuga, potentially connecting cell adhesion with signalling within the nucleus [105]. The binding of α-catenin maintains β-catenin in its hinged configuration, allowing for simultaneous binding of E-cadherin [97, 106]. Reduced levels of E-cadherin and α-catenin proteins have been documented as a common feature in several human cancers [107-109], with a decrease in α-catenin associated with cancer progression due to diminished cell-cell adhesion [110].

## 1.4 Protein Phosphatases

The substrate specificity and catalytic mechanism of protein phosphatases are used to classify them. The two major families of protein phosphatases are protein tyrosine phosphatases and protein serine/threonine phosphatases. These families have several subfamilies with multiple members within the superfamily. Based on structure and gene sequence, the protein tyrosine phosphatase family is divided into three main families (Class I-III) with several sub-families. In contrast, protein serine/threonine phosphatases are subclassified into three structurally distinct families: phosphoprotein phosphatases, metal-dependent protein phosphatases, and aspartate-based phosphatases [111].

One of the key members of the phosphoprotein phosphatases family is protein phosphatase 2A (PP2A), which accounts for 30-50% of all cellular dephosphorylation events [112]. PP2A is a

serine/threonine phosphatase that is highly conserved and universally expressed across eukaryotic cells [113] and regulates a variety of cellular processes, including protein synthesis, cell growth, cellular signalling, apoptosis, and metabolism [114].

### 1.4.1 Structure of PP2A

PP2A is made up of three subunits: a catalytic 'C' subunit (PP2A-C), a scaffolding 'A' subunit (PP2A-A or PR65), and a regulatory 'B' subunit (Figure 1.5). In mammalian cells, the A and C subunits are mostly found as AC dimers (also known as core dimers) or ABC trimers (also known as heterotrimers or holoenzymes), with a small fraction as 'free C' subunits that may be stabilised by binding with other regulatory proteins. For the hydrolysis of Ser/Thr phosphate esters, the PP2A-C subunit requires the presence of two manganese ($Mn^{2+}$) ions in its active site.

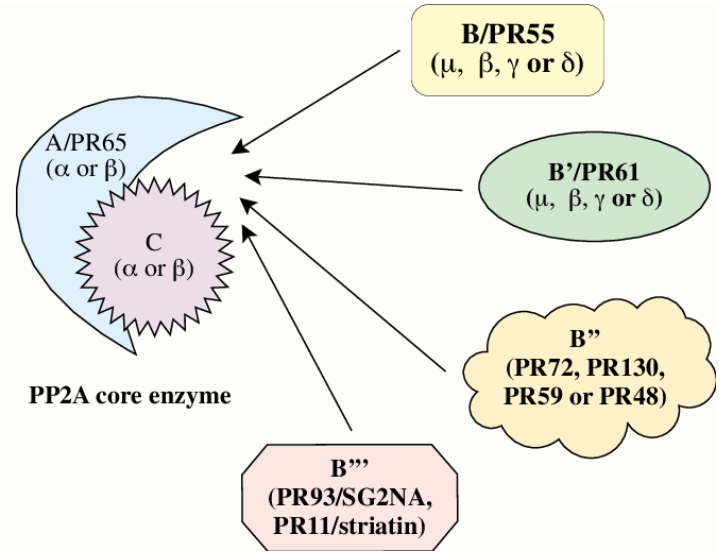


**Figure 1.5: A diagrammatic representation of the structure of Protein Phosphatase 2A (PP2A) showing the scaffolding (A), regulatory (B) and catalytic (C) subunits and isoforms [115].**

#### 1.4.1.1 PP2A: Catalytic Subunit

The catalytic subunit of protein phosphatase 2A (PP2Ac) exhibits a globular structure and is ubiquitously expressed across a wide range of tissues, with particularly high levels observed in the heart and brain. Its expression (PPP2AC) is regulated at the translational level to ensure homeostatic levels [116]. The 37 kDa PP2Ac shares a high degree of sequence conservation, exhibiting 86% amino acid identity between humans and yeast, while also showing 50% similarity with protein phosphatase 1 (PP1) and 40% with protein phosphatase 2B (PP2B). PP2Ac is present in two isoforms, Cα and Cβ, both comprising 309 amino acids and sharing

97% sequence identity. The Cα isoform is primarily localised to the plasma membrane, whereas Cβ is distributed within the cytoplasm and nucleus. The higher expression level of Cα compared to Cβ is attributed to its more active promoter and lower mRNA degradation rate [117]. Notably, the C-terminal tail of PP2Ac (residues 304–309: TPDYEL) is highly conserved and plays a critical role in its interaction with the scaffold and regulatory subunits, including PR61γ [8].

#### 1.4.1.2 PP2A: Scaffold Subunit (PP2A-A or PR65)

The scaffold subunit of protein phosphatase 2A is encoded by two separate genes, *PPP2R1A* and *PPP2R1B*, which give rise to two isoforms: Aα and Aβ. These isoforms are broadly expressed across tissues and exhibit approximately 86% sequence homology [118]. The Aα isoform constitutes the scaffold component in roughly 90% of PP2A complexes, either as part of the core enzyme or the complete holoenzyme, and is highly prevalent in normal tissues, representing about 0.1% of the total cellular protein content. In contrast, the Aβ isoform is incorporated into approximately 10% of PP2A assemblies, reflecting distinct interaction preferences with both the catalytic and regulatory subunits [119]. Both Aα and Aβ isoforms are predominantly localised in the cytoplasm [120].

In its heterotrimeric configuration, the PP2A-A scaffold subunit functions as a structural platform, facilitating the assembly of the catalytic subunit and promoting interactions with the regulatory subunit and various substrates. In contrast, within the dimeric complex, PP2A-A plays a modulatory role by altering the substrate specificity of the catalytic subunit [121]. From a structural perspective, the scaffold subunit is distinct from the other PP2A components. It comprises a HEAT (Huntington/elongation/A-subunit/TOR) repeat domain, consisting of 15 tandem repeats, each approximately 39 amino acids in length. Each repeat contains a pair of α-helices, which are interconnected through inter- and intra-repeat loops. The catalytic subunit associates with HEAT repeats 11 to 15, whereas the regulatory subunit interacts primarily with repeats 1 through 10 [122].

#### 1.4.1.3 PP2A: Regulatory Subunit

The regulatory B subunits of PP2A are classified into four distinct families: (1) B/PPP2R2 (also known as PR55 or B55), (2) B’/PPP2R5 (PR61 or B56), (3) B”/PPP2R3, and (4) B’’’/STRN (Striatin). Each of these subfamilies comprises between three to five isoforms, along with additional splice variants, collectively contributing to a repertoire of at least 26 unique B subunits [111]. The B subunits are considered key regulators of the PP2A holoenzyme,

functioning primarily as modulators that confer both temporal and spatial specificity to the enzyme's activity [123].

#### 1.4.1.3.1 PP2A-B (PR55)

The B55/PR55 regulatory subunit family comprises four isoforms: α, β, γ, and δ. Developmental regulation of these isoforms has been observed, with B55γ expression increasing and B55β expression decreasing progressively after birth [124]. A defining structural feature of the B55 family is the presence of tryptophan-aspartate (WD40) repeats, which are integral to protein-protein interactions and facilitate substrate binding. In neuronal cells, B55α and B55β are predominantly localised in the cytoplasm, while B55γ is associated with the cytoskeletal compartment [125].

#### 1.4.1.3.2 PP2A-B' (PR56/PR61)

The B56 regulatory subunit family comprises five isoforms: α, β, γ, δ, and ε. A distinguishing characteristic of this family is their ability to undergo phosphorylation and their predominantly α-helical structure. These isoforms are capable of directly interacting with the PP2A core enzyme, thereby enhancing its catalytic activity. While the central regions of B56 isoforms share approximately 80% sequence identity, variability in their N- and C-terminal domains contributes to differential tissue-specific expression. Subcellular localization of B56 isoforms is also distinct: B56γ is primarily localized in the nucleus, whereas B56α, B56β, and B56ε are predominantly cytoplasmic. PR61δ (B56δ) is distributed in both the nuclear and cytoplasmic compartments [8].

#### 1.4.1.3.3 PP2A-B" (PR72, PR130) and PP2A-B'" (PR93 or 110)

The B″ and B‴ regulatory subunit families were identified through yeast two-hybrid screening approaches. The B″ family includes the PR72 and PR130 isoforms, which differ primarily in their N-terminal regions, suggesting that these variants arise from alternative splicing events. PR72 expression is restricted to cardiac and skeletal muscle tissues, whereas PR130 is ubiquitously expressed, with particularly high levels in heart and muscle tissues. PR72 possesses two EF-hand-like (EFX) calcium-binding domains, which are essential for inducing conformational changes that facilitate its interaction with the PR65 scaffold subunit [126]. Functionally, PP2A complexes containing the B subunit inhibit simian virus 40 (SV40) replication, whereas those incorporating B″ subunits promote its replication. Furthermore, the B″ subunit has been implicated in regulating the phosphorylation of the retinoblastoma protein

p107 in response to UV-induced DNA damage, thereby contributing to the activation of DNA damage response pathways [127].

### 1.4.2 Regulation of PP2A

The modulation of protein phosphatase 2A (PP2A) biogenesis, activity, and targeting is a highly regulated and complex process. Abnormal regulation or inhibition of PP2A activity is strongly associated with several pathological conditions, particularly cancer [128-130]. Both pharmacological and non-pharmacological mechanisms can reduce PP2A activity, each contributing to disease progression through distinct molecular routes [131-137]. Inhibiting protein phosphatase 2A (PP2A) through pharmacological and non-pharmacological methods yields different outcomes. For example, pharmacological approaches use small molecules with varying specificities and toxicities, while non-pharmacological approaches often involve manipulating the expression of endogenous PP2A-regulating proteins [138] or miRNA [111].

One well-characterised pharmacological inhibitor of PP2A is okadaic acid (OA), which binds to the catalytic site of PP2A, preventing substrate dephosphorylation. Experimental studies demonstrate that topical application of OA to mouse skin induces tumour formation, indicating that pharmacological suppression of PP2A activity can promote oncogenic signalling and tumorigenesis [139, 140]. Another pharmacological inhibitor**,** LB-100**,** selectively inhibits the PP2A catalytic subunit (PP2Acα) by displacing one of its two essential manganese ($Mn^{2+}$) cofactors. This disruption leads to enzyme inactivation and sustained activation of downstream signalling pathways involved in cell proliferation and survival [141]. Although pharmacological inhibitors like OA and LB-100 are valuable research tools for understanding PP2A function, their strong inhibitory effects can mimic disease-like conditions where PP2A activity is pathologically reduced.

Non-pharmacological inhibition of PP2A activity typically occurs through genetic or protein-mediated mechanisms that affect the enzyme's structure, regulation, or holoenzyme assembly. One approach involves knockdown or knockout of the PP2A catalytic subunit**,** which decreases overall enzymatic activity and disrupts dephosphorylation processes in cells [142]. In addition, endogenous protein inhibitors**,** such as SET (Suvar/Enhancer of zeste/Trithorax, also known as I2PP2A) and CIP2A (Cancerous Inhibitor of PP2A)**,** play a crucial role in the non-pharmacological regulation of PP2A [143]. These proteins interact directly with the PP2A holoenzyme, blocking its catalytic activity while also influencing its assembly, disassembly, methylation state, and subunit composition. This level of regulation ensures proper control of PP2A signalling, but overexpression of these inhibitors has been linked to the onset of cancer

and neurodegenerative diseases such as Alzheimer's disease [144, 145]. Furthermore, PP2A activity can also be modulated through post-translational modification (methylation, phosphorylation, and nitration) of its catalytic subunit, including those that alter enzyme stability and substrate specificity [146, 147].

### 1.4.2.1 Phosphorylation

Phosphorylation of a PP2A subunit frequently serves to regulate the feedback [147] loop that controls phosphorylation. For instance, the phosphorylation of the PP2A regulatory subunit B56δ by PKA enhances PP2A activity [148]. Additionally, the phosphorylation of the PP2A catalytic subunit (PP2Ac) leads to its transient inactivation. Phosphorylation of PP2Ac at Tyr307 diminishes phosphatase activity, while methylation at the adjacent Leu309 site increases its phosphatase activity [149, 150]. These modifications influence the binding of regulatory B subunits to the PP2A (AC) core enzyme, thereby affecting PP2A's substrate specificity, targeting, and cellular functions [151]. Furthermore, the susceptibility of PP2A subunits to modification may be regulated by their interactions with non-subunit proteins. For example, the binding of p21-activated kinase 1 (PAK-1) to the PP2A holoenzyme induces a conformational change that leads to a reduction in phosphorylation at Tyr307 [152] and hence increase in phosphatase activity.

### 1.4.2.2 SET

The oncoprotein SET, also known as protein phosphatase 2A inhibitor 2 (I2PP2A), acts as a natural inhibitor of protein phosphatase 2A [153]. It consists of 277 amino acids and has a molecular weight of around 39 kDa. SET was first discovered in acute undifferentiated leukaemia, where it appeared as part of a gene fusion involving the CAN gene [154]. The SET protein interacts directly with the catalytic subunit of PP2A (PP2Ac) via both its N-terminal and C-terminal regions, thereby suppressing PP2A's phosphatase activity [155]. Importantly, SET is a highly potent and specific inhibitor of PP2A and does not affect other phosphatases like PP1, PP2B, or PP2C [156]. To regulate its activity, SET has multiple phosphorylation sites that undergo post-translational modification [135]. SET-mediated PP2A inhibition is an important regulatory mechanism in the promotion of cancer initiation and progression in several types of human leukaemia disease (Figure 9). The biological effect of SET on proliferation and invasion is mediated by PP2A inhibition via binding with the PP2A catalytic subunits [155], which activate AKT and ERK [135].

### 1.4.2.3 CIP2A

Cancerous Inhibitor of PP2A (CIP2A) is an endogenous inhibitor of the PP2A enzyme and functions as a human oncoprotein. It contributes to cancer progression by enhancing cell proliferation, supporting anchorage-independent growth, and promoting resistance to apoptosis. CIP2A is a 90 kDa protein composed of 905 amino acids [111], and it is commonly detected in various cancers, including those affecting the lung, breast, oesophagus, and gastrointestinal tract. Mechanistically, CIP2A directly binds to the PP2A-B56α trimer, displacing the PP2A-A scaffolding subunit. This interaction allows CIP2A to commandeer both the B56α regulatory and PP2Ac catalytic subunits, forming a CIP2A-B56α-PP2Ac pseudotrimer [258]. Additionally, CIP2A interferes with substrate binding by occupying the LxxIxE-motif recognition site on B56α, thereby blocking access for normal substrates [157]. CIP2A is becoming a significant therapeutic target in cancer (Figure 9). In cancer, it is proposed that CIP2A inhibits PP2A, which prevents phosphorylation of Akt and maintains Akt in its phosphorylated (active) state, thus stabilising c-Myc (c-Myc oncogene product), which supports tumorigenesis [158]. Moreover, decreased PP2A activity in the central nervous system, which has high expression of CIP2A, may hasten pathological p-syn aggregation, a key feature in Parkinsons' disease pathogenesis [159].

### 1.4.2.4 Pharmacological Inhibitors

#### 1.4.2.4.1 Okadaic Acid

Okadaic acid (OA) is one of the most common marine toxins and is a polycyclic ether derivative of a C38 fatty acid (Figure 1.6) that is produced by several species of dinoflagellates and is known to accumulate in both marine sponges and shellfish.

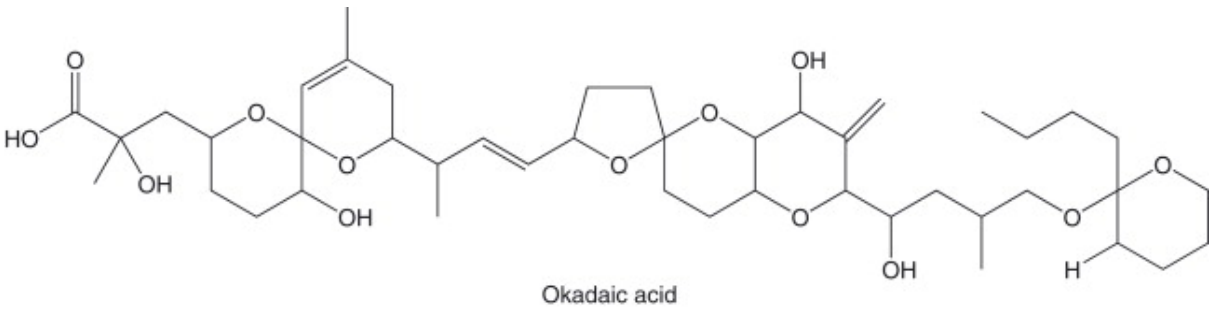

Okadaic acid

**Figure 1.6: Chemical structure of okadaic acid [160].**

Functionally, okadaic acid inhibits several classes of protein serine/threonine phosphatases including PP1, PP2A, PP4, PP5 and PP6 [161, 162], which play critical roles in the regulation of essential cellular processes such as growth, division, death, and cytoskeletal structure maintenance. Within this group of protein phosphatases, OA preferentially inhibits PP2A over PP1 with an $IC_{50}$ value of 7 nM compared to 126 nM for PP1 [163]. The differences in $IC_{50}$ values between these studies likely reflect the assay conditions used, for example, the amount of both enzyme and substrate employed in an assay. Notwithstanding this, the $IC_{50}$ for PP2A is approximately 50–500-fold lower than that for PP1 [162, 164]. In the context of this thesis, OA was used within a concentration range that is relatively selective for PP2A to minimise off target phosphatase inhibition. Okadaic acid causes significant changes in the phosphorylation states of many cellular proteins, which can eventually lead to the collapse of regulatory processes and a variety of cellular disruptions [165]. Okadaic acid is widely utilised as a research tool because of its tumour-promoting properties (Figure 1.7) and its capacity to inhibit protein phosphatase 2A (PP2A). Interestingly, research has also demonstrated that okadaic acid can inhibit the growth of lung cancer cells, both when used alone and in combination with cisplatin. In rodent models studied, the tumour-promoting effects of okadaic acid and related compounds are strongly linked to the upregulation of TNF-α gene expression. Endogenous inhibitors of PP2A, including SET and CIP2A, are critical regulators of cellular function. Overexpression of these proteins leads to marked suppression of PP2A activity, thereby promoting tumour development and progression in human cancers. This mechanism parallels the pathway activated by okadaic acid in rodent carcinogenesis, with TNF-α induction appearing to serve as a key mediator connecting PP2A inhibition to tumour-promoting activity [166, 167].

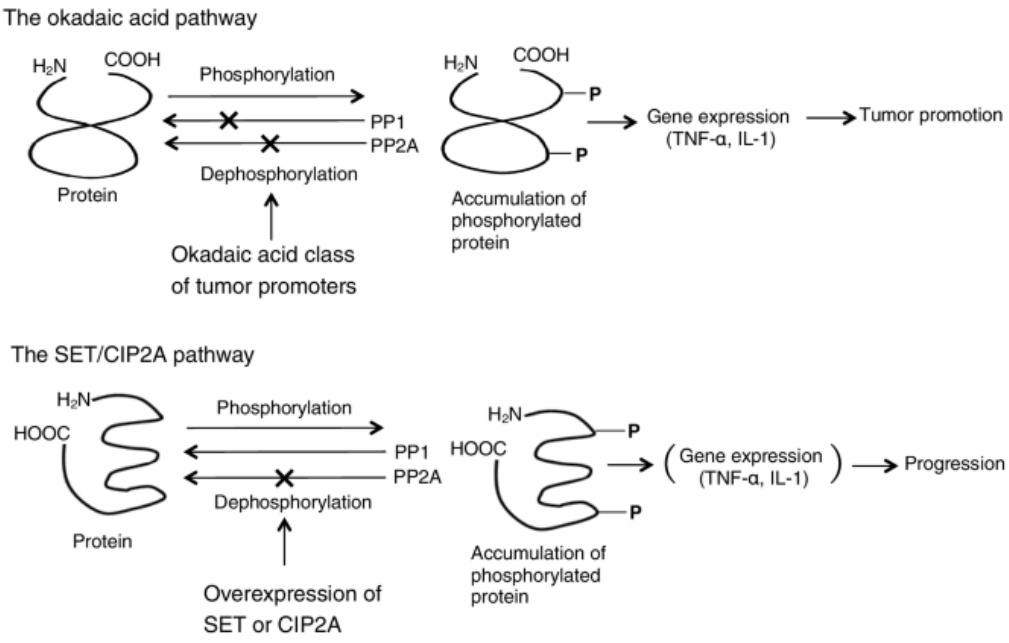


**Figure 1.7: A Schematic illustration of the okadaic acid pathway and the SET/CIP2A pathway for tumour promotion.** Abbreviations: TNF-α, Tumour Necrosis Factor alpha; IL-1, Interleukin-1; PP1, Protein Phosphatase 1; PP2A, Protein Phosphatase 2A [168].

#### 1.4.2.4.2 LB-100

LB-100 is part of a group of chemically modified cantharidins known to inhibit PP2A through direct binding to the enzyme [169]. Structurally, LB-100 (3-(4-methylpiperazine-1-carbonyl)-7-oxabicyclo heptane-2-carboxylic acid) is the first endothall-derived compound to progress into human clinical trials in patients with relapsed solid tumours (Figure 1.8) [170, 171].

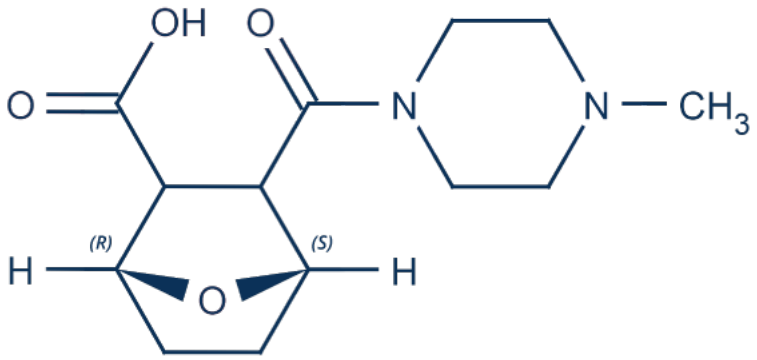


**Figure 1.8: Chemical structure of LB-100 [172].**

LB-100 is membrane-permeable and has shown good tolerability in animal models. It functions as a catalytic inhibitor of both PP2AC and PP5C. In cells, LB-100 inhibits PP2A within the concentration range from 0.85 to 3.9 µM, and PP5C at comparable or slightly higher concentrations[141]. Although LB-100 has growing clinical relevance, its reduced selectivity at pharmacologically relevant doses makes it less suitable as a targeted mechanistic probe in signalling studies compared to OA. For these reasons, LB-100 was discussed but not chosen as the primary reagent. Functionally, LB-100 enhances paracellular endothelial permeability by affecting VE-cadherin-mediated cell–cell adhesion**.** LB-100 may elevate phosphorylation of proteins involved in HIF-1α degradation, leading to reduced HIF-1α protein levels and diminished transcriptional activation of its downstream targets, such as ABCB1 [173]. Furthermore, LB-100 decrease DNA repair mechanisms and disrupts key proteins responsible for cell-cycle checkpoint regulation [171, 174]. It is known to trigger mitotic catastrophe, especially when used in combination with DNA-damaging agents [143]. LB-100 can enhance oncogenic signalling and activate cellular stress response pathways [175]. A study by Lu et al. revealed that combining LB-100 with doxorubicin led to premature mitotic entry and increased cell death in glioblastoma models [171]. Additionally, co-inhibition of PP2A by LB-100 and WEE1 kinase by adavosertib has shown high cytotoxicity in several cancer types, causing DNA replication stress**,** premature mitosis, and cell death [175]. Beyond its effects on cell division, LB-100 can counteract cancer cell senescence**,** promote progenitor cell differentiation**,** enhance drug delivery**,** and drive mitotic catastrophe and apoptosis [176].

### 1.4.2.5 Pharmacological Activators

PP2A plays a key role in numerous signalling pathways that are critical to the development and progression of cancer, and it is widely recognised as a tumour suppressor [177]. In many types of cancer, PP2A activity is reduced or lost. Notably, its dysfunction has been frequently documented in cancers such as colorectal, breast, oral squamous cell carcinoma, and acute myeloid leukaemia (AML) [178]. PP2A can be activated through various mechanisms, which has led to the classification of its activators as direct or indirectly acting [138]. Direct activators, like Small-Molecule Activators of PP2A (SMAPs), enhance PP2A activity by directly binding to the PP2A holoenzyme. On the other hand, indirect activators, such as FTY720, work by interacting with PP2A inhibitors like CIP2A or SET, thereby blocking these suppressors and indirectly promoting PP2A function. Both types of activators ultimately enhance PP2A activity, though the specific downstream signalling effects will vary depending on which PP2A holoenzyme complex is targeted [143, 179].

#### 1.4.2.5.1 SMAPs

Small-molecule activators of PP2A (SMAPs) were developed by modifying FDA-approved tricyclic neuroleptic drugs, specifically by replacing their basic amine groups with neutral polar functional groups [180]. These structural changes led to compounds capable of directly binding to the Aα subunit of the PP2A holoenzyme. Upon binding, SMAPs are believed to induce allosteric conformational changes that activate PP2A's phosphatase function, resulting in the dephosphorylation of key signalling molecules [181]. SMAPs can cross the blood-brain barrier after oral administration and have shown therapeutic potential across various cancers in both cell-based (*in vitro*) and animal (*in vivo*) studies, including in models resistant to standard therapy. For example, they induce apoptosis and suppress tumour growth in KRAS-driven transgenic and xenograft mouse models [182]. In addition to their anticancer activity, SMAPs have shown neuroprotective effects in Alzheimer's disease (AD) models, where they increase PP2A activity, reduced tau phosphorylation and Aβ40/42 levels, and preserved synaptic function and dendritic spine density in the hippocampus of HHcy-AD rats [183]. Furthermore, combining SMAPs such as DT-061 with the tyrosine kinase inhibitor afatinib has been shown to more effectively inhibit the PI3K signalling pathway by promoting degradation of the CIP2A, resulting in enhanced tumour suppression [184].

### 1.4.2.5.2 FTY720

Various drugs, chemicals, and peptides such as metformin [185], FTY720 [186], sodium selenate [187], COG1410 [188], and EHT [189] have been investigated in Alzheimer's disease models for their ability to activate PP2A, though they do so through indirect mechanisms [190]. Among them, FTY720 (fingolimod, Figure 1.9) is a well-known indirect PP2A activator. It is a sphingosine-based immunosuppressant that was approved by the FDA for treating relapsing multiple sclerosis [191]. FTY720 is the first agent of a novel class of sphingosine-1-phosphate (S1P) receptor agonists.

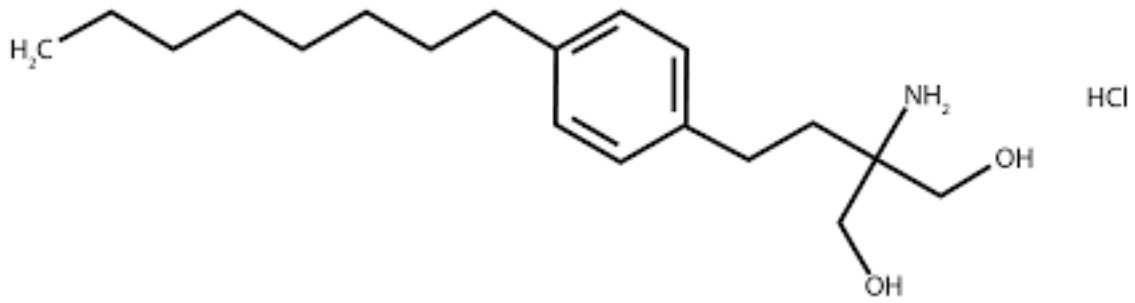


**Figure 1.9: Chemical structure of FTY720 [192].**

Originally derived from ISP-I (myriocin) a natural product isolated from *Isaria sinclairii*, a parasitic fungus, FTY720 was chemically modified to enhance its immunosuppressive potency while reducing toxicity [193, 194]. Once inside the body, FTY720 is phosphorylated to form FTY720-P, a biologically active metabolite that acts as a non-selective agonist for four out of five S1P receptors. FTY720 activates PP2A by disrupting the interaction between PP2Ac and its endogenous inhibitor SET, specifically binding to amino acids 177–277 at the C-terminus of SET. This prevents SET from inhibiting PP2A, thereby restoring its phosphatase activity. This mechanism has shown promise in cancer models, where PP2A reactivation by FTY720 contributes to tumour suppression. In addition to its anticancer potential, FTY720 also shows neuroprotective effects. It reduces neuroinflammation and demyelination by limiting the migration of autoreactive lymphocytes into the central nervous system, thus protecting neurons from immune-mediated damage. Furthermore, FTY720 has exhibited antifungal activity against *Candida albicans* in both *in vitro* studies and mouse models of candidiasis. In addition, FTY720 is particularly effective in autoimmune conditions by preventing excessive immune cell infiltration [195].

## 1.5 Protein Trafficking and Degradation

Intracellular membrane trafficking is a fundamental cellular process that mediates the transport of materials among various organelles. This system is particularly critical in neurons, where protein trafficking underpins essential functions such as neuronal survival, neurite outgrowth, structural remodelling, and synaptic maintenance [196]. The molecular machinery governing intracellular transport is highly intricate, comprising a multitude of regulators that coordinate discrete trafficking events. Disruptions in these processes have been increasingly implicated in human disease [197].

A prominent pathological feature of many neurodegenerative disorders is the aberrant accumulation of misfolded proteins. Intracellular trafficking systems contribute significantly to both the accumulation and clearance of these misfolded species, influencing disease progression. Cellular protein homeostasis is tightly regulated through a balance of synthesis and degradation. Protein half-lives vary widely, ranging from minutes to several days, and these differences in degradation kinetics are vital for cellular regulation and function [198]. Protein degradation predominantly occurs through lysosomal and proteasomal pathways [199], which are mediated by two principal systems: lysosomal proteolysis and the ubiquitin-proteasome pathway (UPP) [200]. Among these, the UPP represents the major mechanism for intracellular protein turnover across diverse tissue types. Despite their functional distinctions, the lysosomal and proteasomal systems exhibit a degree of interconnectivity and coordination [201].

Within the over-arching theme of protein trafficking and degradation, endocytosis plays a pivotal role. It facilitates the internalization and subsequent degradation of a multitude of membrane proteins including cell adhesion molecules, such as the cadherins. Reduced cadherin abundance, driven by endocytosis, is associated with pathological conditions including tumour metastasis [202] and affects endothelial cell behaviour, including migration and vascular permeability [72]. For example, in Kaposi sarcoma, cadherin endocytosis contributes to the disruption of endothelial barrier integrity [203], while certain viruses exploit internalisation of VE-cadherin to facilitate host cell entry [204]. Endocytosis can occur through multiple mechanisms, including both clathrin-dependent pathways and clathrin-independent pathways [205] which include caveolin-dependent endocytosis [206].

### 1.5.1 Clathrin-Mediated Endocytosis

Clathrin-mediated endocytosis is an essential process in vesicular trafficking, enabling the transport of various cargo molecules from the cell surface into the interior. First characterised

over fifty years ago, this mechanism has since led to the identification of more than 50 proteins that are integral to the molecular machinery responsible for the formation of clathrin-coated endocytic vesicles [207]. Clathrin-mediated endocytosis mechanism (Figure 1.10) is initiated by proteins involved in nucleation (Step 1), including FCH and mu domain containing endocytic adaptor 1/2 (FCHO1,2), Intersectin1 (ITSN1), and Epidermal growth factor receptor substrate 15 (EPS15). These proteins cluster bind to the plasma membrane to initiate membrane curvature and recruit other proteins, such as the Adaptor protein 2 complex (AP-2), for cargo selection (Step 2). Clathrin is also recruited by AP-2, which then begins the clathrin coat assembly (Step 3) of the endosome and curves the membrane further, forming the vesicle around the clustered cargo. The vesicle then undergoes scission from the membrane (Step 4) by recruitment of Dynamin via the BAR-domain containing proteins. Uncoating of clathrin (Step 5) is subsequently initiated by Auxilin of G-associated kinase (GAK), which recruits ATPase HSC70 to disassemble the clathrin coat, allowing the machinery to be available for the next endocytosis event [208-210].

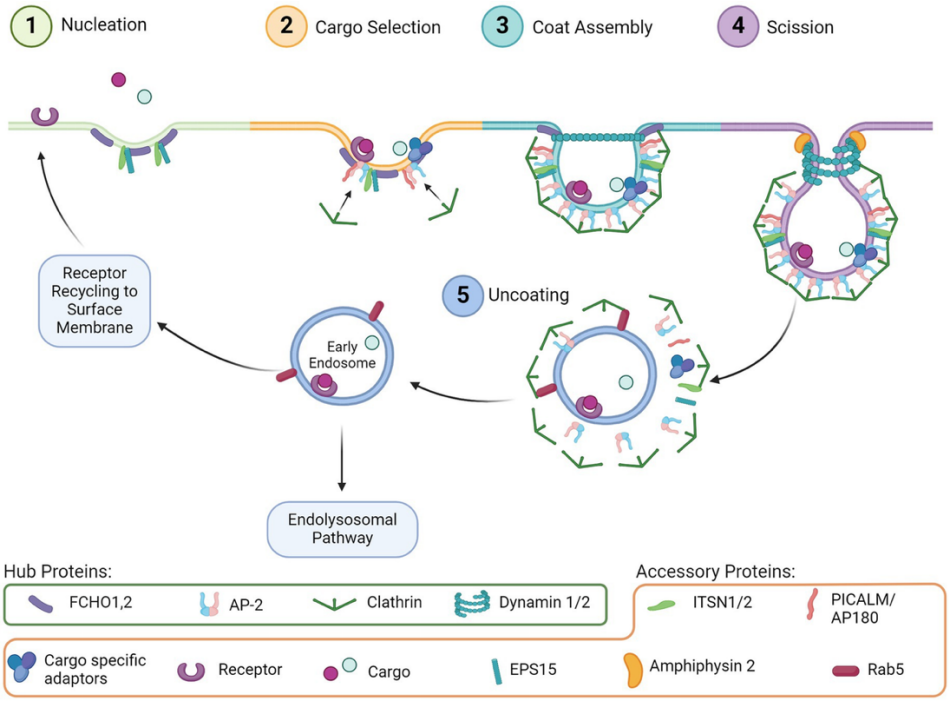


**Figure 1.10: Schematic overview of the clathrin-mediated endocytosis process.** (1) Nucleation: The membrane begins to indent slightly as structural proteins gather at the site. (2) Cargo Selection: Receptors and adaptor proteins link the forming vesicle with specific cargo molecules, while also initiating clathrin recruitment. (3) Coat Formation**:** Clathrin assembles into a lattice structure around the growing vesicle. (4) Scission: Dynamin wraps around the vesicle's neck and, aided by accessory proteins, helps separate the vesicle from the cell membrane. (5) Uncoating**:** The clathrin coat is removed, allowing the vesicle, now an early endosome follow various intracellular pathways, such as returning to the membrane or entering the endolysosomal system [211].

Clathrin-mediated endocytosis generates small (60–120 nm) membrane vesicles that carry a range of cargo, primarily transmembrane proteins and their extracellular ligands, from the plasma membrane of eukaryotic cells into the cytoplasm. These cargo molecules have numerous physiological functions, including nutrient absorption, cellular signalling, developmental regulation via morphogens, and cell adhesion. In neurons, dysregulated clathrin-mediated endocytosis contributes to synaptic dysfunction, amyloid beta (Aβ) processing, and Tau pathology, highlighting its involvement in early Alzheimer's disease pathogenesis. Furthermore, clathrin-mediated endocytosis alterations extend to non-neuronal cell types, including astrocytes and microglia, which play crucial roles in Aβ clearance and neuroinflammation [211].

### 1.5.2 Clathrin -Independent Endocytosis

Clathrin-independent endocytosis facilitates the internalisation of a variety of external ligands, receptors, and pathogens, including several harmful bacterial toxins and viruses [212]. Also known as non-clathrin endocytosis, clathrin-independent endocytosis occurs alongside clathrin-mediated endocytosis and has been observed in numerous *in vitro* cell lines as well as *in vivo* in mice, flies, worms, plants, and yeast. The functions of clathrin-independent endocytosis include the uptake of bulk extracellular proteins and lipids, the removal of activated receptors from the plasma membrane, and the regulation of cellular processes such as spreading, polarisation, and migration. Clathrin-independent endocytosis is also implicated in several diseases, including cancer, lysosomal storage disorders, and atherosclerosis [213]. Several studies have categorised clathrin-independent endocytosis pathways into two types: those that depend on dynamin for membrane scission (dynamin-dependent) and those that utilise other mechanisms (dynamin-independent) [214, 215]. Dynamin, a GTPase enzyme, is essential for the membrane fission step during endocytosis. Caveolae-mediated endocytosis is one of the pathways that falls under the dynamin-dependent category [216].

#### 1.5.2.1 Caveolae-Mediated Endocytosis

Caveolae are flask-shaped invaginations of the plasma membrane that facilitate both endocytosis and transcytosis of various plasma macromolecules, including albumin, insulin, and low-density lipoprotein, as well as certain pathogens such as viruses, bacteria, and their associated toxins [217]. These membrane structures, typically measuring 60–80 nanometres in diameter, were first characterised in the 1950s through electron microscopy [218]. Caveolae are widely distributed across multiple tissues and cell types, including smooth muscle cells, fibroblasts, endothelial cells, macrophages, and adipocytes [219]. Beyond their role in molecular transport, caveolae are implicated in diverse cellular processes, such as signal transduction, lipid metabolism, and vesicular trafficking [220-223].

Caveolae are specialised plasma membrane invaginations formed through the oligomerisation of caveolins, a family of integral membrane proteins with high affinity for membrane cholesterol. There are three caveolin subtypes: caveolin-1, caveolin-2, and caveolin-3. Caveolin-1 and caveolin-2 are primarily involved in caveolae biogenesis in non-muscle cells, whereas caveolin-3 is specific to muscle cells [224]. These proteins collaboratively facilitate the formation and structural maintenance of the characteristic flask-shaped caveolae [225]. Proper assembly of caveolae additionally requires cavin-1 [226-228], while cavin-2, cavin-3, and cavin-4 serve modulatory functions, contributing to the stabilisation and preservation of

caveolar architecture and function [229-231]. Beyond caveolins and cavins, accessory proteins such as Pacsin2 [232, 233] and EHD2 [234] localise to the caveolar neck region, where they further enhance the stability of caveolae at the cell surface [234-236]. The lipid composition of caveolae is also distinctive, enriched with cholesterol, sphingomyelin, and ceramides [237, 238]. During caveolar endocytosis (Figure 1.11), caveolae can pinch off from the plasma membrane and transport their contents to early endosomes or the Golgi apparatus. Notably, caveolae are also capable of dynamic recycling, repeatedly internalising and re-fusing with the plasma membrane without necessarily completing the endocytic process [239].

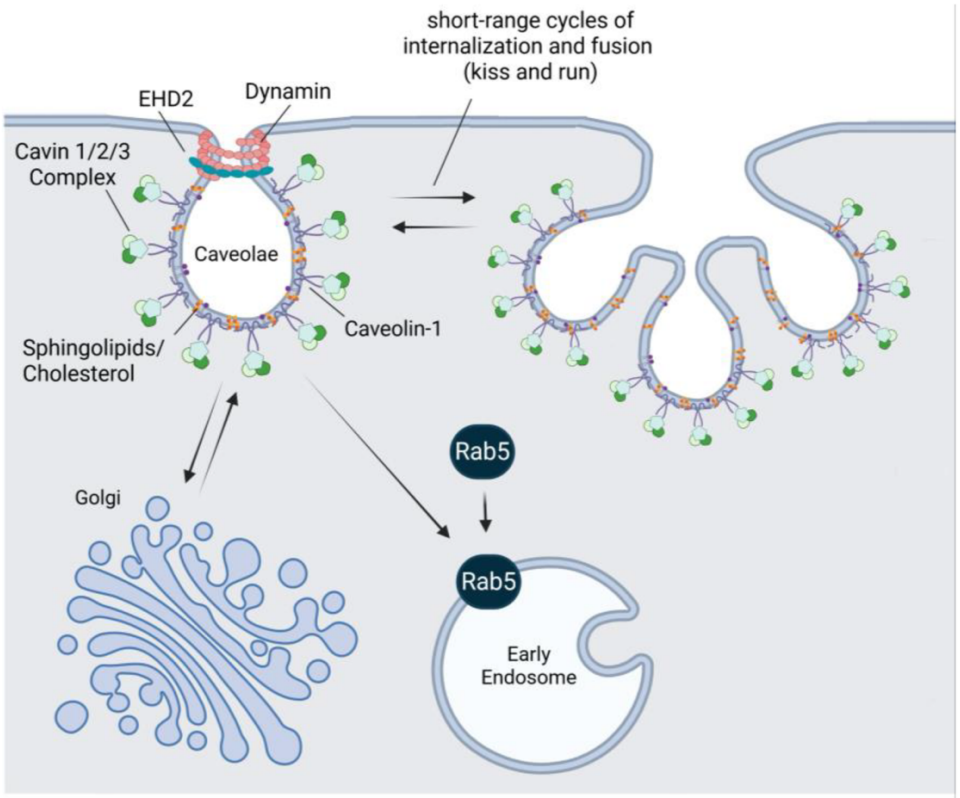


**Figure 1.11: Schematic representation of caveolae-mediated endocytosis [239].**

The internalisation of caveolae is initiated upon binding to specific ligands, triggering a tightly regulated sequence of molecular events. The budding and fission of caveolae from the plasma membrane are modulated by various kinases and phosphatases, notably members of the Src-family tyrosine kinases [217, 240, 241]. A critical step in this process is the phosphorylation of caveolin-1, which facilitates the onset of caveolar membrane scission and internalisation [217]. Detachment of caveolae from the plasma membrane marks the beginning of endocytosis, a step that is mechanistically driven by dynamin-2. This GTPase mediates membrane fission through GTP hydrolysis, supplying the energy required for vesicle release [242, 243]. Accordingly, caveolae-mediated endocytosis is traditionally categorised as a dynamin-dependent pathway.

Genetic ablation of caveolin-1 results in the complete absence of caveolae [244], underscoring its indispensable role in caveolar biogenesis and structural integrity [245].

### 1.5.3 Rab Proteins

Rab proteins, a subfamily within the Ras superfamily of small GTPases, are relatively small proteins that are localised throughout the cytosolic vesicular transport system [246]. The functional characterization of Rab GTPases originated from studies in the yeast *Saccharomyces cerevisiae*, where Novick and colleagues identified several secretion-related genes, designated as SEC (e.g., SEC1, SEC2)[247]. Subsequent research by Gallwitz's group led to the identification of Ras-related YPT1 genes in yeast [248]. It was later discovered that both SEC4 and YPT1 genes encode small GTP-binding proteins that are structurally and functionally homologous, which facilitated the cloning of Rab proteins from a rat brain cDNA library [249].

Rab proteins are universally expressed in eukaryotic cells; some are highly conserved and play fundamental roles in vesicular trafficking, while others are more specialized and restricted to specific cell types in humans [250, 251]. These proteins function as monomers and exhibit sequence homology among family members ranging from 35% to 80% [252]. There are more than 60 distinct proteins in humans, which constitute 41 functional subfamilies with tissue specificity[253]. Ten subfamilies - Rab1, Rab3, Rab4, Rab5, Rab6, Rab8, Rab11, Rab22, Rab27 and Rab40 have also been defined based on distinct subfamily-specific sequence motifs, however, a number of Rab proteins cannot be grouped into these subfamilies [254, 255] (Figure 1.12).

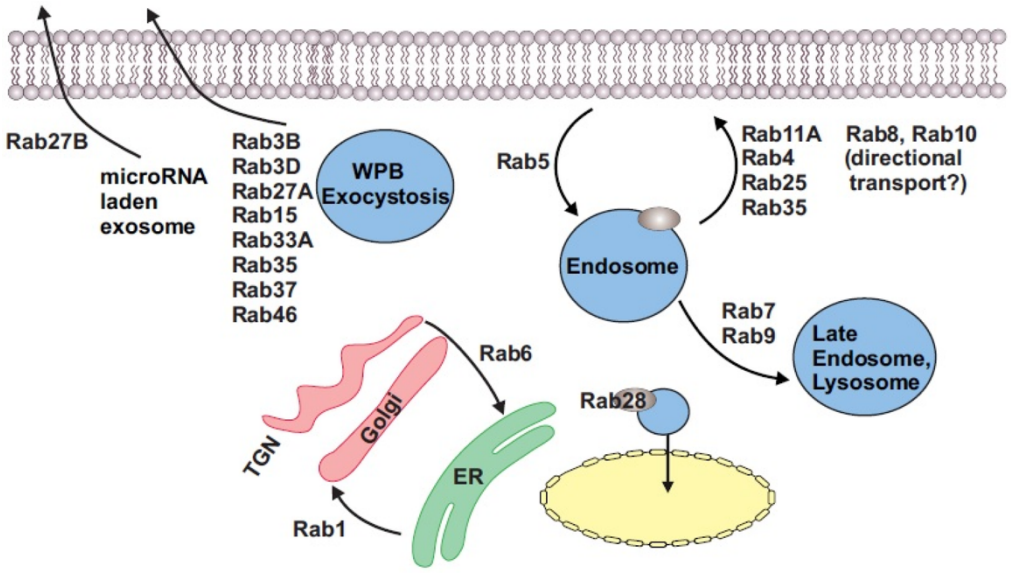


**Figure 1.12: Rab GTPases and their role in endocytic trafficking in endothelial cells.** Abbreviations: WPB, Weibel–Palade Body; TGN, Trans-Golgi Network; ER, Endoplasmic Reticulum**;** Golgi, Golgi Apparatus [256].

Comprising approximately 200 amino acids, Rab proteins possess five conserved motifs essential for GTP binding and hydrolysis. Rab GTPases function as molecular switches that alternate between an active GTP-bound state and an inactive GDP-bound state [246]. In their active form, GTP-bound Rab proteins are associated with the plasma membrane, whereas the GDP-bound inactive form is typically localised in the cytoplasm. The interconversion between these two states is tightly regulated by three key proteins: GDP dissociation inhibitor (GDI), guanine nucleotide exchange factor (GEF), and GTPase-activating protein (GAP). As illustrated in Figure 1.13, GDI acts as a cytosolic regulator, controlling the membrane association and dissociation of Rab GTPases. Upon release from GDI, Rab proteins are activated through the action of GEF, which facilitates the exchange of GDP for GTP. Once activated, Rab-GTP engages with downstream effectors to mediate its cellular functions. Inactivation occurs when GAP catalyses the hydrolysis of GTP to GDP, thereby converting Rab back to its inactive state. GDI then binds to the inactive Rab-GDP, forming a complex that prevents further interaction with effectors and promotes the redistribution of Rab to the cytoplasm, where it can re-enter the activation cycle [257, 258].

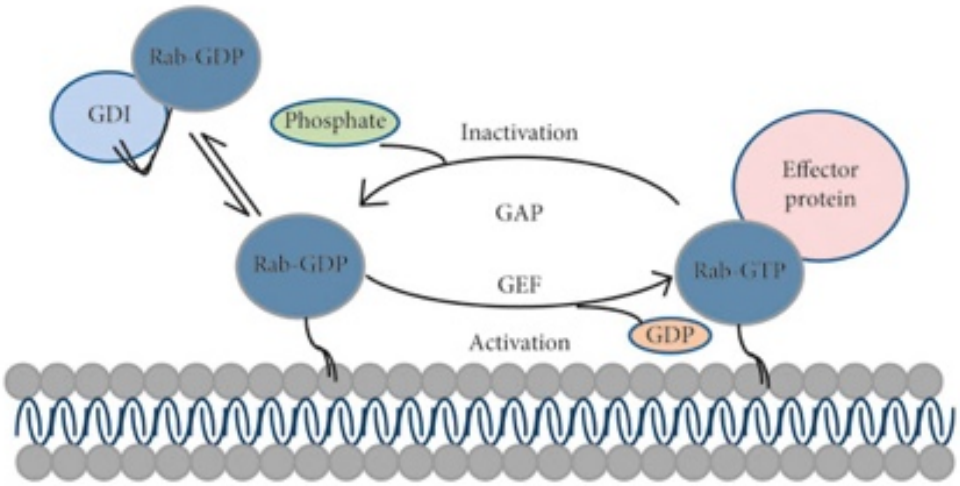


**Figure 1.13: The functional regulation of Rab proteins involves their dynamic transition between active and inactive states [259].**

Rab proteins are associated with specific cellular trafficking pathways. Notably, Rab proteins have been implicated in the regulation of tight junction (TJ) protein trafficking and assembly. For instance, Rab-dependent transport of claudins has been shown to contribute to TJ formation [260]. Furthermore, Rab GTPases, particularly Rab5, are involved in the endocytic trafficking of clathrin-coated vesicles across the blood-brain barrier (BBB) during endothelial transcytosis [261]. Importantly, dysregulated Rab5 activity has been observed in post-mortem brain tissue from Alzheimer's disease (AD) patients and in murine models of AD, suggesting a potential role in the pathogenesis of the disease [262].

### 1.5.3.1 Rab5

Rab5, a well-characterised member of the Ras-related brain (Rab) protein family, is a small GTPase within the Ras superfamily that plays a pivotal role in the regulation of intracellular membrane trafficking. Its functions encompass key processes such as vesicle formation, membrane fusion, endosomal maturation, and receptor-mediated endocytosis [253, 263]. Functionally, Rab5 alternates between an inactive GDP-bound state located in the cytosol and an active GTP-bound state associated with the plasma membrane (Figure 1.14) [264-268].

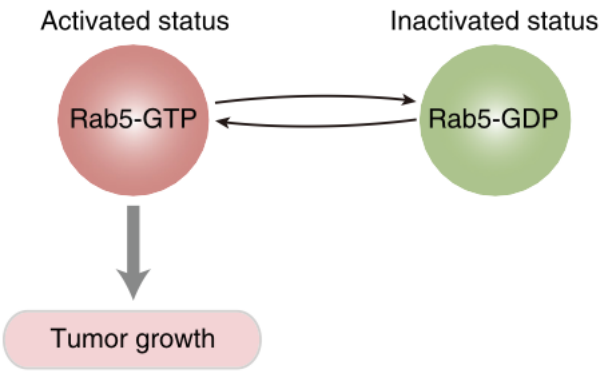


**Figure 1.14: Rab5 exerts its biological function by switching GDP- and GTP-bound states, where Rab5-GTP promotes tumorigenesis [269].**

Structurally, Rab5 adopts a nearly spherical conformation, featuring β-sheets and α-helices at the N-terminal region, while the C-terminus includes a -CCXX motif and a phosphate-binding loop (p-loop). The -CCXX motif undergoes prenylation, a post-translational modification essential for Rab5's association with cellular membranes. The p-loop, critical for GTP binding and hydrolysis, comprises three functionally distinct regions: residues 27–34 facilitate GTP hydrolysis and nucleotide exchange, residues 49–51 form the switch I region, and residues 79–81 constitute switch II [270].

Rab5 is expressed in three isoforms Rab5A, Rab5B, and Rab5C which exhibit a high degree of sequence similarity, sharing more than 80% sequence identity [271, 272]. Among the Rab5 isoforms, Rab5A is the most extensively studied and is often simply referred to as Rab5 in the literature due to its functional prominence [273]. These isoforms are stably anchored to cellular membranes through C-terminal geranyl-geranyl lipid modifications [274]. Notably, all three isoforms possess a conserved phosphorylation consensus motif at amino acid position 123, which is potentially recognized by proline-directed serine/threonine kinases [272]. Among the Rab5 isoforms, Rab5A is particularly significant due to its central role in the endocytic pathway, where it facilitates the internalization of plasma membrane proteins and their subsequent recycling to the cell surface. It is critically involved in the trafficking of G protein-coupled receptors (GPCRs) and contributes to the regulation of junctional protein localization [260, 275-278].

Rab5 proteins are essential for preserving cellular homeostasis through their interaction with a variety of effector molecules, including those containing phosphotyrosine-binding (PTB) domains, leucine zipper motifs [279], early endosome antigen 1 (EEA1), Rabaptin-5/Rabex-5 complexes, and phosphatidylinositol 3-kinases (PI3K) [280]. These effectors preferentially associate with the GTP-bound active form of Rab5, thereby facilitating the docking and fusion of early endosomes [281]. In addition to its central role in endocytic trafficking, Rab5 also participates in a range of other cellular functions, including cell adhesion, migration, mitotic progression, and autophagy [282-285]. Furthermore, Rab5 is implicated in the regulation of myoblast differentiation by modulating the IRS1–IGF–AKT–mTOR signalling cascade during skeletal muscle regeneration [183]. Rab5 contributes to cellular motility by promoting focal adhesion kinase (FAK)-dependent signalling, a mechanism essential for the regulation of cell migration [284]. Additionally, Rab5 influences primary pancreatic cancer cell morphology by suppressing E-cadherin expression, leading to a transition from a spindle-shaped to a rounded cellular form. This morphological shift facilitates enhanced proliferation, invasion, and migratory capacity in pancreatic cancer cells [286]. The involvement of Rab5 in oncogenesis has been widely investigated, with elevated Rab5 expression reported in various human cancers, including breast and pancreatic malignancies. Such overexpression is frequently correlated with tumour progression and unfavourable clinical outcomes (Figure 11) [286, 287].

#### 1.5.3.1.1 RAB5A

Rab5A is a 22-kDa protein consisting of 215 amino acids, encoded on chromosome 3p24.3 [273], and is broadly expressed across a wide range of tissues [288]. Functionally, Rab5A plays a key regulatory role in endocytosis, acting as a rate-limiting factor in homotypic early endosome fusion [265, 266]. Rab5A specifically governs early endosome fusion during endocytosis [265, 266, 289] and contributes to the regulation of vesicle budding events [288]. In epithelial cells, calcium depletion triggers rapid clathrin-mediated internalisation of several junctional proteins such as JAM-A, occludin, ZO-1, E-cadherin, and β-catenin, which are subsequently found to colocalise with Rab5A-positive endosomes [205]. In endothelial cells, Rab5A similarly influences the spatial redistribution of tight junction components, including JAM-A and claudin-1 [260, 277]. Moreover, Rab5A has been identified as a key regulator of Toll-like receptor 4 (TLR4) and epidermal growth factor receptor (EGFR) trafficking, mediating their endocytic recycling in response to lipopolysaccharide (LPS) stimulation [290].

### 1.5.3.2 Rab11

Rab11 proteins are critical regulators of membrane protein trafficking, particularly in maintaining receptor surface expression and mediating transport from the endosomal recycling compartment (ERC) to the plasma membrane [291, 292]. The Rab11 subfamily, consisting of Rab11A, Rab11B, and Rab25 [293], plays a crucial role in the recycling of proteins from endosomes to the plasma membrane, particularly in polarised epithelial cells [294-296]. While Rab11A is expressed ubiquitously [297], Rab11B is predominantly found in the brain, heart, and testis [298] , and Rab25 expression is limited to epithelial cells [293]. Rab11A and Rab11B exhibit 89% amino acid sequence homology, with the most significant differences found in their membrane-binding, hypervariable C-terminal domains [298]. Despite their high sequence similarity and shared localisation to the pericentriolar apical regions, Rab11A and Rab11B appear to target distinct vesicle populations. Rab11a, the first identified and most well-characterised member of this subfamily [292] , is widely expressed and extensively studied within the Rab11 family [299].

Predominantly localised to the trans-Golgi network, recycling endosomes, and post-Golgi vesicles, Rab11 GTPases play essential roles in diverse cellular processes such as cytokinesis, ciliogenesis, oogenesis, and neuritogenesis [300-303]. Functioning through a GTP/GDP-dependent molecular switch, Rab11 directs the recycling of endocytosed cargo and ensures bidirectional endosomal transport, thereby regulating key vesicular trafficking pathways [253, 304]. The Rab11 family exhibits species-specific diversity, with varying numbers of members across yeast, *Drosophila melanogaster, Caenorhabditis elegans,* and *Arabidopsis thaliana* [254, 305, 306]. The activity of Rab11 is tightly regulated by guanine exchange factors (GEFs) and GTPase-activating proteins (GAPs), which modulate its function by controlling GTP/GDP exchange and intrinsic GTPase activity, respectively [307].

Rab11 executes its functions through interactions with a variety of effector proteins. A key group of these effectors, known as Rab11-family interacting proteins (Rab11-FIPs), possesses a Rab-binding domain (RBD) and mediates GTP-dependent interactions with Rab GTPases. These proteins play a critical role in facilitating Rab11-dependent vesicle recycling [308]. Rab11-FIPs are essential for neuronal transcytosis, as they transport proteins from the somatodendritic membrane to the axonal surface. Additionally, Rab11-FIPs link Rab11 to cytoskeletal elements and are responsible for directing vesicular movement along the recycling pathway. The Rab11-FIP family consists of five members (FIP1-5), each characterised by a conserved carboxyl-terminal Rab11-binding domain (BD) [308].

Rab11 plays a vital role in regulating vesicular transport, functions that are essential in highly polarised neuronal cells [303, 309]. It is particularly important for recycling membrane proteins, including receptors critical for signal transduction and neuronal function [307]. Additionally, Rab11 facilitates the trafficking of growth factors necessary for neuronal development, differentiation, and repair. Rab11 is fundamentally involved in preserving neuronal polarity and overseeing vesicular trafficking processes within neurons, which exhibit a high degree of cellular polarisation [388, 395]. Furthermore, Rab11 contributes to the intracellular transport of growth factors essential for neuronal growth, differentiation, and repair mechanisms. Experimental evidence indicates that Rab11 overexpression markedly enhances vesicle trafficking, whereas its reduced expression has been associated with the pathology of various neurodegenerative disorders [307]. In polarised epithelial cells, Rab11 has been observed to localise predominantly within pericentriolar endosomal compartments [310]. A recent study highlighted the dynamic distribution of Rab11 within neuronal cells, where it facilitates the precise delivery of proteins essential for neuronal development [311]. Rab11-dependent trafficking pathways are critical for neuronal migration, a fundamental process in the formation of the mammalian brain. *In vivo* experiments utilising in utero electroporation have demonstrated that disruption of Rab11-mediated endocytic pathways impairs neuronal migration during cerebral cortex development [312].

#### 1.5.3.2.1 Rab11A

Rab11A is a key small GTPase involved in vesicular trafficking and membrane dynamics, processes whose dysregulation has been implicated in tumorigenesis [313]. Rab11A plays a pivotal role in mitotic spindle organisation and orientation, as well as in the recycling of endosomes to the plasma membrane [314, 315]. As the first identified member of the Rab GTPase family, Rab11A is essential for establishing cellular polarity during collective cell migration [316].

Rab11A undergoes multiple posttranslational modifications that are critical for its function. Among these, the prenylation of C-terminal cysteine residues by the addition of geranylgeranyl groups enhances the protein's hydrophobicity, thereby facilitating its membrane association [317]. This lipid modification is catalysed by geranylgeranyl transferase. Notably, the β2-adrenergic receptor (β2AR), a transmembrane protein, has been shown to interact with the α-subunit of geranylgeranyl transferase, thereby modulating the prenylation process in HEK293 cells [318]. In addition to prenylation, Rab11A is subject to ubiquitination, which regulates its proteasomal degradation [313, 319]. This ubiquitination is mediated by the β2AR/HACE1

complex in HEK293 cells [320]. Furthermore, Rab11A activity is regulated through phosphorylation, as well as through its dynamic cycling between GTP-bound and GDP-bound states, which is essential for its role in intracellular trafficking [206, 321].

In polarized epithelial cells, Rab11A localizes to the pericentriolar, microtubule-associated apical recycling endosomes [298, 308] where it regulates the recycling and apical insertion of membrane proteins into the plasma membrane [296]. In epithelial morphogenesis, active Rab11A is essential for E-cadherin trafficking and lumen formation, as it directs E-cadherin to cell–cell junctions. Conversely, inactive Rab11A fails to mediate E-cadherin recycling to the membrane [322, 323]. Rab11A is also crucial in endothelial cells, where its depletion markedly impairs the restoration of adherens junction (AJ) integrity and endothelial barrier function [324]. In murine models of lung vascular injury induced by endotoxemia and polymicrobial sepsis through caecal ligation and puncture (CLP) Rab11A deficiency results in sustained vascular leakage. These findings suggest that Rab11a-mediated recycling of VE-cadherin is essential for maintaining and restoring vascular endothelial barrier integrity via the proper assembly of VE-cadherin at intercellular junctions [324]. Previous research has demonstrated its critical role in cancer progression, primarily through modulation of growth factor signalling pathways [325, 326]. Notably, RAB11A enhances the proliferation and motility of oesophageal cancer cells via activation of WNT signalling [327]. It is also overexpressed in colorectal cancer, where it downregulates E-cadherin expression, thereby promoting epithelial-mesenchymal transition (EMT) [328].

### 1.5.4 Ubiquitin-Proteasome Pathway

The ubiquitin-proteasome pathway is crucial for the regulation of protein homeostasis and trafficking [329]. Proteasomes, which are abundant and stable enzyme complexes found in most cell types, are integral components of this pathway [330-333]. Proteasomes play a critical role in cellular protein quality control by degrading damaged, misfolded, or superfluous proteins, particularly short-lived and soluble misfolded proteins, through the ubiquitin-proteasome system (UPS) [334-336]. Proteins targeted for degradation by proteasomes are typically marked by polyubiquitination. These polyubiquitinated proteins are then processed in the proteasome core, where they are cleaved by internal protease activities into short peptides [337].

Ubiquitination, or ubiquitylation, is a post-translational modification (PTM) in which a ubiquitin molecule is attached to a target protein. This process has diverse roles, including

regulating protein degradation, determining subcellular localisation, and activating kinases. Ubiquitination occurs through a three-step process involving three enzymes: ubiquitin-activating enzyme (E1), ubiquitin-conjugating enzyme (E2), and ubiquitin-protein ligase (E3) [338]. Ubiquitin is a 76-amino acid protein that exists in either its free form or conjugated to a protein as a single ubiquitin (monoubiquitination) or a chain of ubiquitins (polyubiquitination) [329]. The 76-residue ubiquitin protein is attached to target proteins via a lysine isopeptide bond [339, 340]. E1 binds to ubiquitin in an ATP-dependent manner and transfers it to E2, which then interacts with E3 to catalyse the transfer of the ubiquitin molecule from E2 to the substrate [341]. The repeated action of these enzymes results in the polyubiquitination of the substrate [342], and the polyubiquitin chain that forms subsequently directs the protein for degradation by the proteasome (Figure 1.15) [343, 344].

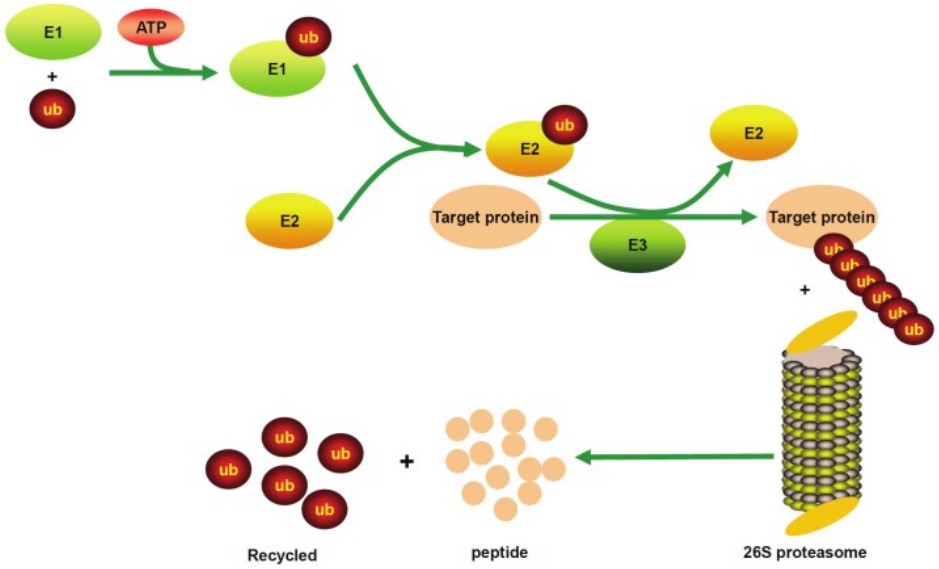


**Figure 1.15: Ubiquitin proteasome system (UPS).** Abbreviations: E1, ubiquitin-activating enzyme; E2, ubiquitin-conjugating enzyme; E3, ubiquitin-protein ligase; E4, chain elongation factor Ub; Ubiquitin [345].

The 26S proteasome is a multiprotein complex consisting of a 20S catalytic core and two 19S regulatory subunits attached to each end of the 20S core. The enzyme has a cylindrical shape and is composed of 28 subunits. 26S proteasome requires ATP hydrolysis, indicating that the 26S proteasome is a eukaryotic ATP-dependent protease [346, 347]. The 19S subunits recognise and bind the polyubiquitin chain, facilitating its cleavage from the target protein. The protein is then translocated into the 20S core, where it undergoes degradation into small oligopeptides, typically consisting of fewer than 25 amino acids [348]. The 20S proteasome is composed of four stacked heptameric rings, organised in an α (1–7): β (1–7): β (1–7): α (1–7)

configuration. The α subunits, located at both termini of the barrel-shaped structure, function as gating mechanisms that regulate substrate access. In contrast, the β subunits situated within the inner rings possess catalytic activity, facilitating the proteolytic degradation of substrates within the core of the complex (Figure 1.16) [349].

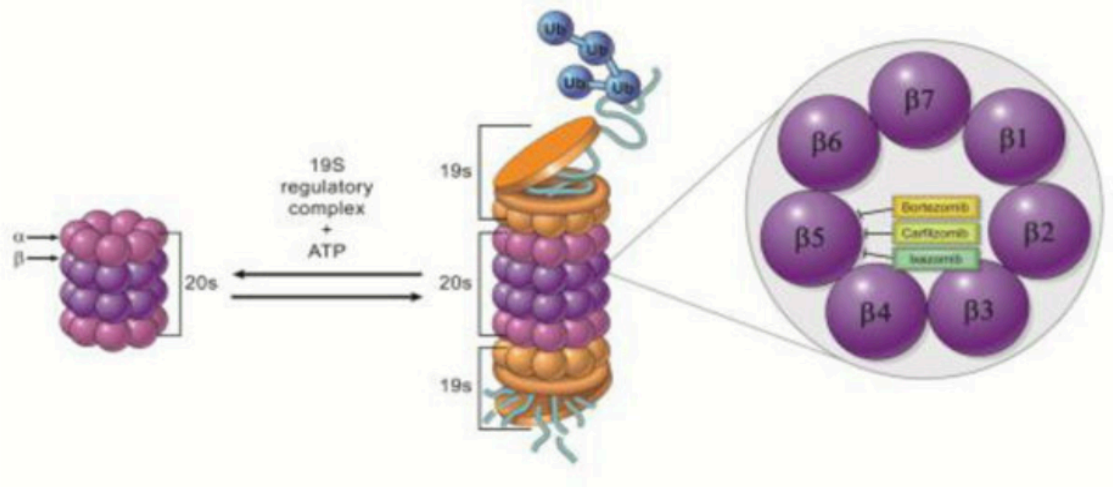


**Figure 1.16: A diagrammatic representation of the structure of the 26S Proteasome [348].**

### 1.5.4.1 Proteosome Inhibitors

Proteasome inhibitors (PIs) are inhibitors that target the cellular mechanisms of protein degradation by inhibiting the β proteolytic subunits of the 20S proteasome [348]. The first synthetic proteasome inhibitor was designed with a peptide backbone containing an aldehyde at the C-terminus, allowing for a reversible interaction with the active site threonine. A modified version, ZLLLal, exhibited increased activity and enhanced cellular permeability, and was later renamed MG-132, which remains a widely used research tool to study proteasomal inhibition [350].

MG-132, a peptide-aldehyde proteasome inhibitor (carbobenzoxyl-L-leucyl-L-leucyl-L-leucinal) (Figure 1.17), is derived from a natural triterpene found in a Chinese medicinal plant called Tripterygium wilfordii. MG132 functions by covalently binding to the active site of the β-subunits of the 20S proteasome, effectively inhibiting the proteolytic activity of the 26S proteasome complex [351]. This targeted inhibition of the ubiquitin-proteasome system has been shown to produce several significant biological effects. For instance, studies have demonstrated that MG132 treatment increases the percentage of proliferating neurons, suggesting a role in promoting neurogenesis or neuronal survival [352]. Additionally, MG132 has been found to attenuate hyperpermeability induced by the recombinant VE-cadherin

cytoplasmic domain (rVE-cad CPD) and protect adherens junctions in cell monolayers, indicating its potential in maintaining endothelial barrier integrity [353]. Another study has shown that acute inhibition of the ubiquitin-proteasome system in neurons leads to an increased recycling pool of vesicles [354]. Numerous studies have indicated that MG132 exhibits neuroprotective properties by mitigating oxidative stress, excitotoxicity, and neurite degeneration [355-359]. Proteasome inhibitors have demonstrated therapeutic efficacy in the management of hematologic malignancies, including multiple myeloma and mantle cell lymphoma, by contributing to improvements in progression-free survival and overall survival [348]. Additionally, evidence suggests that the internalisation of VE-cadherin can be inhibited by the proteasome inhibitor MG132 [360].

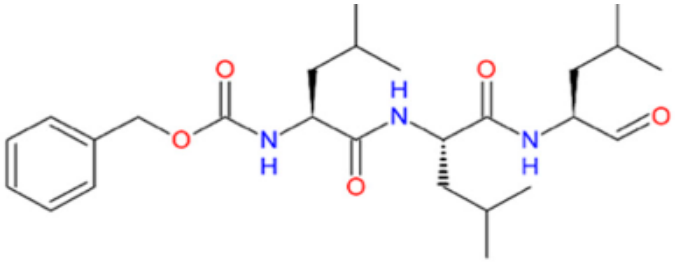


**Figure 1.17: Chemical structure of MG132 [361].**

#### 1.5.4.1.1 Lysosome

Lysosomes are membrane-enclosed organelles that are integral to cellular proteostasis, primarily through the degradation of misfolded and aggregated proteins [337]. They are also responsible for the breakdown of long-lived proteins, insoluble aggregates, damaged organelles, macromolecular complexes, and certain intracellular pathogens [362, 363]. Lysosomes containing a range of acid hydrolases that facilitate the catabolism of biopolymers and various biomolecules. Although present in all eukaryotic cells, their morphology and abundance differ according to cell type and functional status [364]. In addition to serving as cellular recycling centres through mechanisms such as autophagy and micropinocytosis, lysosomes also participate in key signalling pathways, including mTOR and AMPK, highlighting their broader regulatory roles in cell physiology [365].

Lysosomes are highly dynamic organelles that function as terminal degradative compartments, processing macromolecules delivered through secretory, endocytic, autophagic, and phagocytic membrane trafficking pathways [366]. During endocytosis, cell surface proteins are transported to the endosome, where they can either be degraded by lysosomes or recycled to the plasma membrane or other organelles. In the phagocytic pathway, cells engulf large extracellular particles, such as pathogens and dead cells, which are then degraded by lysosomes. The autophagy-lysosome system is responsible for the removal of misfolded or aggregated proteins, damaged organelles, and intracellular pathogens [367]. Some studies suggest that lysosomal inhibitors hinder the degradation of VE-cadherin and lead to the formation of a VE-cadherin fragment during its endocytic processing (Figure 1.18) [368].

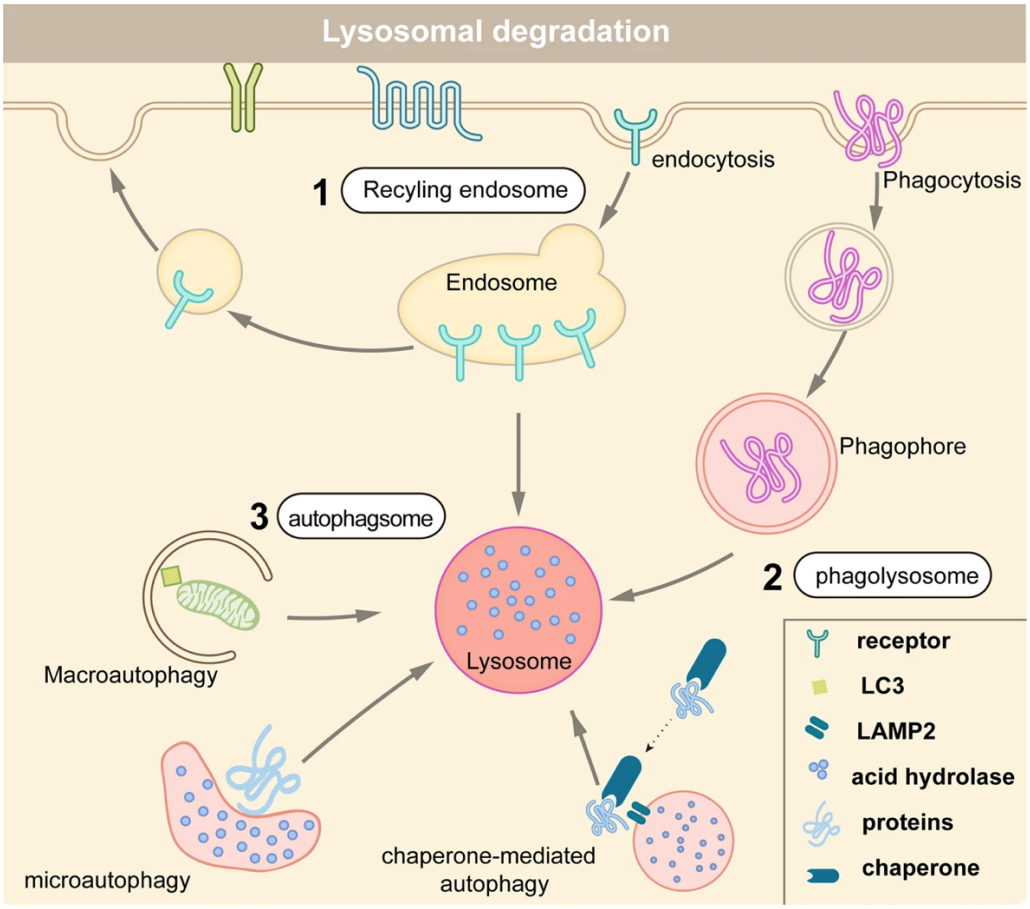


**Figure 1.18: A diagrammatic representation of lysosomal protein degradation through endocytosis, phagocytosis, and autophagy.** (1) Endocytic pathway: cell surface proteins are internalized into endosomes and either degraded in lysosomes or recycled to the plasma membrane or other organelles; (2) Phagocytic pathway: cells engulf and degrade large extracellular particles such as pathogens and dead cells; (3) Autophagy lysosome pathway: misfolded proteins, damaged organelles, and intracellular pathogens are degraded via macroautophagy, microautophagy, or chaperone-mediated autophagy [367].

### 1.5.5.1 Lysosomal Inhibitors

Lysosomal inhibitors exert their effects through distinct molecular mechanisms that disrupt the acidic environment essential for lysosomal function. For example, Bafilomycin A1 specifically targets the vacuolar-type $H^+$-ATPase (v-ATPase) by binding at the interface of transmembrane helices 1, 2, and 4 of the ATP6V0C (subunit c) within the V0 domain. This interaction inhibits the necessary helical swivelling motion, thereby preventing proton translocation and subsequent acidification of the lysosomal lumen [395]. In contrast, chloroquine**,** although mechanistically less defined, is known to neutralise lysosomal pH through an unspecified pathway [369].

Chloroquine, a lipophilic aminoquinoline compound, is widely recognised for its antimalarial properties and its ability to interfere with autophagic and lysosomal degradation pathways under various pathological conditions, including Alzheimer's disease and cerebral ischemia [370, 371]. Its high lipid solubility facilitates efficient translocation across cellular membranes, enhancing its intracellular activity. Structurally, chloroquine is characterised by the substitution of a [5-(diethylamino)pentan-2-yl]amino group at the 4-position and a chlorine atom at the 7-position of the quinoline ring (Figure 1.19) [372].

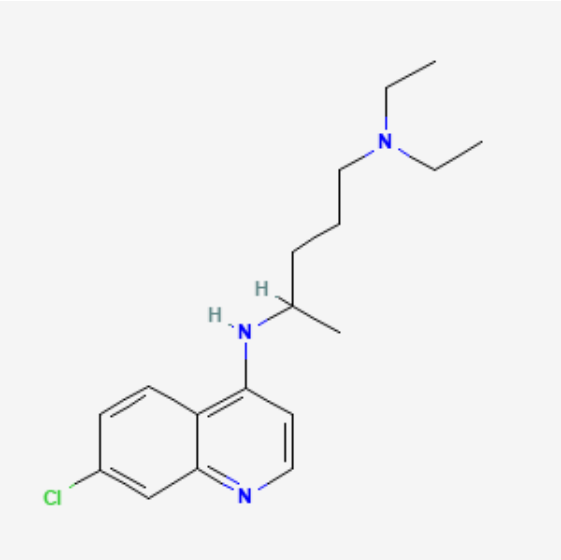


**Figure 1.19: Chemical structure of chloroquine [372].**

Chloroquine acts as a lysosomotropic agent within the cell, meaning it becomes protonated and trapped upon reaching the acidic environment within organelles such as lysosomes [373]. As an autophagy inhibitor, chloroquine has been shown to reduce brain tissue damage and improve

neurological function [374]. Numerous studies have demonstrated that chloroquine provides beneficial effects in various experimentally induced neurological conditions, including traumatic brain injury, cerebral ischemia, Parkinson's disease, and other neurodegenerative disorders [370, 375, 376]. Increasing evidence indicates that chloroquine exerts its neuroprotective actions through a range of mechanisms, including inflammation suppression, oxidative stress reduction, protection against neuronal death, and safeguarding the blood-brain barrier [370, 375]. Chloroquine inhibits autophagic flow by impairing the fusion of autophagosomes with lysosomes. Chloroquine and its derivative, hydroxychloroquine both FDA-approved drugs, are now primarily used in clinical trials focused on tumour treatment via autophagy inhibition [372].

## 1.6 VE-cadherin

### 1.6.1 VE-cadherin Phosphorylation

Protein phosphorylation serves as a crucial regulatory mechanism in a wide range of cellular processes, such as protein synthesis, cell division, signal transduction, cell growth, development, and ageing. Post-translational modifications to VE-cadherin, including tyrosine phosphorylation or cleavage, increase vascular permeability and leukocyte movement across the endothelium [377]. Bradykinin and histamine-mediated phosphorylation of VE-cadherin leads to its internalisation and tagging for degradation following ubiquitination, which in turn increases vascular permeability [378]. Additionally, the phosphorylation of VE-cadherin [379-381] and catenin [382-384] can influence the structural integrity of endothelial junctions. For example, phosphorylation of VE-cadherin at $Tyr^{658}$ and $Tyr^{731}$ within its cytoplasmic domain, prevents binding to p120-catenin and β-catenin [385]. Other studies have linked phosphorylation of these and other tyrosine residues ($Tyr^{685}$) in the cytoplasmic tail of VE-cadherin to the disruption of cell–cell junctions [377]. Besides tyrosine phosphorylation, VE-cadherin is also phosphorylated at $Ser^{665}$ in its cytoplasmic tail. Specifically, VEGF stimulates Src, which directly phosphorylates VE-cadherin at $Tyr^{685}$ and indirectly leads to $Ser^{665}$ phosphorylation via a signalling pathway involving Vav2 (a RhoGEF), Rac1, and the kinase PAK1 [386].

### 1.6.2 VE-cadherin Internalisation

VE-cadherin is a crucial and dynamically regulated adhesion molecule whose presence at the plasma membrane is essential for maintaining cell–cell adhesion and the integrity of junctional complexes. Membrane localisation is primarily modulated through internalisation, which

reduces the availability of VE-cadherin at intercellular junctions, thereby compromising endothelial barrier function [378]. The internalisation process often occurs through a clathrin-mediated pathway that is dependent on p120-catenin, which facilitates the recruitment of VE-cadherin into clathrin-coated pits [387].

Various signalling pathways influence the endocytic process; notably, phosphoinositide 3-kinase (PI3K) signalling promotes VE-cadherin internalisation. For example, Class I PI3Kα activation, in response to TNFα, leads to the destabilisation of VE-cadherin and subsequent disruption of the vascular barrier [388]. In addition to PI3K signalling, numerous other factors, including proinflammatory mediators (TNFα, LPS, histamine, bradykinin), hypoxia and elevated hydrostatic pressure (Table 1) also promote VE-cadherin internalisation. Once internalised, VE-cadherin is trafficked into endosomal compartments where it may either be recycled back to the plasma membrane or targeted for lysosomal degradation [389]. Given that cadherin internalisation weakens cell–cell junctions, this mechanism is closely associated with increased endothelial cell migration and vascular permeability, thereby highlighting its broader implication in endothelial behaviour and vascular homeostasis [390-392].

Conversely, endocytosis/internalisation of VE-cadherin is inhibited by p120-catenin, which binds to the cadherin tail and blocks an endocytic motif within the juxtamembrane domain [203, 393]. The direct interaction between p120-catenin and VE-cadherin prevents clathrin-mediated endocytosis of VE-cadherin [74]. This interaction is vital for maintaining endothelial barrier integrity [394], supporting proper angiogenic remodelling [395] and regulating endothelial adhesion strength and the plasticity of adherens junctions [393]. Recent studies indicate that specific cadherin clusters on the cell surface undergo endocytosis, leading to either degradation or recycling to the plasma membrane [396]

.

| Factor | Cell line | Finding | Reference |
|---|---|---|---|
| VE-cad GGG mutant | Mice | ↓ VE-cad levels, ↑internalisation of VE-cad, and ↓VE-cad-p-120 binding. | [397] |
| VEGF | HUVECs | VE-cad internalised in clathrin dependent manner | [398] |
| Histamine | HUVECs | Induce VE-cad endocytosis. | [399] |
| Lipopolysaccharide | Human vascular endothelial cell line CRL-2922 | ↓ VE-cad levels due early phase clathrin-mediated endocytosis followed by late phase caveolae-mediated endocytosis | [400] |
| TNFα | HUVECs | VE-cad degradation and ↑ human endothelial cell permeability | [401] |
| Ubiquitin ligase K5 | Primary and immortalised (HMEC-1) endothelial cells | K5 triggers VE-cad endocytosis by displacing p120, leading to ↓VE-cad levels | [203] |
| LPS and Pseudomonas | Rat lung microvascular endothelial cells (LMVECs) | LPS causes VE-cad internalization, ↓ presence on the cell surface | [402] |
| Lactate | HUVECs | Activates calpain1/2 via ERK, leading to VE-cad cleavage and ↑endocytosis | [403] |
| Calpain | COS7 cells | VE-cad localises to clathrin-rich areas and is cleaved by calpain | [393] |
| Extracellular calcium | Bovine aortic endothelial cells | Low calcium (0.12 mM) ↑ permeability and triggers cad endocytosis | [404] |
| Hydrostatic pressure | Lung endothelial cells | High pressure activates Piezo1, leading to VE-cad internalization | [405] |
| Desacetylvinblastine monohydrazide (DAVLBH) | HUVECs | DAVLBH disrupts VE-cad distribution in a dose-dependent manner and promotes its internalization. | [406] |
| Thrombin | HLMVECs | ↑ the co-localization of VE-cad at cell-cell adhesion junctions. | [407] |
| Bradykinin | HUVECs | Phosphorylation, internalization, and ubiquitination of VE-cad, leading to ↑permeability | [408] |
| Hypoxia | HUVECs | VE-cad internalization, ↓ cell adhesion and ↑ permeability. | [409] |
| BMP6 | HUVECs | ↑ permeability, triggers VE-cad internalization and Src-dependent phosphorylation | [410] |
| Semaphorin 3A | hCMEC/D3 | Phosphorylation (Ser) and internalisation of VE-cad, disrupting cell junctions and barrier integrity | [411] |

**Table 1.1: Summary of factors implicated in the internalisation of VE-cadherin.** Abbreviations: VEGF, Vascular Endothelial Growth Factor; VE-cad, VE-cadherin; HUVECs, Human Umbilical Vein Endothelial Cells; TNFα, Tumour Necrosis Factor alpha; HMEC-1, Human Microvascular Endothelial Cells – line 1; HLMVECs, human lung microvascular endothelial cells; ERK, Extracellular Signal-Regulated Kinase; BMP6, Bone Morphogenetic Protein 6; hCMEC/D3, Human Cerebral Microvascular Endothelial Cell line / Clone D3.

### 1.6.3 VE-cadherin Recycling

Endocytic recycling is a fundamental process responsible for maintaining the surface expression of membrane proteins, thereby preserving cellular homeostasis [412]. The regulation of cadherin levels at the plasma membrane is governed by a dynamic balance between endocytosis and degradation, which reduce surface cadherin, and synthesis and recycling, which restore cadherin availability [413]. Recycling pathways comprise three main transport routes: a direct route from sorting endosomes to the plasma membrane, and an indirect route that involves trafficking through recycling endosomes before returning to the cell surface [414]. Specifically, the recycling of VE-cadherin between the plasma membrane and intracellular compartments plays a pivotal role in adherens junction remodelling, a process essential for reestablishing endothelial barrier function [415, 416]. The endosomal recycling system is one of the primary mechanisms for modulating plasma membrane composition by returning internalised proteins and lipids to the cell surface [291]. Proteins targeted for recycling are transported back via exocytosis, a process regulated by small GTPases, the exocyst complex, and the interaction of complementary SNARE proteins on opposing membranes. In both yeast and mammalian systems, the exocyst complex consists of eight core subunits: Sec3, Sec5, Sec6, Sec8, Sec10, Sec15, Exo70, and Exo84 [71, 417]. Notably, Sec5, Sec6, and Sec15 are critical for the recycling of Drosophila E-cadherin. Loss of these components in epithelial cells results in the accumulation of Drosophila E-cadherin within enlarged recycling vesicles and disrupts its proper delivery to the plasma membrane [418]. In endothelial cells, there is little information on the recycling of internalised VE-cadherin back to the plasma membrane; however, Rab11a and its effector protein FIP2 and Rab4 have been implicated [412]. However, several factors induce VE-cadherin recycling in several different tissues and cell types (Table 2).

| Factor | Cell line | Finding | Reference |
|---|---|---|---|
| p18 and Rab11a | Human pulmonary microvascular endothelial cells (HPMVECs) and Male C57BL/6J mice | The p18 protein binds to VE-cadherin through its VE-cadherin-binding domain before Rab11a interacts with it. Overexpressing p18 boosts VE-cadherin trafficking to adherens junctions. Additionally, p18 helps maintain pulmonary endothelial barrier integrity by regulating Rab11a's interaction with VE-cadherin and Rab11a activation. Overall, both p18 and Rab11a are key players in recycling VE-cadherin. | [419] |
| Transmembrane Domain containing Protein 4(CMTM4) | GFP-labelled HUVECs, dsRED-labelled pericytes Zebrafish | CMTM4 is a crucial regulator of angiogenesis, helping recycle VE-cadherin back to endothelial adherens junctions. The study shows that CMTM4 strongly colocalizes with Rab4 and VE-cadherin, suggesting it plays a role in the rapid recycling of VE-cadherin to the cell surface at these junctions. | [420] |
| Metformin | chionrochidoroid plexus in rats | Prolonged metformin treatment reverses VE-cadherin internalization and ↓VEGF levels. Metformin prevents VE-cadherin disassembly at the plasma membrane by inhibiting the VEGF/VEGFR2/p-Src signalling pathway, helping restore VE-cadherin's proper localization at the cell surface. | [421] |
| Phospholipase D2 | Mouse lung microvascular endothelial cells (MLMVECs) | Phospholipase D2 (PLD2) helps restore endothelial barrier integrity by promoting VE-cadherin dephosphorylation through a PTPN14-dependent mechanism. Additionally, phosphatidic acid (PA), produced by PLD activity, regulates VE-cadherin recycling and supports barrier repair by enhancing its dephosphorylation. | [407] |
| GSTpi (Phase II metabolic enzyme) | HUVEC | Glutathione S-transferase pi (GSTpi) prevents the dissociation of the VE-cadherin/catenin complex and stops VE-cadherin internalization, helping maintain endothelial barrier function. It also blocks TNF-α-induced VE-cadherin internalization and the resulting ↑ in permeability in human endothelial cells. | [422] |
| Intraflagellar transport proteins (IFT20) | HDLECs | IFT20 is crucial for recycling VE-cadherin to adherens junctions by regulating its vesicular trafficking, which helps maintain endothelial cell–cell adhesion | [423] |

**Table 1.2: Various factors lead to the recycling of VE-cadherin.**

## 1.7 Blood-Brain Barrier Dysfunction

BBB dysfunction is linked to multiple sclerosis, hypoxic and ischemic insult, Parkinson's and Alzheimer's disease, epilepsy, brain tumours, glaucoma, and lysosomal storage diseases. Barrier dysfunction can range from minor changes in BBB permeability caused by tight junction opening to chronic barrier breakdown, as well as changes in transport systems and enzymes. Barrier dysfunction is also linked to basement membrane breakdown. Under normal conditions, the BBB is relatively impermeable, but under pathological conditions, several factors, such as vasoactive agents, cytokines, and chemical mediators, result in BBB dysfunction and increased BBB permeability [14]. Interestingly, proinflammatory stimuli, such as lipopolysaccharide (LPS, aka endotoxin), reduce vascular integrity by disrupting VE-cadherin adhesion in endothelial cells [424].

### 1.7.1 VE-cadherin in BBB Dysfunction

VE-cadherin is an important target of BBB breakdown because it is a structural component of vascular integrity in the brain [425]. The integrity of the BBB is crucial for preserving cerebral homeostasis and supporting optimal neurological function [426]. When the BBB is compromised, it facilitates the infiltration of toxins, plasma proteins, and immune cells from the bloodstream into the brain, which can induce inflammatory responses. This disruption is implicated in the pathogenesis of various cerebrovascular and neurological conditions, including ischemia/reperfusion stroke, hypertension, cerebral cavernous malformation, amyotrophic lateral sclerosis, Alzheimer's disease, Parkinson's disease, multiple sclerosis, and depression [412, 427-430]. Consequently, strategies aimed at restoring BBB integrity have become a critical focus for therapeutic intervention in these disorders [427, 431-434]. Evidence suggests that reduced expression of VE-cadherin at endothelial junctions contributes to compromised vascular integrity, leading to conditions such as cerebral cavernous malformation, oedema, diabetic retinopathy, and solid tumours. Conversely, the restoration of VE-cadherin expression at cell junctions is associated with endothelial barrier repair and disease regression [435-440]. Laboratory studies further indicate that targeting VE-cadherin function may offer an effective strategy for normalising vascular structures in cancer therapy [441]. Research on acute lung injury has shown that elevated levels of VE-cadherin and enhanced cadherin binding at adherens junctions can improve pulmonary barrier function, both *in vitro* and *in vivo*, when the novel endosomal adaptor protein p18 is overexpressed [442].

Various therapeutic strategies are being investigated to enhance BBB integrity by targeting tight junction proteins, reducing permeability, and stabilising the barrier [54, 443, 444]. Studies on

stroke have shown that inhibitors of RhoA and ROCK effectively reverse oxygen-glucose deprivation/reperfusion (OGD/R)-induced hyperpermeability of human brain microvascular endothelial cell monolayers and prevent the internalisation of VE-cadherin [445]. Another study demonstrated that overexpression of NTN4 increased VE-cadherin expression and decreased permeability in human umbilical vein endothelial cells (HUVECs). This effect was mediated through the activation of the NF-κB signalling pathway, revealing a novel regulatory mechanism for VE-cadherin expression and providing new directions for research on NTN4 in endothelial barrier-related diseases [446]. Research has demonstrated that microRNA miR-27a directly downregulates VE-cadherin expression [447]. The use of CD5-2, a blocker that selectively inhibits the interaction between miR-27a and VE-cadherin, has been shown to enhance VE-cadherin expression [437]. In a mouse model of cerebral cavernous malformation, which is characterised by a disrupted BBB, treatment with CD5-2 significantly decreased BBB permeability which stabilised the vasculature and therefore lessened lesion severity [440].

Glucocorticoids, steroids primarily used for their anti-inflammatory effects, represent another approach for restoring BBB integrity and function. These agents have been tested in various preclinical models and as therapies for brain tumours and multiple sclerosis (MS). They act through glucocorticoid receptors to reduce the expression of inflammatory molecules and increase the expression of endothelial junction proteins, such as occludin, claudin-5, and VE-cadherin, which are critical for maintaining BBB integrity [448].

In addition, FTY720 has been shown to effectively prevent the movement of junction proteins within endothelial cells, thereby preserving BBB integrity, reducing ischemia/reperfusion-induced damage, and decreasing neuroinflammation [449]. This compound is especially noteworthy as it was the first oral medication approved for the treatment of relapsing-remitting MS due to its ability to rapidly cross the BBB and accumulate in the CNS [450-452]. Research suggests that FTY720 does not facilitate the translocation of adherens or tight junction proteins across the membrane [453]. In a different study, Sarai et al. (2009) observed that prolonged exposure to FTY720 (for 3 hours) resulted in enhanced peripheral localisation of both VE-cadherin and β-catenin in human microvascular endothelial cells (HMVEC) [454]. Conversely, other research suggests that FTY720 may have potential therapeutic applications in protecting against endothelial barrier dysfunction associated with severe *Plasmodium falciparum* malaria [455].

Under pathological conditions, the expression levels, phosphorylation states, or localisation of junctional molecules alter, leading to the disruption of junction integrity. By either limiting or

reversing these changes, it is possible to inhibit the paracellular permeability of the BBB and restore its integrity, thereby improving disease outcomes [456].

### 1.7.2 PP2A in BBB Dysfunction

The PP2A family plays a critical role in regulating essential cellular functions. The BBB is altered in certain pathological conditions, such as neurodegenerative disorders, causing upregulated PP2A subunits, which lead to BBB dysfunction [457]. PP2A regulates the phosphorylation status of tight junction and adherens junction proteins [458]. Many junctional proteins contain multiple phosphorylation sites, which can regulate protein-protein interactions during the assembly and disassembly of junction complexes. Modifications in the phosphorylation status of tight junction (TJ) proteins play a crucial role in regulating BBB permeability. Most studies on phosphorylation/dephosphorylation processes focus on three key TJ proteins: the transmembrane proteins occludin and claudin-5, and the scaffolding protein ZO-1[18]. In epithelial cells, phosphorylation of tyrosine residues in occludin is associated with TJ complex assembly, although specific sites, $Tyr^{398}$ and $Tyr^{402}$, have been linked to barrier dysfunction [459]. Blocking PP2A with okadaic acid enhances the phosphorylation and integration of ZO-1, occludin, and claudin-1 into tight junctions as they form [458]. Disrupted regulation of PP2A influences various Ser/Thr protein kinases implicated in Alzheimer's disease (AD) pathogenesis [457]. In AD brains, reduced PP2A activity contributes to Tau and APP hyperphosphorylation, promoting the formation of neurofibrillary tangles (NFTs) and excessive production of β-amyloid (Aβ) [190].

## 1.8 Metformin

PP2A has been linked to insulin resistance and type 2 diabetes [460]. Metformin has been widely used to treat type 2 diabetes and other metabolic syndromes since the 1960s [461]. It was first isolated from the extracts of the plant *Galega officinalis* (French lilac) in the 1920s [462], and was subsequently approved for the treatment of diabetes mellitus in Europe and Canada in 1957, and in the United States in 1995 [463]. Chemically, metformin (N, N-dimethyl-biguanide) is synthesised from dimethylamine hydrochloride and 2-cyanoguanidine (Figure 1.20) [463, 464]. Having been prescribed for over six decades, metformin is recognised for its strong safety profile and high efficacy in blood glucose management [462].

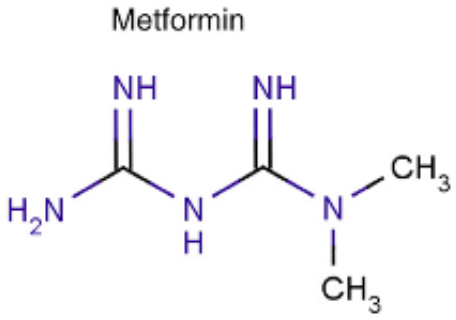


**Figure 1.20: Chemical structure of Metformin [465].**

### 1.8.1 Mechanism of Action -Diabetes

Metformin lowers blood glucose primarily by activating adenosine monophosphate-activated protein kinase (AMPK) through lysosomal or mitochondrial pathways. This activation improves insulin sensitivity by inhibiting acetyl-CoA carboxylase (ACC), promoting CREB-binding protein (CBP) coactivator activity to reduce gluconeogenesis gene expression, suppressing mTORC1 to limit anabolic processes, and reducing cAMP levels to further inhibit glucose production (Figure 1.21). In addition to its AMPK-dependent pathway, metformin can also function independently of AMPK by inhibiting complex I of the mitochondrial electron transport chain in liver, muscle, and skeletal muscle cells [466], which in turn alters the AMP: ATP and NADH: $NAD^+$ ratios, or by directly inhibiting fructose-1,6-bisphosphatase [467].

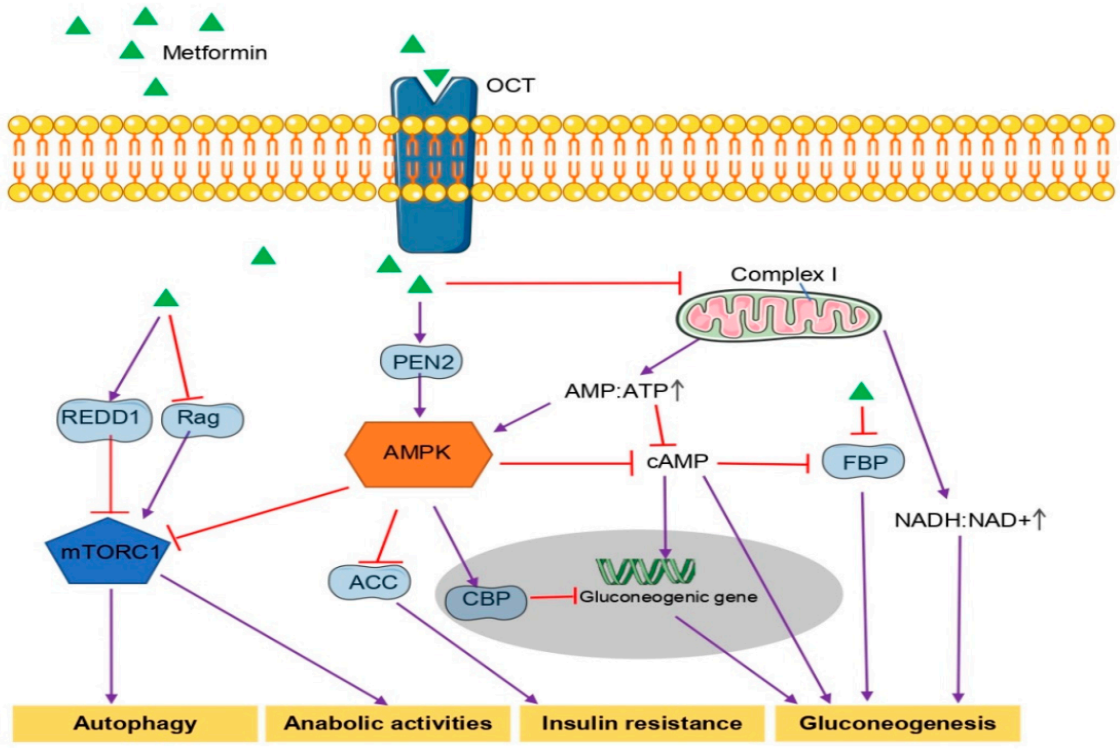


**Figure 1.21: The mechanism through which metformin exerts its hypoglycaemic effects.** AMPK enhances insulin sensitivity by inhibiting acetyl-CoA carboxylase (ACC), activating CREB-binding protein (CBP) to suppress the expression of gluconeogenesis genes, and inhibiting mechanistic target of rapamycin complex 1 (mTORC1) to limit cellular anabolic processes. Additionally, metformin reduces gluconeogenesis by lowering cyclic AMP (cAMP) levels. Metformin's glucose-lowering effect can also occur independently of AMPK activation, through alterations in the AMP: ATP and NADH: $NAD^+$ ratios via mitochondrial mechanisms or by directly targeting fructose-1,6-bisphosphatase (FBP). Key regulatory components involved include REDD1 (regulated in development and DNA damage response 1), Rag family GTPases (Rag), presenilin enhancer 2 (PEN2), organic cation transporters (OCT), ATP, AMP, NADH, and NAD+ [467].

In addition to its hypoglycaemic effects, metformin enhances cognitive and mood functions in some patients with type 2 diabetes mellitus (T2DM). Furthermore, it has been reported to exert beneficial effects in various neurological disorders, including major depressive disorder (MDD), Alzheimer's disease (AD), and Fragile X syndrome (FXS) [467]. Clinical and animal studies have demonstrated that metformin provides neuroprotective benefits in a range of neurological conditions [468-470]. Importantly, metformin increases PP2A activity and decreases tau phosphorylation at PP2A-dependent epitopes *in vitro* and *in vivo* in Alzheimer's disease [185]. Moreover, protein phosphatase 2A (PP2A) plays a role in cellular processes such

as insulin signalling, cell proliferation, and apoptosis by dephosphorylating key signalling molecules, including AKT, AMPK, p53, and c-Myc, all of which are involved in metformin signalling pathways [471].

### 1.8.2 Pleiomeric Actions

Metformin has gained significant attention for its broad therapeutic applications across numerous diseases [472]. It has proven effective not only in treating type 2 diabetes mellitus (T2DM) but also in managing conditions like obesity, cancer, cardiovascular diseases, inflammatory disease and neurological disorders [473]. In the context of breast cancer, metformin interferes with the mTOR signalling pathway by enhancing phosphorylation at the inhibitory Ser789 site of IRS-1, an effect that depends on AMPK activation. It also suppresses the expression of IGF-1R and insulin receptor (IR) genes. The co-expression of IGF-1R with the drug-resistance protein MRP1 has been linked to reduced responsiveness to cancer therapies [474].

It also shows promise as an anti-ageing, antiviral, and anti-inflammatory agent [475]. Regarding the latter metformin influences inflammatory pathways by modulating NF-κB signalling, affecting immune cell differentiation, and lowering the secretion of inflammatory cytokines [476, 477]. Remarkably, it reduces levels of several cytokines in the bloodstream even in non-diabetic individuals, including CCL11 a molecule associated with aging and tissue degeneration [461, 478]. The anti-inflammatory properties of metformin are largely attributed to its action on the AMPK-mTOR pathway. Yet, evidence suggests it can also suppress inflammation through alternative mTOR-related mechanisms independent of AMPK. For instance, metformin has been shown to directly inhibit mTORC1 via a Rag GTPase-dependent route, bypassing the typical TSC1/2 or AMPK pathways [479].

Although long-term use of metformin has been associated with impaired absorption of vitamin $B_{12}$ in the small intestine, potentially resulting in neuropathy, anaemia, or cognitive deficits if left unrecognised, metformin has also demonstrated neuroprotective effects in various neurodegenerative disorders, including Alzheimer's disease, Parkinson's disease, Huntington's disease, and multiple sclerosis [473]. In Alzheimer's disease, metformin activates AMPK, which contributes to lowering amyloid-beta levels and reducing brain inflammation. It also enhances the Nrf2 pathway, boosting antioxidant activity, decreasing neuronal death, and improving mitochondrial function factors that may help combat memory decline. In Parkinson's disease, metformin protects dopamine-producing neurons by stimulating AMPK,

encouraging mitochondrial biogenesis through PGC-1α, and reducing oxidative stress. It also limits inflammation by inhibiting microglial activation and reducing pro-inflammatory cytokines like TNF-α, IL-1β, and IL-6. Additionally, metformin enhances autophagy, helping remove damaged proteins and organelles, and further supports antioxidant defences by modulating Nrf2-regulated genes. In Huntington disease, metformin has shown promise by activating AMPK and inhibiting the MID1/PP2A/mTOR complex, leading to reduced translation of mutant huntingtin protein [480, 481]. This decreases its harmful buildup. The drug also improves cognition, reduces behavioural symptoms, enhances mitochondrial health and autophagy, increases brain-derived neurotrophic factor (BDNF), and lessens glial-driven inflammation [482]. Finally, emerging studies suggest it may also benefit individuals with multiple sclerosis by reducing inflammation and oxidative damage in the central nervous system [483, 484].

## 1.9 Immortalized Cell lines

Cell lines are vital assets for biomedical studies, diagnostic tests, and clinical applications [485]. An immortalised cell line refers to a culture of cells that has been derived from a primary cell culture, typically used to increase the cell population and extend their lifespan. Immortalised cells are those that have surpassed the Hayflick limit through genetic modifications, allowing for a theoretically unlimited number of divisions [486]. The process of immortalisation involves artificially bypassing the restriction on cell divisions by altering the expression of genes associated with cellular aging. First experiments aimed at artificially immortalising cells took place in the 1960s, where researchers obtained immortalised cell lines from rats and hamsters using polyomaviruses [487] and chemical carcinogens [488]. Immortalised cell lines of rats and hamsters were obtained. Immortalisation is a complex process consisting of multiple stages, during which cells undergo various selection processes after being transfected with the required genetic material [489]. These manipulations can alter the characteristics of the resulting cell line compared to the primary culture, potentially restricting its application in biomedical research [490]. The first publication documenting altered cell properties following immortalisation was published in early 2013[491].

That said, immortalised cell lines are commonly utilised instead of primary cells to examine biological mechanisms as they have multiple benefits over primary cells [492]. They not only serve as convenient tools in fundamental research but are also finding increasing application in translational and preclinical studies. This trend is attributed to their advantages over primary cells, including the ability to generate larger quantities of cells and maintain them for extended

durations, the ease of genetic alterations, and the elimination of donor-to-donor variability when comparing results across different experiments [493]. This makes them particularly important in understanding the pathophysiology of disease, including neurodegeneration and also valuable tools in drug discovery [493]. The most well-defined cell line to study the human BBB is hCMEC/D3.

### 1.9.1 hCMEC/D3

The hCMEC/D3 cell line was derived from human temporal lobe microvessels isolated during surgery for epilepsy control. The primary isolate was enriched for cerebral endothelial cells (CEC). Cells were sequentially immortalised by lentiviral vector transduction with the catalytic subunit of human telomerase (hTERT) and SV40 large T antigen in the first passage, after which CEC were selectively isolated by limited dilution cloning and clones were extensively characterised for brain endothelial phenotype [494].

The hCMEC/D3 cell line preserves a consistent and physiologically normal endothelial phenotype, which includes the ability to swiftly develop networks of capillary-like vascular structures within a three-dimensional extracellular matrix [495, 496]. This cell line displays a spindle-like, elongated shape comparable to primary brain endothelial cell cultures. Additionally, it demonstrates contact inhibition when it reaches confluence while cultured on collagen types I or IV, expressing brain endothelial/epithelial markers alongside adherence and tight junction proteins, as well as functional ABC transporters.

The hCMEC/D3 cell line is the first extensively characterised human brain endothelial cell line, which embodies many of the distinctive features of the blood-brain barrier, even in the absence of coculture with glial cells. This cell line serves as a valuable model for investigating the biology of human brain endothelium concerning neuroinflammatory or infectious diseases, as well as for large-scale screening of CNS drug candidates [497], as well as an *in vitro* model of BBB function [498-504]. These adherent cells were grown in endothelial cell-specific medium with 5% FBS.

### 1.9.2 EAHY926

A widely utilised and well-defined permanent human endothelial cell line is EA.hy926 [505]. This cell line was established in 1983 through the fusion of human umbilical vein endothelial cells (HUVEC) with a human lung cancer cell line, A549 [506]. EA.hy926 cells exhibit several endothelial characteristics akin to those of HUVECs and are regarded as the immortal equivalent of primary HUVECs [507]. Similar to primary HUVECs, EA.hy926 cells display

comparable permeability, alteration of tight junction proteins, and modifications in structural proteins after thrombin treatment [508], along with a reduction in angiogenesis due to high-glucose exposure under hypoxic circumstances [509]. Additionally, both HUVECs and EAhy926 cells exhibit a comparable senescence phenotype after receiving doxorubicin treatment [510]. This is an adherent cell line that is cultured in Dulbecco's Modified Eagle Medium (DMEM) supplemented with 10% foetal bovine serum.

### 1.9.3 bEND3

bEnd3 cells are an immortalised mouse brain endothelial cell line originally generated in 1990 [511]. They represent a promising option for studying the blood–brain barrier because they grow quickly, preserve blood–brain barrier traits throughout multiple passages, create functional barriers, and are easy to manipulate with various molecular techniques [512]. bEnd.3 cells develop monolayers in culture and exhibit essential features of the blood-brain barrier phenotype, including the expression of crucial tight junction proteins like zonula occludens (ZO), claudins, and occludin, along with key endothelial cell markers such as endothelial NOS (eNOS) and von Willebrand Factor (vWF) [512, 513]. This is an adherent cell line that is cultured in Dulbecco's Modified Eagle Medium (DMEM) supplemented with 10% foetal bovine serum.

## 1.10 Aims

The overall scope of this thesis is to examine the role of PP2A in the regulation of VE-cadherin in human brain microvascular endothelial cells. It specifically examines whether okadaic acid, a PP2A inhibitor, affects the expression and abundance of VE-cadherin in hCMEC/D3 cells, and assesses the resulting impact on blood-brain barrier (BBB) integrity using an in vitro model. Additionally, the study seeks to identify proteins influenced by protein phosphatase inhibition, investigate those involved in VE-cadherin trafficking, and evaluate whether increasing PP2A activity through metformin can help restore BBB function.

Protein phosphatases remain relatively underexplored and are not yet comprehensively characterized [514]. Existing studies indicate that protein phosphatase 2A (PP2A) contributes to the regulation of epithelial tight junction formation and the preservation of barrier integrity [515]. Nevertheless, its specific role in modulating adherens junction components particularly vascular endothelial (VE)-cadherin at the blood-brain barrier (BBB) is not well understood. Given the essential function of VE-cadherin in endothelial cell cohesion and BBB integrity, this study aimed to investigate the effects of okadaic acid (OA), a known PP2A inhibitor, on VE-cadherin abundance and expression, alongside PP2A activity and protein levels. Furthermore, the mechanism underlying VE-cadherin reduction upon PP2A inhibition was examined, focusing on whether this process occurs via proteasomal or lysosomal degradation. The potential of proteasome inhibition to counteract OA-induced effects was also assessed. Consequently, this study evaluated the influence of OA on BBB integrity by determining whether OA disrupts endothelial barrier function.

Wuerger et al. recently employed an integrative transcriptomic, proteomic, and phosphoproteomic strategy to demonstrate that okadaic acid, a known inhibitor of protein phosphatase 2A (PP2A), influences key cellular processes such as energy metabolism, inflammatory signalling, cytoskeletal organisation, and signal transduction in human HepaRG liver [516, 517]. Similarly, in primary rat neuronal cultures, okadaic acid was shown to differentially regulate 320 proteins involved in anatomical structure development, cellular transport, differentiation, and signalling pathways [518]. Despite these findings, a comparable comprehensive or even targeted proteomic investigation into the effects of okadaic acid in human brain microvascular endothelial cells has yet to be conducted. Addressing this gap is crucial for advancing our understanding of PP2A's role in modulating blood-brain barrier (BBB) function under both physiological and pathological conditions. Accordingly, this study explored the global proteomic alterations in hCMEC/D3 cells following PP2A inhibition via

okadaic acid treatment. Differentially expressed proteins were identified, and subsequent enrichment analysis of Kyoto Encyclopaedia of Genes and Genomes (KEGG) pathways and associated biological processes were performed using the ShinyGO platform. Additionally, the STRING database was utilised to examine potential direct (physical) and indirect (functional) protein-protein interactions. The involvement of Rab5a and Rab11A in VE-cadherin internalisation and recycling was also investigated.

Given that okadaic acid functions as an inhibitor of PP2A activity, strategies aimed at modulating and restoring PP2A function may offer therapeutic potential in counteracting its deleterious effects. Previous studies have demonstrated that metformin can activate PP2A across a range of cell types, including human skeletal muscle cells, macrophages, primary cortical neurons, and in various animal models. However, whether metformin exerts similar effects on PP2A activity in human brain microvascular endothelial cells (hCMEC/D3) remains unconfirmed. Therefore, this study investigated the impact of metformin on PP2A activity, expression, and protein abundance in hCMEC/D3 cells. In addition, given reports that metformin can enhance tight junction integrity, evidenced by its ability to reverse hydrocephalus and increase VE-cadherin expression in the choroid plexus of a rat model of intraventricular haemorrhage [519]. The potential of metformin to reverse okadaic acid-induced reductions in VE-cadherin abundance was evaluated in a time-dependent manner.

Overall, this thesis aims to examine whether okadaic acid influences VE-cadherin expression and abundance in human brain microvascular endothelial cells (hCMEC/D3), to uncover the underlying molecular mechanisms, and to assess potential impacts on blood-brain barrier (BBB) function using an in vitro model. A proteomic analysis was conducted to identify key pathways and protein interactions affected by okadaic acid, with a focus on understanding its regulatory effect on VE-cadherin. Selected differentially expressed proteins were further investigated to determine their role in mediating this effect. Additionally, the study evaluated whether metformin modulates PP2A catalytic subunit (PP2Ac) activity and expression in hCMEC/D3 and explored its capacity to reverse okadaic acid-induced changes, particularly in relation to VE-cadherin abundance.

# Chapter 2

# Materials

## 2.1 Consumables

| | |
|---|---|
| 6-well plate | Sarstedt |
| 12-well plate | Sarstedt |
| 24-well plate | Sarstedt |
| 96-well plate | Sarstedt |
| Cell scrapper | Sarstedt |
| PCR 8 tube strip and caps | Applied Biosciences |
| Serological pipettes | Sarstedt |
| 12-well transwell inserts | Stem Cell™ Technologies |
| T75-cell culture (filtered cap) | VWR |
| Filtered pipette tips<br>(2, 10, 20, 200, 1000 µL) | Fisher Brand |
| Pipette tips<br>(2, 10, 20, 200, 1000 µL) | Sarstedt |
| 50 mL tubes | Sarstedt |
| 15 mL tubes | Sarstedt |
| T25-cell culture (filtered cap) | VWR |
| Serological pipettes | Sarstedt |

**Table 2.1: List of consumables**

## 2.2 Equipment

| | |
|---|---|
| MX3000p, Real Time PCR machine | Applied Biosystem |
| Analytical balance | Mettler, AE240 |
| Autoclave | Dixon |
| Fluorescence microscope | EVOS fl |
| Automated pipettes | Gilson, Inc. (2 µL, 10 µL, 100 µL, 200 µL, 1000 µL, 5000 µL, 300 µL Pipetman Ultra 8-channel) |
| Centrifuge | Hettich Zentrfugen, EBA 12R/mikro 22R |
| Digital imaging | Fusion Fx imaging system, Vilber Lourmat |
| Freezer (-80 °C) | ThermoFisher Scientific |
| Gel electrophoresis system | Bio-Rad, Mini-Protean |
| Incubator (37C, 5% CO2, 95% rh) | HERAcell 240i |
| Laminar flow hood | Mason Technology, BioBan 48 |
| Luminometer | ThermoFisher Scientific, Fluoroskan AscentFL |
| Microplate reader | BioTek EL 808 |
| pH meter | Mettler-Toledo Inc., MP320 |
| Thermocycler | MJ Research Inc, PTC-100 |
| Heat Block | Thermoscientific |

**Table 2.2: List of Equipment**

# Chapter 3

# The Mechanism of VE-cadherin Degradation in the Blood-Brain Barrier Post Protein Phosphatase 2A Inhibition Using Okadaic Acid

## 3.1 Introduction

The BBB is a distinctive cellular barrier, the structural integrity of which protects the central nervous system from pathogen infiltration. Structurally, it is a monolayer of endothelial cells connected through a tight junction and adherent junction, lining the cerebrovascular system. While tight and adherent junctions involve a multitude of protein-protein interactions, a crucial component of adherent junctions and BBB architecture is vascular endothelial cadherin (VE-cadherin) [520]. VE-cadherin is a transmembrane protein unique to endothelial cells and is recognised for its role in supporting the initial phases of vascular connection and fusion [75]. Research indicates that VE-cadherin plays a crucial role in the stabilisation of cell-cell junctions and the regulation of vascular barrier integrity [521, 522]. VE-cadherin is a highly dynamic adhesion molecule, and its presence at the plasma membrane correlates with cell-cell adhesion and the functioning of the junctional complex [378]. The internalisation of VE-cadherin is believed to reduce VE-cadherin levels at junctions, hence impacting endothelial barrier function [415]. The disruption of VE-cadherin may result from tyrosine phosphorylation, internalisation, endocytosis, and/or lysosomal degradation [424].

VE-cadherin internalisation is linked to the loosening of cell-cell junctions, which influences endothelial behaviours, including cell migration and permeability [523]. The internalisation of VE-cadherin can occur in a clathrin-dependent or clathrin-independent mechanism [387]. Moreover, *Le, Yap & Stow,* J. (1999) showed that some pools of E-cadherin on the cell surface undergo endocytosis and recycling back to the plasma membrane [524]. These observations suggest that cadherin endocytosis is an important regulatory mechanism controlling cell surface levels and perhaps regulates overall levels of VE-cadherin expression [387]. This has been observed across several mammalian cell types and tissues [393] and regulates the stability of endothelial cell junctions [397]. Additionally, the reorganisation of adherens junctions is essential for collective migration during angiogenesis [525-527]. Certain findings suggest that controlled cadherin endocytosis is crucial for both dynamic cell movement and the formation of a stable tissue architecture [397]. Endocytosis may facilitate the degradation of contacts that result in decreased cadherin expression in epithelial cells, which is linked to various diseases, including tumour metastasis [202] and contributes to various disease mechanisms. For example, in an experimental model of acute pancreatitis, the internalisation of E-cadherin by pancreatic acinar cells is increased [528].

Phosphorylation and dephosphorylation because of the coordinated action of protein kinases and phosphatases are critical in regulating junctional protein-protein interactions and function.

Changes in the phosphorylation state of tight junction proteins is an important regulator of BBB permeability [17]. VE-cadherin has an important role in the control of vascular permeability *in vitro* and *in vivo* [529-531]. VE-cadherin phosphorylation on serine and tyrosine residues has been shown to provoke its internalisation both in *vitro* and in *vivo*, leading to an increase in vascular permeability [378, 390, 411, 532]. The cytosolic tail of VE-cadherin contains nine putative phospho-tyrosine sites, including $Tyr^{645}$, $Tyr^{658}$, $Tyr^{685}$, $Tyr^{731}$, and $Tyr^{733}$. These sites may be involved in barrier integrity. Indeed, many vasculopromoting agents, such as VEGF and histamine, increase the phosphorylation of VE-cadherin and associated catenin, resulting in a loosening of VE-cadherin/catenin binding [523]. In addition to tyrosine phosphorylation, serine phosphorylation of VE-cadherin is reported to be involved in the regulation of endothelial barrier function [150]. One study demonstrated that phosphorylation of VE-cadherin at a serine residue triggers its internalisation by recruiting β-arrestin 2, which facilitates clathrin-dependent endocytosis of VE-cadherin [533]. Another study showed that Sema3A promotes VE-cadherin serine phosphorylation and internalisation, leading to the disruption of cell-cell junctions and a loss of barrier integrity in brain endothelial cells [411].

Serine/threonine phosphorylation represents more than 98% of all protein phosphorylation in mammalian cells [534]. PP2A is the major phosphatase responsible for dephosphorylation of Ser and Thr residues [145]. It was also the first phosphatase found to associate with tight junction complexes [458]. The inhibition of protein phosphatases by various protein phosphatase inhibitors is a strategy for understanding the role of these enzymes in numerous cellular processes [165]. Diarrhetic Shellfish Poisoning (DSP) was documented in humans in the late 1970s [535]. The infection resulted from shellfish contaminated with okadaic acid and its derivatives, dinophysistoxin 1(DTX-1), DTX-2, DTX-4, 7-*O*-palmitoyl-OA and 7-*O*-docosahexaenoyl-O [536]. In laboratory animals, these toxins caused epithelial damage and fluid accumulation in the gastrointestinal tract, and at elevated levels cell death. OA and its derivatives have been shown to function as tumour promoters, and when injected into the brains of animals, okadaic acid induces neuronal damage similar to that seen in Alzheimer's disease [536]. Reports show that neuronal damage induced by okadaic acid corresponds with the hyperphosphorylation of tau protein, the development of neurofibrillary tangles, and an accumulation of β-amyloid [537]. In 1988, Bialojan and Takai [538] discovered that okadaic acid inhibited a particular protein phosphatase, type 2 phosphatase, *in vitro* at nanomolar concentrations. Consequently, it was proposed that intracerebral injection of okadaic acid, due to its ability to block protein phosphatases, would serve as a valuable model for Alzheimer's

disease [539]. Moreover, numerous investigations indicate that pharmacological inhibition of PP2A enhances the paracellular permeability of the endothelial barrier [540-542]. However, the mechanism underlying PP2A inhibition using okadaic acid in the blood-brain barrier remains inadequately explored.

Okadaic acid, a protein phosphatase 2A inhibitor, stimulates caveolae-dependent internalisation [543]. The okadaic acid-induced phosphatase inhibition causes severe alterations in the phosphorylation states of many cellular proteins that can eventually lead to the collapse of regulatory processes and a variety of cellular disruptions [165]. With regard to junctional proteins, okadaic acid-mediated inhibition of PP2A enhances the phosphorylation and targeting of ZO-1, occludin, and claudin-1 to tight junctions during junctional biogenesis [515]. The functional modifications include abnormalities in the expression of tight junctional proteins, their distribution, and the local microenvironment that may facilitate the opening of tight junctions [544]. A study showed that okadaic acid, which inhibits PP2A, disrupts cell-to-cell adhesion in human mammary epithelial cells, resulting in the internalization of E-cadherin [150]. Decreased cadherin expression or cadherin loss has been noted in stroke, traumatic brain injury, and brain tumours, and is accompanied by a loss of blood-brain barrier integrity [544].

Protein phosphatases are inadequately researched and insufficiently characterised [514]. Evidence suggests that PP2A plays a role in regulating epithelial tight junction assembly and maintaining barrier integrity [515]. However, its involvement in controlling adherent junctional proteins, particularly VE-cadherin at the BBB, remains unclear. The present study aims to: 1) investigate if okadaic acid alters VE-cadherin expression and abundance in human brain microvascular endothelial cells and elucidate its underlying mechanisms and 2) assess any functional consequence on BBB function using a surrogate *in vitro* model.

## 3.2 Materials and Methods

### 3.2.1 Cell Culture

Human cerebral microvascular endothelial cells (hCMEC/D3) were purchased from American Type Culture Collection (ATCC; cat No SCC066), while bEnd.3 cells and EAhy926 were obtained from Professor Matt Campbell (Department of Genetics, TCD) and Dr Mark Ward (Department of Histopathology, TCD), respectively. hCMEC/D3 cells were removed from liquid nitrogen and rapidly thawed at 37°C in preparation for culturing in EndoGRO-MV culture medium (Merck, Cat. #SCME-BM) containing 5% foetal bovine serum (FBS), supplemented with 100 U/mL penicillin, 100 mg/mL streptomycin and the supplements provided with the kit (Merck, Cat. #SCME004-S). All plasticware in which hCMEC/D3 were cultured was pre-coated with a 5% (w/v) solution of rat tail collagen type I (08115, EMD Millipore Corp, USA) in Dulbecco's phosphate-buffered saline (DPBS) containing $Ca^{2+}$ and $Mg^{2+}$ (D8662, Sigma-Aldrich). The collagen solution was added to the culture and incubated for one hour at 37°C in an incubator. The solution was then aspirated, and the culture surface rinsed with Dulbecco's phosphate-buffered saline (DPBS) containing $Ca^{2+}$ and $Mg^{2+}$ (D8662, Sigma-Aldrich) before cell seeding. Cells were plated at a density of $2x10^6$ per T-75 flask. The culture medium was changed every 3 to 4 days until the cells reached ~80% confluence. The hCMEC/D3 cells were used up to passage 45.

bEND.3 and EAhy926 cells were cultured in Dulbecco's Eagle's medium (Sigma D5796) supplemented with 10% foetal bovine serum (FBS Sigma F9665), 100 U/mL penicillin/streptomycin (Sigma P0781), and L-glutamine. The culture medium was changed every 2-3 days. The bEND.3 and EAhy926 cells were used at passages 5–20 and 32-38, respectively.

All cells were maintained in a humidified atmosphere at 37°C and 5% $CO_2$, and experiments were performed under serum-free conditions. hCMEC/D3 cells were preserved by freezing in hCMEC/D3 medium supplemented with 10% DMSO. bEND3 and EAHY926 cell lines were frozen in Complete growth medium, supplemented with 5% (v/v) DMSO. Cells were frozen at a controlled rate (1°C/h) utilising a Mr Frosty container in a -80°C freezer.

### 3.2.2 Cell Trypsinisation and Counting

To trypsinise the cells, the culture medium was aspirated, and the cells were washed with

Dulbecco′s phosphate buffered saline,1xPBS (D8662, Sigma-Aldrich) before the addition of a 0.25% trypsin-EDTA solution (T4049, Sigma-Aldrich). The cells were incubated for 2-3 minutes at 37°C to release the cells, before stopping the reaction by the addition of full serum medium. The cell suspension was centrifuged at 300 x g for 5 minutes to harvest the cell pellet. The cell pellet was reconstituted in 8-10 mL of full growth medium. From this, a 50 µL aliquot was removed and an equal volume of a 0.4% solution of trypan blue (Gibco, USA) added, and the cells incubated for 2 minutes. An aliquot (10 µL) of the cell suspension was added to both chambers of the haemocytometer and observed using light microscopy under a 10x magnification. The number of unstained cells (viable) was determined from four areas consisting of 16 squares designated by gridlines on the haemocytometer, and the average was determined. The viable cell count per millilitre was calculated by multiplying the average number of cells by the trypan blue dilution factor.

### 3.2.3 Protein Cell Extraction

The cell culture medium was removed, and the cells were washed in sterile ice-cold PBS (D8662, Sigma-Aldrich) with gentle swirling before being aspirated. RIPA buffer (110 µL/well for a 6-well plate; Trizma Base 50 mM, NaCl 150 mM, EDTA 2 mM, NP-40 0.5% v/v) was supplemented with 100x protease inhibitor cocktail Set I (539131-EMD Millipore Corp, Germany) and the cells detached using a cell scraper. The cell suspension was transferred to a 1.5 mL Eppendorf tube and incubated on ice for approximately 15 minutes. The cell suspension then underwent three freeze-thaw cycles at -80°C to ensure complete lysis. Cell debris was removed by centrifugation at 400xg for 10 minutes, and the supernatant transferred to a clean sterile 1.5 mL Eppendorf tube. Protein samples were stored at -80°C for protein quantification and downstream analysis.

### 3.2.4 Bradford Assay

Protein content in the cell lysates was quantified using a Bradford assay. A protein standard curve was generated using the method of serial dilution to cover a concentration range of 0-1500 µg/mL based upon bovine serum albumen (BSA, Cat # A7888) as the reference standard. The protein standards, blank control, and unknown protein samples (5 µL) were added in duplicate to a 96-well plate and mixed with 250 µL of Bradford reagent (B6916; Sigma, Dublin). The colour was allowed to develop for 15 minutes at room temperature in the dark before the absorbance was determined at a wavelength of 595 nm using a spectrophotometer (BIO-TEK EL808). The absorbance from the duplicates was averaged, the background subtracted, and the standard curve constructed. The protein concentration in the unknown

samples was interpolated from the standard curve (Graphpad Prism v10) and adjusted to account for dilution. The protein samples were then standardised to 1 mg/mL using distilled water as the diluent.

### 3.2.5 Immunoblotting /Western blot

#### 3.2.5.1 SDS-PAGE and Dry Transfer

Protein samples (20 µg) were heated for 30 seconds in a sample loading buffer consisting of lithium dodecyl sulphate (LDS) 5% v/v, glycerol 50% v/v, Tris-HCl 1 M, bromophenol blue 2.5 mg, phenol red 2.5 mg, and ficoll 400 5% v/v, and cooled on ice for 3 minutes. The denatured samples were subjected to sodium dodecyl sulphate-polyacrylamide gel electrophoresis (SDS-PAGE) using an 8% stacking gel and 12% resolving gel (Table 3.1). A molecular weight ladder (Fisher BioReagent, EZ-Run™ Prestained Protein Ladder, 10-170 kDa) was included on the gel to establish the relative molecular sizes of the proteins. Gels were run at 120 V for 1 h with 25 mM Tris Base, 192 mM glycine, and 0.1% (v/v) SDS as the running buffer.

An iBlot 2 system was used to dry-transfer the proteins from the gel to a PVDF membrane. In brief, the iBlot 2 transfer stack was separated into the bottom and top stacks. The SDS-PAGE gel was sandwiched between the bottom and top stacks and compressed with a ruler to eliminate air bubbles. The sandwich was then placed in the apparatus, and the following program was run for either 7 min (P0) or 6 min (P1) for large-sized (kDa) or small proteins (kDa), respectively. Following transfer, if the membranes were not used straight away, they were labelled and stored dry between sheets of filter paper at 4 °C.

| Gene | Resolving gel | | Stacking gel |
|---|---|---|---|
| | 8% | 12% | 5% |
| $dH_2O$ | 4.6 mL | 3.3 mL | 1.4 mL |
| 30%(w/v) Acrylamide /Bisacrylamide | 2.7 mL | 4.0 mL | 0.33 mL |
| Tris (1.5 M, pH 8.8) | 2.5 mL | 2.5 mL | - |
| Tris (1 M, pH 6.8) | - | - | 0.25 mL |
| 10% (w/v) SDS | 0.1mL | 0.1 mL | 0.02 mL |
| 10% (w/v) ammonium persulfate | 0.1mL | 0.1 mL | 0.02 mL |
| TEMED | 0.006 mL | 0.004 mL | 0.002 mL |

**Table 3.1: Composition of the resolving and stacking gel used for PAGE.**

### 3.2.5.2 Immunodetection of Proteins

The PVDF membrane was blocked in TBS-T (Tris 10 mM, NaCl 100 mM, HCl 1 M, and Tween-20 0.1 % v/v) containing 5% milk or 2% BSA for 1 h. The blocking solution was then removed and the membranes probed overnight at 4°C with, anti-VE-cadherin mouse (BV9, cat. # sc-52751), anti-VE-cadherin rabbit (Abcam, cat. # AB205336), anti-PP2Ac (1D6, cat. # sc-80665), anti-Ub (A-5, cat. # sc-166553), anti-pan-cadherin (E-11, cat. # sc-515872), anti-HSP90 (AC-16, cat. # sc-101494), Rab5A (E-11, cat. # sc-166600) or Rab11A (Abcam, cat. #AB128913) as appropriate. Primary antibodies were used at either a 1:500 or 1:3000 dilution in blocking buffer. The next day, the membrane was rinsed with TBS-T and then incubated at room temperature for 1 hour with TBS-T + 5% milk containing an HRP-conjugated anti-mouse or anti-rabbit secondary antibody at a 1:1000 and 1:5000 dilution, respectively. Following washing with TBS-T for 15 min and twice for 5 min at room, the membrane was exposed to the chemiluminescence reagents (3.2 µL of 30% hydrogen peroxide and 6 mL of 250 mM luminol, 90 mM 4-iodophenylboronic acid, and 100 mM Tris-HCl), for 2 minutes before being sandwiched between acetate sheets. The protein bands were visualised and recorded using a Fusion Fx imaging system (Vilber Lourmat) and underwent densitometric analysis using Bio1D software. The membranes were then stripped in a solution consisting of 62.5 mM, pH 6.8 Tris-HCl, 2% (v/v) SDS, and 0.83 µL β-mercaptoethanol (M7154; Sigma Aldrich), before being re-probed with a 1:2000 dilution of an HRP-conjugated actin antibody (C4, cat # sc-47778).

### 3.2.6 Semi-Quantitative Real-Time PCR

#### 3.2.6.1 RNA extraction and Quantification

hCMEC/D3 cells were cultured in 6-well plates at a density of 4 x $10^5$ cells per well or in 12-well plates at a density of 2 x $10^5$ cells per well. The cells were subsequently lysed in Tri Reagent™ on ice (1 mL per 4 x $10^5$ cells; Sigma Aldrich). Chloroform was then added (200 µL/mL of TriReagent), shaken vigorously and incubated at room temperature for 10 minutes. To separate the organic and aqueous phases, the samples were centrifuged at 12,000 g for 15 minutes at 4°C. The upper aqueous phase containing RNA was carefully removed to avoid the interphase and transferred to a new Eppendorf tube. The RNA was precipitated by the addition of isopropanol (500 µL/mL of TriReagent) and collected by centrifugation at 12,000 g for 10 minutes at 4°C. The supernatant was discarded, and the RNA pellet was washed with 75% and 100% ethanol consecutively. Following air drying, the RNA pellet was reconstituted in nuclease-free water (Promega, P119E) and heated at 65°C for 5 minutes to aid dissolution.

RNA quantification and purity were determined spectrophotometrically using a NanoDrop (Thermofisher Scientific, NanoDrop ND 8000). In brief, the nucleic acid option of the Nanodrop software (ND1000) was selected, the upper and lower pedestal cleaned with Nano Pure water (2 µL) and the machine blanked against the sample elution buffer. The upper and lower pedestals were cleaned again, and 2 µL of the experimental sample was added. Absorbance was then determined at a wavelength of 260 nm, while purity was assessed by measuring the ratio of the sample absorbance at 260 and 280nm; a ratio of approximately 2.0 was considered acceptable RNA purity.

#### 3.2.6.2 Validation of mRNA Quality

The RNA quality was examined using agarose gel electrophoresis. Agarose gels of 1% (w/v) were prepared by dissolving 0.5 g of agarose (A9539) in 100 mL 1xTAE buffer (Tris base, glacial acetic acid and 0.5 M EDTA pH 8.0), followed by heating in a microwave oven. The agarose solution was cooled to hand-hot, 3µL of Gel Red Nucleic Acid stain was added (SCT122, Millipore), and the gel was cast in a 10 cm × 6.2 cm Bio-Rad Mini Sub-Cell GT gel casting tray to form a 6.5 mm thick gel. An 8-tooth well-forming comb was set at a height of 1 mm from the bottom. The gel was allowed to set for 20 min, then covered with 100 mL 1xTAE running buffer. Before electrophoresis, the comb was removed from the gel, and the gel with its supporting plate was transferred to a Bio-Rad Mini Sub-Cell GT electrophoresis unit. The RNA sample was prepared using 1-2 µg with 4 µL of 6x RNA loading dye (15% w/v Ficoll

400, 0.15% w/v xylene cyanol and 0.2% w/v orange G) before loading the wells. The gels were then run at 100 V until the marker dye was 2/3 down the gel. Gel images were captured using UV detection in a Fusion Fx imaging system (Vilber Lourmat).

Intact RNA is depicted by two clear bands corresponding to 28s rRNA and 18 rRNA in a ratio of approximately 2:1, respectively, with minimal smearing as can be seen in Figure 3.1. A third minor band corresponding to 5S rRNA was also noted (Figure 3.1).

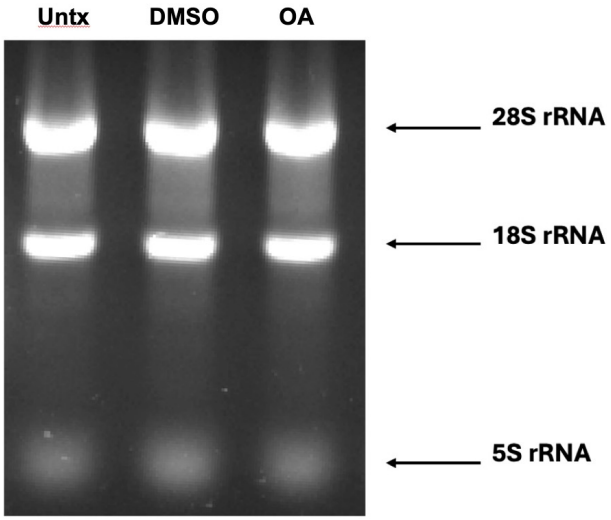


**Figure 3.1: Assessment of the integrity of the RNA samples isolated using TRI reagent.** A typical midi gel (1% w/v agarose) showing 28S rRNA,18S rRNA and 5S rRNA bands. The image is presented as a negative for clarity. DMSO was used at a concentration of 0.01%, and OA was used at a concentration of 10 nM.

### 3.2.6.3 DNase Treatment and cDNA Synthesis

To remove potential DNA contamination, RNA samples (1 µg) were DNase-treated by adding 1 µL of a 10X DNase I Reaction Buffer, 1 µL of DNase I Amp Grade, and molecular-grade water to give a total volume of 10 µL. The reaction was incubated for 15 minutes at room temperature, and the reaction was stopped by adding 1 µL of a 25 mM EDTA solution and heating to 65°C for 10 min. The RNA was then reverse transcribed to complementary DNA (cDNA) as follows. To each DNase-treated sample (11 µL), random hexamer primers (1 µL; Thermo Fisher Scientific, SO142) were added and the mixture incubated at 65°C for 5 minutes in a thermocycler. To this, 4 µL of 5X Reaction Buffer from the RevertAid Reverse Transcriptase kit (EP0442), 0.5 µL (20 U) of RiboLock RNase Inhibitor (Thermo Fisher

Scientific), 0.2 µL of 100 mM dNTP Mix (Thermo Fisher Scientific, R0191), and 1 µL (200 U) of RevertAid Reverse Transcriptase were added, and the volume brought to 20 µL. After a brief spin, the samples were placed in a thermocycler, and the following cycling conditions were run: 25°C for 10 minutes and then 42°C for 60 minutes. The reaction was terminated by heating at 70°C for 10 minutes.

### 3.2.6.4 Semi-Quantitative Real-Time PCR and Validation of RT-PCR

mRNA expression was determined using semi-quantitative RT-PCR with target-specific primers (Table 3.2) and SYBR Green GoTaq DNA polymerase (Promega, A6002). Lyophilised primers were reconstituted in molecular grade PCR water to create 100 µM master stocks, from which 10 µM working primer stocks were prepared by diluting the master stock 1:10 with molecular grade water. The RT-PCR reaction mix consisted of 10 µL of 2X SYBR Green mix, 50 ng of cDNA template, 500 nM of each forward and reverse primer, and brought to 20 µL with molecular grade water. Each PCR run included a non-template control, and all samples were processed in triplicate. The samples were placed in the thermocycler (Mx3000P QPCR System) programmed as follows: 1 cycle at (95°C for 2 min), followed by 40 cycles at (95°C for 15 sec, 62°C for 1 min, 72°C for 15 sec), with a final hold step at 4°C. Gene expression was quantified using the comparative Ct method $2^{\wedge(-\Delta\Delta Ct)}$.To optimise each primer, the validity of the primer sequences was confirmed through nucleotide search (Primer-BLAST; NCBI), while specificity and amplicon size were assessed using a dissociation curve added to the end of the PCR run. Reference housekeeping genes, such as glyceraldehyde-3-phosphate dehydrogenase (GAPDH) and glycosylphosphatidylinositol (GPI), were employed for normalisation of the gene of interest.

| Gene | NMID | Forward Sequence | Reverse Sequence |
|---|---|---|---|
| **VE-cadherin** | NM_001795.4 | ATACCAAGGTCCACTTC | GTGAGGATGCAGAGTAA |
| **GPI** | NM_001329911.2 | TCTATGCTCCCTCTGTGTTAGA | CTCCTCCGTGGCATCTTTATT |
| **GAPDH** | NM_002046.5 | CTCTGCTCCTCCTGTTCGAC | GCGCCCAATACGACCAAATC |

**Table 3.2: List of primers including gene identification numbers and sequence.**

The dissociation curve results were utilised to evaluate the amplification of non-specific products and to check for DNA contamination. Nevertheless, if specific amplification was observed in the NTC samples, the experiment's results were deemed invalid.

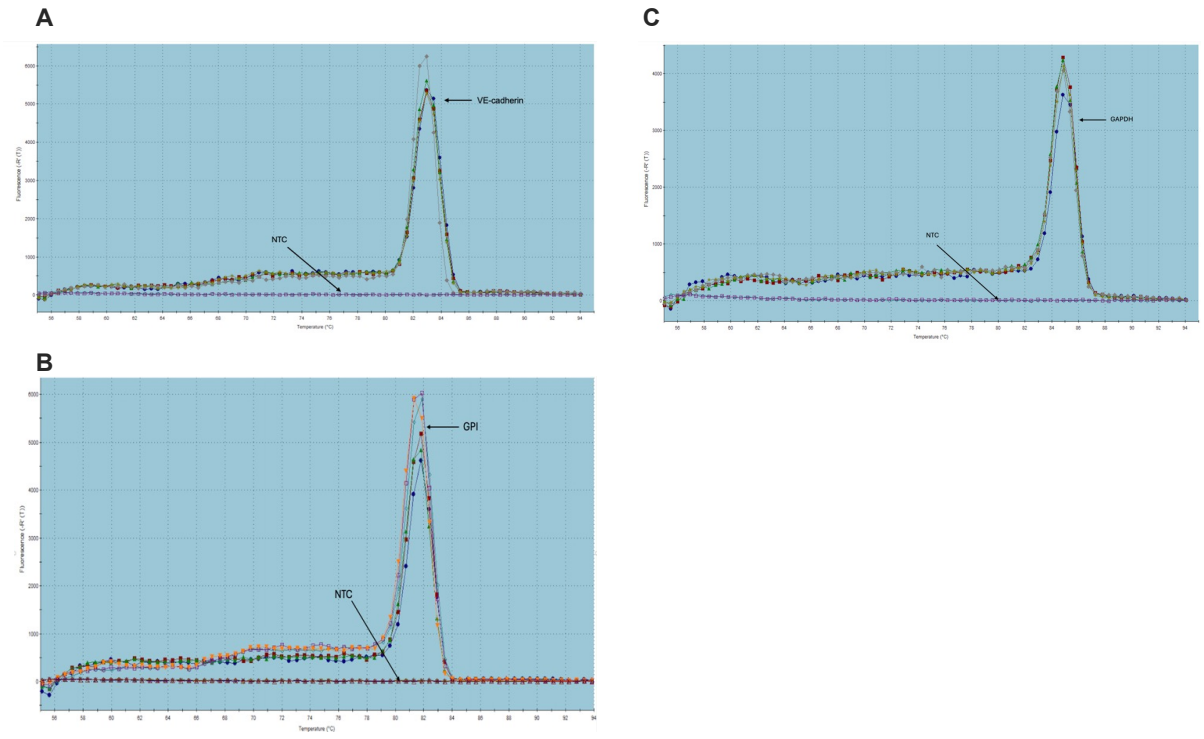


**Figure 3.2: Representative dissociation curves for VE-cadherin, GPI and GAPDH mRNA using SYBR green.** Dissociation curve of real-time SYBR Green PCR products of VE-cadherin (A), housekeeping gene GPI (B) and GAPDH (C). Temperature is plotted on the x-axis with the derivative of the fluorescence level on the y-axis. A single melt peak at 83, 85, and 82℃ indicates a single PCR product is being amplified in these samples (A, B and C), whilst No Template Control samples have low melting temperatures and non-specific amplification.

### 3.2.7 Permeability Assay

hCMEC/D3 cells were cultured on collagen-coated inserts with a pore size of 0.4 µm at a density of 4 × $10^5$ cells per/ 12 well until a confluent layer of cells developed. The monolayer was rinsed with Dulbecco′s Phosphate Buffered Saline,1xPBS (D8662, Sigma-Aldrich), and the culture medium was changed to serum-free medium for 2 h. The cells were then exposed to DMSO (0.01%) or okadaic acid (10 nM) for 24 h. The medium was then removed from the insert, and FITC-labelled dextran (200 µL) prepared in serum-free medium was added. The insert was then placed in a new plate containing 500 µL of serum-free medium. Following a

30-minute incubation period at room temperature, 100 µL of the medium in the bottom chamber was reserved and added to a 96-well plate for the determination of fluorescence. The fluorescence was measured using a fluorimeter (Thermofisher Scientific, Fluroskan Ascent FL) at an excitation wavelength of 485 nm and an emission wavelength of 530 nm (Figure 3.3).

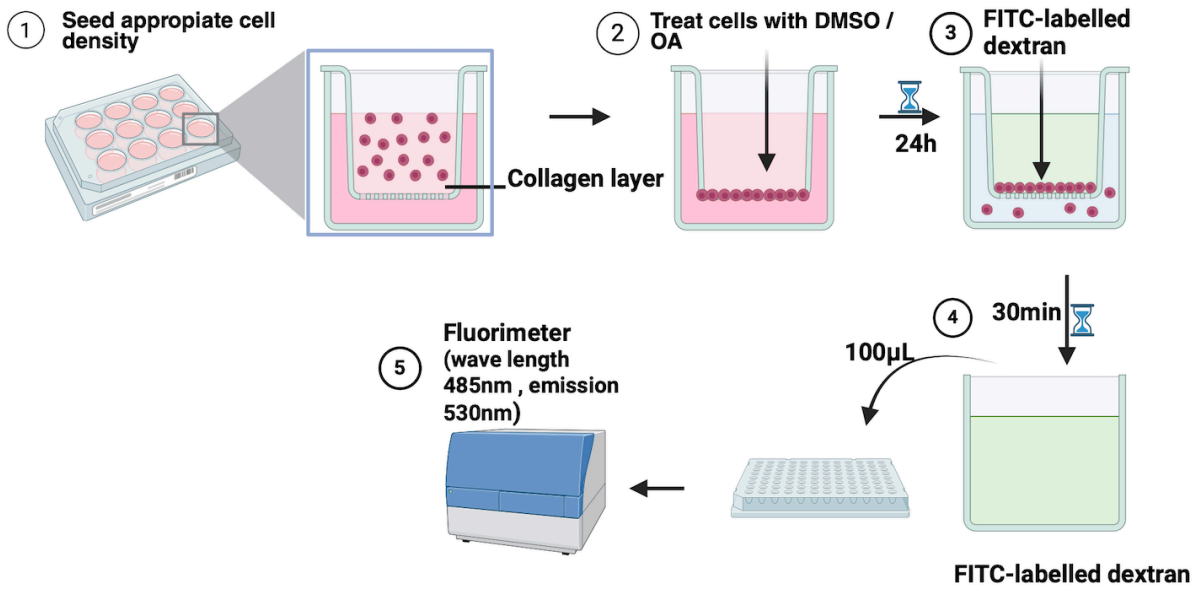


**Figure 3.3.: An illustrative diagram of the permeability assay protocol.**

### 3.2.8 PP2Ac Phosphatase Activity Assay

A commercially available PP2A immunoprecipitation assay (17-313RF, Merck Millipore) was used to determine PP2Ac activity following extraction in RIPA buffer. The PP2A immunoprecipitation phosphatase assay kit is used to detect purified PP2A or PP2A from a cellular lysate. It utilises the malachite green and contains components that have been matched to optimise sensitivity and range of detection. Protein (100 µg) was incubated for 2 h at 4°C with 4 µg of anti-PP2A (C subunit, clone 1D6) and protein-A-agarose. The mixture was centrifuged five times (Microcentrifuge Technico mini, 50 sec), during which beads were washed three times with 700 µL TBS and once with 500 µL Ser/Thr assay buffer. Then, beads were incubated with 60 µL diluted phosphopeptide and 20 µL Ser/Thr assay buffer at 30°C for 10 min in a constant temperature shaker. Finally, the mixture was centrifuged briefly (1 min), and the supernatant (25 µL) transferred to another 96-well plate (1⁄2 volume microtiter plate). A standard curve for phosphate was prepared by serial dilution of a 0.1 mM working solution of the phosphate standard in distilled water. The working solution was made by adding 125 µL of Phosphate Standard (Solution C Catalogue # 20-103) to 1125 µL of distilled water. As with the

samples, 25 µL of each phosphate standard was added to the microtiter plate along with distilled water as a blank. The working solution of malachite green was prepared by adding 10 µL of solution B to each millilitre of solution A. This working solution (100 µL) was added to each well and carefully mixed to avoid creating bubbles (Figure 3.4). The colour was allowed to develop for 15 minutes at room temperature, and the absorbance was read at a wavelength of 650 nm on a microtiter plate reader (VARIOSKAN LUX, Thermo Scientific).

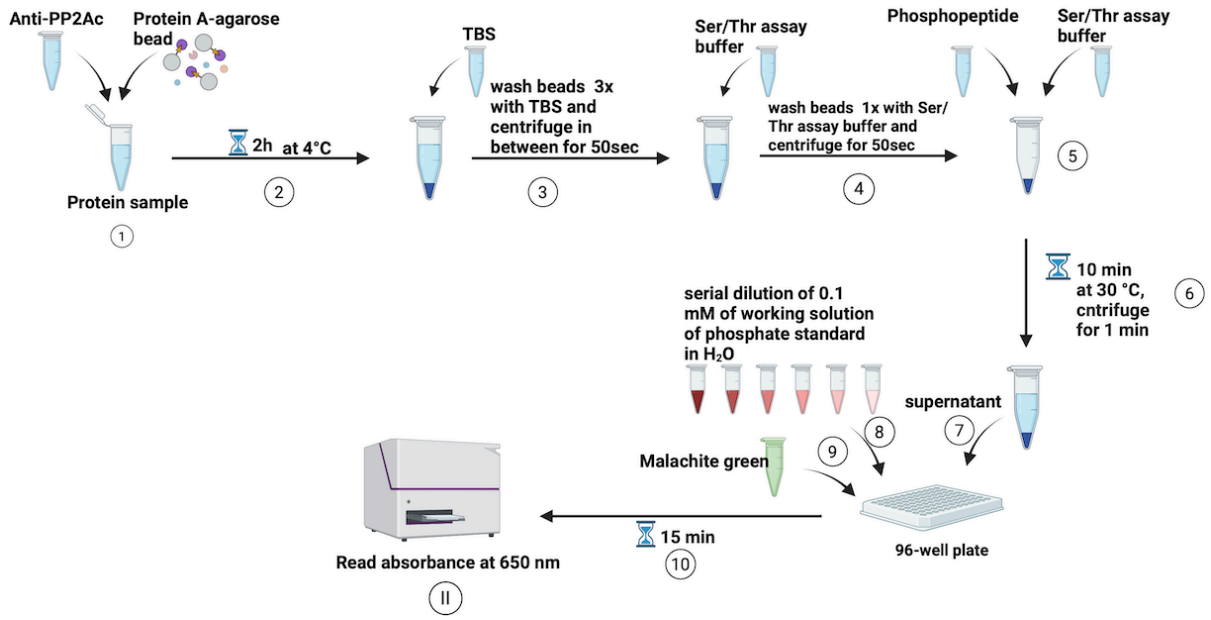


**Figure 3.4: An illustrative diagram of the PP2A phosphatase activity assay protocol.**

### 3.2.9 VE-Cadherin Immunoprecipitation Assay (Pull-down assay)

hCMEC/D3 cells were plated at a density of 600,000 cells in a T-25 flask and exposed to okadaic acid (10 nM) or DMSO (0.01%; solvent control) in a serum-free medium for 24 h. Cells were lysed in RIPA buffer containing 100x protease inhibitor Cocktail Set I (EMD Millipore Corp, USA) for 30 minutes with gentle rotation. The samples were then centrifuged at 12,000 rpm for 5 minutes at 4°C, and the supernatant was reserved for immunoprecipitation following quantification of protein concentration using a Bradford assay section (3.2.4). To the protein samples (100 µg), 1 µg of mouse control m-IgG$^{K}$ antibody and 20 µL of protein A/G-agarose conjugated agarose beads were added (Calbiochem, USA) and allowed to incubate for 30 minutes. The supernatant was mixed with 2 µg of anti-VE-cadherin antibody or 1 µg of mouse control m-IgG$^{K}$ (negative control) after centrifuging at 12000 rpm for 5 minutes and incubating for 1h at 4 °C with rotation. Following the incubation period, 20 µL of A/G-agarose conjugated agarose beads were added (Calbiochem, USA) and incubated overnight with

rotation at 4°C. Following an overnight incubation period, the mixture was centrifuged at 8,000 rpm for 2 minutes at a temperature of 4°C. After centrifugation, the beads were rinsed 5 times with PBS to remove unspecific binding. To the supernatant, 50 µL of 2x SDS without β-mercaptoethanol was added. The samples were then heated at 100°C for 5 minutes and centrifuged. Finally, 5% β-mercaptoethanol was added to the mixture and heated again. The mixture was then loaded onto an 8% SDS gel, and VE-cadherin abundance was quantified using Western Blot. The total amount of VE-Cadherin was adjusted to the level of α-actin protein.

### 3.2.10 Immunofluorescence Microscopy

hCMEC/D3 cells were cultured to confluence on collagen type I-coated 96 well plate (10,000 /well). After five days, the medium was removed and the cells washed once with prewarmed PBS before being fixed for 10 minutes with 4% β-formaldehyde in PBS pH 7.4 at room temperature. Cells were blocked with 5% BSA in PBS for one hour at room temperature to prevent unspecific binding of antibodies. Following this, the cells were incubated overnight at 4°C with anti-VE-cadherin rabbit (primary antibody 1:50; cell signalling cat. #2158S) dissolved in 5% BSA in PBS. Cells were washed three time with PBS and incubated for 1 h at room temperature with a secondary goat anti-rabbit Alexa Fluor 488 antibody (1:200, Abcam cat. #AB 150077) dissolved in 5% BSA in PBS, and the plate was covered in aluminium foil and kept in the dark. Following this, the cells were washed with PBS three times for five minutes each. The cell nuclei were counterstained with 4′,6-diamidino-2-phenylindole (DAPI) and images captured using an EVOS cell imaging system at 20x magnification.

### 3.2.11 Cell viability: MTT Assay

hCMEC/D3 cells were cultured on collagen-type I-coated 96-well plates at a density of 10,000 cells per well and cultured until they reached 75-80% confluence. The cells were washed with PBS and incubated in serum-free medium for 2 h before being exposed to okadaic acid (10 nM), dimethylsulphoxide (DMSO; 0.1% v/v, solvent control for okadaic acid, Triton X-100 (1%, positive control), or serum-free media for a further 24 h. After 22 h, MTT [3-(4,5-dimethylthiazol-2-yl)-2,5-diphenyltetrazolium bromide; 5 mg/mL in serum-free medium] was added. The plates were covered with aluminium foil and incubated at 37°C, 5% $CO_2$, and 95% humidified air for the remaining 2 h. The liquid was then removed from the plates, and 600 µL of DMSO was added to each well. The plates were then incubated for 2 minutes at 37°C to aid solubilisation of the purple formazan crystals. The purple colour was quantified by measuring

the absorbance at a wavelength of 540 nm using a spectrophotometer (BioTek, EL 808, Bedfordshire, UK). The absorbance of each well was adjusted for background by subtracting the absorbance of the blank (no cells) wells. Cell viability was expressed as a percentage of the average absorbance value from the vehicle-treated control cells (serum-free medium).

### 3.2.12 Whole Cell Lysate and Membrane/Cytosolic Fractionation

hCMEC/D3 cells were seeded on collagen-coated (section 3.2.1) Petri dishes (Thermo Scientific, USA) at a density of $4x10^6$ cells per dish and allowed to attach overnight. Following attachment, the cells were pretreated with MG132 (5 µM; proteasomal inhibitor) for 30 minutes before being exposed to DMSO (0.01%, v/v), okadaic acid (10 nM) or medium alone for 8 h. Whole-cell lysates were obtained by lysing the cells in M-PER reagent containing a Halt protease and phosphatase inhibitor cocktail (100x; 78440, ThermoScientific, USA). The dishes were agitated gently for 5 minutes, and the lysate was transferred to a microcentrifuge tube. Cell debris was removed by centrifugation (14000 x g for 10 minutes at 4°C), and the supernatant was transferred to a sterile 1.5 ml sample tube and stored at -80°C for protein quantification and Western blot analysis. The cells for the whole cell lysate and membrane fraction were taken from different petri dishes.

Membrane and cytosolic fractions were obtained using the Mem-PER™ Plus kit (Thermo Scientific, USA). Following aspiration of the culture medium, cells were resuspended in 1x PBS, released from the petri dish by scraping and collected by centrifugation at 400 x g for 20 minutes. The cell pellet was washed twice with the cell wash solution and re-pelleted each time by centrifugation (400 x g for 20 minutes). For isolation of the cytosolic protein fraction, cells were suspended in permeabilisation buffer containing a Halt protease and phosphatase inhibitor cocktail (100x; 78440, ThermoScientific, USA), vortexed and incubated at 4°C for 10 minutes with continuous mixing. Cellular debris was removed by centrifugation at 16000 x g for 15 minutes, and the supernatant containing the cytosolic proteins was transferred to a separate tube. The pellet was retained for the extraction of membrane proteins.
The reserved pellet was resuspended in solubilisation buffer containing a Halt protease and phosphatase inhibitor cocktail (100x; 78440, ThermoScientific, USA) by pipetting, incubated at 4°C for 30 minutes under continuous mixing. After 30 minutes, the mixture was centrifuged at 16000 x g for 15 minutes at 4°C, and the supernatant (membrane fraction) was transferred to a fresh tube and stored at -80 °C for downstream analysis.

The purity of subcellular fractions obtained from the identical starting sample was assessed by testing for the presence of pan-cadherin protein (membrane fraction) and Hsp90 protein (cytosolic fraction) using Western blot analysis (section 3.2.5). Quantitative analysis of the blots was not performed because the primary purpose of this experiment was to verify the purity of the fractions rather than to compare protein abundance between samples, in accordance with the instructions provided in the kit used.

### 3.2.13 Data and Statistical Analysis

All data were normalised to the appropriate control and expressed as either an absolute value, a percentage or a ratio. Protein concentration was interpolated from standard curves using non-linear regression (Graphpad Prism version 10). Data were analysed by one-way ANOVA with post hoc analysis (Dunnett's, Bonferroni) as appropriate (Graphpad Prism version 10). Protein abundance was normalised relative to β-actin, and mRNA expression was normalised to the geometric mean of GAPDH and GPI. Sample sizes (3-5) were determined based on power calculations to ensure at least 80% power to detect biologically meaningful differences at a significance level of $P < 0.05$. Increasing the sample size improves the statistical power of the study, enhancing the reliability of the results and supporting their suitability for publication in high-impact journals. Data are expressed as mean ± S.E.M., and a value of $P < 0.05$ was taken to indicate statistical significance.

## 3.3 Result

### 3.3.1 Effect of Okadaic Acid on VE-cadherin Abundance in hCMEC/D3 Cells

As okadaic acid has been used as a model of memory impairment in rats [545], I wanted to establish if it could be used as a model to alter VE-cadherin abundance in hCMEC/D3. To this end, I exposed hCMEC/D3 cells to increasing concentrations of okadaic acid (1-20 nM) for 24 h and investigated its effect on VE-cadherin abundance using Western blot. At the lower end of the concentration range of (1 and 5 nM), okadaic acid did not alter VE-cadherin abundance compared to the untreated group (medium alone; Figure 3.5A, B). In contrast, at a concentration of 10 and 20 nM, okadaic acid decreased VE-cadherin abundance by approximately 50 and 70% (Figure 3.5A, B; $P<0.05$), respectively, compared to the untreated group. DMSO (0.01% v/v; solvent control) did not change VE-cadherin abundance in hCMEC/D3 cells. From the immunoblots presented in Figure 3.5B and C, single bands were detected with a molecular weight of 130 kDa (Figure 3.5B) and 43 kDa (Figure 3.5C), consistent with the expected molecular weight for VE-cadherin and β-actin.

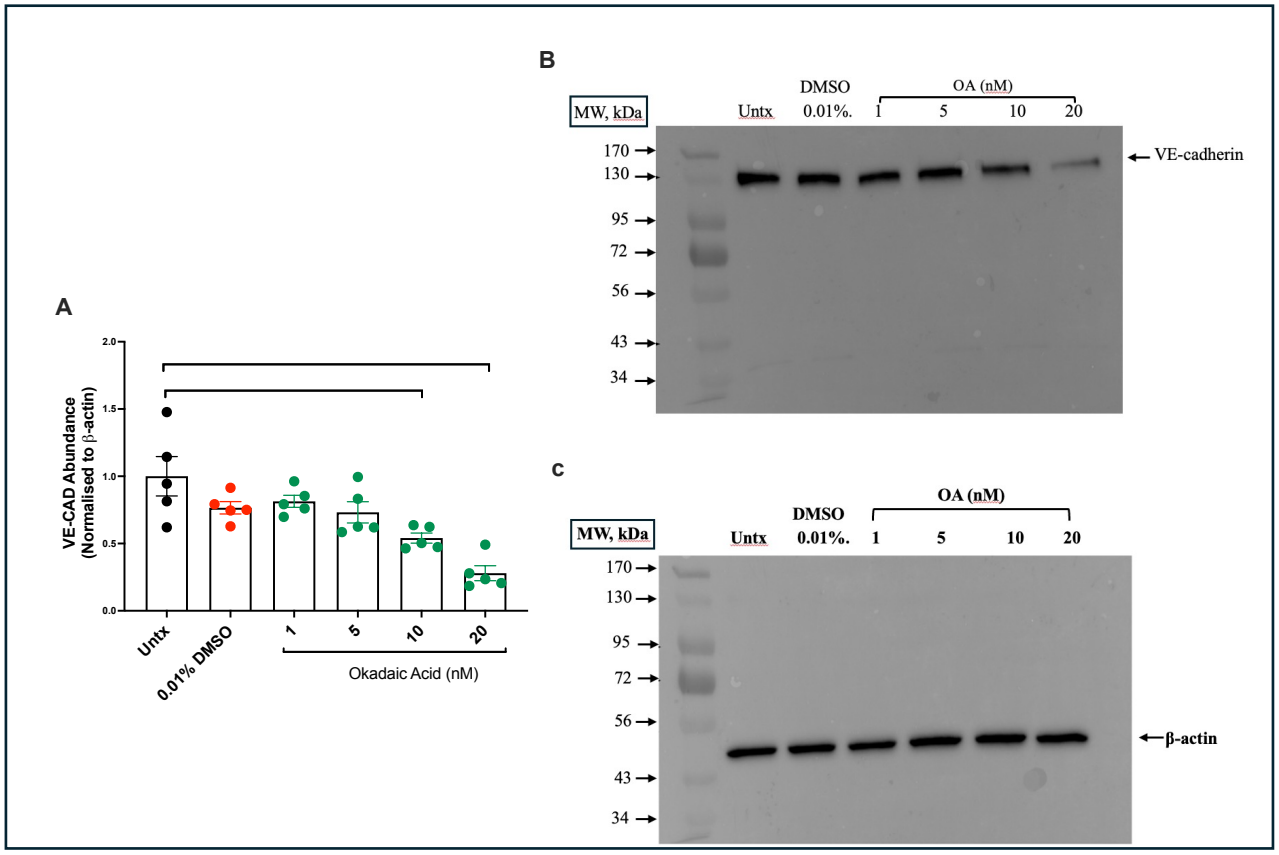


**Figure 3.5: Concentration-dependent effect of okadaic acid on VE-cadherin abundance.**

### 3.3.2 Effect of Okadaic Acid on VE-cadherin Abundance in bEND3 and EAhy926 Cell Lines

To determine if the effect of okadaic acid on VE-cadherin abundance was translatable to other endothelial cell lines, I also investigated its effect in bEND3 (mouse brain endothelial) and EAhy926 (immortalised human umbilical endothelial) cells. Okadaic acid did not appear to alter VE-cadherin abundance in bEND3 cells at any concentration studied (20-50 nM, Figure 3.5A, C, exploratory data; n=2) compared to the untreated group (Untx). Similarly, okadaic acid (10-40 nM) did not alter VE-cadherin abundance in EAhy926 cells compared to the control group (Untx; Figure 3.6B, D; n=2). DMSO had not altered VE-cadherin abundance in either cell line compared to the medium alone (Untx; Figure 3.6A-D). Based on this, I focused subsequent work on the hCMEC/D3 cell line.

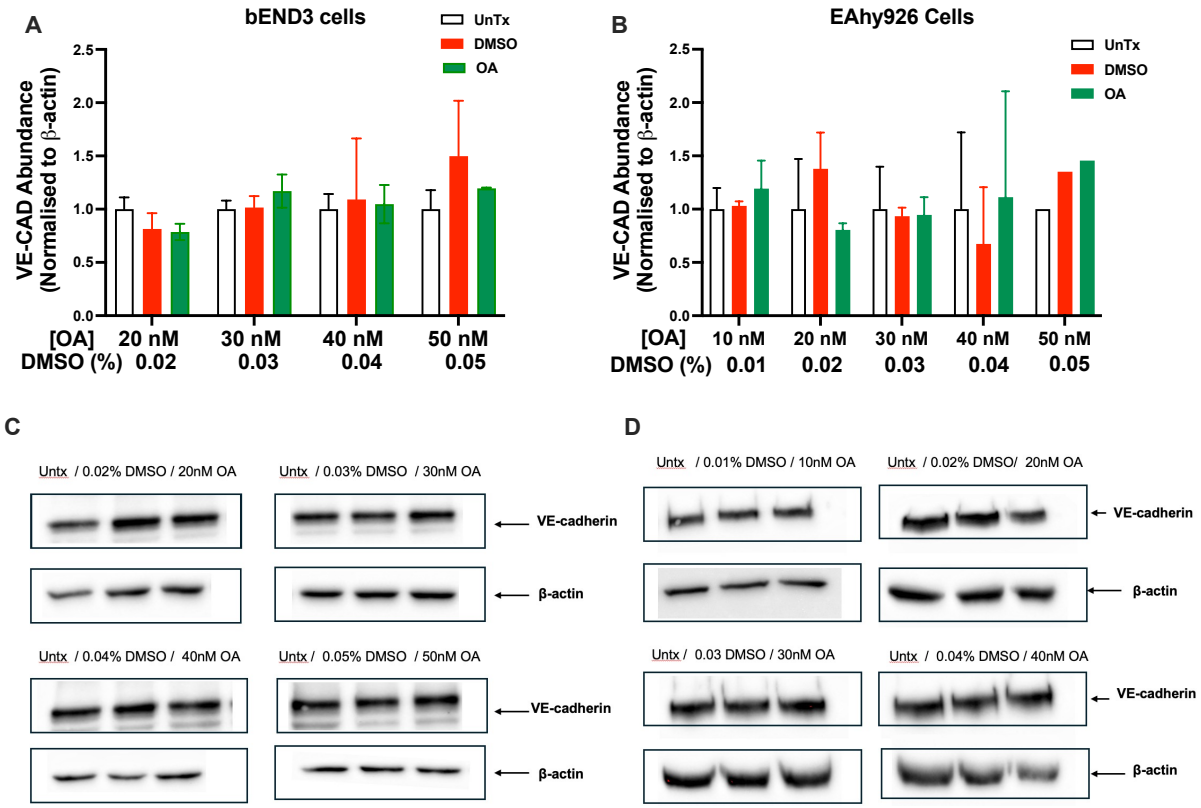


**Figure 3.6: Effect of okadaic acid on VE 1VE-cadherin abundance in bEND3 and EAhy926.** Mouse brain endothelial cells (bEND3; A, C) and immortalised human umbilical endothelial cells (Eahy926; B, D) were exposed to okadaic acid (OA; 10-50 nM), DMSO (0.01-0.05 % v/v; solvent control) or medium only (Untx) for 24 h. VE-cadherin abundance was determined in cell lysates using Western blot. Data were normalised to β-actin and expressed relative to the untreated group and presented as mean ± S.E.M. (n=2). Data are analysed using a one-way ANOVA with post hoc analysis (Dunnett's test, relative to Untx at each concentration). Representative blots are presented in C (bEND3) and D (Eahy926).

### 3.3.3 Effect of Okadaic Acid on hCMEC/D3 Cell Viability

To confirm that the okadaic acid-mediated reduction in VE-cadherin was not due to effects on cell viability, an MTT assay was utilised. Okadaic acid at concentrations of 10 and 20 nM (Figure 3.7A, B) did not alter the viability of hCMEC/D3 cells following 24 h exposure compared to medium alone (Untx) or DMSO (0.01 and 0.02% v/v). Similarly, DMSO did not alter cell viability at any concentration studied (Figure 3.7A, B). As expected, Triton X100 (1% v/v; positive control) decreased cell viability by 80-90% compared to the untreated group (Figure 3.7A, B).

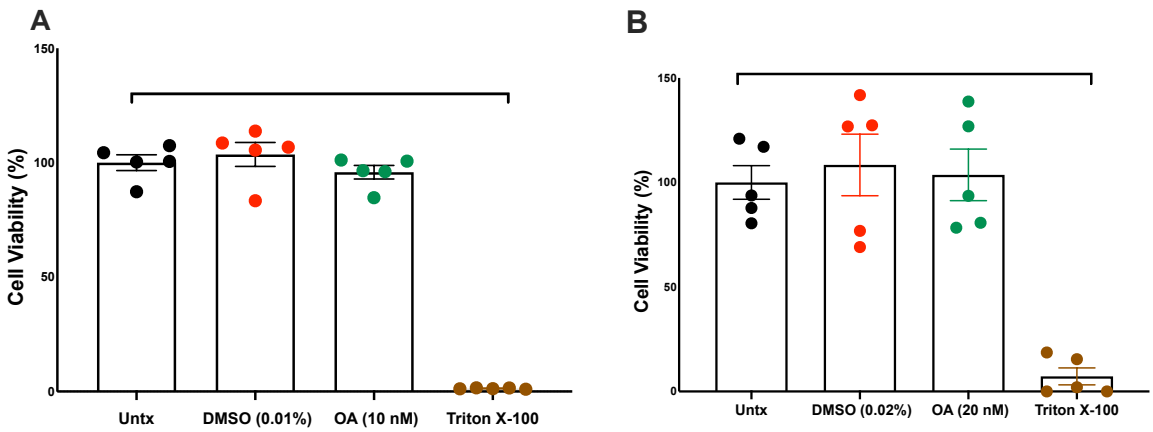


**Figure 3.7: Effect of okadaic acid on cell viability.** hCMEC/D3 cells were exposed to DMSO (A: 0.01% v/v; B 0.02% v/v), okadaic acid (A: 10nM; B: 20nM), medium alone Untx (A, B) or Triton X-100 (1% v/v; positive control; A, B) for 24h and the effect on cell viability using an MTT assay. Data were analysed using one-way ANOVA with *post hoc* analysis (Dunnett's test) and presented as mean ± S.E.M. Horizontal bars indicate statistical significance at $P<0.05$ (n=5).

### 3.3.4 Effect of Okadaic Acid on VE-cadherin Abundance and mRNA Expression

To confirm and extend the data from the okadaic acid dose-response relationship, the effect of okadaic acid (10 nM and 20 nM) on VE-cadherin abundance and mRNA expression was investigated in hCMEC/D3 cells. Consistent with the earlier experiment, exposure to okadaic acid (10 and 20 nM) for 24 h decreased VE-cadherin abundance by 50% and 70% ($P<0.05$), respectively, compared to medium alone (Untx; Figure 3.8A, B). DMSO (0.01% and 0.02% v/v) did not alter VE-cadherin abundance compared to Untx (Figure 3.8A, B). Interestingly, okadaic acid at a concentration of 10 nM increased ($P<0.05$, Figure 3.7C) VE-cadherin mRNA

expression by 1.5-fold, while at the higher concentration of 20 nM VE-cadherin mRNA expression was decreased by 77% ($P<0.05$; Figure 3.8D). DMSO (0.01 and 0.02% v/v) did not affect VE-cadherin mRNA expression compared to the Untx group (Figure 3.8C, D). Based upon these data, okadaic acid was used at a concentration of 10 nM in all further experiments.

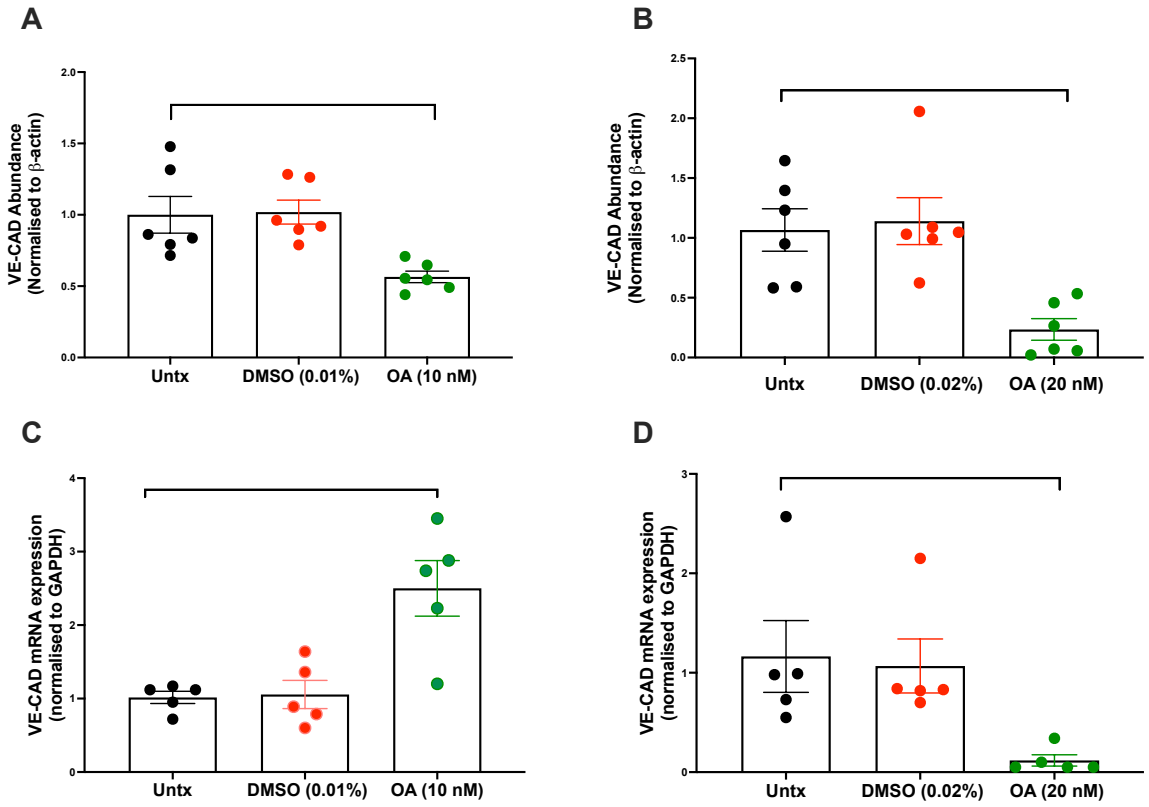


**Figure 3.8: Effect of okadaic acid on VE-cadherin abundance (A, B) and mRNA expression (C, D) in hCMECD3 cells.** Cells were exposed to 10 nM (A and C) or 20 nM (B and D) okadaic acid (OA) for 24 h. DMSO (0.01% A, C; 0.02% v/v B, D) was included as the solvent control. VE-cadherin abundance was determined in cell lysates using Western blot (A, B), while mRNA expression was determined using semi-quantitative PCR (C, D). Data were normalised to β-actin or the geometric mean of GAPDH and GPI and expressed relative to the untreated group as appropriate. Data were analysed using a one-way ANOVA with post hoc analysis (Dunnett's test) and presented as mean ± S.E.M. Horizontal bars indicate statistical significance at $P<0.05$ (n=5, C /D or n=6, A/B).

### 3.3.5 Effect of Okadaic Acid on Protein Phosphatase 2Ac (PP2Ac) Activity and Abundance

Exposure of hCMEC/D3 cells to okadaic acid (10 nM) for 24 h decreased PP2Ac activity by 60% compared to the untreated group (Figure 3.9A; $P<0.05$). When the effect of okadaic acid on PP2Ac abundance was investigated, it was found to be unaltered compared to the control group (Figure 3.9B). DMSO (0.01% v/v) did not affect PP2Ac activity or abundance compared to those exposed to medium alone (Untx; Figure 3.9A, B). These data indicate that OA inhibits PP2Ac activity independently of a change in PP2Ac abundance.

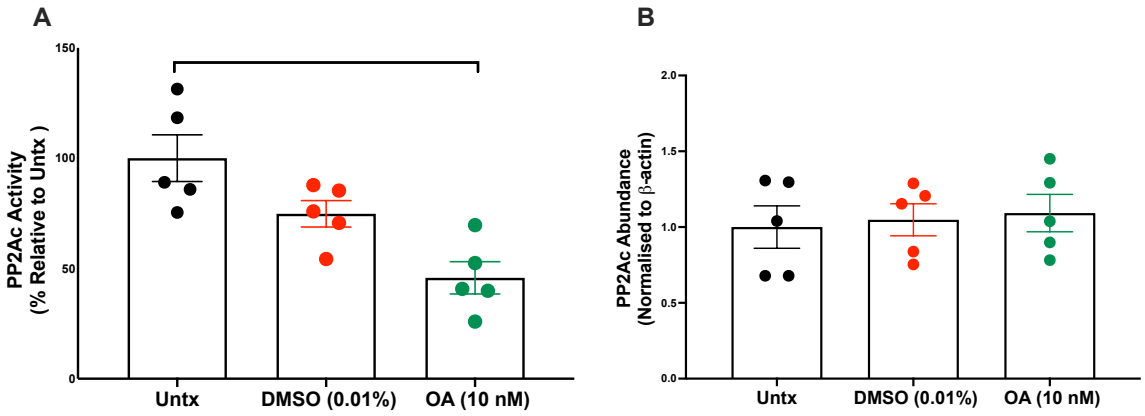


**Figure 3.9: Effect of okadaic acid on PP2Ac activity and abundance.** hCMEC/D3 cells were exposed to okadaic acid (OA; 10 nM) and its effect on PP2Ac activity was determined using a PP2Ac immunoprecipitation activity assay (A), while abundance was measured using Western blot (B). PP2Ac activity was expressed relative to the control group (Untx), while abundance was normalised to β-actin and expressed relative to the untreated group (B). Data were analysed using a one-way ANOVA with *post hoc* analysis (Dunnett's test) and presented as mean ± S.E.M. Horizontal bars indicate statistical significance at $P<0.05$ (n=5).

### 3.3.6 Effect of Proteasomal and Lysosomal Inhibition on Okadaic Acid-Mediated Downregulation of VE-cadherin

To investigate if proteasomal or lysosomal degradation could underpin the mechanism by which okadaic acid reduces VE-cadherin abundance, hCMEC/D3 cells were exposed to MG132 (proteasomal inhibitor) or chloroquine (lysosomal inhibitor). The initial MG132 experiments were conducted with a limited set of conditions to establish the baseline response of VE-cadherin to proteasomal inhibition. Based on these results, additional conditions were included in the chloroquine experiments to allow a more comprehensive comparison and interpretation

of lysosomal inhibition effects. In the presence of MG132 (5 μM), okadaic acid (10 nM) did not reduce VE-cadherin abundance compared to the untreated group with MG132 (Figure 3.10A). In contrast, okadaic acid, in the presence of chloroquine (100 μM), still reduced VE-cadherin abundance by approximately 70% compared to the untreated (Untx with chloroquine) group (Figure 3.10B; $P<0.05$). DMSO did not affect the abundance of VE-cadherin in the presence of either MG132 or chloroquine (Figure 3.10A, B).

To extend the data obtained in the presence of MG132, I investigated if okadaic acid increased the ubiquitination of VE-cadherin using a pull-down assay. In hCMEC/D3 cells okadaic acid increased ubiquitination of VE-cadherin by 70% compared to medium alone (Untx; Figure 3.9C; $P< 0.05$). DMSO had no effect (Figure 3.10C). Negative control (Isotype control) was mouse IgG mk.

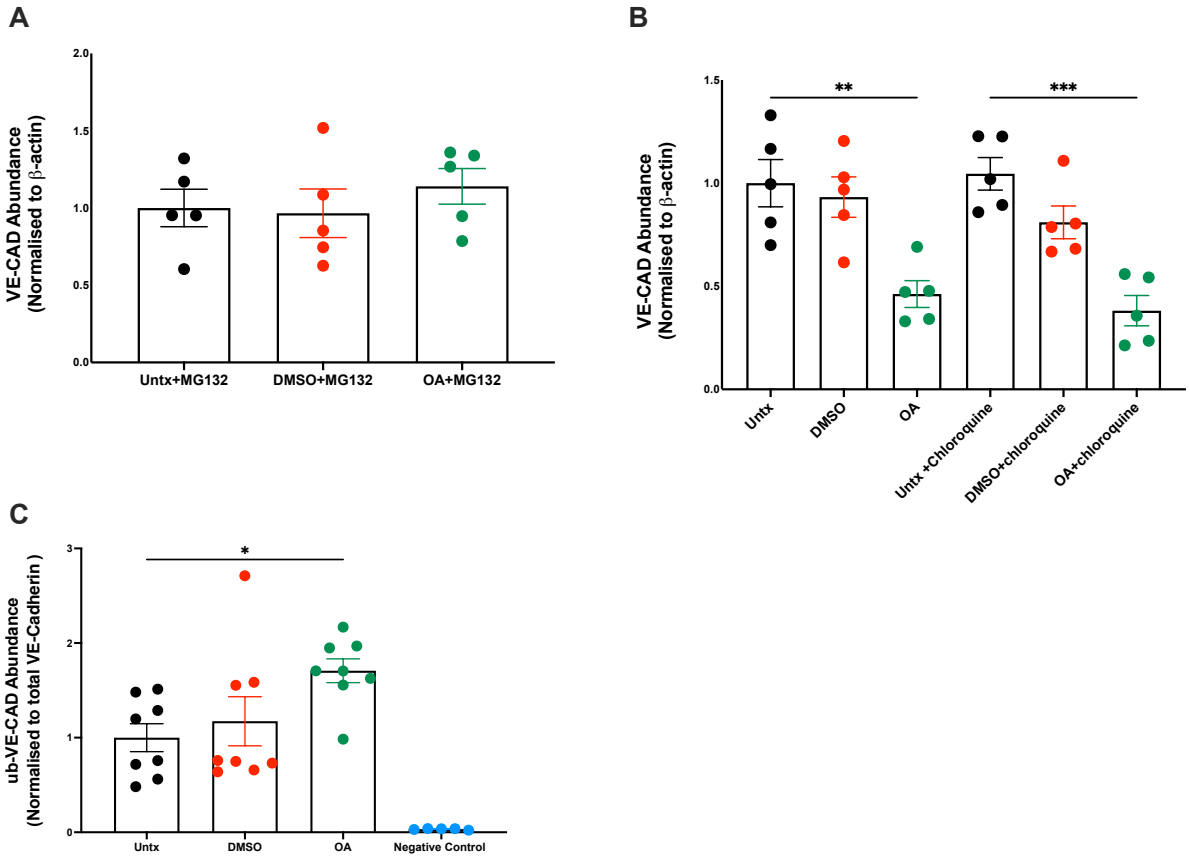


**Figure 3.10: Effect of proteasomal and lysosomal inhibition on VE-cadherin abundance and ubiquitination following exposure to okadaic acid in hCMECD3 cells.** Proteasomal degradation was investigated using MG132 (5 µM) after exposure of cells to OA and DMSO for 8 hours (A), lysosomal degradation was assessed using chloroquine (100 µM) after exposure of cells to OA and DMSO for 24 hours (B), and VE-cadherin was immunoprecipitated from whole cell lysate (C). The abundance of VE-cadherin and Ubiquitin-VE-cadherin was assessed via Western blot (A, B, C), normalised to β-actin, and expressed relative to the untreated group as mean ± S.E.M. (n=5 or 8). Data were analysed using a one-way ANOVA with *post-hoc* analysis (Dunnett's test). Horizontal bars denote statistical significance at $P<0.05$.

### 3.3.7 Effect of Okadaic Acid on Membrane and Cytosolic Location of VE-cadherin in hCMEC/D3 Cells

Membrane and cytosolic fractionation were used to determine if the reduction of VE-cadherin in whole-cell lysate is associated with loss from the plasma membrane. Okadaic acid (10 nM) reduced VE-cadherin abundance in the whole cell lysate by approximately 60% and by around 50% in the membrane fraction compared to the untreated group (Figure 3.11A-D; $P < 0.05$). In the cytosolic fraction, VE-cadherin was undetected in all groups (Figure 3.11E); β-actin

abundance in all figures (Figure 3.11B, D and E). DMSO (0.01% v/v) did not affect the abundance of VE-cadherin in either the whole cell or membrane fractions compared to the untreated group (Figure 3.11A-D).

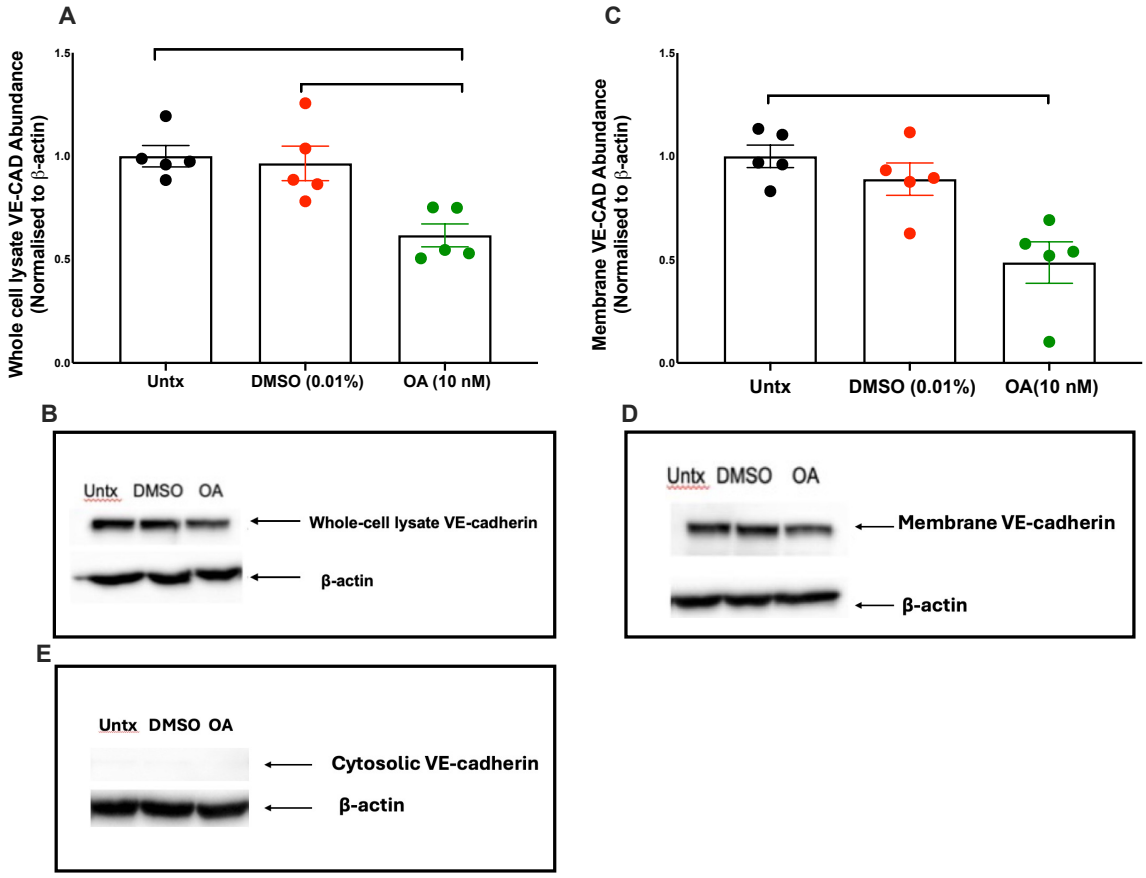


**Figure 3.11: VE-cadherin abundance by cellular compartment following exposure to okadaic acid.** The effect of okadaic acid (OA; 10nM), media alone or DMSO (0.01%) on VE-cadherin abundance in Whole-cell lysate (A, B), membrane fraction (C, D) and cytosolic fraction (E) was determined using Western Blot. VE-cadherin abundance was normalised to β-actin and expressed relative to the untreated group (Untx). Data were analysed using a one-way ANOVA with a *post hoc* analysis (Dunnett's test). Horizontal bars indicate statistical significance at $P<0.05$ (n=5). Representative blots are presented in B and D.

### 3.3.8 Effect of Okadaic Acid on Whole Cell Lysate, Membrane and Cytosolic Location of Pan-cadherin and HSP90 in hCMEC/D3 Cells

The purity of the whole cell lysate, cytosolic, and membrane fractions was assessed by probing for Pan-cadherin (membrane fraction; Figure 3.10A, B and C) and HSP-90 (cytosolic fraction; Figure 3.12A, B and C). The presence of pan-cadherin was detected in both whole-cell lysate (Figure 3.12A) and membrane fractions (Figure 3.12C) but was undetectable in the cytosolic

fraction (Figure 3.12B). Additionally, the abundance of HSP90 was much higher in the cytosolic rather than whole cell lysate or membrane fractions. Together, these data demonstrate the intensity of the fractionation process.

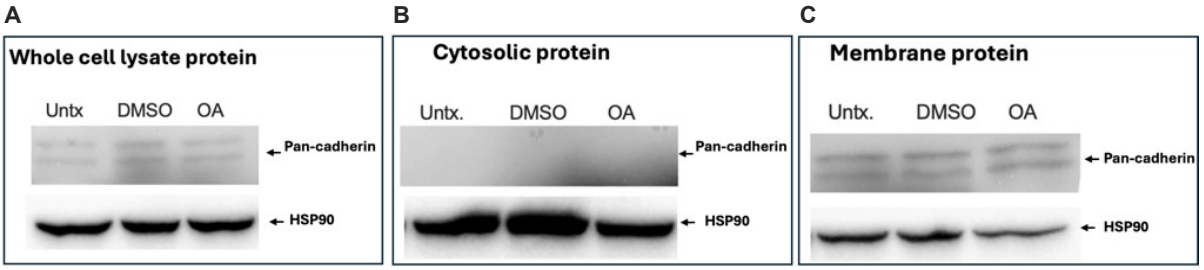


**Figure 3.12: Pan-cadherin and HSP90 abundance by cellular compartment following exposure to okadaic acid.** The effect of okadaic acid (OA; 10nM), media alone or DMSO (0.01%) on Pan abundance in Whole-cell lysate (A), membrane fraction (C) and cytosolic fraction (B) was determined using Western Blot. Representative blots are presented in A, B and C.

### 3.3.9 Effect of Proteosome Inhibitor (MG132) in Combination with Okadaic Acid on VE-cadherin Abundance in hCMEC/D3

To expand the subcellular fraction and earlier data, I investigated if proteasomal inhibition by MG132 could restore VE-cadherin and increase it in the cytosolic fraction. In the presence of MG132 (5 μM), okadaic acid did not alter VE-cadherin abundance in whole cell lysate compared to the Untx or DMSO groups (Figure 3.13A, B). Likewise, okadaic acid did not affect VE-cadherin abundance in the membrane fraction compared to Untx or DMSO groups in the presence of MG132 (Figure 3.13C, D). Interestingly, in the presence of MG132 alone or in combination with okadaic acid or DMSO, VE-cadherin was not detected in the cytosolic fraction (Figure 3.13E). In the presence of MG132, DMSO (0.01% v/v) did not alter VE-cadherin abundance in whole cell lysate or membrane fractions compared to the Untx plus MG132 group (Figure 3.13A-E). Figures 3.11 and 3.13 are conceptually connected and should be interpreted together, as both examine VE-cadherin distribution across subcellular fractions. Figure 3.11 shows the effect of okadaic acid alone, whereas Figure 3.13 extends this analysis by assessing okadaic acid in combination with MG132, although these experiments were conducted using separate sample sets. Together, Figures 3.11 and 3.13 show that okadaic acid reduces membrane-associated VE-cadherin and that this loss is prevented by proteasomal

inhibition with MG132, indicating that the reduction in VE-cadherin occurs via a proteasome-dependent degradation pathway rather than redistribution to the cytosol.

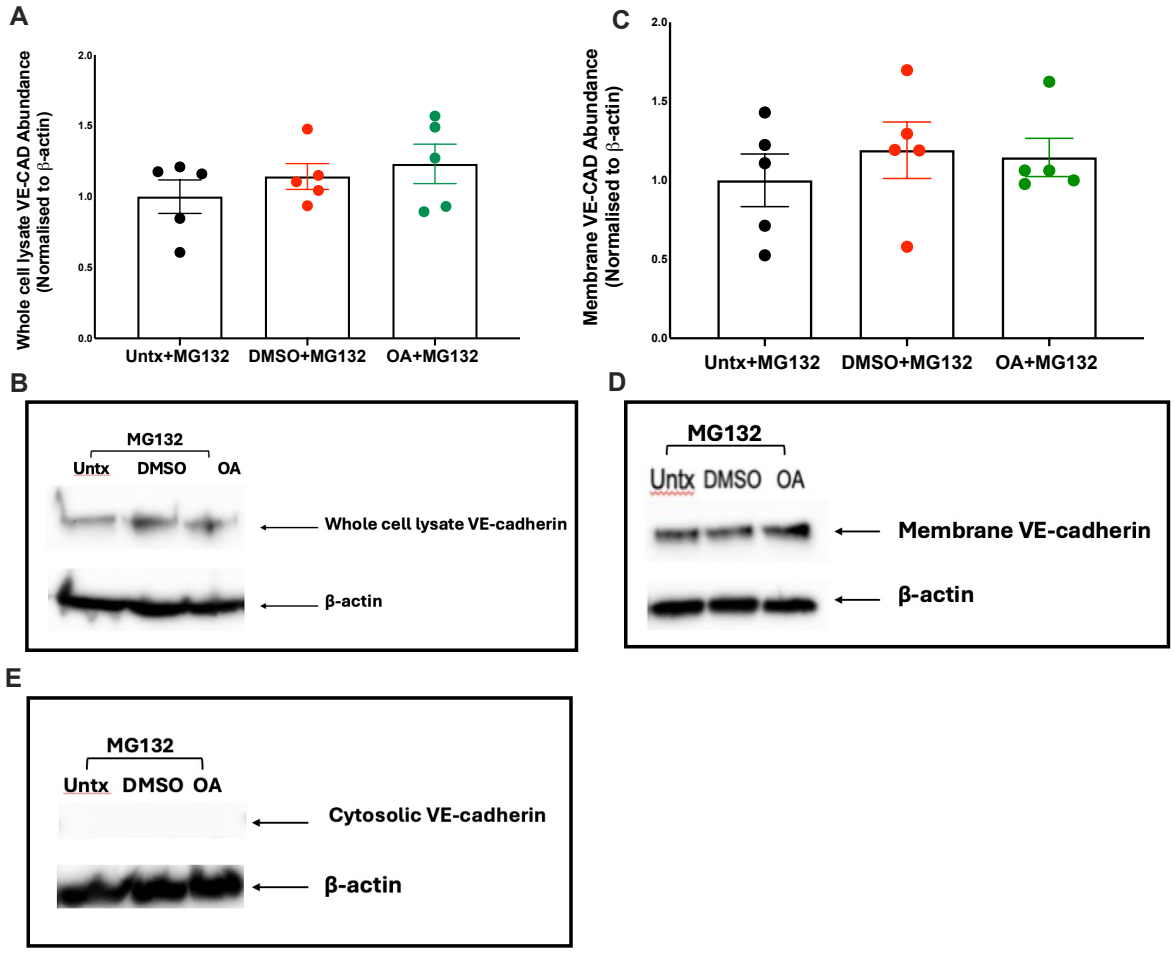


**Figure 3.13: VE-cadherin abundance in whole cell lysate, cytosolic and membrane fractions following exposure to okadaic acid in combination with MG132.** Exposing hCMEC/D3 cells to the proteasome inhibitor MG132 (5 µM) in combination with okadaic acid (OA; 10 nM) for 8 hours. Subsequently, the fractions were obtained with M-PER mammalian protein extraction reagent and Mem-PER plus membrane protein extraction kit. VE-cadherin abundance in whole cell lysate, cytosolic and membrane fractions was assessed via Western blot, normalised to β-actin, expressed relative to the untreated group, and reported as mean ± S.E.M. (n=5). A representative Western blot (C-E) display for data obtained from whole cell lysate, cytosolic and membrane fractions obtained from cells treated with okadaic acid combined with the proteasome inhibitor MG132. Data were analysed with a one-way ANOVA with a *post hoc* analysis (Dunnett's test).

### 3.3.10 Effect of Proteosome Inhibitor (MG132) in Combination with Okadaic Acid on Pan-cadherin and HSP90 Abundance in hCMEC/D3

To read out any possible confounding influence of MG132 on subcellular fraction, the purity of the whole cell lysate, cytosolic, and membrane fractions was evaluated using Pan-cadherin (membrane fraction) and HSP-90 (cytosolic fraction) as specific markers (Figure 3.14A-C). Pan-cadherin was detected in both the whole-cell lysate (Figure 3.14A) and membrane fractions (Figure 3.14C) but was undetectable in the cytosolic extracted fraction (Figure 3.14 B), verifying the quality of the fractionation protocol of HSP90 was as expected the abundance of HSP90 (cytosolic marker) was enriched in the cytosolic fraction compared to either the whole cell or membrane fractions (Figure 3.14A and C).

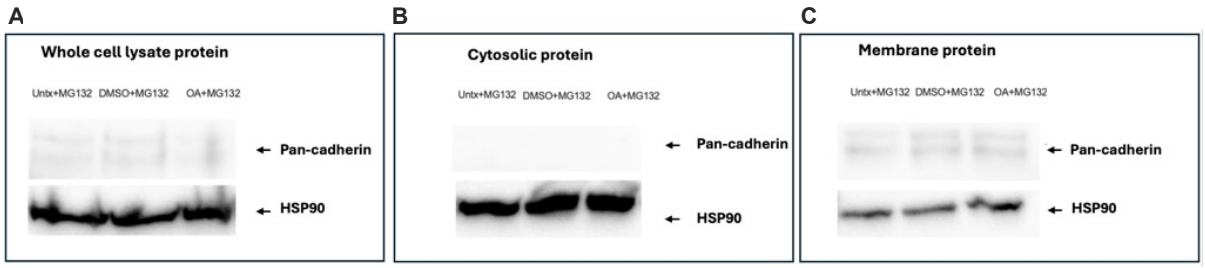


**Figure 3.14: Pan-cadherin and HSP90 abundance in whole cell lysate, cytosolic and membrane fractions following exposure to okadaic acid in combination with MG132.** Exposing hCMEC/D3 cells to the proteasome inhibitor MG132 (5 µM) in combination with okadaic acid (OA) (10 nM) for 8 hours. Subsequently, the fractions were obtained with M-PER mammalian protein extraction reagent and Mem-PER plus membrane protein extraction kit. Pan-cadherin and HSP90 abundance in whole cell lysate (A), cytosolic (B) and membrane fractions (C) was assessed via western blot. A representative Western blot (C-E) displays data obtained from whole cell lysate, cytosolic and membrane fractions obtained from cells treated with okadaic acid combined with the proteasome inhibitor MG132 (A-C).

### 3.3.11 Effect of Okadaic Acid on VE-cadherin Localisation in hCMEC/D3

An immunofluorescence approach was used to visualise VE-cadherin localisation in hCMEC/D3 before and after exposure to okadaic acid (10 nM). In the absence of okadaic acid, VE-cadherin was predominantly localised at the plasma membrane (Figure 3.15). Following exposure to okadaic acid, VE-cadherin can be seen to redistribute to the cytoplasm (Figure 3.15). Annotations (arrows) have been added to the images to indicate the regions of positive VE-cadherin immunoreactivity, including membrane-associated and cytoplasmic staining.

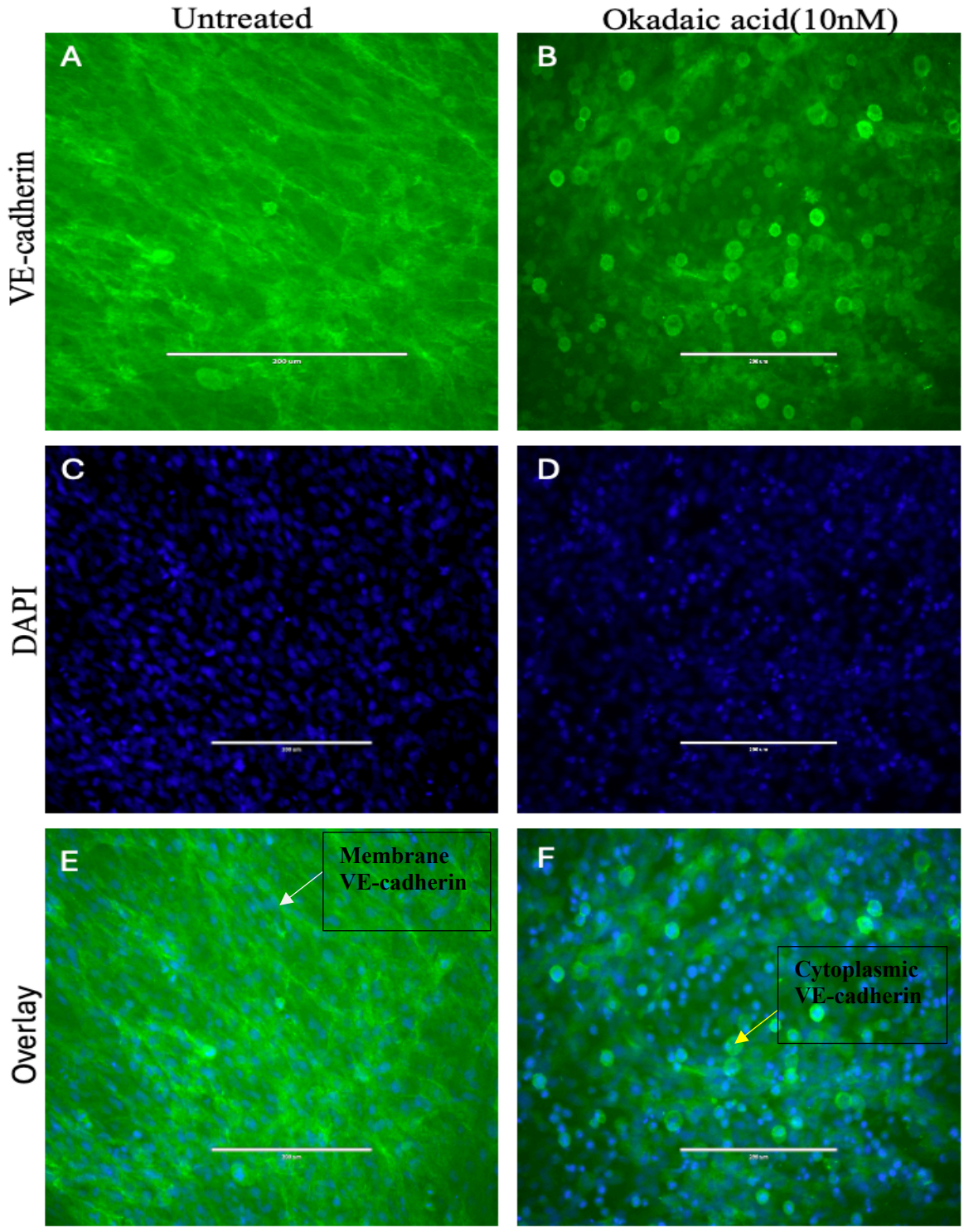


**Figure 3.15: VE-cadherin localisation in hCMEC/D3 cells following exposure to okadaic acid.** A representative image from one experiment showing VE-cadherin localisation in the absence (Untx) and presence of okadaic acid OA (10 nM B, D and F). VE-cadherin staining (green), DAPI nuclear staining (blue), Scale bar (200 µm, 20X). White arrows indicate membrane-localised VE-cadherin in the control condition, and yellow arrows indicate cytoplasmic VE-cadherin following okadaic acid treatment.

### 3.3.12 Effect of Okadaic Acid on Permeability of hCMEC/D3 Monolayers

To investigate the functional effect of okadaic acid on a surrogate marker of blood-brain barrier permeability, a transwell permeability assay was used. Okadaic acid at a concentration of 10 nM enhanced the permeability of hCMEC/D3 cells to FITC-labelled dextran by 187.1% compared to the untreated group (Figure 3.16; $P < 0.05$). Lipopolysaccharide (positive control) increased the permeability of hCMEC/D3 by 67% compared to control (Figure 3.16; $P < 0.05$), while DMSO (0.01%) did not affect cell permeability.

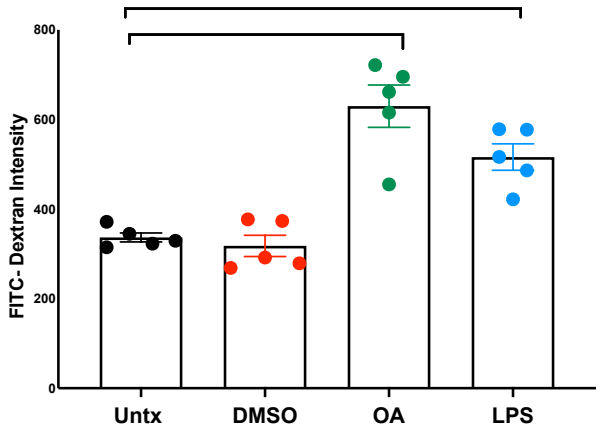


**Figure 3.16: Impact of okadaic acid on h 1hCMECD3 permeability.** Cell permeability was assessed using a FITC-labelled dextran-based transwell assay. hCMEC/D3 cells were exposed to okadaic acid (OA, 10 nM), Lipopolysaccharide (LPS, 50 µg/ml; positive control), DMSO (0.01% v/v) or medium (Untx) for 24 h, and the translocation of FITC-labelled dextran measured. Data were analysed using a one-way ANOVA with a *post hoc* analysis (Dunnett's test). Horizontal bars indicate statistical significance at $P<0.05$ (n=5).

## 3.4 Discussion

In my study, I developed a model using okadaic acid to study the role of PP2A in modulating BBB function. Specifically, I examine the impact of protein phosphatase inhibition on the adherens junction protein VE-cadherin, a key component of BBB integrity. VE-cadherin's function in preserving blood-brain barrier integrity is well documented [70]. In this study, I show that okadaic acid decreases the abundance of VE-cadherin in hCMEC/D3 cells at a concentration of 10 nM and 20 nM. This is attributed to selective inhibition of PP2A as OA has a higher affinity toward PP2A than PP1 (Ki=0.032 nM for PP2A vs 147 nM for PP1) [546]. Despite this, it is worth considering that even a modest inhibition of protein phosphatase 1 (PP1) may influence cellular signalling, as PP1 and PP2A share multiple substrates and signalling pathways. To definitively attribute the observed effect to PP2A inhibition, a targeted genetic approach using siRNA or overexpression of endogenous inhibitors would need to be used. The decrease in VE-cadherin abundance observed in this study is consistent with previous reports demonstrating that PP2A activity contributes to the stabilisation of endothelial junctional complexes. Inhibition of PP2A has been shown to impair adherens and tight junction organisation in endothelial cells through increased phosphorylation and internalisation of junctional proteins [411]. Thus, the reduction in VE-cadherin following OA treatment aligns with the known consequences of PP2A inhibition within endothelial barriers. Hence, a concentration of 10 nM of okadaic acid was used in subsequent experiments to minimise the possibility of inhibiting PP1 [538], PP4, PP5 and PP2B [547].

To determine if the impact of okadaic acid on VE-cadherin is applicable to other endothelial cell lines and across species, I examined its effects on immortalised human umbilical vein endothelial cells (EAhy926) and mouse brain microvascular endothelial cells (bEND3). In these cell lines, okadaic acid did not alter VE-cadherin abundance at concentrations up to 50 nM. There may be several factors contributing to this: 1) variations in tissue source; hCMEC/D3 are human microvascular endothelial cells immortalised via a lentivirus including hTERT and SV40 large T antigen, whereas EAhy926 are human umbilical vein endothelial cells fused with A549 epithelial cells from a human adenocarcinoma, and bEND3 cells are brain endothelial cells derived from a mouse with endothelium [494], 2) Difference in cell type: immortalised cells (bEND3, EAhy926). Immortalisation is a complex process that involves multiple stages where cells are subjected to different selection criteria after being introduced to the required genetic material [489]. These modifications can alter the characteristics of the resulting cell line when compared to the original culture [490], and 3) Species difference, human (hCMEC/D3, EAhy926) and mouse (bEND3).

Then I examined the impact of okadaic acid on cell viability to determine a concentration range devoid of cytotoxicity and to improve the assays [548]. The MTT cytotoxicity experiment revealed that okadaic acid at concentrations of 10 and 20 nM did not affect cell viability in hCMEC/D3 cells. Our findings support research indicating that treatment of NRK-52E cells with 10 nM okadaic acid is not cytotoxic [549]. Additionally, the dose-dependent effect of DMSO, the solvent for okadaic acid, was examined and determined to be non-toxic at concentrations of 0.01% and 0.02%. This is consistent with previous work indicating that DMSO (0.5%) does not impact cell viability in human dermal fibroblast cells [550].

The current investigation demonstrated that okadaic acid, at concentrations of 10 nM and 20 nM, reduced the abundance of VE-cadherin in hCMEC/D3 cells. The impact of okadaic acid on VE-cadherin abundance correlates with a study indicating that okadaic acid lowers E-cadherin abundance in MCF-7 breast cancer cells [551]. Conversely, halcone–semicarbazone hybrid molecule CS-11, a small molecule that inhibits PP2A-β-catenin signalling, has been found to increase E-cadherin abundance. It demonstrates that CS-11 significantly upregulates E-cadherin on the cell membrane, thereby facilitating the further recruitment of excess β-catenin to the cell surface. This process ultimately results in a decrease in the availability of active β-catenin in the nucleus and strengthens adhesion junctions, which may help to prevent the early spread of metastatic cancer cells [552].

Interestingly, our results demonstrate that the effect of okadaic acid (OA) on VE-cadherin expression is concentration-dependent. At 10 nM OA, VE-cadherin mRNA expression increased, while protein abundance was reduced; at 20 nM, both mRNA and protein levels were decreased. This apparent discrepancy between mRNA and protein levels at the lower OA concentration, although surprising, is not unusual. It is generally accepted that mRNA expression and protein abundance are often correlated [553]; however, transcription and translation are highly regulated processes, and protein levels can be modulated independently of mRNA. For example, VE-cadherin translation may be reduced despite elevated mRNA levels due to translational repression, which can occur under cellular stress, limited energy availability, or via regulatory mechanisms such as microRNAs or repressor proteins binding to the mRNA [554]. Additionally, this effect could reflect concentration-dependent differences in protein degradation. In line with these observations, OA has been shown to influence the transcription of other genes in a concentration-dependent manner: low OA concentrations (e.g., 10 nM) can elevate cell cycle genes such as cyclin D, whereas moderate to high OA levels can upregulate apoptotic pathways [555-557]

Our findings indicate that okadaic acid reduces PP2Ac activity in endothelial cells, as demonstrated by p62 immunostaining [558]. Interestingly, OA treatment did not alter PP2Ac protein abundance, consistent with previous reports in Hep3B and Huh-7 cell lines [559]. These results align with the known role of PP2A in maintaining endothelial barrier integrity [560]. Furthermore, OA has been shown to promote the relocation of VE-cadherin and β-catenin from the cell membrane to the cytoplasm or nucleus, leading to disruption of cell–cell junctions [561].

In the present study, I examined the processes of adherent junction destabilisation mediated by okadaic acid. Our results indicate increased ubiquitination of VE-cadherin mediated by the ubiquitin–proteasome pathway, which is supported by the elevated abundance of ubiquitinated VE-cadherin. This is consistent with other studies demonstrating the necessity of the ubiquitin E3 ligase, CHFR (checkpoint with forkhead and ring finger), as an essential component in ubiquitin-dependent degradation of VE-cadherin [562]. Conversely, lysosomal activity was not implicated in the decrease of VE-cadherin mediated by okadaic acid, as chloroquine did not prevent okadaic acid-induced VE-cadherin reduction. It is possible that chloroquine may not have prevented OA-mediated loss of VE-cadherin if used at a suboptimal concentration for lysosomal inhibition. However, this is unlikely to be the case as chloroquine at a concentration of 100 μM inhibits autophagy-associated lysosomal degradation at 50-100 μM in multiple mammalian cell types, including endothelial cells [372, 563, 564]. While other studies use chloroquine with a concentration range of 10–50 μM, multiple reports indicate that up to 100 μM is required in some cell types to produce strong LC3-II accumulation and clear blockage of autophagosome-lysosome fusion [372, 565]. My data is inconsistent with one study, showing that internalised VE-cadherin co-localises with early endosomes and that chloroquine significantly impedes the downregulation of VE-cadherin in cells expressing the VE-cadherin mutant IL-2R-VE-cadcyto mutant [368]. Nevertheless, my data indicate that VE-cadherin is degraded following exposure to OA through a mechanism involving ubiquitination of VE-cadherin, proteasomal degradation, and this process is not related to lysosomal degradation.

The modulation of VE-cadherin localisation and integrity is essential for endothelial barrier function [17]. I investigated whether VE-cadherin may be localised from the membrane to the cytoplasm or nucleus in hCMEC/D3 cells. We focused on the expression of VE-cadherin in the regions of intracellular connections to visualise its localisation in endothelial cells. Through Western blotting and immunostaining, our findings show that VE-cadherin translocate from the membrane after exposure to okadaic acid, as evidenced by a reduction in the abundance of VE-cadherin in both whole cell and membrane fractions. This could be explained by the degradation

of VE-cadherin following internalisation, which supports my previous data that showed enhanced ubiquitination of VE-cadherin via the ubiquitin-proteasome system. In the absence of okadaic acid, VE-cadherin was concentrated at the membrane, but not in the cytosolic fraction. This contrasts with one study that has shown okadaic acid prompts the movement of VE-cadherin from the membrane to the cytoplasm in human keratinocytes [56]. Fluorescence microscopy results reveal alterations in cell morphology, with VE-cadherin being internalised and redistributed throughout the cytoplasm, and a small amount found in the nucleus, correlating with changes in cell interaction. Additional investigation utilising confocal immunostaining is necessary to confirm the presence of VE-cadherin in the nucleus. That said, research indicates that E-cadherin is localised within the nucleus in colorectal cancer samples and cell lines [57], along with findings that okadaic acid promotes the translocation of E-cadherin from the membrane in untreated cells to the cytoplasm in cells exposed to okadaic acid [58].

Significantly, in my study, the investigation examines whether the proteasome inhibitor MG132 may reduce the impact of okadaic acid on VE-cadherin abundance. According to the literature, the concentration of MG132 was limited to 5 μM for 8h, as higher doses were reported to reduce cell viability in 293T cells [566]. This dose falls within the widely accepted low-micromolar range **(**1–10 μM**)** that has been shown to effectively inhibit proteasome activity while maintaining acceptable cell viability. MG132 exhibits well-established time- and dose-dependent cytotoxicity; therefore, the use of a mid-range concentration such as 5 μM provides a balance between achieving robust proteasomal inhibition and avoiding excessive, non-specific apoptosis. Several studies have demonstrated that treatment with 5 μM MG132 for 6–12 hours is sufficient to block proteasome function and induce accumulation of ubiquitinated proteins [567, 568]. In addition, an exposure time of 8 hours was chosen rather than 24 hours, following findings in human pulmonary fibroblast (HPF) cells**,** where prolonged MG132 treatment induced growth inhibition and cell death, accompanied by elevated reactive oxygen species (ROS) levels and depletion of glutathione (GSH). For instance, treatment with 30 μM MG132 for 24 hours resulted in substantial cytotoxicity in HPF cells [569]. Thus, the chosen dose (5 μM, 8 h) lies within the widely validated experimental range. Our findings showed that MG132 inhibits the degradation of VE-cadherin, as evidenced by the abundance of VE-cadherin in the presence of the proteasome inhibitor. This finding is consistent with previous studies showing that treatment with okadaic acid completely reverses the dephosphorylation of eNOS-associated Akt (threonine 308/serine 473) in MG132-treated cells [29]. This confirmed that the proteasome is involved in the degradation of VE-cadherin. Our findings verified the

potential of proteasome inhibitors to restore VE-cadherin abundance. Based on the existing literature, we hypothesised that the proteasome inhibitor would mitigate the impact of okadaic acid on VE-cadherin abundance, as MG132 inhibits protein degradation, as shown in several studies [570, 571]. VE-cadherin, a component of endothelial adherens junctions that coordinates the paracellular pathway, has its protein production partially regulated through the transcellular route.

Considering the critical function of VE-cadherin in preserving the integrity of the blood-brain barrier and the finding that okadaic acid elevates blood-brain barrier permeability, our data suggest that okadaic acid enhances BBB permeability via PP2A-mediated degradation of VE-cadherin. Our results align with previous research demonstrating that okadaic acid (100 nM) increases the permeability of rat pulmonary microvascular endothelial cells (RPMVECs) [572].

In conclusion, the present data show that okadaic acid facilitates the breakdown of VE-cadherin via a sequence of transcellular processes, initiating disassembly from endothelial adherens junctions and subsequent degradation by the proteasome. This leads to the breakdown of endogenous VE-cadherin, ultimately resulting in the rupture of adherens junctions and endothelial hyperpermeability. The breakdown of VE-cadherin can be inhibited by the proteasome inhibitor MG132, which can restore the damage to VE-cadherin caused by okadaic acid in endothelial cells. Our findings indicate that the permeability of the endothelial barrier increased and was associated with the internalisation and translocation of VE-cadherin from the membrane.

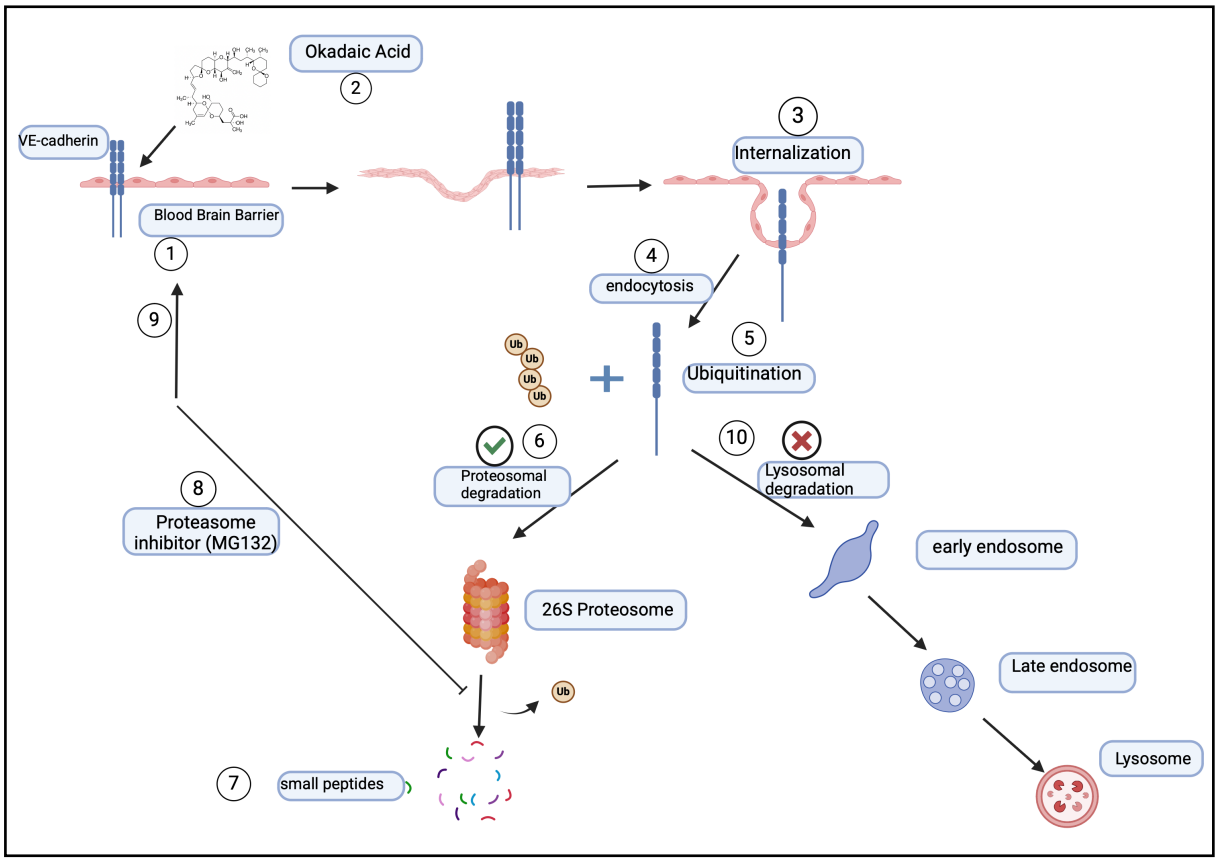


**Figure 3.17: Schematic overview of the mechanism of VE-cadherin degradation in Blood blood-brain barrier post protein phosphatase 2A inhibition using okadaic acid**

# Chapter 4

# Proteomic Microarray Analysis of Okadaic Acid-Treated hCMEC/D3 Cells Reveals Differentially Expressed Proteins Involved in VE-Cadherin Recycling and Degradation

## 4.1 Introduction

The blood-brain barrier (BBB) plays a crucial role in maintaining normal central nervous system function by carefully controlling the exchange of materials between the bloodstream and the brain [573]. The preservation of the BBB largely depends on the expression of tight junctions and adherens junctions that connect neighbouring endothelial cells [574]. Within the family of proteins that make up the adherens junction, vascular endothelial (VE)-cadherin plays a key role in regulating endothelial cell-cell adhesion and hence normal endothelial barrier function [378]. In addition, VE-cadherin is also coupled to several intracellular signalling pathways associated with VEGF and TGFβ that modulate endothelial development and morphogenesis [75, 575, 576]. Unsurprisingly, dysregulation of VE-cadherin is linked with the pathophysiology of several diseases, including cancer [577], atherosclerosis [578], Alzheimer's [579] [579] and inflammation [399]. Many of these diseases/conditions are associated with the loss of VE-cadherin, primarily mediated through enhanced degradation. For example, Tiruppathi *et al*., recently showed an increase in degradation of VE-cadherin in lung samples from patients with sepsis/Acute Respiratory Distress Syndrome(ARDS) and in human microvascular lung endothelial cells following exposure to lipopolysaccharide [562].

Endocytic trafficking of VE-cadherin is an early step in the pathway to degradation. It facilitates the dynamic remodelling of the adherens junctions and is crucial for endothelial cells to sprout, migrate and restore a compromised BBB following vascular injury [415, 416]. This is a complex process involving internalisation, early endosomal sorting, endocytic recycling and late endosomal sorting, leading to lysosomal or proteasomal degradation [580]. While multiple proteins are involved in these processes, monomeric small GTPases known as Rabs play a significant role in vesicular formation, the movement/delivery of vesicles along cytoskeletal structures, and targeted docking/fusion at specific sites through recruitment of effector proteins [581]. The Rab GTPase family has around 70 members, the majority of which are involved in endocytic trafficking [582]. At the expense of GTP, they facilitate the development of multiprotein complexes on the cytoplasmic surfaces of intracellular membranes. These protein assemblies are reversible and under spatial and temporal regulation. This allows fine-tuning of where intracellular vesicles are trafficked [582]. For example, Rab5A is involved in the internalisation and trafficking of membrane receptors to early endosomes by directing vesicle fusion and receptor sorting [421]. This has been shown for VE-cadherin in human pulmonary microvascular endothelial cells [176] but not brain microvascular endothelial cells. In another study using human lung microvascular endothelial cells, Rab11A was found to facilitate

trafficking of VE-cadherin from the endosomal recycling compartment back to the plasma membrane, which maintained endothelial function [324]. Despite these two studies, further insight into the role of Rab11A and Rab5A in VE-cadherin trafficking is sparse regarding human brain microvascular endothelial cells.

In chapter 3, I showed that okadaic acid (PP2A inhibitor) decreased VE-cadherin abundance in brain microvascular endothelial cells because of proteasomal degradation rather than lysosomal degradation. This extends earlier studies showing that inhibition of PP2A by semaphorin 3A or okadaic acid internalises VE-cadherin and redistributes it to either the cytoplasm or nucleus [411, 560]. While this is important for our understanding of the regulation of adherens junctions, it is worth noting that PP2A accounts for approximately 50% of the serine and threonine phosphatase activity in the cell [112] . When this is taken into consideration with the fact that serine and threonine phosphorylation account for more than 75% of the phosphoproteome [583], the impact of inhibiting PP2A is likely far-reaching. Indeed, using a combined transcriptomic, proteomic, and phosphoproteomic approach, Wuerger *et al*. recently showed that okadaic acid (PP2A inhibitor) impacts energy homeostasis, inflammation, signal transduction and cytoskeletal rearrangement in human HepaRG liver cells [516, 517]. Similarly, in rat primary neurone cultures, okadaic acid differentially regulated 320 proteins associated with anatomical structural development, transport, cell differentiation and signal transduction [518]. However, a similar comprehensive or limited proteomic analysis has not been established for okadaic acid in human brain microvascular endothelial cells. Addressing this deficit will enhance our understanding of how okadaic acid/PP2A modulates blood-brain barrier function under physiological and pathophysiological conditions.

Therefore, the current chapter aimed to investigate in human brain microvascular endothelial cells:

1) The effect of okadaic acid on the cellular proteome using a microarray approach to establish key functional networks and protein-protein interrelationships
2) Interrogate the dataset to identify further mechanistic insight into how okadaic acid may modulate VE-cadherin, and
3) Investigate targets of interest from the list of differentially expressed proteins to see if they modulate the effect of okadaic acid on VE-cadherin abundance.

## 4.2 Materials and Methods

### 4.2.1 Cell Culture

hCMEC/D3 cells were plated onto surfaces coated with rat tail collagen (08225, EMD Millipore Corp, USA) and cultured in EndoGRO-MV medium (Merck, Cat. #SCME-BM) supplemented with 5% foetal bovine serum (FBS), growth factors, 100 U/mL of penicillin, and 100 mg/mL of streptomycin. The cells were maintained in a humidified environment at 37°C with 5% $CO_2$, and the culture medium was refreshed every 3 to 4 days. Following trypsinisation, cells were counted after being stained with trypan blue. Comprehensive details regarding the cell culture methods can be found in Chapter 3, section 3.2.1.

### 4.2.2 High Content Proteomic Screening (Immuno-Based Microarray)

A limited proteomic screening assay was undertaken in collaboration with Sciomics (Heidelberg, Germany) using the scioDiscover 2.0 assay. This is a high-content immune-based microarray assay targeting 1438 proteins covering fundamental pathways associated with cancer, neurological disorders and organ failure. The array is spotted with 1,929 antibodies, with each antibody present in quadruplets. The assay has a sensitivity comparable to that of an ELISA with a fM-pM range and a high dynamic range (0.5 - 5000-fold).

hCMEC/D3 were plated at a density of 300,000 cells per well in 6-well plates and exposed to DMSO (0.01% v/v; control) or okadaic acid (10 nM) in serum-free medium. After 24 h, the medium was removed and the cells washed in ice-cold PBS (phosphate-buffered saline). Following washing, the PBS was completely removed and the plates snap-frozen and stored at -80°C until shipping. Plates were sealed and shipped overnight on dry ice.

Proteins were extracted using scioExtract buffer (Sciomics) and quantified using a BCA (bicinchoninic acid) assay and standardised to a uniform protein concentration following in-house protocols. A reference sample was generated by pooling an identical volume from each sample. The experimental samples and reference sample were labelled with scioDye 2 and scioDye 1, respectively. The labelling reaction was quenched after 2 h, and the buffer was replaced by PBS; all labelled samples were stored at -20°C until required. Samples were analysed using a reference-based design. In brief, the arrays were blocked using scioBlock on a Hybstation HS 4800 (Tecan, Austria) before being competitively incubated with the labelled reference. After 3 h, the slides were washed with PBSTT (1x), rinsed with 0.1x PBS and again with water, before being dried under nitrogen. Slides were scanned on a Powerscanner (Tecan,

Austria) at constant laser power and PMT settings. Spot segmentation was performed using GenePix Pro 6.0 (Molecular Devices, Union City, CA, USA). The raw data (median signal intensities) were analysed using LIMMA (linear models for the microarray), an R package from Bioconductor. Rab11a, cadherin 5 (VE-cadherin), and UBP4 were the three proteins verified through Western blot analysis.

### 4.2.3 Protein Extraction and Quantification

Following removal of the culture medium, the cells were rinsed with sterile ice-cold PBS (D8662, Sigma-Aldrich). The cells were then lysed using RIPA buffer supplemented with a 100x protease inhibitor cocktail Set I (539131-EMD Millipore Corp, Germany) and collected with the aid of a cell scraper. The resulting cellular suspension was placed in an Eppendorf tube and left on ice for 15 minutes before being subjected to three freeze-thaw cycles at -80°C to ensure complete cell lysis. After centrifugation (400 x g for 10 minutes), the cell debris was discarded, and the supernatant transferred to a sterile 1.5 mL sampling tube, which was then stored at -80°C for protein quantification and subsequent Western blot analysis.

Protein concentration in the cell lysate was determined using a Bradford assay, with absorbance readings taken at 595 nm using a spectrophotometer (BIO-TEK EL808). The absorbance values were converted to concentrations using a standard curve established with bovine serum albumin as the reference protein. Unless indicated otherwise, all samples were adjusted to a concentration of 1 mg/mL. Detailed protocols for the isolation and quantification of proteins can be found in chapter 3, sections 3.2.3 and 3.2.4, respectively.

### 4.2.4 SDS-PAGE and Western Blotting

Protein samples (20 µg) were combined with a 5x loading buffer, heated at 95°C for 30 s, and subsequently cooled on ice for 3 minutes. SDS-PAGE was performed using 8% gels, with a molecular weight marker included. Following electrophoresis, proteins were transferred to a PVDF membrane via the iBlot 2 Dry Blotting System. The membranes were blocked for 1 h (4°C) in TBS-T containing either 5% milk or 2% BSA and then incubated overnight at 4°C with a primary antibody. The following day, the membranes were washed and then exposed to HRP-conjugated secondary antibody (specific to either mouse or rabbit) in TBS-T with 5% milk for 1 h at room temperature in the dark under rotation. Protein bands were detected using chemiluminescence, with images captured on a Fusion Fx imaging system. The membranes were then stripped and re-probed with an HRP-conjugated β-actin antibody. Comprehensive protocols can be found in chapter 3, sections 3.2.5.1. and 3.2.5.2. respectively.

### 4.2.5 RNA Cell Extraction and cDNA Synthesis

Cells were lysed in Tri Reagent™ (Sigma Aldrich), and the aqueous phase separated following the addition of chloroform and centrifugation. The aqueous phase containing RNA was transferred to a new tube and the RNA was precipitated upon addition of isopropanol. The RNA was further purified by washing with 75% and 100% ethanol, air-dried, and reconstituted in nuclease-free water. RNA quantity and purity were assessed by measuring the 260/280 absorbance ratio using a spectrophotometer (NanoDrop).

To remove any potential DNA contamination, the RNA samples were treated with DNase I (Invitrogen). cDNA was synthesised using the RevertAid Reverse Transcriptase kit (Thermo Fisher) with random hexamer primers. Detailed protocols for RNA isolation, clean-up, and reverse transcription can be found in Chapter 3, sections 3.2.5.1 and 3.2.5.2. respectively.

### 4.2.6 Semi-Quantitative Real-Time PCR

mRNA expression was assessed using semi-quantitative reverse transcription PCR (RT-PCR) with primers specific to the targets and SYBR Green GoTaq DNA polymerase. The reactions were run on the Mx3000P QPCR System. Primers were prepared at a stock concentration of 100 µM and diluted to a working concentration of 10 µM for use. The reaction mix contained 10 µL of 2X SYBR Green mix, 50 ng of cDNA, 500 nM of each primer (forward and reverse, IDT), and molecular-grade water, resulting in a total volume of 20 µL. A non-template control was included in the setup. The PCR conditions consisted of an initial denaturation at 95°C for 2 minutes, followed by 40 cycles of 95°C for 15 s, 62°C for 1 minute and 72°C for 15 s. mRNA expression was quantified using the comparative Ct method, full details are available in Chapter 3, section 3.2.6.3.

| Gene | NMID | Forward Sequence | Reverse Sequence |
|---|---|---|---|
| **Rab11A** | NM_004663 | GCAACAAGAAGCATCCAGG | GCACCTACTGCTCCACGAT |
| **GPI** | NM_001329911.2 | TCTATGCTCCCTCTGTGTTAGA | CTCCTCCGTGGCATCTTTATT |
| **GAPDH** | NM_002046.5 | CTCTGCTCCTCCTGTTCGAC | GCGCCCAATACGACCAAATC |

**Table 4.1: List of primers detailing gene name, NMID number and sequence.** Abbreviations: GPI, glucose-6-phosphate isomerase; GAPDH, glyceraldehyde-3-phosphate dehydrogenase.

### 4.2.7 Rab11A or Rab5A siRNA knockdown (Cell Transfection)

hCMEC/D3 cells were plated at a density of $6 \times 10^4$ in 24-well plates so that they would be 70–90% confluent 24 h before the start of the transfection protocol. On the day of transfection, the growth medium containing FBS was removed and the cells rinsed once with 1xPBS before being replaced with a serum-free growth medium. The cells were maintained in a humidified environment at 37°C with 5% $CO_2$ for 2 h. Meanwhile, 2 µL of Lipofectamine 2000 (Thermo Fisher Scientific) was diluted in 48 µL of Opti-MEM and mixed gently. The Rab5A and Rab11A siRNA probes were purchased from Thermo Fisher based on sequences published in the literature [176, 324]. The siRNA probes were diluted in Gibco™ Opti-MEM™ I reduced serum medium to a final siRNA concentration of 20 nM. The diluted siRNA was combined with the diluted Lipofectamine 2000, mixed gently, and incubated at room temperature for 30 minutes. Following this, 400 µL of the serum-free medium was added to the siRNA-Lipofectamine 2000 complexes, mixed gently, and transferred to each well containing the cells. The cells were then incubated at 37°C in a $CO_2$ incubator, and mRNA or protein was isolated 24, 48, and 72 h post-transfection.

### 4.2.8 Data and Statistical Analysis

Microarray data was normalised using a specialised invariant Lowess method. For analysis of the samples, a one-factorial linear model was fitted via least squares regression with LIMMA, resulting in a two-sided t-test or F-test based on moderated statistics. All presented P values were adjusted for multiple testing by controlling the false discovery rate according to Benjamini and Hochberg. Differences in protein abundance between different samples or sample groups are presented as log-fold changes (*logFC*) calculated for base 2. Proteins with a (*logFC*) > 0.5 and an adjusted $P < 0.05$ were defined as differentially expressed and displayed in blue in the volcano plot. The differentially expressed proteins were ascribed to functional networks using the KEGG hierarchy classification system (https://www.genome.jp/kegg/) and ShinyGO

(https://bioinformatics.sdstate.edu/go/), while protein-protein interactions and cluster analysis were interrogated through string analysis (https://string-db.org).

All other data were normalised to the appropriate control and expressed as either an absolute value, a percentage or a ratio. Protein abundance was normalised relative to β-actin, and mRNA expression was normalised to the geometric mean of GAPDH and GPI. Protein concentration was interpolated from standard curves using non-linear regression (Graphpad Prism version 10). Data were analysed by one-way ANOVA with post hoc analysis (Dunnett's or Bonferroni) as appropriate (Graphpad Prism version 10).

## 4.3 Result

### 4.3.1 Proteomic Screening: Effect of Okadaic Acid on hCMEC/D3 Cells

Hierarchical cluster analysis and principal component analysis of the complete dataset indicated that sample FZ007 (okadaic acid group) was an outlier (Figure 4.1A and B). This sample consistently showed abnormal expression patterns compared to the other samples, including unusually high background noise, low signal-to-noise ratio, and failure to cluster with its experimental group. Because such deviations can distort downstream statistical analyses, it was removed from all subsequent analyses to maintain the reliability and biological validity of the results. Of the 1438 proteins screened, okadaic acid differentially altered the abundance of 104 proteins compared to the control group (DMSO) in the filtered data set. For visualisation purposes, these are presented in the volcano plot (Figure 4.2) and listed in Tables 4.2 and 4.3. Okadaic acid increased the abundance of 64 proteins (positive LogFC value; Table 4.2), while 40 were downregulated (negative LogFC value; Table 4.3) compared to the control group. The relative expression levels of the differentially regulated proteins are summarised in a heatmap (Figure 4.3).

When the list of differentially expressed proteins was interrogated further, KEGG analysis mapped them to 216 known biological pathways and networks. From this list, key ones related directly to the broad theme of the thesis were selected (Table 4.4). This included 7 proteins implicated in neurodegeneration (hsa05022), 8 were associated with membrane trafficking (hsa04131), 2 were associated with the ubiquitin system (hsa04121), 4 were cell adhesion molecules (hsa04514), and 2 were tight junction proteins (hsa04530). Interestingly, ubiquitin carboxyl-terminal hydrolase 4 (UBP4), cadherin 1 (CADH1), Rab11A and cathepsin (CATH) were upregulated, while cadherin 5 (CADH5), ubiquitin+1 (UBB) and Rab1A were downregulated in the okadaic acid group.

Based on the proteomic results and KEGG pathway analysis, genes for the microarray study were selected using a systematic and objective process to ensure biological relevance and technical feasibility. Genes corresponding to the key proteins and pathways identified (e.g., neurodegeneration, membrane trafficking, ubiquitin system, cell adhesion, tight junctions) were first identified using literature searches, pathway databases (e.g., KEGG, Reactome), and prior experimental evidence. The technical team then evaluated which genes could be reliably measured on the microarray platform, considering probe availability and hybridisation efficiency. Genes were excluded if they lacked validated probes, showed extremely low or

highly variable baseline expression, or were not directly related to the pathways of interest. This approach ensured that the final gene panel was scientifically meaningful, technically robust, and capable of detecting genuine changes in gene expression.

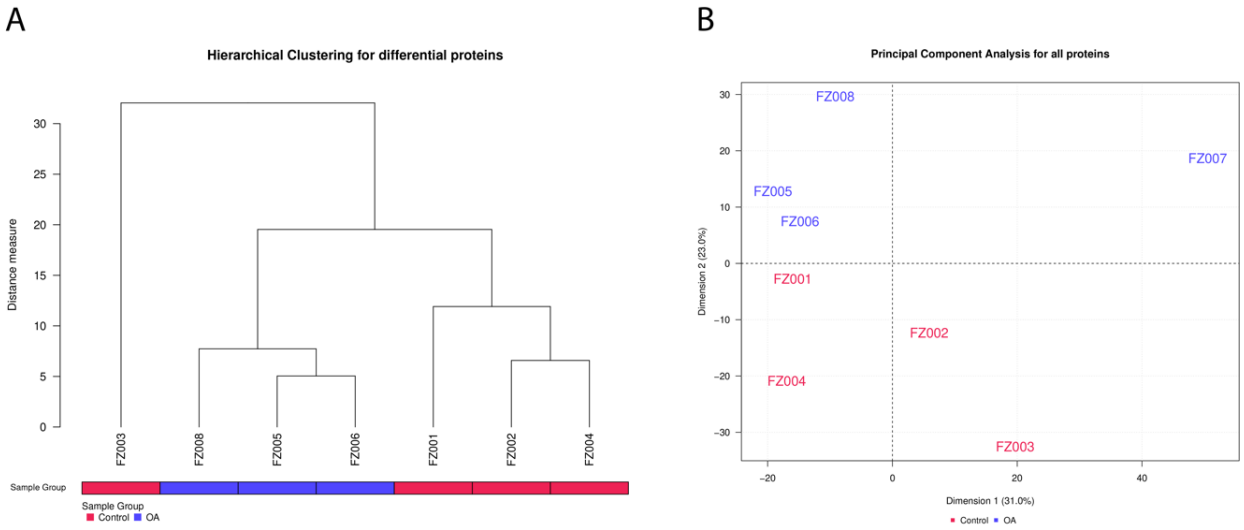


**Figure 4.1: Hierarchical clustering and principal component analysis of all differentially expressed proteins in hCMEC/D3 cells following exposure to okadaic acid.** hCMEC/D3 cells were exposed to okadaic acid (10 nM; blue) or DMSO (0.01% v/v, control; red) for 24 h and protein abundance determined using a high content immune-based microarray (Sciomics, Germany). (A) A dendrogram representing hierarchical clustering of differentially expressed proteins, with the y-axis representing dissimilarity between clusters. (B) A scatter plot representing principal component analysis of differentially expressed proteins. The percentages on the axis labels describe the ratio of total variance explained by the respective principal component. In this plot, the location of a sample is defined by its first two principal components, i.e. linear combinations of protein features with the largest variance across the samples. Samples with a similar profile are close.

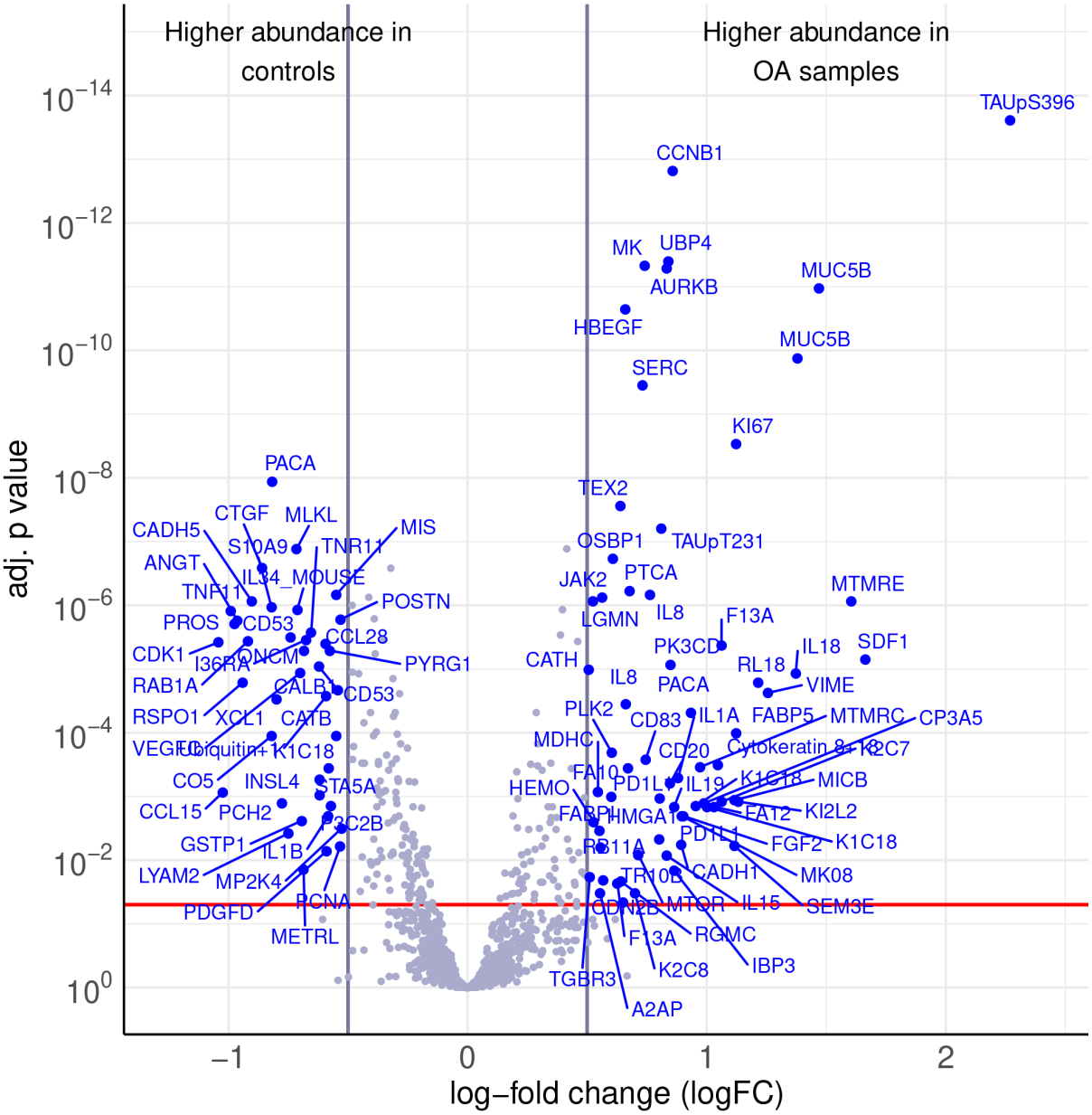


**Figure 4.2: Volcano plot visualising differential protein abundance following exposure to okadaic acid in hCMEC/D3 cells**. hCMEC/D3 cells were exposed to okadaic acid (10 nM) or DMSO (0.01% v/v, control) for 24 h, and protein abundance was determined using a high-content immune-based microarray (Sciomics, Germany). The proteins are plotted as their corresponding adjusted P values against their corresponding $Log_2$-fold change (logFC) in abundance. The horizontal red line indicates an adjusted P value of 0.05, while the blue vertical lines indicate the logFC cutoff at ± 0.5. Proteins that are differentially expressed (logFC > 0.5 and adjusted P value < 0.05) are displayed with their names in blue. A positive logFC value indicates higher abundance in the okadaic samples compared to the control and *vice versa*.

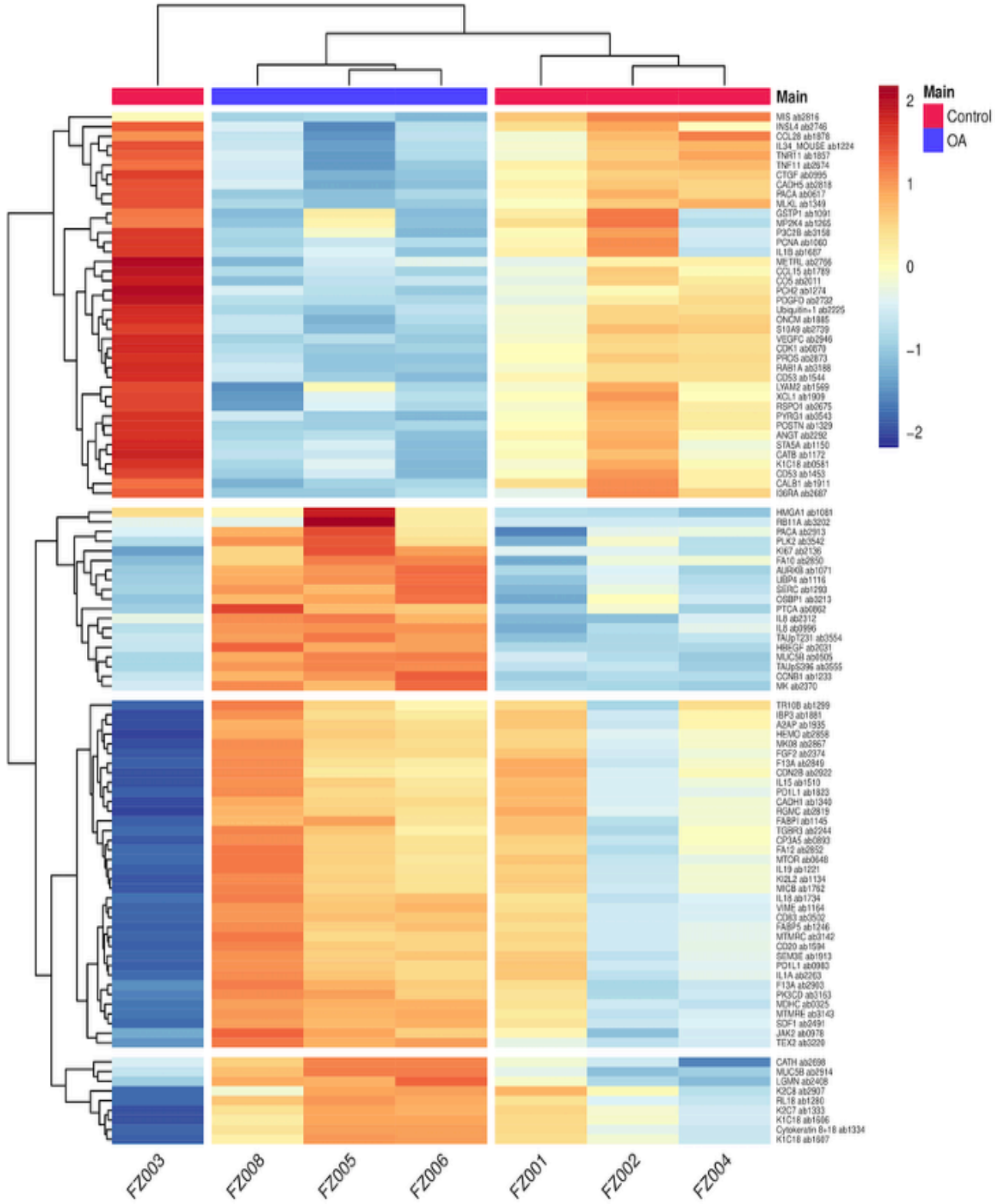


**Figure 4.3: Heatmap displaying the relative abundance of proteins identified as being differentially expressed following exposure to okadaic acid (10 nM).** Values were centred and scaled by proteins (P<0.05). The y-axis displays proteins with similar expression levels, and the x-axis represents similar samples.

| Protein | Antibody ID | Uniprot Name | Uniprot-Entry | HGNC | logFC | Aver Exp | Adj. p Val |
|---|---|---|---|---|---|---|---|
| **TAUpS396** | ab3555 | | P10636 | MAPT | 2.27 | 11.14 | 2.4e-14 |
| **SDF1** | ab2491 | SDF1 HUMAN | P48061 | CXCL12 | 1.66 | 14.00 | 7.1e-06 |
| **MTMRE** | ab3143 | MTMRE-HUMAN | Q8NCE2 | MTMR14 | 1.60 | 13.78 | 8.7e-07 |
| **MUC5B** | Ab055 | MUC5B-HUMAN | Q9HC84 | MUC5B | 1.47 | 12.09 | 1.1e-11 |
| **MUC5B** | ab2914 | MUC5B-HUMAN | Q9HC84 | MUC5B | 1.38 | 12.48 | 1.3e-10 |
| **IL18** | ab1734 | IL18-HUMAN | Q14116 | IL18 | 1.37 | 14.36 | 1.2e-05 |
| **VIME** | ab1164 | VIME-HUMAN | P08670 | VIM | 1.26 | 13.95 | 2.4e-05 |
| **RL18** | ab1280 | RL18-HUMAN | Q07020 | RPL18 | 1.22 | 12.45 | 1.6e-05 |
| **K12L2** | ab1134 | KI2L2-HUMAN | P43627 | KIR2DL2 | 1.13 | 12.33 | 1.2e-03 |
| **FABP5** | ab1246 | FABP5-HUMAN | Q01469 | FABP5 | 1.12 | 14.26 | 1.0e-04 |
| **K167** | ab2136 | K167-HUMAN | P46013 | MK167 | 1.12 | 12.64 | 2.9e-09 |
| **SEM3E** | ab1913 | SEM3E-HUMAN | O15041 | SEMA3E | 1.12 | 13.87 | 6.oe-03 |
| **MICB** | ab1762 | MICB-HUMAN | Q29980 | MICB | 1.12 | 13.13 | 1.1e-03 |
| **K2C7** | ab1333 | K2C7-HUMAN | P08729 | KRT7 | 1.06 | 13.40 | 1.2e-03 |
| **F13A** | ab2903 | F13A-HUMAN | P00488 | F13A1 | 1.06 | 11.57 | 4.2e-06 |
| **Cytokeratin 8+18** | ab1334 | | P05787 | KRT8 | 1.05 | 11.20 | 3.2e-04 |
| **FA12** | ab2852 | FA12-HUMAN | P00748 | F12 | 1.03 | 11.31 | 1.5e-03 |
| **K1C18** | ab1606 | KIC18-HUMAN | P05783 | KRT18 | 1.00 | 12.78 | 1.5e-03 |
| **CP3A5** | ab0893 | CP3A5-HUMAN | P20815 | CYP3A5 | 0.99 | 13.10 | 1.3e-03 |
| **MTMRC** | ab3142 | MTMRC-HUMAN | Q9C0I1 | MTMR12 | 0.97 | 14.03 | 3.5e-04 |
| **K1C18** | ab1607 | K1C18-HUMAN | P05783 | KRT18 | 0.95 | 11.25 | 1.4e-03 |
| **PACA** | ab2913 | PACA-HUMAN | P18509 | ADCYAP1 | 0.94 | 12.22 | 4.9e-05 |
| **FGF2** | ab2374 | FGF2-HUMAN | P09038 | FGF2 | 0.90 | 14.03 | 2.0e-03 |
| **MK08** | ab2867 | MK08-HUMAN | P45983 | MAPK8 | 0.90 | 12.96 | 2.0e-03 |
| **CADH1** | ab1340 | CADH1-HUMAN | P12830 | CDH1 | 0.89 | 13.71 | 5.7e-03 |
| **IL1A** | ab2263 | IL1A-HUMAN | P01583 | IL1A | 0.88 | 11.85 | 5.1e-04 |
| **IBP3** | ab1881 | IBP3-HUMAN | P17936 | IGFBP3 | 0.86 | 12.54 | 1.5e-02 |
| **IL19** | ab1221 | IL19-HUMAN | Q9UHD0 | IL19 | 0.86 | 13.24 | 1.5e-03 |
| **CCNB1** | ab1233 | CCNB1-HUMAN | P14635 | CCNB1 | 0.86 | 13.22 | 1.5e-13 |
| **PK3CD** | ab3163 | PK3CD-HUMAN | O00329 | PIK3CD | 0.85 | 11.33 | 8.6e-06 |
| **CD20** | ab1594 | CD20-HUMAN | P11836 | MS4A1 | 0.85 | 13.43 | 6.2e-04 |
| **UBP4** | ab1116 | UBP4-HUMAN | Q13107 | USP4 | 0.84 | 12.04 | 4.0e-12 |
| **IL15** | ab1510 | IL15-HUMAN | P40933 | IL15 | 0.83 | 12.61 | 8.5e-03 |
| **AURKB** | ab1071 | AURKB-HUMAN | Q96GD4 | AURKB | 0.83 | 10.75 | 5.2e-12 |
| **TAUpT231** | ab3554 | | P10636 | MAPT | 0.81 | 8.48 | 6.2e-08 |
| **PD1L1** | ab0983 | PD1L1-HUMAN | Q9NZQ7 | CD274 | 0.80 | 13.85 | 1.1e-03 |
| **PD1L1** | ab1823 | PD1L1-HUMAN | Q9NZQ7 | CD274 | 0.80 | 13.48 | 4.7e-03 |
| **IL8** | ab2312 | IL8-HUMAN | P10145 | CXCL8 | 0.76 | 8.57 | 6.8e-07 |
| **CD83** | ab3502 | CD83-HUMAN | Q01151 | CD83 | 0.75 | 14.15 | 2.6e-04 |
| **MK** | ab2370 | MK-HUMAN | P21741 | MDK | 0.74 | 9.80 | 4.7e-12 |
| **SERC** | ab1293 | SERC-HUMAN | Q9Y617 | PSAT1 | 0.73 | 13.85 | 3.5e-10 |
| **MTOR** | ab0648 | MTOR-HUMAN | P42345 | MTOR | 0.71 | 11.51 | 8.3e-03 |
| **K2C8** | ab2907 | K2C8-HUMAN | P05787 | KET8 | 0.70 | 10.01 | 3.3e-02 |
| **PTCA** | ab0862 | PTCA-HUMAN | Q14761 | PTPRCAP | 0.68 | 9.62 | 6.0e-07 |
| **FA10** | ab2850 | FA10-HUMAN | P00742 | F10 | 0.67 | 7.89 | 3.6e-04 |
| **IL8** | ab0996 | IL8-HUMAN | P10145 | CXCL8 | 0.66 | 8.72 | 3.6e-05 |
| **HBEGF** | ab2031 | HBEGF-HUMAN | Q99075 | HBEGF | 0.66 | 9.07 | 2.2e-11 |
| **CDN2B** | ab2922 | CDN2B-HUMAN | P42772 | CDKN2B | 0.65 | 12.23 | 4.6e-02 |
| **RGMC** | ab2819 | RGMC-HUMAN | Q6ZVN8 | HJV | 0.64 | 13.50 | 2.2e-02 |
| **TEX2** | ab3220 | TEX2-HUMAN | Q8IWB9 | TEX2 | 0.64 | 13.30 | 2.8e-08 |
| **F13A** | ab2849 | F13A-HUMAN | P00488 | F13A1 | 0.63 | 13.52 | 2.3e-02 |
| **OSBP1** | ab3213 | OSBP1-HUMAN | P22059 | OSBP | 0.61 | 13.38 | 1.9e-07 |
| **PLK2** | ab3542 | PLK2-HUMAN | Q9NYY3 | PLK2 | 0.60 | 11.60 | 2.1e-04 |
| **HMGA1** | ab1081 | HMGA1-HUMAN | P17096 | HMGA1 | 0.60 | 9.96 | 1.0e-03 |
| **TR10B** | ab1299 | TR10B-HUMAN | O14763 | TNFRSF10B | 0.57 | 10.59 | 2.1e-02 |
| **JAK2** | ab0978 | JAK2-HUMAN | O60674 | JAK2 | 0.56 | 12.69 | 7.5e-07 |
| **RB11A** | ab3202 | RB11A-HUMAN | P62491 | RAB11A | 0.56 | 8.49 | 6.3e-03 |
| **A2AP** | ab1935 | A2AP-HUMAN | P08697 | SERPINF2 | 0.55 | 10.67 | 3.3e-02 |
| **HEMO** | ab2858 | HEMO-HUMAN | P02790 | HPX | 0.55 | 12.99 | 3.4e-03 |
| **MDHC** | ab0325 | MDHC-HUMAN | P40925 | MDH1 | 0.55 | 13.86 | 8.4e-04 |
| **FABP1** | ab1145 | FABPI-HUMAN | P12104 | FABP2 | 0.53 | 12.50 | 2.5e-03 |
| **LGMN** | ab2408 | LGMN-HUMAN | Q99538 | LGMN | 0.52 | 9.47 | 8.6e-07 |
| **TGBR3** | ab2244 | TGBR3-HUMAN | Q03167 | TGFBR3 | 0.51 | 11.15 | 1.8e-02 |
| **CATH** | ab2698 | CATH-HUMAN | P09668 | CTSH | 0.51 | 12.66 | 1.0e-05 |

**Table 4.2: List of proteins upregulated following exposure to okadaic acid.** Included in the table are the protein name, targeting antibody, Uniprot-Identifier, HGNC code, logFC value, average expression and adjusted P value.

| Protein | Antibody ID | Uniprot Name | Uniprot-Entry | HGNC | logFC | Aver Exp | Adj. p Val |
|---|---|---|---|---|---|---|---|
| **MP2K4** | Ab1265 | MP2K4-HUMAN | P45985 | MAP2K4 | -0.53 | 15.08 | 3.2e-03 |
| **POSTN** | Ab1329 | POSTN-HUMAN | Q15063 | POSTN | -0.53 | 14.11 | 1.7e-06 |
| **PCNA** | Ab1060 | PCNA-HUMAN | P12004 | PCNA | -0.53 | 13.27 | 6.0e-03 |
| **CALB1** | Ab1911 | CALB1-HUMAN | P05937 | CALB1 | -0.54 | 10.14 | 2.1e-05 |
| **MIS** | Ab2816 | MIS-HUMAN | P03971 | AMH | -0.55 | 11.96 | 6.8e-07 |
| **CATB** | Ab1172 | CATB-HUMAN | P07858 | CTSB | -0.55 | 14.88 | 1.1e-04 |
| **P3C2B** | Ab3158 | P3C2B-HUMAN | O00750 | PIK3C2B | -0.57 | 13.50 | 1.4e-03 |
| **PYRG1** | Ab3543 | PYRG1-HUMAN | P17812 | CTPS1 | -0.58 | 13.33 | 5.1e-06 |
| **K1C18** | Ab0581 | K1C18-HUMAN | P05783 | KRT18 | -0.58 | 13.68 | 3.6e-04 |
| **IL1B** | Ab1687 | IL1B-HUMAN | P01584 | IL1B | -0.58 | 14.51 | 2.1e-03 |
| **PDGFD** | Ab2732 | PDGFD-HUMAN | Q9GZP0 | PDGFD | -0.59 | 10.04 | 7.2e-03 |
| **Ubiquitin+1** | Ab2225 | | P0CG47 | UBB | -0.59 | 12.64 | 2.7e-05 |
| **CCL28** | Ab1878 | CCL28-HUMAN | Q9NRJ3 | CCL28 | -0.59 | 14.99 | 4.0e-06 |
| **STA5A** | Ab1150 | STA5A-HUMAN | P42229 | STAT5A | -0.62 | 12.10 | 9.5e-04 |
| **INSL4** | Ab2746 | INSL4-HUMAN | Q14641 | INSL4 | -0.62 | 12.02 | 5.4e-04 |
| **CD53** | Ab1453 | CD53-HUMAN | P19397 | CD53 | -0.62 | 15.08 | 9.1e-06 |
| **TNR11** | Ab1857 | TNR11-HUMAN | Q9Y6Q6 | TNFRSF11A | -0.65 | 15.43 | 2.7e-06 |
| **I36RA** | Ab2687 | I3RA-HUMAN | Q9UBH0 | IL36RM | -0.68 | 15.17 | 3.5e-06 |
| **ONCM** | Ab1885 | ONCM-HUMAN | P13725 | OSM | -0.68 | 12.20 | 5.1e-06 |
| **METERL** | Ab2766 | METRL-HUMAN | Q641Q3 | METRNL | -0.69 | 10.90 | 1.4e-02 |
| **GSTP1** | Ab1091 | GSTP1-HUMAN | P09211 | GSTP1 | -0.69 | 14.21 | 2.4e-03 |
| **VEGFC** | Ab2946 | VEGFC-HUMAN | P49767 | VEGFS | -0.70 | 13.07 | 1.2e-05 |
| **IL34-MOUSE** | Ab1224 | IL34-MOUSE | Q8RLR4 | I134 | -0.71 | 15.58 | 1.2e-06 |
| **MLKL** | Ab1349 | MLKL--HUMAN | Q8NB16 | MLKL | -0.72 | 15.13 | 1.3e-07 |
| **CD53** | Ab1544 | CD53-HUMAN | P19397 | CD53 | -0.74 | 14.45 | 3.2e-06 |
| **LYAM2** | Ab1569 | LYAM2A-HUMAN | P16581 | SELE | -0.75 | 13.19 | 3.8e-03 |
| **PCH2** | Ab1274 | PCH2-HUMAN | Q15645 | TRIP13 | -0.78 | 12.40 | 1.3e-03 |
| **XCL1** | Ab1909 | XCL1-HUMAN | P47992 | XCL1 | -0.80 | 12.17 | 3.0e-05 |
| **PACA** | Ab0617 | PACA-HUMAN | P18509 | ADCYAP1 | -0.82 | 13.94 | 1.2e-08 |
| **CO5** | Ab2011 | CO5-HUMAN | P01031 | C5 | -0.82 | 12.64 | 1.1ee-04 |
| **S10A9** | Ab2739 | S10A9-HUMAN | P06702 | S100A9 | | 14.47 | 1.1e-06 |
| **CTGF** | Ab0995 | CTGF-HUMAN | P29279 | CTGF | -0.86 | 14.71 | 2.6e-07 |
| **CADH5** | Ab2818 | CADH5-HUMAN | P33151 | CADH5 | -0.90 | 14.45 | 8.7e-07 |
| **RAB1A** | Ab3188 | RAB1A-HUMAN | P62820 | RAB1A | -0.92 | 13.21 | 3.7e-06 |
| **RSPO1** | Ab2675 | RSPO1-HUMAN | Q2MKA7 | RSPO1 | -0.94 | 13.43 | 1.6e-05 |
| **ANGT** | Ab2292 | ANG1-HUMAN | P01019 | AGT | -0.96 | 13.52 | 1.8e-06 |
| **PROS** | Ab2873 | RSPO1-HUMAN | P07225 | PROS1 | -0.98 | 15.14 | 2.0e-06 |
| **TNF11** | Ab2674 | TNF11-HUMAN | O14788 | TNFSF11 | -0.99 | 14.90 | 1.2e-06 |
| **CCL15** | Ab1789 | CCL15-HUMAN | Q16663 | CCL15 | -1.02 | 12.65 | 8.6e-04 |
| **CDK1** | Ab0870 | CDK1-HUMAN | P06493 | CDK1 | -1.04 | 12.88 | 3.8e-06 |

**Table 4.3: List of proteins downregulated following exposure to okadaic acid.** Included in the table are the protein name, targeting antibody, Uniprot-Identifier, HGNC code, logFC value, average expression and adjusted P value.

| Pathway ID | Pathway Description | Protein Count | Protein Abbreviation | Protein Name |
|---|---|---|---|---|
| **ihsa05022** | **Neurodegeneration** | 7 | **IL1A** | interleukin 1 alpha |
| | | | **IL1B** | interleukin 1 beta |
| | | | **MAPT** | microtubule associated protein tau |
| | | | **MTOR** | mechanistic target of rapamycin kinase |
| | | | **MAPK8** | mitogen-activated protein kinase 8 |
| | | | **RAB1A** | RAB1A, member RAS oncogene family |
| | | | **UBB** | ubiquitin B |
| **hsa04514** | **Cell Adhesion** | 4 | **CADH1** | cadherin 1 |
| | | | **CADH5** | cadherin 5 |
| | | | **SELE** | selectin E |
| | | | **CD274** | CD274 molecule |
| **hsa04530** | **Tight junction** | 2 | **PCNA** | proliferating cell nuclear antigen |
| | | | **MAPK8** | mitogen-activated protein kinase 8 |
| **hsa04131 (KEGG Brite)** | **Membrane trafficking** | 8 | **PIK3CD** | phosphatidylinositol-4,5-bisphosphate3-kinase catalytic subunit delta |
| | | | **IGFBP3** | insulin like growth factor binding protein 3 |
| | | | **RAB11A** | RAB11A, member RAS oncogene family |
| | | | **RAB1A** | RAB1A, member RAS oncogene family |
| | | | **OSBP** | oxysterol binding protein |
| | | | **MAPT** | microtubule associated protein tau |
| | | | **MTOR** | mechanistic target of rapamycin kinase |
| | | | **MUC5B** | mucin 5B, oligomeric mucus/gel-forming |
| **hsa04121 (KEGG Brite)** | **Ubiquitin system** | 2 | **UBB** | ubiquitin B |
| | | | **USP4** | ubiquitin specific peptidase 4 |

**Table 4.4: KEGG Pathway Enrichment Analysis of proteins differentially modulated by okadaic acid.** This table summarises the significantly enriched Kyoto Encyclopaedia of Genes and Genomes (KEGG) pathways identified in the differentially expressed protein set following exposure to okadaic acid (10 nM) compared to solvent control (DMSO; 0.01%). Each row corresponds to a KEGG pathway identification number with associated details: pathway descriptor, number of proteins in the set, protein abbreviation and name. Upregulated and downregulated proteins are highlighted in blue and red, respectively.

### 4.3.2 Biological and Functional Protein Associations

The list of proteins differentially regulated by okadaic acid was assigned to different biological processes (Figure 4.4) using ShinyGO (version 0.82)[584-586], which is based upon Ensembl Release 104. It was found that 26.2% of all proteins differentially regulated were related to cellular processes, 21.8% were associated with biological regulation, 16.3% were linked with a response to stimulus, and 9.9% were involved in metabolic processes. It should be noted that several of the differentially regulated proteins contribute to more than one biological process.

The data set was further interrogated to investigate physical (direct) and functional (indirect) protein associations using the STRING database (http://string-db.org), following the addition of the catalytic subunit of protein phosphatase 2A (PPP2CA) to the list. The network presented in Figure 4.5 was generated from multiple lines of evidence (medium confidence = 0.400), which included experimental data, curated database entries, text mining, co-expression,

neighbour, gene fusion and co-occurrence. The mode for network presentation was interactive SVG (scalable vector graphics). Within this protein interactome, UBB was found to be directly linked to USP4 (ubiquitin carboxyl-terminal hydrolase 4), CDH1 (cadherin 1), Vim (vimentin), PPP2CA (catalytic subunit of PP2Ac) and, indirectly, to CDH5 (VE-cadherin), RAB1A and RAB11A (Figure 4.5). Importantly, PPP2CA was directly linked to Rab11A, AURKB (aurora kinase B), MTOR (mechanistic target of rapamycin), CDK1 (cyclin-dependent kinase 1), CCNB1 (cyclin B1) and MAPT (microtubule-associated protein tau). Multiple direct protein-protein interactions can be seen around JAK2 (Janus kinase 2), CXCL8 (interleukin 8), IL-1, IL-15, and IL-18. To explore clustering from this network, the data set underwent Markow cluster analysis MCL). This resulted in 16 clusters being identified (Figure 4.6). The top 5 clusters were around cytokine receptor binding (33 proteins), transcriptional regulation of the cell cycle (13 proteins), intermediate filaments (6 proteins), complement and coagulation cascades (6 proteins) and short-term memory (4 proteins). Together, these data highlight the pleiotropic effect of okadaic acid on a cell at a fundamental level through protein degradation (e.g. USP4 and UBB), kinase signalling (e.g. MAPK8 and MAP2K4), control of the cell cycle (e.g. PCNA, RAB11A and PPP2CA) and inflammation (e.g. IL-19, IL-15 and IL-18).

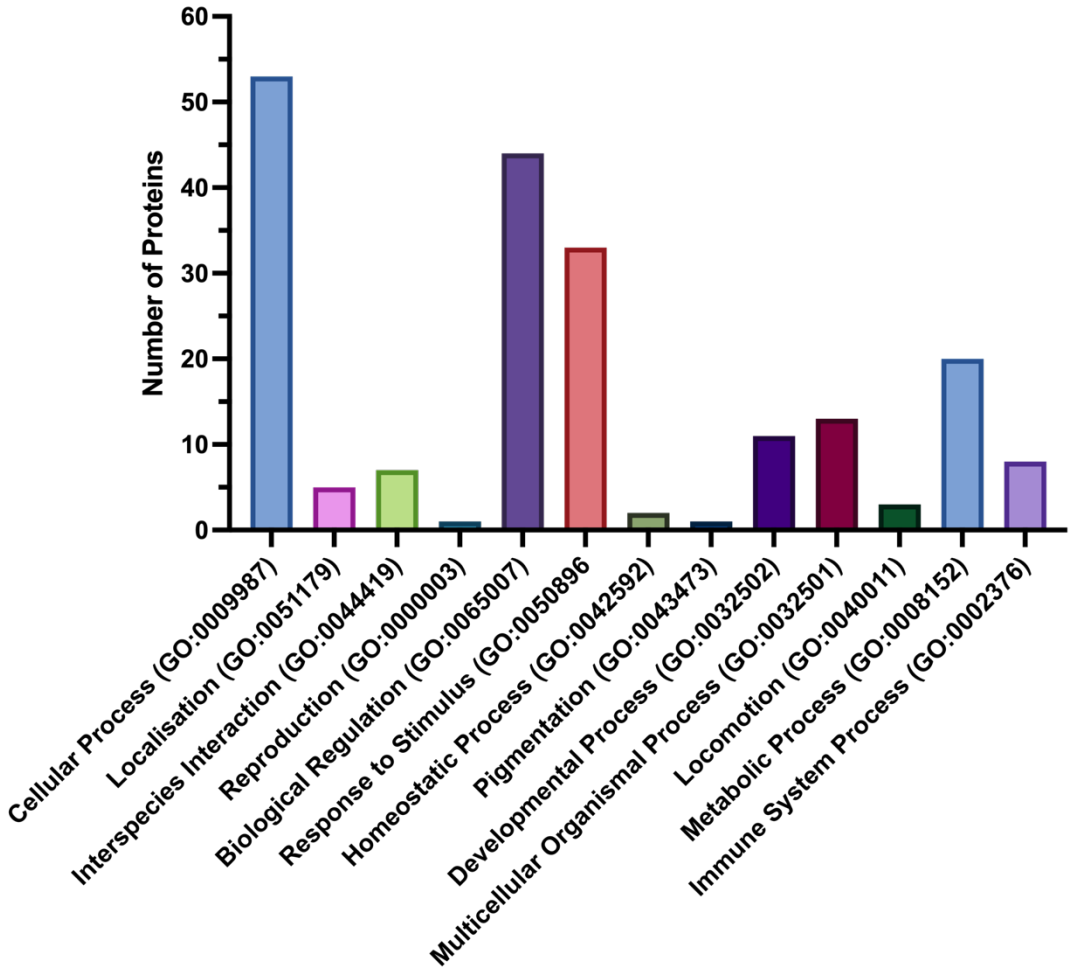


**Figure 4.4: Grouping of differentially expressed proteins following exposure to okadaic acid (10 nM) according to their biological process.** Distribution of the proteins between biological processes was based on Ensembl release 104. The data set was filtered for unclassified associations.

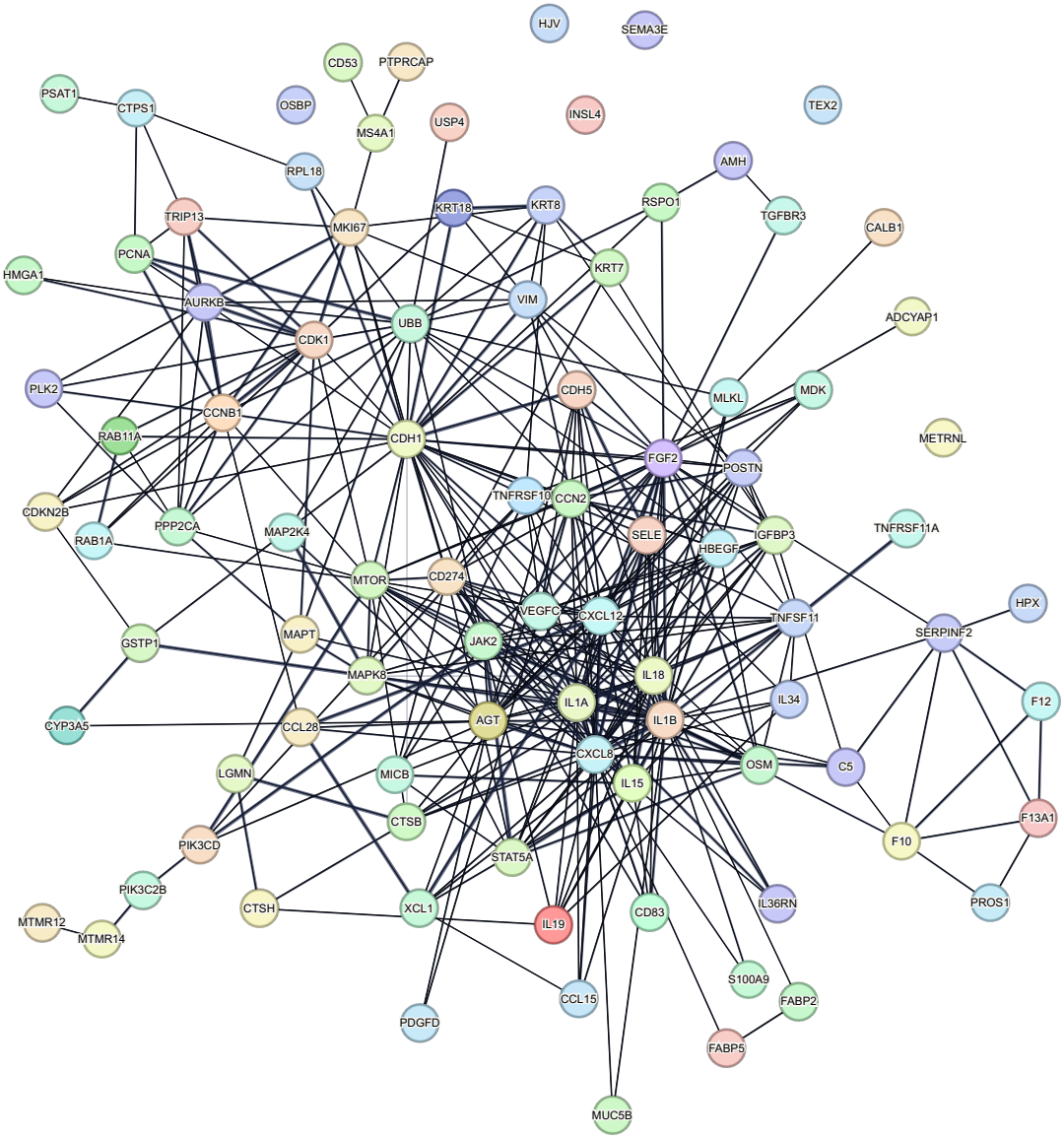


**Figure 4.5: Protein Interactome Network Constructed via STRING Analysis.** This graphic depicts the protein–protein interaction network of differentially expressed proteins following exposure to okadaic acid (10 nM), upon STRING analysis. Each node represents an individual protein included in the dataset, while the connecting lines denote predicted functional associations derived from multiple lines of evidence, including experimental data, curated database entries, text mining, co-expression, and computational predictions. The abbreviated protein name is centralised on the node, while line thickness reflects the confidence score of each interaction, with thicker edges indicating higher confidence based on the integrated data sources. The network was generated using STRING (v12.0), applying a high-confidence interaction score threshold (e.g., >0.4 to minimise false positives. The abbreviated protein names are defined in Tables 2 and 3.

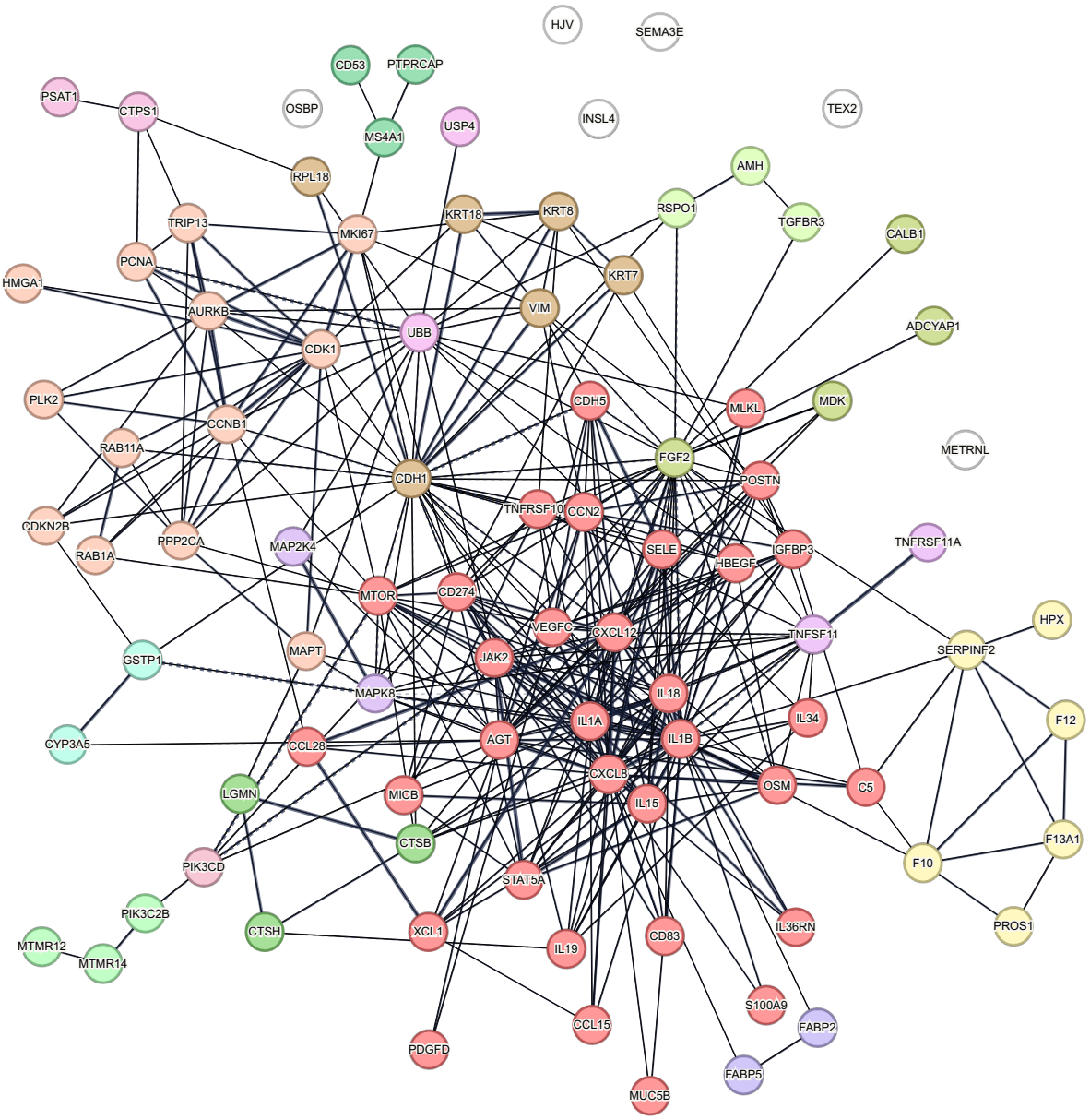


**Figure 4.6: MCL cluster analysis.** Nodes represent proteins, and lines represent edge associations. Clusters are shown by colours and were identified using the Markov Cluster Algorithm (inflation = 3).

| color | cluster Id | gene count | description |
|---|---|---|---|
| | Cluster 1 | 33 | + Viral protein interaction with cytokine and cytokine receptor |
| | Cluster 2 | 13 | + TP53 Regulates Transcription of Cell Cycle Genes |
| | Cluster 3 | 6 | + Intermediate filament |
| | Cluster 4 | 6 | + Complement and coagulation cascades |
| | Cluster 5 | 4 | + Short-term memory |
| | Cluster 6 | 3 | Type II transforming growth factor beta receptor binding |
| | Cluster 7 | 3 | Endosome lumen |
| | Cluster 8 | 3 | Phosphatidylinositol phosphate phosphatase activity, and Phosphatidylinositol pho... |
| | Cluster 9 | 3 | CD53, MS4A1, PTPRCAP |
| | Cluster 10 | 2 | CYP3A5, GSTP1 |
| | Cluster 11 | 2 | + Triglyceride catabolism |
| | Cluster 12 | 2 | JNK (c-Jun kinases) phosphorylation and activation mediated by activated human ... |
| | Cluster 13 | 2 | + Positive regulation of fever generation by positive regulation of prostaglandin se... |
| | Cluster 14 | 2 | TNFR1-induced NFkappaB signaling pathway |
| | Cluster 15 | 2 | CTPS1, PSAT1 |
| | Cluster 16 | 1 | PIK3CD |

### 4.3.3 Rab11A knockdown: Design and Assay validation in hCMEC/D3 cells

Based on the microarray data showing upregulation of Rab11A following exposure to okadaic acid and its known role in VE-cadherin recycling [324], I went on to investigate if knockdown of Rab11a would modify okadaic acid-mediated loss of VE-cadherin. Before this could be addressed, the assay had to be optimised and validated.

As the first step in this process, a series of experiments were designed to compare the knockdown efficiency of four different transfection reagents at a constant siRNA concentration (20nM) and transfection time. The four transfection reagents tested were Nanocin (Tecrea), PolyFect (Qiagen), Lipofectamine 2000 (Thermo Fisher Scientific) and TransIX-X2® system (Mirus Bio), and knockdown was assessed for Rab11A mRNA expression. In hCMEC/D3 cells, Lipofectamine 2000, PolyFect and TransIX-X2 decreased Rab11A mRNA expression by 88%, 63% and 73%, respectively, compared to medium alone (Untx; Figure 4.7; $P<0.05$). Nanocin tended to decrease Rab11A expression, but this failed to reach significance compared to Untx (Figure 4.7). Based on these data, Lipofectamine 2000 was used in all further experiments.

Having settled on Lipofectamine 2000 as the transfection reagent, the next step was to investigate the effect of transfection time on Rab11a knockdown. Cells were transfected with Lipofectamine 2000/siRNA complexes for 24, 48 and 72 h and knockdown was determined at the protein level using Western blot analysis. In these screening experiments, Rab11A abundance was decreased at all time points, but greatest at the 24 h time point (85% reduction) compared to mock-transfected cells (Figure 4.8). Over the same period, transfection with the negative control siRNA did not affect Rab11A abundance compared to mock-transfected cells. Based on this, all subsequent transfection experiments assessed Rab11A knockdown at 24 hours.

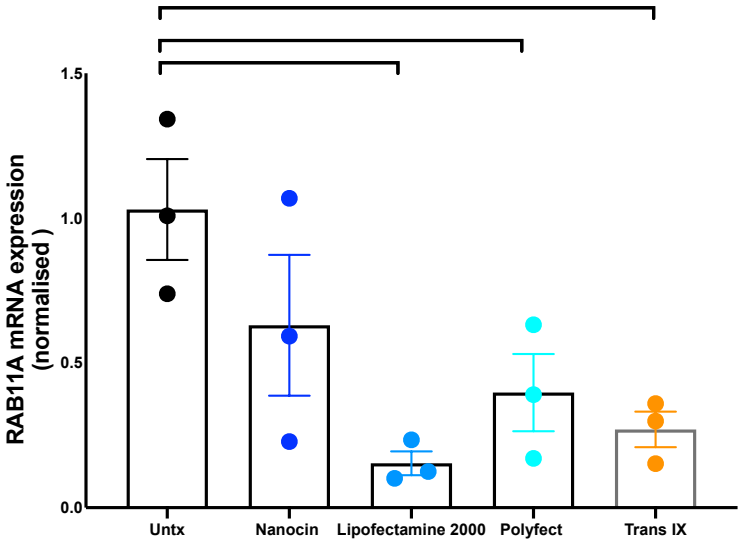


**Figure 4.7: Effect of different transfection reagents on Rab11A mRNA expression.** hCMEC/D3 cells were transfected using either Nanocin, Lipofectamine 2000, PolyFect or TransIX-X2 transfection reagents for 24 h, and Rab11A knockdown was determined at the level of transcription using semi-quantitative PCR (qPCR). Data were normalised to the geometric mean of GAPDH and GPI and expressed relative to the untreated group. Data were analysed using a one-way ANOVA with *post hoc* analysis (Dunnett's test) and presented as mean ± S.E.M. (n=3). Horizontal bars indicate statistical significance at $P<0.05$.

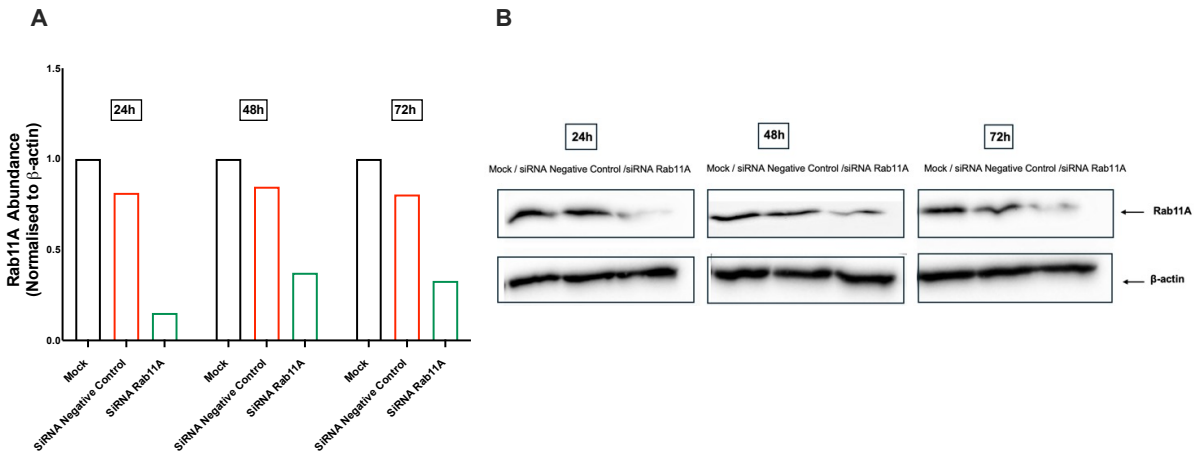


**Figure 4.8: Effect of Rab11A Knockdown on Rab11A abundance over time.** hCMEC/D3 cells were transfected with Rab11a siRNA, negative control siRNA or transfection reagent (mock) for 24, 48 and 72 h (A). At each time point, cells were lysed and Rab11A abundance was determined using Western blot (n=1). Representative immunoblots are presented in B.

### 4.3.4 Effect of Okadaic Acid on Rab11A Abundance in hCMEC/D3

As microarray analysis of the proteome showed that okadaic acid caused a moderate upregulation of Rab11A abundance (LogFC 0.56; cutoff >0.05), this finding was re-evaluated using a Western blot approach. In hCMEC/D3, exposure to okadaic acid (10 nM) for 24 h did not affect Rab11A abundance compared to cells exposed to medium alone (Untx; Figure 4.9A, B). Similarly, DMSO (0.01% v/v; solvent control) did not alter Rab11A abundance compared to Untx (Figure 4.9 A, B).

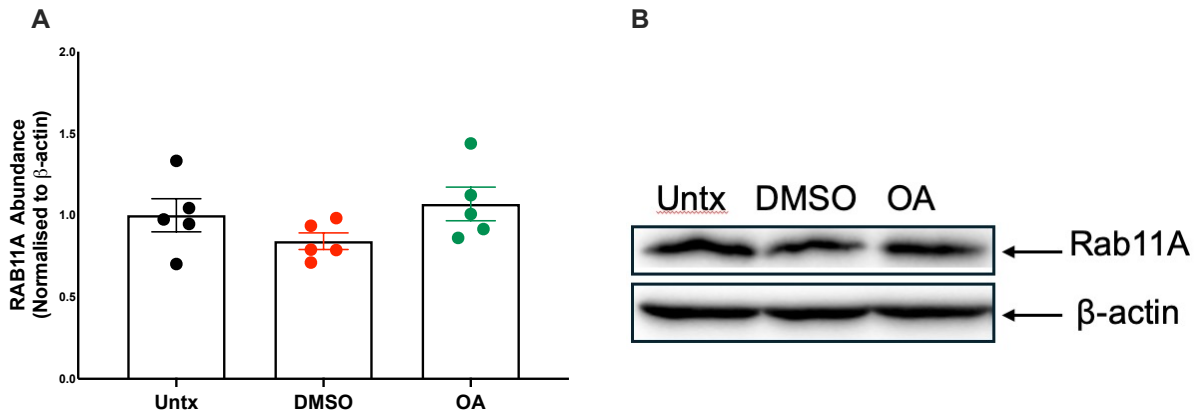


**Figure 4.9: Effect of okadaic acid on Rab11A abundance in hCMEC/D3.** Cells were exposed to okadaic acid (10 nM), DMSO (0.01%) or medium alone (Untx) for 24 h, and Rab11A abundance was determined in cell lysates using Western blot (A and B). Data were normalised to β-actin and expressed relative to the untreated group (Untx). Data were analysed using a one-way ANOVA with *post hoc* analysis (Dunnett's test) and presented as mean ± S.E.M. (n=5). A representative immunoblot is presented in B.

### 4.3.5 Effect of Rab11A knockdown on Rab11A Abundance in the Absence and Presence of Okadaic Acid

Rab11A knockdown decreased the abundance of Rab11A in hCMEC/D3 cells by 60% compared to mock-transfected cells (Figure 4.10 A, C; $P<0.05$). Transfection with negative control siRNA did not alter Rab11A abundance compared to the mock-transfected control group (Figure 4.10 A, C). Importantly, Rab11A knockdown decreased Rab11A abundance by 66% following exposure to okadaic acid (10 nM), compared to the mock-transfected group exposed to okadaic acid (Figure 4.10 B, D; $P<0.05$). Transfection with the negative control siRNA exposed to okadaic acid did not alter Rab11A abundance compared to the mock-transfected group exposed to okadaic acid (Figure 4.10 B, D).

### 4.3.6 Effect of Rab11A knockdown on VE-cadherin Abundance in the Absence and Presence of Okadaic Acid

In hCMEC/D3 cells, knockdown of Rab11A did not alter VE-cadherin abundance compared to mock-transfected cells (Figure 4.11 A, C). Similarly, transfection with negative control siRNA did not alter VE-cadherin abundance relative to mock-transfected cells (Figure 4.11 A, C). Rab11A siRNA did not change VE-cadherin abundance in the presence of okadaic acid (10 nM) compared to mock-transfected cells exposed to okadaic acid (Figure 4.11 B, D). Negative control transfected cells did not alter VE-cadherin abundance compared to mock-transfected cells exposed to okadaic acid (Figure 4.11 B, D). In the negative control transfected group, okadaic acid did not affect VE-cadherin abundance compared to the mock transfected group in the presence of okadaic acid (Figure 4.11 B, D).

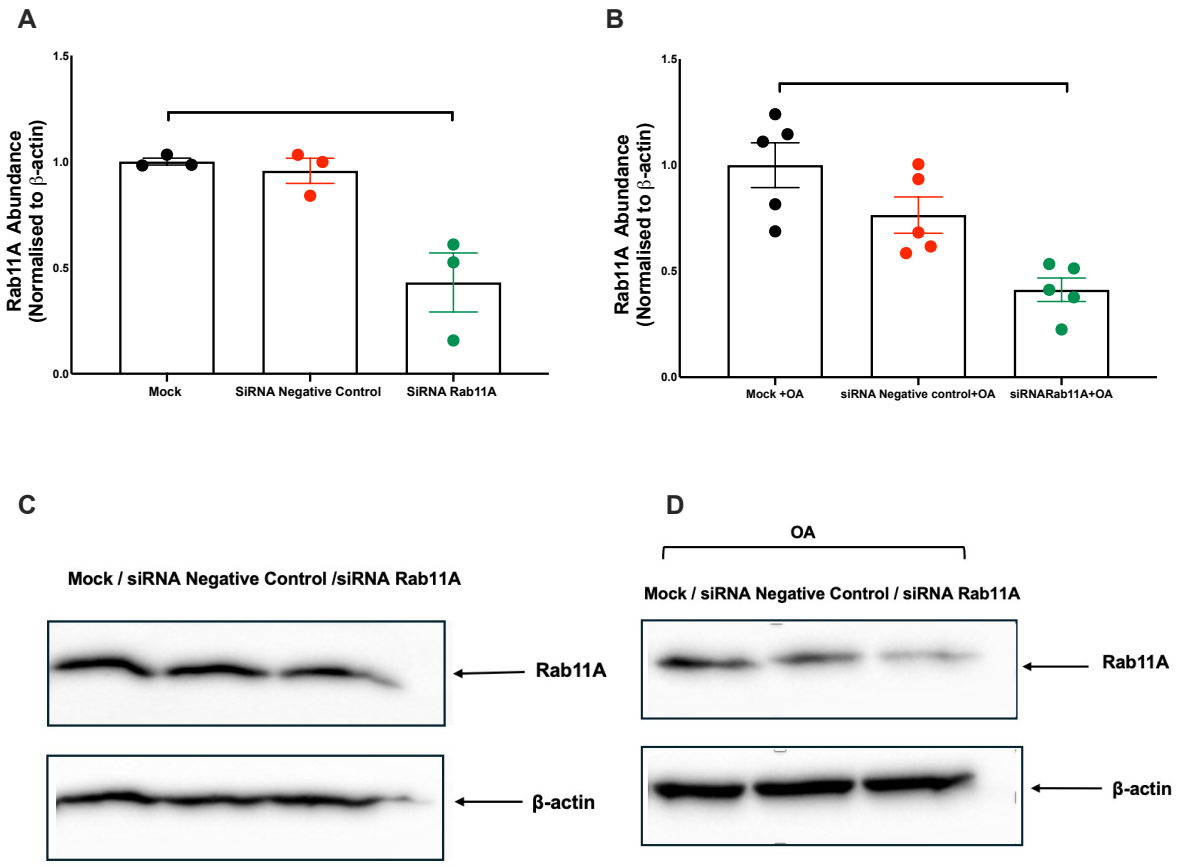


**Figure 4.10: Effect of Rab11A knockdown on Rab11A abundance in the absence or presence of okadaic acid.** Cells were transfected with either Rab11A siRNA, negative control siRNA or transfection reagent (mock) for 24 h in the absence (A and C) or presence of okadaic acid (OA; B and D). Rab11A abundance was determined in cell lysates using Western blot. Data were normalised to β-actin and expressed relative to mock-transfected cells exposed to medium alone or okadaic acid as appropriate. Data were analysed using a one-way ANOVA with *post hoc* analysis (Dunnett's test) and presented as mean ± S.E.M. Horizontal bars indicate statistical significance at $P<0.05$ (n=3 or 5). Representative immunoblots are presented in C and D.

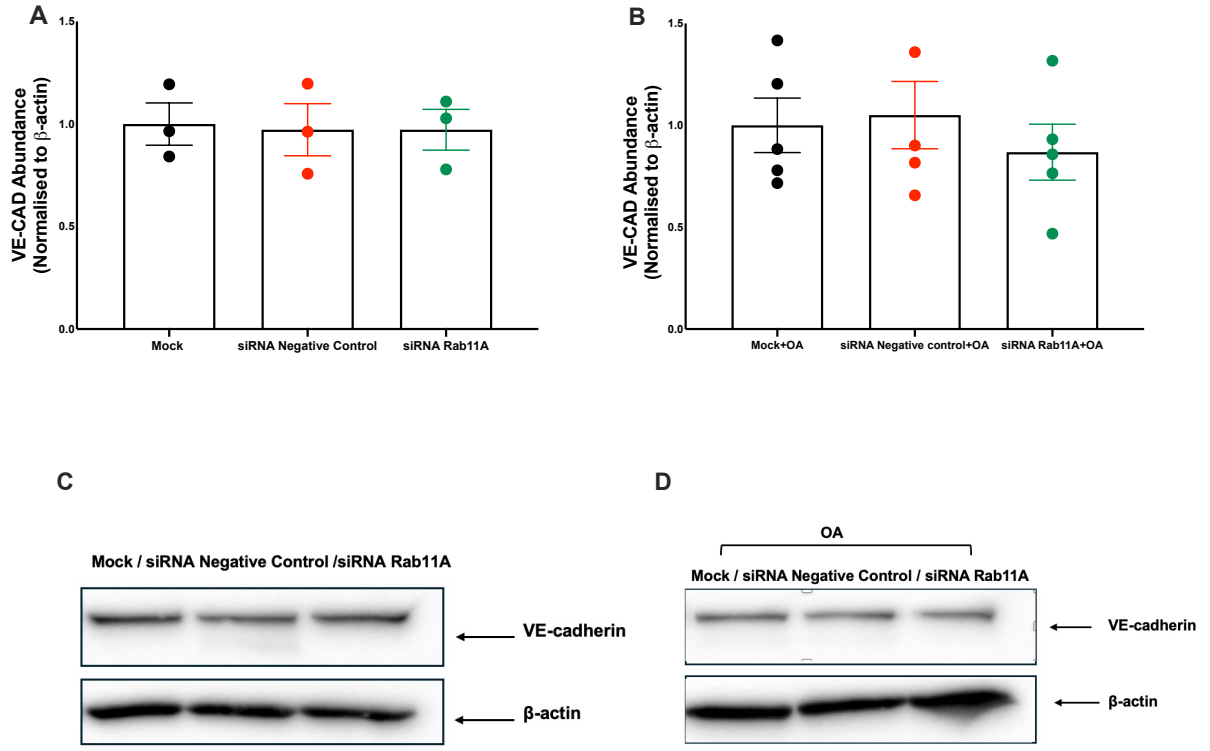


**Figure 4.11: Effect of Rab11A knockdown on VE-cadherin abundance in the absence or presence of okadaic acid.** hCMEC/D3 Cells were transfected with Rab11A siRNA, negative control siRNA or transfection reagent (mock) for 24 h in the absence (A and C) or presence of okadaic acid (OA; B and D), and Rab11A abundance was determined using Western blot. Data were normalised to β-actin and expressed relative to mock-transfected cells exposed to medium alone or okadaic acid as appropriate. Data were analysed using a one-way ANOVA with *post hoc* analysis (Dunnett's test) and presented as mean ± S.E.M. (n=3 or 5). Representative immunoblots are presented in C and D.

### 4.3.7 Effect of Rab11A knockdown on PP2Ac Abundance

As Rab11A knockdown did not prevent OA-mediated downregulation of VE-cadherin, and the micro-array screen showed an indirect association between PP2Ac and Rab11A, I wanted to investigate if knockdown of Rab11A affects PP2Ac abundance. In hCMEC/D3 cells, knockdown of Rab11A decreased PP2Ac abundance of approximately 30% compared to mock-transfected cells (Figure 4.12 A, C; $P<0.05$), while transfection with negative control siRNA had no effect compared to mock-transfected cells (Figure 4.12 A, C). This raised the possibility that okadaic acid may affect Rab11A-dependent downregulation of PP2Ac. In cells transfected with Rab11A siRNA, okadaic acid did not alter PP2Ac abundance compared to mock-transfected cells in the presence of okadaic acid (Figure 4.12 B, D). Similarly, okadaic acid did not change PP2Ac abundance in the negative control siRNA group compared to the mock-transfected group in the presence of okadaic acid (Figure 4.12 B, D).

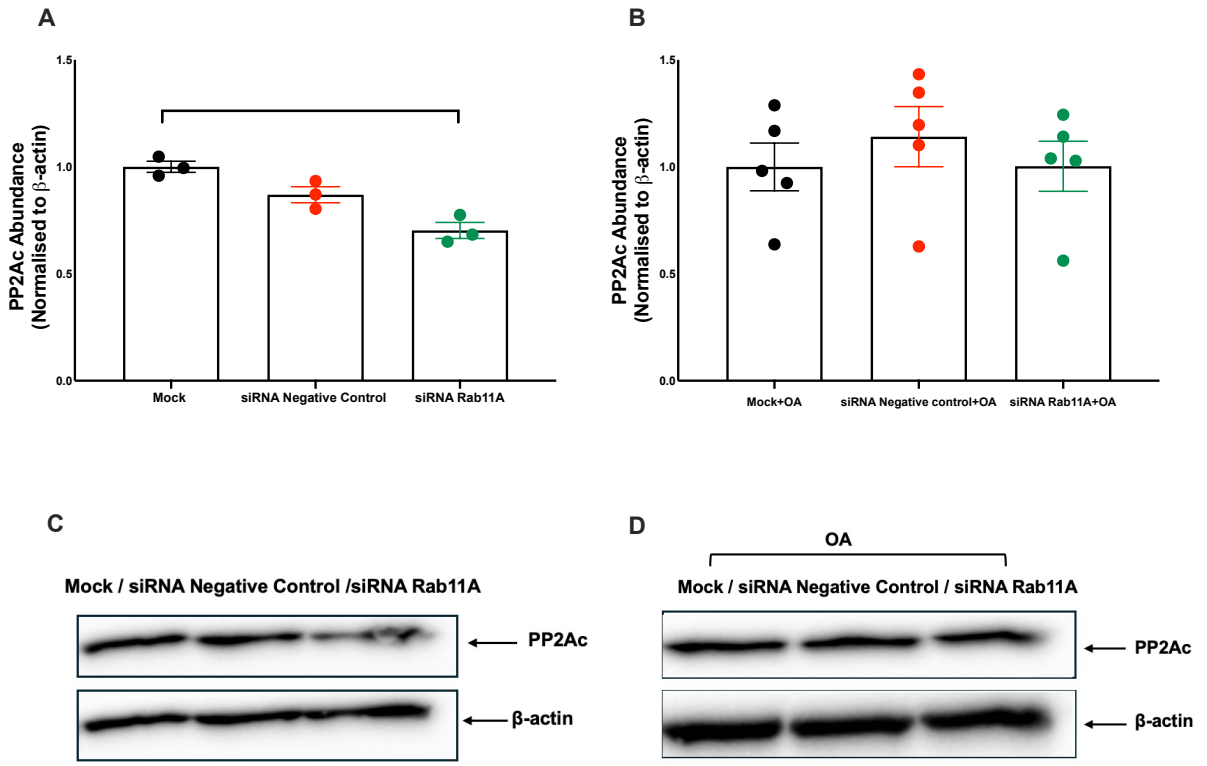


**Figure 4.12: Effect of Rab11A knockdown on PP2Ac abundance in the absence or presence of okadaic acid.** hCMEC/D3 cells were transfected with Rab11A siRNA, negative control siRNA or transfection reagent (mock) for 24 h in the absence (A, C) or presence of okadaic acid (OA, 10 nM; B, D). PP2Ac abundance was determined in cell lysates using Western blot. Data were normalised to β-actin and expressed relative to mock-transfected cells exposed to medium alone or okadaic acid as appropriate. Data were analysed using a one-way ANOVA with *post hoc* analysis (Dunnett's test) and presented as mean ± S.E.M. Horizontal bars indicate statistical significance at $P<0.05$ (n=3 or 5). Representative immunoblots are presented in C and D.

### 4.3.8 Effect of Okadaic Acid on Rab5A Abundance

As the data indicated that Rab11a was not involved in VE-cadherin trafficking, I was curious to investigate if an alternative Rab GTPases may be involved. While the Rab family comprises over 60 members with diverse functions, I decided to focus on Rab5a, which was not part of the microarray, as it is a key regulator of early endocytosis and has been shown to promote LPS-induced internalisation of VE-cadherin in human pulmonary microvascular endothelial cells [176]. On this basis, I explored whether Rab5A could be involved in okadaic acid-mediated VE-cadherin abundance in hCMEC/D3. Exposure to okadaic acid (10 nM) or DMSO (0.01% v/v) for 24 h did not alter Rab5a abundance compared to the Untx group (Figure 4.13 A, B).

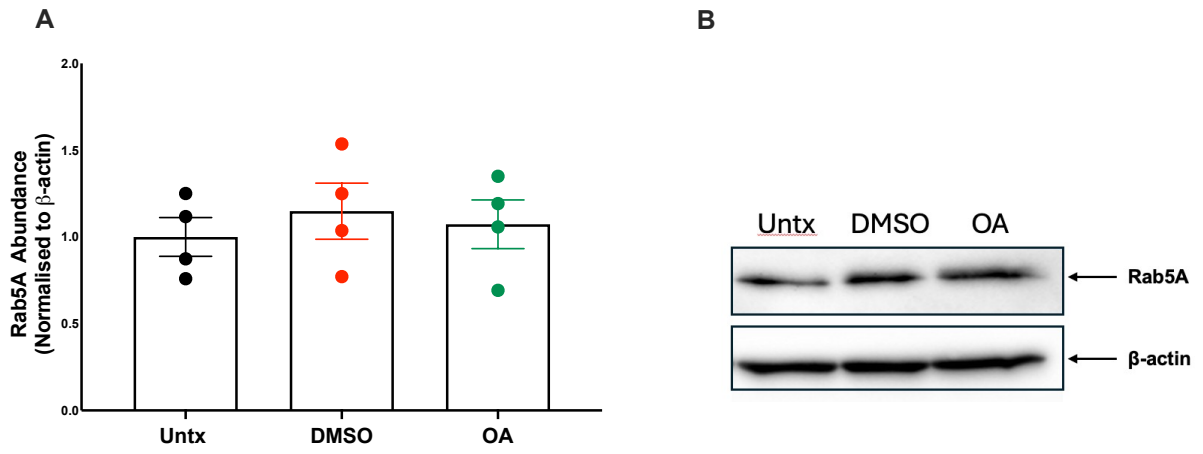


**Figure 4.13: Effect of Okadaic acid on Rab5A abundance in hCMEC/D3.** Cells were exposed to okadaic acid (OA, 10 nM), DMSO (0.01% v/v) or medium (Untx) for 24 h, and Rab5A abundance was determined in cell lysates using Western blot (A, B). Data were normalised to β-actin and expressed relative to the untreated group. Data were analysed using a one-way ANOVA with *post hoc* analysis (Dunnett's test) and presented as mean ± S.E.M. (n=4). A representative immunoblot is presented in B.

### 4.3.9 Effect of Rab5A Knockdown on Rab5A Abundance in the Absence and Presence of Okadaic Acid

Transfection of hCMEC/D3 cells with Rab5A siRNA decreased Rab5A abundance by 66% compared to mock-transfected cells (Figure 4.14 A, C; $P<0.05$). Transfection with negative control siRNA did not alter Rab5A abundance compared to mock-transfected cells (Figure 4.14 A, C). In the presence of okadaic acid (10 nM), transfection with Rab5A siRNA reduced Rab5A abundance by 47% compared to the mock+OA group (Figure 4.14 B, D). Okadaic acid did not change Rab5A abundance in the negative control siRNA group compared to the mock-transfected group in the presence of okadaic acid (Figure 4.14 B, D).

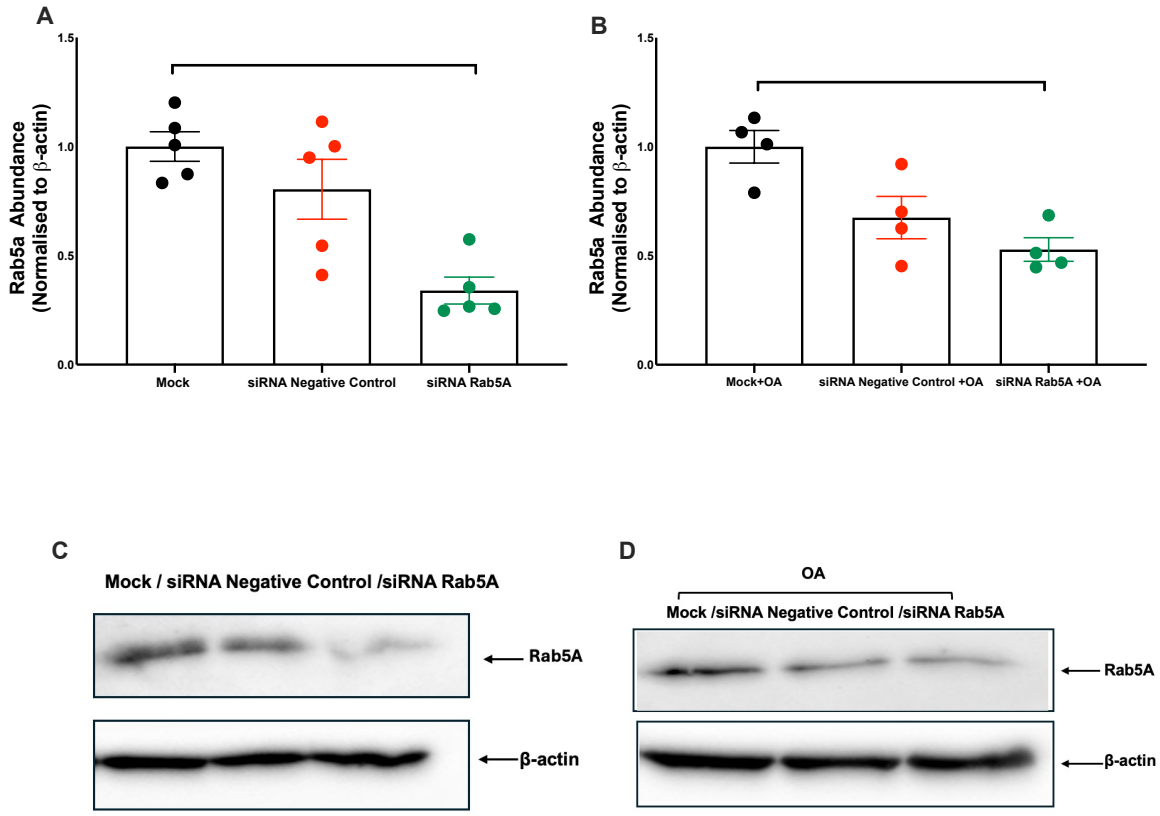


**Figure 4.14: Effect of Rab5A knockdown on Rab5A abundance in the absence or presence of okadaic acid.** Cells were transfected with either Rab5A siRNA, negative control siRNA or transfection reagent (mock) for 24 h in the absence (A and C) or presence of okadaic acid (OA, 10 nM; B and D). Rab5A abundance was determined in cell lysates using Western blot. Data were normalised to β-actin and expressed relative to mock-transfected cells exposed to medium alone or okadaic acid as appropriate. Data were analysed using a one-way ANOVA with *post hoc* analysis (Dunnett's test) and presented as mean ± S.E.M. Horizontal bars indicate statistical significance at $P<0.05$ (n=4 or 5). Representative immunoblots are presented in C and D.

### 4.3.10 Effect of Rab5A Knockdown on VE-cadherin Abundance in the Absence or Presence of Okadaic Acid

Transfection with either Rab5A siRNA or negative control siRNA did not alter VE-cadherin abundance in hCMEC/D3 cells compared to mock-transfected cells (Figure 4.15 A, C). In the presence of okadaic acid (10 nM), VE-cadherin abundance was unchanged following Rab5A siRNA transfection compared to those mock-transfected (Mock+OA; Figure 4.15 B, D). Similarly, okadaic acid did not change VE-cadherin abundance in the negative control siRNA group compared to the mock-transfected group in the presence of okadaic acid (Figure 4.15 B, D).

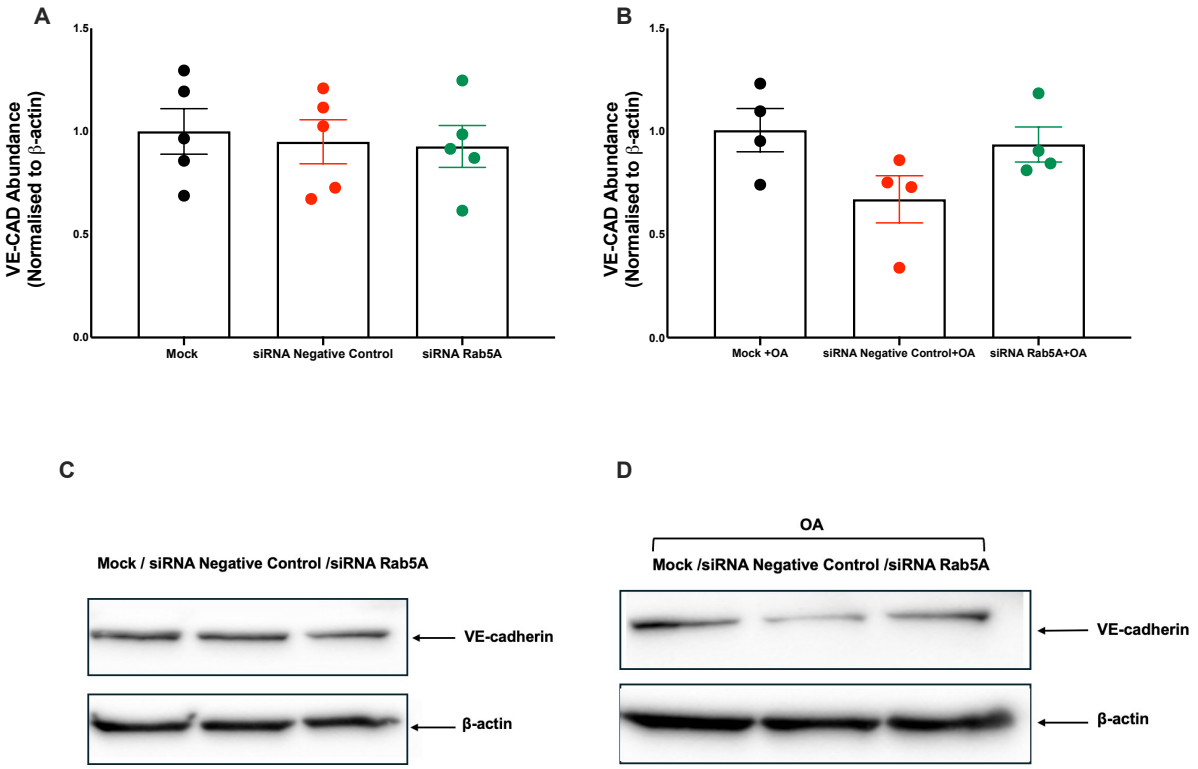


**Figure 4.15: Effect of Rab5A knockdown on VE-cadherin abundance in the absence or presence of okadaic acid.** hCMEC/D3 cells were transfected with siRNA targeting Rab5A or negative control siRNA and exposed to medium alone or okadaic acid (10 nM; B and D) for 24 h. VE-cadherin abundance was determined in cell lysates using Western blot. Data were normalised to β-actin and expressed relative to mock-transfected cells exposed to medium alone or okadaic acid as appropriate. Data were analysed using a one-way ANOVA with *post hoc* analysis (Dunnett's test) and presented as mean ± S.E.M. (n=4 or 5). Representative immunoblots are presented in C and D.

### 4.3.11 Effect of Rab5A Knockdown on PP2Ac Abundance Following Exposure to Okadaic Acid

Okadaic acid (10 nM) did not alter PP2Ac abundance in cells transfected with Rab5A siRNA compared to mock-transfected cells (Figure 4.16 A, B). Likewise, okadaic acid did not change PP2Ac abundance in the negative control siRNA group compared to the mock-transfected group in the presence of okadaic acid (Figure 4.16 A, B).

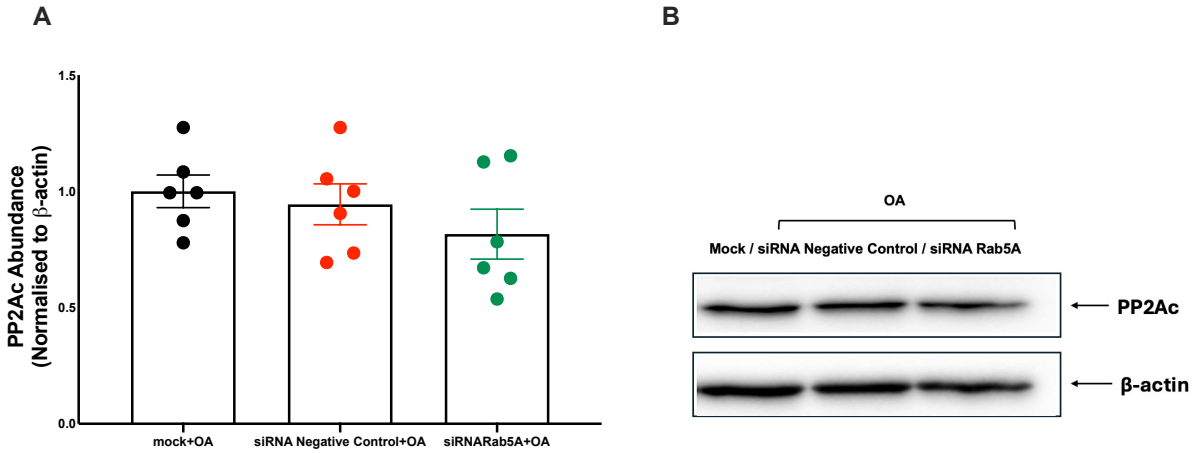


**Figure 4.16: Effect of Rab5A knockdown on PP2Ac abundance in hCMEC/D3 following exposure to okadaic acid.** hCMEC/D3 cells were transfected with Rab5A siRNA or negative control siRNA for 24 h and exposed to okadaic acid (OA, 10 nM), and the effect on PP2Ac abundance was determined using Western blot (A, B). Data were analysed using one-way ANOVA with *post hoc* analysis (Dunnett's test) and presented as mean ± S.E.M. (n=6). A representative immunoblot is presented in B.

## 4.4 Discussion

The present study shows that okadaic acid (10 nM) differentially regulates the expression of 104 proteins (64 upregulated and 40 downregulated) mapping to fundamental cellular, biological, stress and metabolic biological processes. Importantly, 60 of the proteins formed a protein interactome network, with UBB (ubiquitin B) being directly linked to USP4 (ubiquitin carboxyl-terminal hydrolase 4), PPP2CA (PP2A catalytic subunit), CADH1 (cadherin 1), VIM (vimentin) and indirectly to CDH5 (VE-cadherin), Rab1A and Rab11A. Similarly, PPP2CA interacts directly with Rab11A, AURKB (aurora kinase B), MTOR (mechanistic target of rapamycin), CDK1 (cyclin-dependent kinase 1), CCNB (cyclin B) and MAPT (microtubule-associated protein tau). Regarding protein clustering, the top clusters were around cytokine receptor binding, regulation of the cell cycle, intermediate filaments and complement/coagulation cascades. Within the context of this thesis, many of these differentially regulated proteins confirm and extend our earlier finding that okadaic acid decreased VE-cadherin abundance through proteasomal degradation. When the role of Rab11A was investigated further, along with Rab5A (not covered in the microarray profile), they were not found to affect okadaic acid-mediated loss of VE-cadherin or PP2Ac abundance directly.

Although several studies have investigated the effects of okadaic acid on the cellular proteome, these have focused on murine [587] and human liver [516, 517], mouse intestine [588], human cancer cells [589, 590] and embryonic rat cortical neurones [518]. Despite this, there is a paucity of data regarding endothelial cells and in particular human brain microvascular endothelial cells. While important, most of the above studies are limited as they use okadaic acid within a concentration range 33-500 nM, which far exceeds the $IC_{50}$ for PP2Ac (7 nM), but encompasses the $IC_{50}$ (126 nM) for inhibition of PP1 [163]. However, Swingle *et al*. report an $IC_{50}$ for PP2A inhibition of okadaic acid of around 0.1-0.3 nM and an $IC_{50}$ for PP1 of 15-50 nM [162]. The differences in $IC_{50}$ values between these studies likely reflect the assay conditions used, for example, the amount of both enzyme and substrate employed in an assay. Notwithstanding this, the $IC_{50}$ for PP2A is approximately 50–500-fold lower than that for PP1 [162, 164]. Hence, the data obtained in the present study more likely represent effects associated with the inhibition of PP2A.

Using a mass spectrometry-based approach, okadaic acid was shown to differentially regulate 46 proteins in murine liver [587], 58 in murine intestine [588], 104 and 947 in human HepaRG

cells [516, 517], 67 in lipid rafts from SH-SY5Y neuroblastoma cells [590], 39 in MCF-7 breast cancer cells [589] and 320 phosphoproteins in rat embryonic cortical neurones [518]. Our data, obtained using an immune-based microarray approach, is in broad agreement with these studies as okadaic acid differentially regulated 104 proteins. There were major protein clusters around cytoskeleton (e.g. CDK1, Taups396 and Taupt231), stress responses (oxidative/inflammatory), e.g. IL1B, IL1A and MK08, cell differentiation e.g. JAK2, MK08 and STA5A and signal transduction (e.g. PCNA, CDK1 and MK). As this thesis focuses on how okadaic acid modulates VE-cadherin and BBB function, subsets of proteins were extracted from the dataset based on KEGG pathway enrichment. The pathways of particular interest were neurodegeneration (Hsa05022), cell adhesion (Hsa04514), tight junctions (Hsa04530), membrane trafficking (Hsa04131) and the ubiquitin system (Hsa04121; Table 4).

### 4.4.1 Neurodegeneration

Hallmarks of neurodegenerative diseases include pathological protein aggregation, cytoskeletal abnormalities, dysregulated cellular phosphorylation and inflammation. For example, in Alzheimer's disease hyperphosphorylation of Tau is a key feature noted in human brain [591, 592] and experimental models of Alzheimer's disease [593, 594]. This may be a consequence of dysregulated kinase or phosphatase activity. In an early study, the phosphatase angle was investigated by Harris *et al*. [595]. They showed that okadaic acid increased phosphorylation of Tau in human brain slices [595]. With hindsight, this is not surprising as PP2A is the main phosphatase responsible for dephosphorylation of Tau, accounting for approximately 70% of the dephosphorylation of phospho-Tau [596]. This correlates well with other studies showing PP2A activity to be decreased in patients with Alzheimer's disease [597, 598], Parkinsonism, dementia of Guan [591], and dementia with Lewy bodies [599]. The current study supports these observations to show that okadaic acid increases levels of microtubule-associated protein Tau (MAPT; aka Tau-pS396), mutations of which are associated with misfolding and aggregation of Tau protein [600]. In addition, bioinformatic analysis of the current dataset extends these studies to show that okadaic acid reduces Rab1A abundance. This is interesting as Rab1A increases Tau secretion by neurons and HeLa cells [601]. Therefore, a reduction in Rab1A would decrease Tau secretion and contribute to the increase in Tau and p-Tau levels found in the CSF of patients with Alzheimer's disease [601]. I also show that the expression of two kinases, MTOR and MAPK8, were upregulated by okadaic acid in the current study, both of which play key roles in the development of Alzheimer's disease. MTOR has a dual function in Alzheimer's disease as it inhibits insulin signalling and reduces autophagic removal

of β-amyloid and phosphor-Tau [602] which contribute to disease progression. Interestingly, β-amyloid monomers activate the MAPK8/JNK1-MAPK9/JNK2 pathway in Alzheimer's disease [603], leading to amyloid plaque formation.

Inflammation is also a key driver in the pathophysiology of neurodegenerative diseases, including Alzheimer's disease [604], and causes BBB dysfunction [605]. In brain tissue from patients with Alzheimer's disease, interleukin-1 (IL-1) abundance is up-regulated around amyloid plaques [606]. Mechanistically, this may be due to IL-1-mediated activation of the β-amyloid precursor protein promoter [607]. Consistent with these data, I show that pharmacological inhibition of PP2A by okadaic acid increased IL-1A abundance, tying PP2A to neurodegeneration and Alzheimer's disease. Surprisingly, okadaic acid reduced IL-1β abundance. This was unexpected, as a meta-analysis shows IL-1β to be increased in Alzheimer's disease [608]. However, in neuroblastoma cells and primary cultured neurons, IL-1β up-regulates α-cleavage but down-regulates β-cleavage of amyloid precursor protein (APP), which increases sAPPα production but decreases sAPPβ and Aβ production [609]. Therefore, the okadaic acid mediated decrease in IL-1β observed in the present study would be consistent with increased sAPPβ and Aβ, and thus plaque formation. Still, it is worth noting that Alzheimer's disease is associated with either an increase in α-secretase or a decrease in β-secretase or both in brain tissue from 80% of patients with the disease [610].

### 4.4.2 Ubiquitin system

As alluded to above, misfolded protein aggregation is also a hallmark of neurodegenerative diseases, which can manifest as amyloid-β (Aβ) aggregates in Alzheimer's disease [611]. This may be due to altered synthesis and processing of amyloid β or disrupted proteolysis, because reduced proteasomal function is observed in brain tissues from patients with Alzheimer's disease [612]. Notably, protein aggregates themselves can inhibit proteasomal function [613]. Proteasomal degradation is a multi-step process involving tagging of proteins for destruction by ubiquitin, followed by their degradation by the 26S proteasome. In Alzheimer's disease, a growing body of evidence has focused on the ubiquitin+1 ($UBB^{+1}$) frameshift mutant as it associates with the formation of amyloid β plaques and neurofibrillary tangles [614]. In the latter study, $UBB^{+1}$ was found in the brain of all patients at postmortem [615]. $UBB^{+1}$ is a modified ubiquitin with a 19-amino-acid C-terminal extension [614] which interferes with normal proteasomal function, favouring the accumulation of abnormal proteins [616]. Recent

work by Maniv *et al*. shows that $UBB^{+1}$ caused extracellular deposition of amyloid-β (Aβ) and insoluble hyperphosphorylated Tau aggregates under *in vitro* conditions [615]. Mechanistically, this was attributed to competition between $UBB^{+1}$ and ubiquitin for UCHL1, a deubiquitinating enzyme, which manifests as increased levels of amyloid precursor protein (APP), secreted Aβ peptides, and ultimately Aβ build-up [615]. Our proteomic data would be at variance with this, as UBB (ubiquitin+1) was reduced following exposure to okadaic acid. However, the expression of USP4, a deubiquitinating enzyme that removes conjugated ubiquitin from target proteins, was increased by okadaic acid. Hence, the net effect may depend on the relative contribution of UBB and USP4 on amyloid β homeostasis in a particular situation. Either way, these data contribute to our understanding of okadaic acid and UBB in neurodegeneration and Alzheimer's disease. However, proteolysis of amyloid β and its precursors is likely more complicated, as ubiquitinated APP can undergo lysosomal rather than proteasomal degradation [617].

### 4.4.3 Membrane trafficking

Not surprisingly, KEGG pathway enrichment analysis showed overlap between the neurodegeneration and membrane trafficking pathways following exposure of brain microvascular endothelial cells to okadaic acid. Commonalities within the dataset were MAPT, MTOR, and Rab1A. As in Alzheimer's disease, another neurodegenerative disease known as frontotemporal lobar degeneration with tau (FTLD-Tau), is associated with abnormal accumulation of Tau protein in nerve cells, leading to their damage and death [618]. Interestingly, approximately 5-20% of patients with familial frontotemporal dementia have genetic mutations in the microtubule-associated protein tau (MAPT) [619, 620] and defective trafficking of organelles [621, 622]. The latter can impact cellular clearance pathways, leading to protein aggregation and neurodegeneration [623].

As stated earlier, MTOR has a dual function in Alzheimer's disease as it inhibits insulin signalling and reduces clearance of β-amyloid and phosphor-Tau [602]. While there is little evidence to support a direct interaction between mTOR and insulin growth factor binding protein-3 (IGFBP3), there is crosstalk with the IGF signalling pathway. Dysregulation of which is a key contributor to the pathology of Alzheimer's disease. For example, levels of IGFBP-3 are noted in ageing plaques and neurofibromin complexes in human brain [624] and that β-amyloid increases expression of IGFBP-3 protein in brain pericytes [625]. How this is directly linked to membrane trafficking in the brain is unclear. However, in corneal epithelial

cells, the secretion of IGFBP-3 mediates intracellular trafficking of IGF-1R receptor in response to stress [626].

MTOR is part of a well-established signal transduction pathway (PI3K/AKT/mTOR pathway) whereby PI3K activation leads to AKT activation, which in turn, activates mTOR [627]. Therefore, it is not surprising that okadaic acid increased PI3KCD (phosphatidyl inositol-4,5-bisphosphate 3-kinase catalytic subunit delta; aka, PI3Kδ or p110delta isoform of PI3K) levels in the present study and was highlighted in the protein interactome and following cluster analysis. In the context of Alzheimer's disease PI3Kδ influences the trafficking of APP and formation of amyloid plaques [628] and contributes to the neuroinflammatory component of Alzheimer's disease through increased trafficking and secretion of TNFα [629]. Interestingly, PI3Kδ is involved in the regulation of Rab5 GTPase, and hence endocytic trafficking [630].

Interestingly, I found okadaic acid increased the abundance of mucin-5B in brain microvascular endothelial cells with pathway enrichment analysis linking this to membrane trafficking. To the best of my knowledge, there has been no published work linking mucin-5 B to okadaic acid, PP2A, neurodegeneration or Alzheimer's disease. This is therefore a novel finding and difficult to explain within the context of this thesis. However, perturbations of mucin trafficking are well established in the pathophysiology associated with breast and colorectal cancer [631].

The current study showed that okadaic acid increased the abundance of oxysterol binding protein (OSBP) in brain microvascular endothelial cells. This corroborates earlier work showing okadaic acid to increase phosphorylation of OSBP [632]. Functionally, this may impact cholesterol trafficking within cells [633] as OSBP facilitates the trafficking of cholesterol from the endoplasmic reticulum to the trans-Golgi network [634]. However, the facilitated trafficking of cholesterol is unlikely to impact the development of Alzheimer's disease for several reasons. Firstly, reduced trafficking and biosynthesis of brain cholesterol is a notable feature in patients with Alzheimer's disease and in animal models. Secondly, the binding of amyloid precursor protein to cholesterol can lead to the production of amyloid-β and downregulation of ApoE-mediated cholesterol uptake [635], which may influence the onset of amyloid deposition. Interestingly, a confocal study indicates that ApoE colocalises with Rab11A, implicating the latter in endosomal recycling of cholesterol in CHO cells [636]. This ties in with our microarray data showing that okadaic acid increases Rab11A abundance.

The Rab GTPases are a family of small proteins that play a central role in Alzheimer's disease by regulating membrane trafficking within neurons, the dysregulation of which results in the abnormal trafficking of proteins like amyloid-β and tau [637]. In the current study, okadaic acid decreased the abundance of Rab1A but increased Rab11A. Rab1A is associated with both endoplasmic to Golgi and post-endosomal transcytosis of vesicles [638], and is implicated in regulating amyloid-β generation [639]. While few if any studies have investigated the role of Rab1A in Alzheimer's disease *per se*, its overexpression potentiates mTORC1 signalling in normal and cancer cells [640, 641]. This could represent a pathway through which it may contribute to the pathophysiology of Alzheimer's disease, as MTOR reduces autophagic removal of β-amyloid and phosphor-Tau, [602] as Rab1A was downregulated in the present study. Additionally, Rab1A also affects actin polymerisation and cell morphology through inhibition of mTOR signalling [642]. While Rab1A plays a general role in endocytic vesicle processing, it is also involved in the trafficking of EGF and transferrin [643].

In Alzheimer's disease, Rab11 controls endosomal recycling of β-secretase to the plasma membrane and hence increased production of Aβ [644]. Our microarray data would be consistent with an increase in membrane trafficking of β-secretases, as okadaic acid increases the abundance of Rab11A in brain microvascular endothelial cells. However, the increase in Rab11A abundance was not confirmed using a Western blot approach. It is difficult to reconcile the disparity between the microarray data and that obtained using Western blot. This might simply reflect the enhanced sensitivity of micro-immunoassays, such as those using microfluidic devices or surface-based assays for detection of low-abundance proteins over the standard Western blot approach [645]. Despite this, there is no existing literature that directly examines the effect of okadaic acid on Rab11A, although some studies have explored its impact on vesicle trafficking. For example, in goldfish bipolar cells, okadaic acid modulated the mobility and transport of recently internalised vesicles within ribbon-containing synaptic terminals [646]. However, the present study found that Rab11A knockdown did not alter the effect of okadaic acid on VE-cadherin abundance or PP2Ac abundance following a 24 h exposure. In contrast, Yan et al. report that Rab11A knockdown in endothelial cells reduces VE-cadherin abundance within 48 to 72 hours, followed by a gradual return to baseline levels, paralleling the expression pattern of Rab11A [412]. Importantly, in the latter study no effect was noted at the 24 h time point, which is consistent with our findings, but it would be worth extending our study to look at later time points in any future experiments. My data would indicate that Rab11A is not involved in recycling of VE-cadherin back to the plasma membrane following exposure to okadaic acid in brain microvascular endothelial cells.

Although Rab5A was not included on the immune-microarray, I decided to investigate if Rab5A was involved in okadaic-acid-mediated loss of VE-cadherin on the premise that Rab5 is a key regulator of endocytosis, mediating the fusion of endocytic vesicles with early endosomes [647]. siRNA silencing reduced Rab5A abundance by 66% and was unaffected by exposure to okadaic acid. In addition, Rab5A knockdown did not alter VE-cadherin or PP2Ac abundance under control conditions or in the presence of okadaic acid. Together, these data indicate that Rab5A is not involved in VE-cadherin internalisation in brain microvascular endothelial cells. However, in human pulmonary microvascular endothelial cells, lipopolysaccharide increases Rab5A abundance and internalisation, an effect which was reversed following knockdown of Rab5A [176]. The disparity with our data could be due to the use of different stimuli (lipopolysaccharide vs okadaic acid) or tissue selectivity of the response (lung vs brain). Alternatively, it may simply reflect a multitude of mechanisms by which VE-cadherin can be regulated, which include phosphorylation and management of localisation at the cell surface, regulated endocytosis and transcriptional regulation [648]. However, this requires further investigation to gain consensus.

### 4.4.4 Cell Adhesion

Neurodegenerative diseases are also associated with dysregulation of molecules involved in mediating cell-cell contacts. In the present study, pathway analysis linked several differentially regulated proteins to the cell adhesion (hsa04514) and tight junction (hsa04530) pathway descriptors. Cell adhesion molecules (CAMs) are key mediators of interactions between cells and their environment, essential for cell survival, movement, activation, and adaptability [649]. There are four main families of CAMs: cadherins, immunoglobulin superfamily members, selectins, and integrins that facilitate adhesion among vascular cells. Among these, E-cadherin is the most extensively studied and is predominantly found in adherens junctions of mature epithelial cells, where it links the actin cytoskeletons of neighbouring cells [650]. Our findings align with previous research indicating that okadaic acid alters the expression of EMT-related adhesion molecules such as Cadherin-6B (Cad6B) and E-cadherin (Cadherin 1). Another study also found that the formation of the E-cadherin/catenin complex is regulated by protein phosphatases [84].

VE-cadherin (also known as cadherin 5 or CD144) plays a key role in forming adherens junctions (AJs) and maintaining the barrier function of endothelial cells [72]. In our study, we found decreased VE-cadherin levels, consistent with other studies suggesting it may serve as

an early indicator of endothelial damage in the preclinical phase of Alzheimer's disease, based on cerebrospinal fluid and gene expression data [651]. E-selectin, a member of the selectin family and expressed on activated endothelial cells, facilitates the initial rolling and eventual stable adhesion of leukocytes at inflammatory sites [652-654]. Recent evidence suggests that E-selectin not only mediates adhesion but also interacts with the actin cytoskeleton via proteins like α-actinin, vinculin, filamin, and signalling molecules such as focal adhesion kinase (FAK) and paxillin, indicating a signalling function previously unrecognized [652, 655]. In our study, E-selectin expression decreased following exposure to okadaic acid. This is consistent with prior work showing that okadaic acid prevents leukocyte-induced E-selectin dephosphorylation in activated HUVECs [652]. Another adhesion-related protein impacted by okadaic acid is CD274 (also known as PD-L1 or B7-H1), which is relevant in various cancers [656]. PD-L1 is expressed on multiple immune and endothelial cells, including dendritic cells, lymphocytes, and, under certain conditions, epithelial cells, especially during inflammation [657, 658]. In our findings, PD-L1 expression was upregulated after okadaic acid treatment, consistent with other studies reporting that OA can enhance PD-L1 expression [659].

### 4.4.5 Tight junction

One research study showed that okadaic acid impacts tight junction proteins in intestinal Caco-2 cells at concentrations relevant to food exposure [660]. c-Jun N-terminal kinase (JNK) is part of the mitogen-activated protein kinase (MAPK) family [661]. MAPKs are known to contribute to the abnormal hyperphosphorylation of tau proteins in Alzheimer's disease (AD) brains with reduced PP2A activity [662]. In our study, okadaic acid increased the expression of MAPK8, which is consistent with other research reporting JNK activation in neurofibrillary degeneration in neurons of Alzheimer's disease [663, 664]. The activation of several kinases, including Ser/Thr kinases, MAPK, ERK, PKA, JNK, PKC, CaMKII, Calpain, and GSK3β, has been linked to AD pathology [665]. Additional studies have demonstrated that kinases such as Raf-1, MEK, and MAPKs (including ERK) become hyperphosphorylated in response to okadaic acid [666, 667]. MAPKs like JNK, p38, and ERK have also been reported to be upregulated in neurodegenerative diseases such as Alzheimer's disease and Parkinson's disease [668].

In the present study, okadaic acid also affected the expression of PCNA (proliferating cell nuclear antigen), a protein involved in tight junction signalling. PCNA plays a crucial role in DNA replication and repair [669]. While it is typically absent in adult neurons, PCNA is found in the nuclei of vulnerable neurons in patients with Parkinson's disease and in dopaminergic neurons of MPTP-treated mice [670]. PCNA expression was also upregulated in HepaRG cells

exposed to 33 nM okadaic acid [516]. Furthermore, studies have observed increased expression of PCNA, along with markers like Mcm2 and Ki67, in glial cells and neurons, correlating with greater Alzheimer-type pathology [671]. The significance of PCNA in Alzheimer's disease is further supported by autopsy-based immunohistochemical studies showing the presence of cell cycle-related proteins such as Ki67, PCNA, cdc2, cdc25A, cdk4, and various cyclins in Alzheimer's disease-affected brains [672-677].

In conclusion, the present study provides novel insights into how okadaic acid (10 nM), a potent PP2A inhibitor, disrupts the proteomic landscape of human brain microvascular endothelial cells, with implications for neurodegeneration and blood-brain barrier dysfunction. Through a detailed proteomic and bioinformatic analysis, okadaic acid was shown to differentially regulate 104 proteins, with functional clustering highlighting roles in cytoskeletal integrity, cell adhesion, inflammation, membrane trafficking, and protein degradation, processes central to Alzheimer's disease pathology. Notably, key molecules such as MAPT, MTOR, Rab1A, Rab11A, and UBB were differentially expressed, reinforcing connections to Tau pathology, impaired autophagy, and amyloid-β accumulation. Despite Rab11A's increased abundance in the microarray data, functional studies indicated it is not directly involved in VE-cadherin recycling at the 24-hour mark, suggesting time-dependent effects or alternate trafficking routes. Additionally, the upregulation of MAPK8, PCNA, and PD-L1 supports a broader inflammatory and stress response, while the novel finding of increased mucin-5B introduces a potentially unexplored mechanism in neurovascular dysfunction. Overall, these findings expand our understanding of okadaic acid's molecular effects and underscore the importance of phosphatase regulation in endothelial health and neurodegenerative disease progression. To fully elucidate the mechanism by which okadaic acid reduces VE-cadherin levels, additional experiments are needed to explore the roles of other candidate proteins that may contribute to its trafficking or transcriptional regulation.

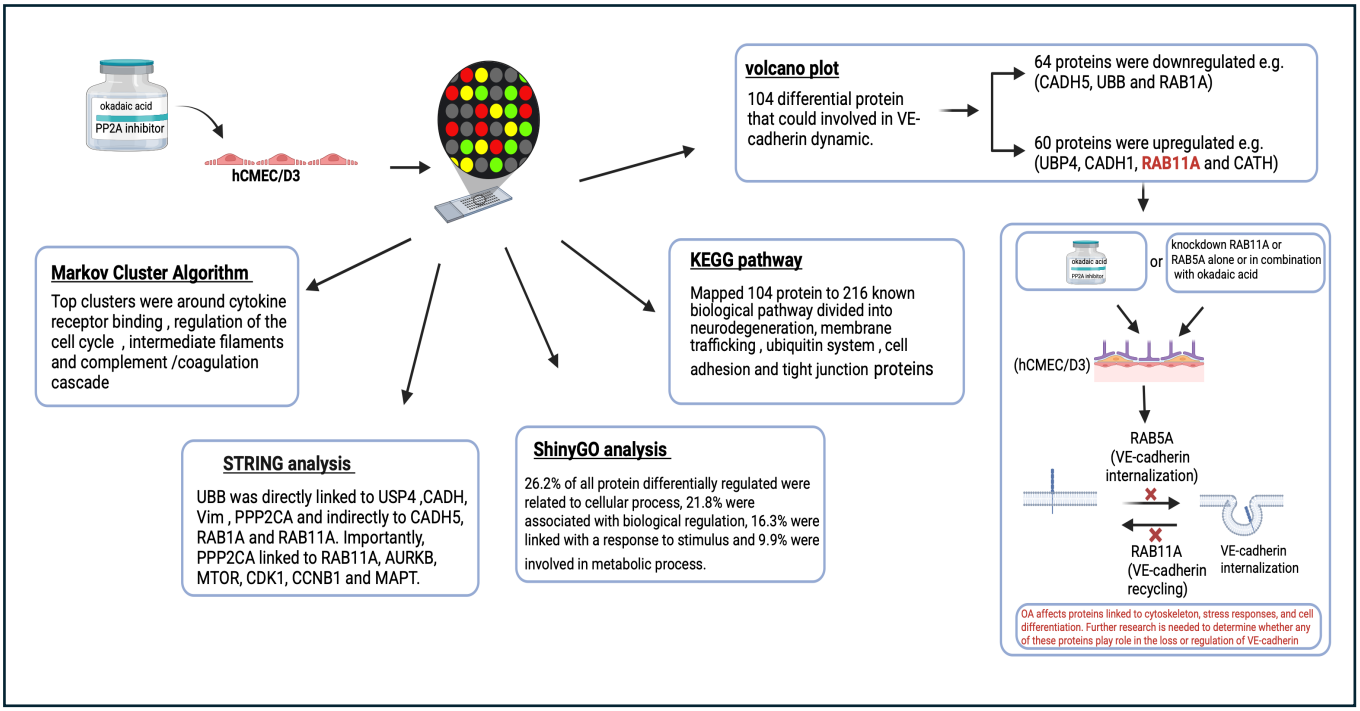


**Figure 4.17: A schematic summary of the Proteomic Microarray data from hCMEC/D3 cells following exposure to okadaic acid, revealing a protein network of differentially expressed proteins implicated in numerous biological processes, including VE-Cadherin recycling and degradation**

# Chapter 5

# Investigation of the Effect of Metformin on Protein Phosphatase 2A and VE-cadherin in Brain Microvascular Endothelial Cells

## 5.1 Introduction

The blood-brain barrier is crucial for sustaining brain homeostasis and safeguarding the central nervous system (CNS). Disruption of the BBB has been noted following traumatic head injuries, strokes, oedema, and inflammation, as well as in Alzheimer's and Parkinson's diseases [678]. In research on neurodevelopmental disorders, the role of PP2A has been extensively investigated as PP2A accounts for about 71% of the total tau phosphatase activity in the human brain [596]. For example, in Alzheimer's disease, it is well documented that Tau protein is hyperphosphorylated [594] and has been associated with a diminished activity of PP2A in both grey and white matter [679]. Additionally, a study by Sontag et al. showed that levels of the PP2ABαC heterotrimeric complex, which is the primary isoform of neuronal PP2A that interacts with tau, are reduced [147].

As such, the activation of PP2A presents a promising strategy to prevent and treat Alzheimer's disease and related tauopathies [680]. Intriguingly, there is also a strong relationship between Alzheimer's disease and type 2 diabetes mellitus [681-684]. It is interesting to speculate that protein phosphatase 2A may represent a commonality between these two conditions, as it is also dysregulated in type II diabetes mellitus and is involved in the development of insulin resistance [685, 686]. Similarly, type 2 diabetes mellitus is associated with Parkinson's disease (PD) [158, 385] , which is also associated with dysregulation of PP2A. This raised the possibility that therapeutic agent used for diabetes, such as metformin, may serve as potential treatments for neurological disorders, offering new perspectives on their management [687, 688].

One such drug, metformin, has been used since the 1960s in the treatment of type 2 diabetes and other metabolic disorders is of particular interest as it can cross the blood-brain barrier and is neuroprotective [460]. Metformin also reduces tau phosphorylation at PP2A-dependent sites in both experimental and animal models related to Alzheimer's disease [185, 471, 689-691]. This is in keeping with other studies, which demonstrate that metformin activates PP2A activity in human skeletal muscle cells, macrophages, primary cortical neurons, and in mice. However, this remains to be established for brain microvascular endothelial cells. Metformin also improves memory function in the senescence-accelerated mouse-prone 8 (SAMP8) model of spontaneous Alzheimer's disease by reducing amyloid precursor protein c99 (APPc99) and tau phosphorylation [682]. Within the context of this thesis, which focuses on PP2A-mediated regulation of VE-cadherin, metformin offsets hypoxia and VEGF-induced endothelial barrier

permeability in murine endothelial monolayers by enhancing expression of tight junction proteins such as occludin, claudin-3, claudin-5, zonal occludin-1 (ZO-1), and zonal occludin-2 (ZO-2) [685, 692]. Interestingly, in a recent study, metformin reversed hydrocephalus and upregulated VE-cadherin expression in choroid plexus in a rat model of intraventricular haemorrhage [421]. Based on these studies, metformin may be considered an option for addressing BBB dysfunction induced by okadaic acid through maintenance of adherent junctions via upregulation of VE-cadherin abundance. However, this remains to be established.

It is important to emphasise that the primary aim of this chapter is to investigate the potential cellular mechanisms of action of metformin, including its interaction with PP2A and effects on VE-cadherin in brain microvascular endothelial cells. While type 2 diabetes mellitus is associated with blood-brain barrier dysfunction, this study does not aim to model the chronic effects of diabetes or tight glycaemic control. Addressing such long-term effects would require experimental approaches involving varied glucose concentrations and comparisons with other antidiabetic agents, which are beyond the scope of the present work.

Therefore, the aims of this chapter were to:

1. Investigate if metformin directly modulates PP2Ac activity and abundance in brain microvascular endothelial cells and whether it can reverse the inhibitory effect of okadaic acid.
2. Determine if metformin in the absence or presence of okadaic acid can modify VE cadherin abundance in human brain microvascular endothelial cells.

## 5.2 Method

### 5.2.1 Cell Culture

Full details of the cell culture protocols can be found in Chapter 3, section 3.2.1. In brief, hCMEC/D3 cells were seeded onto collagen type 1 coated plates (rat tail collagen, 08225, EMD Millipore Corp, USA) and cultured in EndoGRO-MV medium (Merck, Cat. #SCME-BM) containing 5% foetal bovine serum (FBS), growth factors (Merck, Cat. #SCME004-S), 100 U/mL penicillin, and 100 mg/mL streptomycin. The cells were kept in a humidified atmosphere at 37°C and 5% $CO_2$, and the medium was changed every 3 to 4 days until the cells reached approximately 80% confluence. To subculture confluent cells, they were treated with 0.25% trypsin-EDTA solution (Sigma-Aldrich) and subsequently counted using a haemocytometer after trypan blue staining. The hCMEC/D3 cells were used up to passage number 45.

### 5.2.2 Cell Viability: LDH Assay

hCMEC/D3 cells were seeded in 96-well plates at a density of 10,000 cells per well and exposed to increasing concentrations of metformin (10 µM - 50 mM), dimethylsulphoxide (DMSO; 0.0001% to 1% v/v) or Triton-X100 (1% v/v; positive control). DMSO was used as the solvent control for okadaic acid. The cells were exposed to metformin or DMSO for 24 hours. The plates were then centrifuged at 250 × g for 10 minutes, and the supernatants were transferred to a new 96-well plate. The LDH Cytotoxicity Assay reagent mixture (Roche, Cat. #11644793) was prepared according to the manufacturer's instructions by mixing 250 µL from the blue cap bottle with 11.25 mL from the red cap bottle, which is sufficient for 100 samples at each. This reagent mix (100 µL) was added to each well and incubated for 30 minutes at room temperature in the dark. Absorbance was measured at 490 nm using a BioTek EL 808-plate reader (Bedfordshire, UK). Cell death was quantified based on the kit protocol and expressed as a percentage relative to the LDH release induced by 1% Triton X-100, representing 100% cell death.

### 5.2.3 Protein Extraction and Quantification

Before cell lysis, the culture medium was removed, and the cells were washed in sterile ice-cold PBS (D8662, Sigma-Aldrich). Cells were then lysed in RIPA buffer supplemented with 100x protease inhibitor cocktail Set I (539131-EMD Millipore Corp, Germany) and harvested using a cell scraper. The cell suspension was then placed in an Eppendorf tube and incubated on ice for approximately 15 minutes before undergoing three freeze-thaw cycles at -80°C. Cell debris was removed by centrifugation (400 x g, 10 min) and the supernatant was transferred to

a sterile 1.5 mL sampling tube and stored at -80°C for protein quantification and downstream Western blot analysis.

Protein content in the cell lysate was quantified using a Bradford assay. Absorbance was determined at a wavelength of 595 nm using a spectrophotometer (BIO-TEK EL808). Absorbance of the unknown samples was interpolated from a standard curve using bovine serum albumin as the reference protein. The protein content in all samples was standardised to 1 mg/mL unless otherwise stated. Full details of the protocols for protein isolation and quantification can be found in chapter 3, section 3.2.3. and 3.2.4. respectively.

### 5.2.4 SDS-PAGE and Western Blotting

Protein samples (20 µg) were mixed with sample loading buffer (x5) and heated at 95°C for 30 seconds before being cooled on ice for 3 minutes. Following denaturation, the samples were subjected to sodium dodecyl sulphate-polyacrylamide gel electrophoresis (SDS-PAGE) on either an 8% or a 12% gel. To determine the relative molecular weight of the protein bands, a molecular weight ladder (Thermo Fisher) was included on each gel. Following electrophoresis, proteins were transferred to a Polyvinylidene fluoride (PVDF) membrane using the iBlot 2 Dry Blotting System from Amersham. Membranes were blocked in TBS-T with 5% milk or 2% BSA for one hour at 4°C, and probed with the primary antibody overnight at 4°C. The following day, the membranes were washed with TBS-T, incubated with an HRP-conjugated secondary antibody specific to mouse or rabbit at room temperature for 1 hour in TBS-T + 5% milk. The protein bands were visualised using chemiluminescence detection and the image captured on a Fusion FX imaging system (Vilber Lourmat). Densitometric analysis of the protein bands was performed using Bio1D software. Membranes were stripped with a stripping solution and re-probed with an HRP-conjugated βactin antibody. A detailed description of the protocols can be found in chapter 3, 3.2.5.1 and 3.2.5.2. respectively.

### 5.2.5 RNA Cell Extraction and cDNA Synthesis

hCMEC/D3 cells grown in 6-well or 12-well plates were lysed in Tri Reagent™ (Sigma Aldrich). After the addition of 200 µL of chloroform and a 10-minute incubation at room temperature, the mixture was centrifuged at 12,000 g for 15 minutes at 4°C. The upper aqueous phase, which contained the RNA, was transferred to a new Eppendorf tube, and RNA precipitated by the addition of isopropanol. Following centrifugation (12,000 g for 10 minutes at 4°C), the supernatant was removed, and the RNA pellet was washed with increasing concentrations of ethanol (75% and 100% v/v). The RNA pellet was air dried and reconstituted

in nuclease-free water, with heat at 95°C for 5 minutes to aid in dissolving. RNA quantity and purity were analysed by measuring the 260/280 ratio on a spectrophotometer (Nanodrop).

The RNA samples were treated with DNase I (Invitrogen) before undergoing reverse transcription. cDNA synthesis was performed using the RevertAid Reverse Transcriptase kit (Thermo Fisher) and random hexamer primers. Detailed protocols associated with RNA isolation, clean-up and reverse transcription can be found in Chapter 3, sections 3.2.6.1 and 3.2.6.2.

### 5.2.6 Semi-Quantitative Real-Time PCR

mRNA expression was analysed using semi-quantitative reverse transcription polymerase chain reaction (RT-PCR) with target-specific primers and SYBR Green GoTaq DNA polymerase (Promega, A6002) on an Mx3000P QPCR System (Agilent Technologies). Lyophilised primers were reconstituted to give a stock solution of 100 µM and further diluted to give a 10 µM working concentration for RT-PCR. The reaction mix consisted of 10 µL of 2x SYBR Green mix, 50 ng cDNA template, 500 nM of each forward and reverse primer, and molecular grade water to a final volume of 20 µL. A non-template control was included for each primer set. The PCR cycling conditions were as follows: an initial denaturation at 95°C for 2 minutes, followed by 40 cycles of 95°C for 15 seconds, 62°C for 1 minute, 72°C for 15 seconds. Gene expression was quantified using the comparative Ct method; detailed protocols are described in Chapter 3, section 3.2.6.3.

| Gene | NMID | Forward Sequence | Reverse Sequence |
|---|---|---|---|
| **PPP2CA** | NM_00 2715.2 | TGGAGCCTCAGCGAGCGG | GGCTCTTGACCTGGGACT |
| **VE-cadherin** | NM_001795.4 | ATACCAAGGTCCACTTC | GTGAGGATGCAGAGTAA |
| **GPI** | NM_001329911.2 | TCTATGCTCCCTCTGTGTTAGA | CTCCTCCGTGGCATCTTTATT |
| **GAPDH** | NM_002046.5 | CTCTGCTCCTCCTGTTCGAC | GCGCCCAATACGACCAAATC |

**Table 5.1: List of primers including gene identification numbers and sequence**

### 5.2.7 PP2A Phosphatase Activity Assay

PP2Ac activity was determined using a PP2A immunoprecipitation phosphatase assay kit from Merck Millipore. In brief, 100 µg of protein was combined with 4 µg of anti-PP2A (C subunit, clone 1D6) and protein-A-agarose. The immunoprecipitate was collected by centrifugation (Microcentrifuge Technico mini, 50s) and washed three times with 700 µL TBS and once with 500 µL of the Ser/Thr assay buffer. The immunoprecipitate was incubated with 60 µL of diluted phosphopeptide and 20 µL Ser/Thr assay buffer at 30°C for 10 min in a constant temperature shaker. Following this, malachite green was added, and the absorbance was determined at a wavelength of 620 nm in a microtiter plate reader (Varioskan Lux, Thermo Scientific). A full description of the protocol can be found in chapter 3, section 3.2.8.

### 5.2.8 Data and Statistical Analysis

Data were normalised to the appropriate control and presented as either an absolute value, a percentage, or a ratio. Using non-linear regression (GraphPad Prism version 10), protein concentration was determined from a standard curve. Statistical analysis was conducted using one-way ANOVA with appropriate *post hoc* analysis (Dunnett's) in GraphPad Prism version 10. The data are presented as mean ± S.E.M., and a P value of less than 0.05 was considered statistically significant.

## 5.3 Result

### 5.3.1 Effect of Metformin and DMSO on Cell Viability

In preliminary experiments to optimise the LDH assay, the effect of cell number (781 to 50,000 cells / well) on Triton X100 (1% v/v; positive control) mediated LDH release was investigated alone and in combination with DMSO (0.01% v/v) compared to medium alone. Exposure to Triton X100 (1% v/v) for 24 h increased LDH release in a cell number-dependent manner compared to medium alone (Untx; Figure 5.1A). This response was unaltered by co-exposure to DMSO (0.01% v/v; Figure 5.1A). Based on this data, the effect of increasing concentrations of DMSO (0.0001 - 1% v/v) and metformin (10 µM-50 mM) on LDH release using 25,000 cells per assay well was investigated. DMSO and metformin had a minimal effect on LDH release (less than 10% reduction) compared to those exposed to medium alone (Figure 5.1B). Although these findings are preliminary and based on a single experiment, it was decided to use metformin at a concentration of 15 mM in all subsequent experiments.

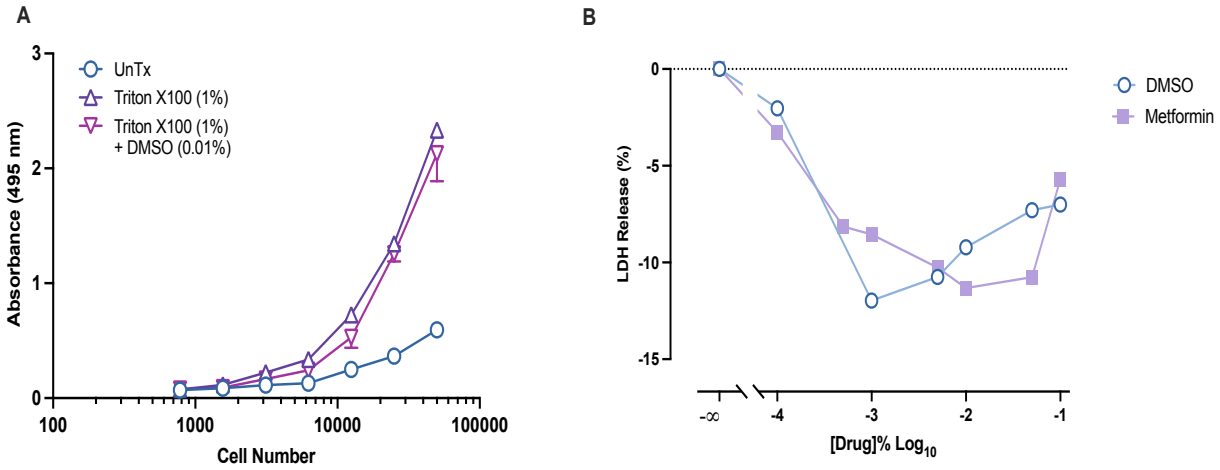


**Figure 5.1: Optimisation of the lactate dehydrogenase (LDH) cytotoxicity assay.** The effect of cell number on LDH release following exposure to Triton-X100 (1% v/v, positive control) alone and in combination with DMSO (0.01% v/v) (A) or in response to increasing concentrations of DMSO (0.0001-1%) or metformin (10 µM- 50 mM; B) were investigated in hCMEC/D3 cells. LDH release in the culture medium was measured using a commercial kit after 24 h (n=1).

### 5.3.2. Does Metformin Affect PP2Ac Abundance and Activity?

The effect of metformin on PP2Ac abundance was determined using Western blot. When hCMEC/D3 cells were exposed to metformin (15 mM) for 24 h, no effect on PP2Ac protein abundance was observed compared to the untreated group (medium alone; Figure 5.2A, B). To extend this finding, the effect of metformin on PP2Ac activity was investigated using a PP2Ac immunoprecipitation activity assay. In hCMEC/D3 cells exposed to metformin (15 mM), there was no observable effect on PP2Ac activity compared to the untreated group (medium alone; Figure 5.2C).

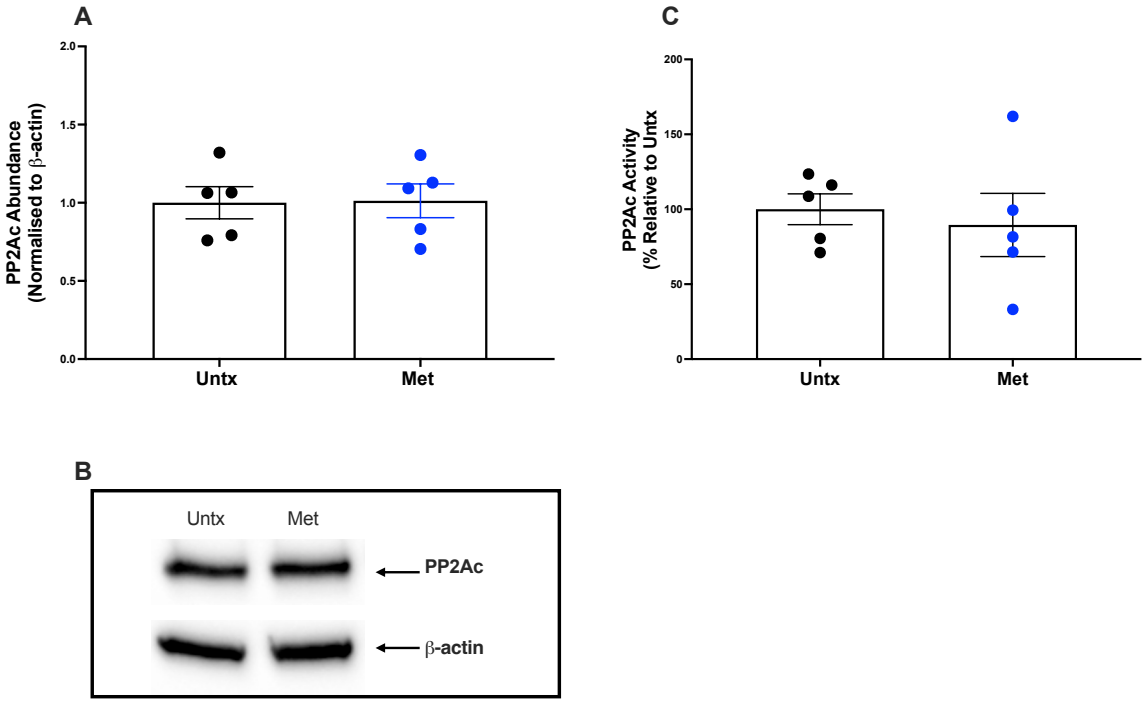


**Figure 5.2: Effect of Metformin on PP2Ac abundance and activity.** hCMEC/D3 cells were exposed to metformin (Met; 15 mM) and its effect on PP2Ac abundance determined in cell lysates using Western blot (A, B), while PP2Ac activity was determined using a PP2Ac immunoprecipitation activity assay (C). A representative immunoblot is presented in B. PP2Ac abundance was normalised to β-actin and expressed relative to the untreated group (A, B), while PP2Ac activity was expressed relative to the control group (Untx; C), Data were analysed using an unpaired t-test and presented as mean ± S.E.M. Horizontal bars indicate statistical significance at $P<0.05$ (n=5).

### 5.3.3 Does Metformin Alter the Effect of Okadaic Acid on PP2Ac Activity and mRNA Expression?

As I showed in chapter 3 (section 3.3.5) that okadaic acid decreased PP2Ac activity, I investigated if metformin could reverse this effect before looking at its effect on VE-cadherin. In hCMEC/D3 cells, metformin (15 mM) did not affect PP2Ac activity compared to the untreated group (Figure 5.3A). While okadaic acid (10 nM) decreased PP2Ac activity by 60% compared to the control group (Untx; Figure 5.3A), as shown in earlier experiments. Interestingly, exposure to metformin (15 mM) and okadaic acid (10 nM) PP2Ac activity was decreased by 58% compared to the untreated group ($P<0.05$; Figure 5.3A). To extend this finding and rule out possible effects at the level of transcription, I looked at the effect of metformin and okadaic acid alone and in combination on PPP2Ac expression in hCMEC/D3 cells. Neither metformin (15 mM) nor okadaic acid (10 nM) alone or in combination affected PPP2Ac expression compared to cells exposed to medium alone (Figure 5.3B). DMSO (0.01% v/v; solvent control) did not alter the PP2Ac activity or PPP2Ac expression compared to the control group (Figure 5.3 A, B).

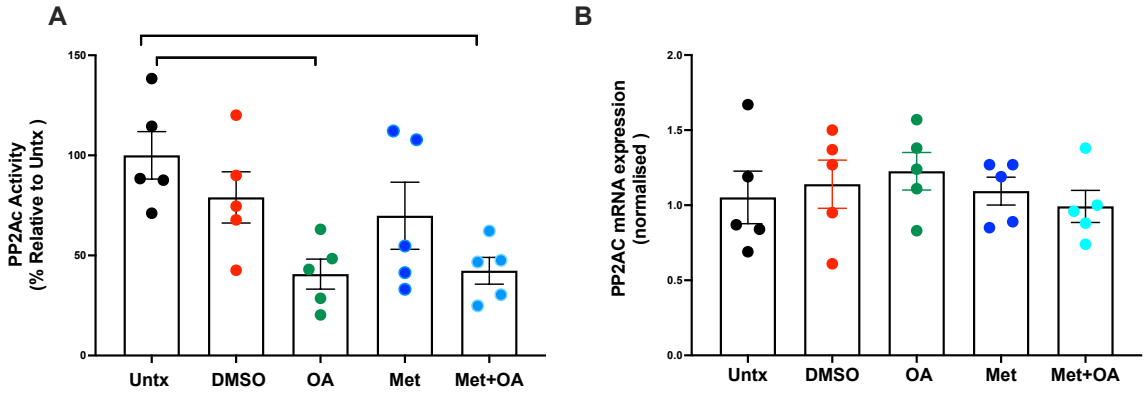


**Figure 5.3: Effect of Metformin (Met, 15 mM) and Okadaic Acid (OA, 10 nM) alone and in combination on PP2Ac activity and mRNA expression.** PP2Ac activity was determined using an immunoprecipitation assay kit (Millipore). The data were normalised to the Untx control (medium alone) and expressed as a percentage (A). PPP2Ac mRNA expression was determined by RT-PCR and normalised to the geometric mean of GAPDH and GPI and expressed relative to the untreated group (B). DMSO (solvent control) was used at a concentration of 0.01% (v/v) in both experiments (A, B). Data were analysed using a one-way ANOVA with *post hoc* analysis (Dunnett's test) and presented as mean ± S.E.M. Horizontal bars indicate statistical significance at $P<0.05$ (n=5).

### 5.3.4 Effect of Metformin Alone and in Combination with Okadaic Acid on VE-cadherin Abundance and mRNA Expression

The effect of metformin and okadaic acid alone and in combination on VE-cadherin abundance and mRNA expression was investigated using Western blot and RT-PCR. Metformin had no effect (Figure 5.4 A) on VE-cadherin abundance, while okadaic acid (10 nM) decreased it by 47% compared to the untreated group in hCMEC/D3 cells (medium alone; Figure 5.4 A; $P<0.05$). Similarly, okadaic acid in combination with metformin (15 mM) also reduced VE-cadherin abundance by 53% (Figure 5.4 A; $P<0.05$) compared to control (Untx). When the effect on VE-cadherin expression was explored, okadaic acid (10 nM; $P<0.05$) increased VE-cadherin expression while metformin (15 mM) had no effect (Figure B). In the presence of okadaic acid and metformin, VE-cadherin expression was increased compared to the untreated group (Figure 5.4 B; $P<0.05$). DMSO (0.01%) did not alter VE-cadherin abundance or expression in hCMEC/D3 cells compared to control (Untreated, Figure A, B).

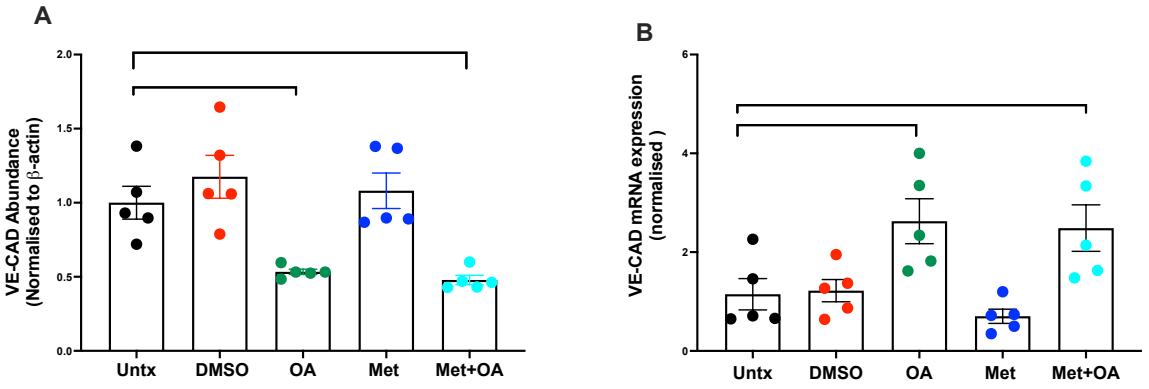


**Figure 5.4: Effect of Metformin (15mM) alone and in combination with Okadaic Acid (10nM) on VE-cadherin abundance and mRNA expression.** VE-cadherin abundance was determined by Western blot and normalised to β-actin abundance (A). VE-cadherin mRNA expression was determined by RT-PCR and normalised to the geometric mean of GAPDH and GPI. DMSO was used at a concentration of 0.01% (v/v) in both experiments (A, B). Data are analysed using a one-way ANOVA with *post hoc* analysis (Dunnett's test) and presented as mean ± S.E.M. Horizontal bars indicate statistical significance at $P<0.05$ (n=5).

### 5.3.5 Temporal Effect of Metformin Alone and in Combination with Okadaic Acid on VE-cadherin Abundance

As exposure to metformin for 24 h failed to alter okadaic acid-mediated attenuation of VE-cadherin abundance, it raised the possibility of a transient response. To address this, the effect of metformin (15 mM) and okadaic acid (10 nM) alone and in combination was studied at several time points over 24 h. As expected, there was no change in VE-cadherin abundance in any of the treatment groups at baseline (0 h; Figure 5.5A). Exposure of hCMEC/D3 cells to metformin decreased VE-cadherin abundance at the 4 h time point compared to the DMSO group (Figure 5.5 B; $P<0.05$, 40%). While a similar decrease was observed compared to the control group, this failed to reach significance. However, at 8 hours, metformin decreased VE-cadherin abundance by 57% compared to the untreated group (Figure 5.5C; $P < 0.05$). This effect was gradually lost as no effect was noted at the 10 and 24 h time points (Figure 5.5). Okadaic acid did not affect VE-cadherin abundance at the 4 h time point but decreased it from 8 h onwards (Figure 5.5C; $P<0.05$). At the 8 h timepoint, okadaic acid decreased VE-cadherin abundance by 64%.

When cells were exposed to okadaic acid in combination with metformin, VE-cadherin abundance was decreased at the 4 h time point compared to Untx and DMSO groups (Figure 5.5 B; $P<0.05$). This likely reflects the ability of metformin to decrease VE-cadherin abundance at this time point as okadaic acid alone had no effect at this time point. Interestingly, when cells were exposed to okadaic acid in combination with metformin at the 10 h timepoint, VE-cadherin abundance was higher than in the corresponding okadaic acid group (Figure 5.5D; $P<0.05$). This would indicate that at this time point, metformin can reverse okadaic acid-mediated loss of VE-cadherin. A similar effect was observed at the earlier 8 h time point, but this failed to reach significance (Figure 5.5C). In keeping with the earlier data, the combination of metformin and okadaic acid did not affect VE-cadherin abundance at the 24 h time point (Figure 5.5 E). DMSO (0.01% v/v) did not alter VE-cadherin abundance compared to the Untx group at any time point studied.

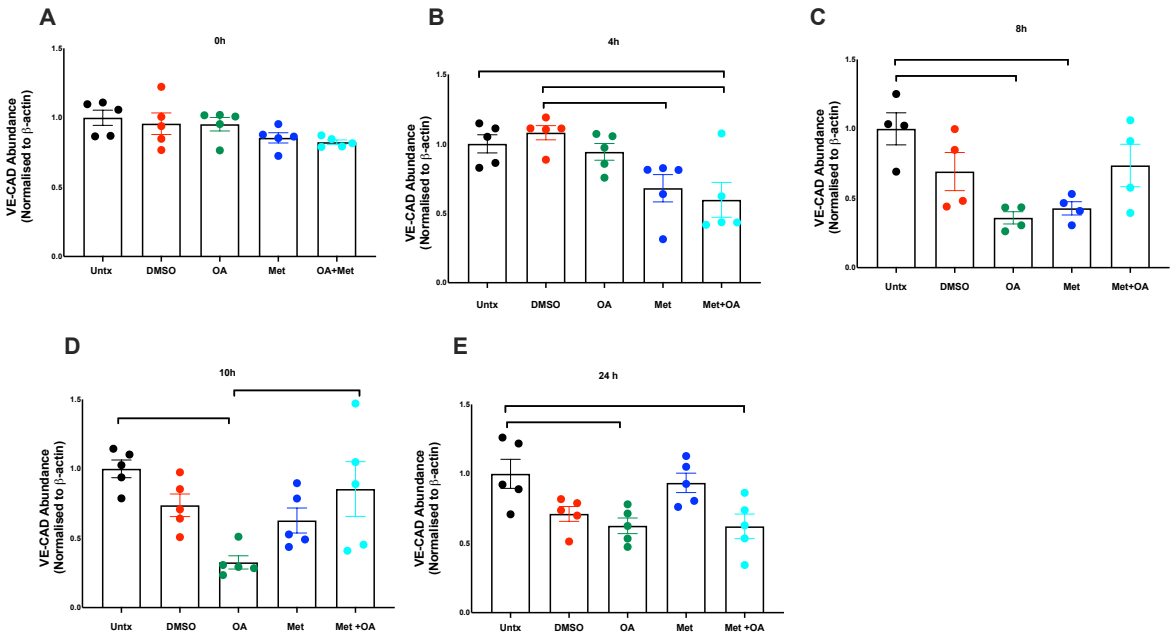


**Figure 5.5: Temporal Effect of Metformin alone and in combination with Okadaic Acid on VE-cadherin Abundance.** hCMECD3 were exposed to okadaic acid (OA, 10 nM), metformin (Met, 15mM) alone or in combination over 24 h. DMSO (0.01%) was used as a solvent control. VE-cadherin abundance was determined using Western blot and normalised to β-actin abundance (loading control). Data are analysed using a one-way ANOVA with *post hoc* analysis (Bonferroni) and are presented as mean ± S.E.M. Horizontal bars indicate statistical significance at $P<0.05$ (n=5).

## 5.4 Discussion

In the present study, I show that metformin does not modulate PP2Ac activity in human brain microvascular endothelial cells, but that it decreases VE-cadherin abundance and attenuates okadaic acid-mediated loss of VE-cadherin in a transient time-dependent manner at a concentration which does not affect cell viability. Moreover, metformin does not attenuate the okadaic acid-mediated increase in VE-cadherin mRNA expression.

In preliminary experiments, the dose-dependent effect of metformin on cell viability (lactate dehydrogenase) release was investigated, and it was found to have little effect up to a concentration of 100 mM. A review of the literature surrounding the *in vitro* application of metformin indicated that concentrations used are typically in the range of 1-100 mM [693]. Based upon this and the lack of toxicity in the preliminary experiments, I decided to use a concentration of 15 mM in the current series of experiments. This aligns with other studies using metformin (15 mM) in Panc1, Panc28, L3.6pL cells [688] and NSCLC cells [694]. However, it should be noted that many in *vitro* studies, including my own, use metformin at a concentration which exceeds the peak plasma level of metformin reported in clinical trials, which is 5 mg/mL or 30 µM [695]. In this study, metformin was applied directly to brain microvascular endothelial cells, at concentrations in excess of those typical achieved clinically. This approach allows direct assessment of cellular mechanisms, such as effects on PP2A activity and VE-cadherin regulation, without interference of systemic metabolism, organ interactions, or indirect effects that occur *in vivo*. However, it is important to acknowledge that the concentrations used may not reflect pharmacological levels achievable in patients, and therefore the effects observed may differ when other tissues, pharmacokinetics, and indirect systemic influences are involved. Therefore, while my acute high-dose experiments are useful for mechanistic insights, caution is needed when interpreting these findings for clinical relevance, and complementary *in vivo* studies are required to confirm therapeutic potential.

In the present study, metformin (15 mM, 24 h) did not alter PP2Ac activity in hCMEC/D3 cells, which is in agreement with data obtained in murine C2C12 microtubules, although using a lower concentration (500 µM metformin) [696]. Conversely, other studies reported metformin-induced activation of PP2A in A549 and H1651 lung cancer cell lines [697], and murine primary neurons and human epithelial cells HeLa; 10mM ) [185], human skeletal muscle cells from lean, insulin-sensitive individuals [471], human subcutaneous white adipose tissue (10 µM metformin) [698] and in myeloproliferative neoplasm (15 mM) cells [699]. Nevertheless, there are several differences between these studies and the present work, which include the

concentration of metformin used (15 mM vs 10 mM or 2.5 mM), time point (24 h vs 4 h) and species (human vs murine). Interestingly, in the study by Kickstein *et al*., which used 2.5 mM metformin and a time point of 4 h, metformin did not affect PP2Ac activity upon immunoprecipitation of the catalytic subunit (PP2Ac) as in our study, but increased it when the holoenzyme was pulled down via immunoprecipitation with an antibody directed against the scaffolding subunit of PP2A (PP2A-A subunit-specific antibody) [185]. Hence, metformin does not directly activate PP2Ac activity but mediates its activity via a component of the PP2A holoenzyme. It would be interesting to use the latter approach in any follow-up work.

The effect of metformin on PP2Ac may be more complex. For example, in primary cardiomyocytes, the proinflammatory response to high glucose is inhibited by metformin through reduced phosphorylation of PP2Ac at $Tyr^{307}$, which disrupts the interaction between PP22Ac, A4 and MID1 [700]. To expand the findings of the current study, the effect of metformin on PP2Ac abundance and mRNA expression was investigated to rule out any confounding influence on PP2Ac activity. However, exposure to metformin (15 mM) for 24 h did not alter either protein or mRNA expression of PP2Ac. This supports a recent paper showing that metformin (4 mg/mL) does not affect PP2A protein abundance in PS19 mice [689]. While there is a paucity of data regarding the effect of metformin on PPP2Ac expression, Hanawa et al. show there is no effect on expression of the PPP2R4 regulatory subunit in endometrial cancer cell lines (HEC265 and HEC1B) [460]. However, the present study raises the possibility that PP2Ac activity may be too pronounced (saturated) to detect induction by metformin, so its effect in the presence of okadaic acid was also investigated. While okadaic acid reduced PP2Ac activity as reported in chapter 3 of this thesis and widely within the literature [558, 701, 702], metformin did not attenuate or modify okadaic acid-mediated inhibition of PP2Ac activity. This supports our finding that metformin does not modulate PP2Ac activity in hCMEC/D3 cells under my experimental conditions, i.e. when assayed following immunoprecipitation of the catalytic subunit.

Metformin is associated with a wide range of effects encompassing anti-inflammatory [703] and preservation of cellular junctions [421, 704]. In the latter study, Shen *et al.* found that metformin prevents internalisation and loss of VE-cadherin in choroid plexus in a rat model of intraventricular haemorrhage [421]. However, in the present study, exposure to metformin for 24 h did not affect VE-cadherin abundance in brain microvascular endothelial cells. However, when the temporal effect was investigated, metformin decreased VE-cadherin abundance at the 4 and 8 h time points, before returning towards baseline levels. The disparity between the study by Shen and co-workers and the present study may reflect differences in the species used

(human vs rat), physiological state (normal vs cancer) and/or the concentration of metformin used (15 mM vs 50 mg/kg i.e. for 7 days). Although it likely reflects the experimental condition used, as in the present study, cells were "physiological" (unstimulated conditions) while those of Shen and co-workers were observed under "pathophysiological" (experimental model of intraventricular haemorrhage) conditions. Outside of these two studies, there is a paucity of data addressing the effect of metformin on VE-cadherin abundance. However, metformin does not affect occludin, claudin-5, zonal occludin-1 (ZO-1) and zonal occludin-2 (ZO-2) abundance in rat brain microvascular endothelial cells or bEnd3 cells [685, 705], or E-cadherin abundance in airway epithelial cells [706] under "physiological" conditions. These studies are in keeping with our finding that metformin has little effect on VE-cadherin under "physiological" conditions, with the caveat that a temporal decrease is noted following short-term exposure. However, under "pathophysiological" conditions, metformin reverses the downregulation of ZO-1, claudin-1 and occludin in a dextran sulphate sodium model of colitis [707], and ZO-1, occludin, claudin-1, claudin-3 and claudin-5 following exposure to lipopolysaccharide or in a rat model of sepsis [692, 708].

In the present study, okadaic acid was used a pharmacological tool to represent a generalised "pathophysiological" model of hyperphosphorylation, as occurs in Alzheimer's disease [595] and cancer [709]. Consistent with earlier data presented, okadaic acid decreased VE-cadherin abundance while increasing VE-cadherin mRNA expression (chapter 3). The increase in VE-cadherin mRNA levels does not always result in a corresponding increase in VE-cadherin abundance because gene expression is a multi-step process with regulation occurring at the transcriptional, post-transcriptional, translational, and post-translational levels. This means that while more mRNA may be available, factors such as translation repression, protein degradation, or feedback regulation could prevent a corresponding increase in protein abundance [710, 711].

When the effect of okadaic acid on VE-cadherin abundance was investigated over time, a decrease was detected as early as 8 h. The temporal response to okadaic acid is extremely variable ranging from minutes to hours depending on the endpoint being measured. For example, in mouse peritoneal macrophages, an increase in phospholipase A2 activity is detectable as early as 30 min after exposure to okadaic acid [712], while a decrease in collagen synthesis in fibroblasts observed after 12 h [713]. The latter is in keeping with the current data, and likely reflects the half-lives of VE-cadherin [~6 h; 401] and intracellular collagen [~7h;714] compared to the kinetics around activation of phospholipase A2 [715].

As in the earlier experiments, metformin failed to alter the effect of okadaic acid on VE-cadherin abundance, apart from at the 10 h time point. At this time point, metformin attenuated the okadaic acid-mediated loss of VE-cadherin. It is difficult to explain such a transient effect of metformin on VE-cadherin abundance. However, metformin can temporarily increase VE-cadherin expression and prevent its internalization, through modification of the VEGF signalling [421]. For example, metformin through inhibition of VEGFR2 [421] could counterbalance/offset the effect of increased VEGF as a consequence of okadaic acid [716].

In conclusion, metformin does not alter PP2Ac activity or modify VE-cadherin levels in brain microvascular endothelial cells. Importantly, it does not offset downregulation of VE-cadherin following pharmacological inhibition of PP2A by okadaic acid. However, there is a short-lived transient effect which requires further investigation to ascertain the underlying mechanism. These data contribute to our understanding of how okadaic acid and PP2Ac inhibition modulate adherens junctional proteins but rule out any therapeutic benefit in targeting this system with metformin due to the transient nature of any effects.

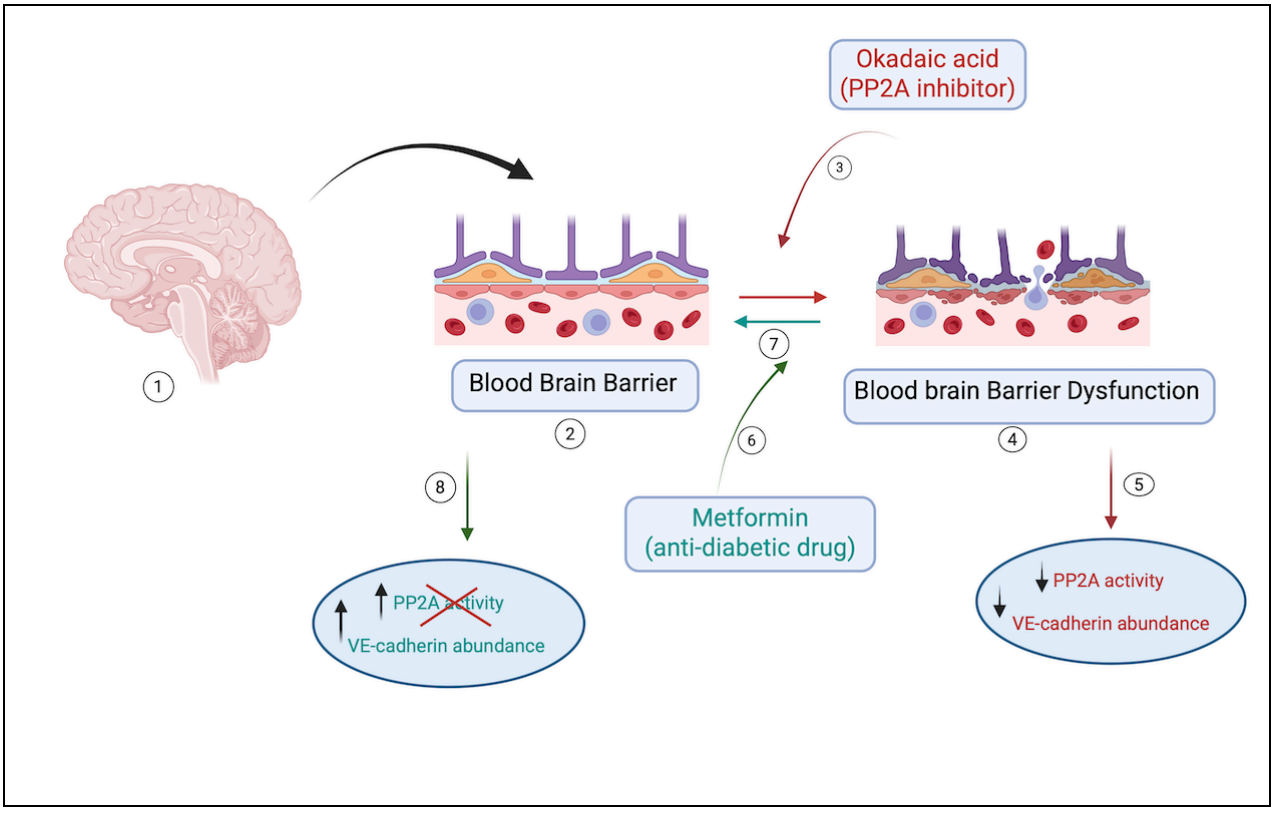


**Figure 5.6: Schematic summary of the effect of okadaic acid and metformin on PP2A activity and VE-cadherin abundance in endothelial cells associated with the blood-brain barrier.**

# Chapter 6

# Conclusion and Future Work

## 6.1 Conclusion

Protein phosphatases are critical enzymes in microvascular endothelial cells, with protein phosphatase 2A (PP2A) being of particular importance. PP2A's role is often explored using okadaic acid, a potent and selective inhibitor. By inhibiting PP2A, okadaic acid allows researchers to study its involvement in cell growth, development, and various signalling pathways. In this thesis, I used human cerebral microvascular endothelial cells (hCMEC/D3) as a model of the BBB. A key protein in maintaining BBB integrity is VE-cadherin, which forms part of the adherens junctions that connect endothelial cells. My research centres on the role of PP2A in regulating the BBB. In the initial phase of the study, I investigated how PP2A affects the adherens junction protein VE-cadherin by using okadaic acid to inhibit its activity. While PP2A's role in regulating tight junctions and maintaining the blood-brain barrier has been previously explored [560, 717-719]. Its involvement in controlling adherens junctions, particularly VE-cadherin, remained unclear. The current research informs the mechanism driving VE-cadherin degradation and its impact on a surrogate marker of BBB integrity.

Okadaic acid was shown to potently disrupt BBB integrity by targeting VE-cadherin. Exposure of hCMEC/D3 cells to okadaic acid (10nM) led to a marked reduction in VE-cadherin protein levels without inducing cellular toxicity, highlighting a specific, non-lethal mechanism of barrier compromise. This effect was mediated through inhibition of PP2A, a serine/threonine phosphatase that plays a crucial role in maintaining endothelial homeostasis. Mechanistically, okadaic acid-induced degradation of VE-cadherin occurred through enhanced ubiquitination and proteasomal processing rather than lysosomal proteolysis. This indicates that PP2A activity directly or indirectly regulates the post-translational stability of VE-cadherin. The specificity of this effect was observed in human brain endothelial cells but not in other endothelial cell lines. These findings establish a foundational framework for understanding how molecular toxins such as okadaic can compromise BBB integrity by targeting adherens junction proteins. The disruption of adherens junctions, along with internalisation and translocation of VE-cadherin, results in increased endothelial permeability. This underscores the importance of PP2A activity in maintaining BBB stability and identifies VE-cadherin as a target of phosphatase inhibition.

Then I expand these findings, noting that a previous study in rat primary neuron cultures showed that okadaic acid altered the expression of 320 proteins linked to structural development, cellular transport, differentiation, and signal transduction [518]. However, a comparable proteomic analysis, either broad or focused, has not been conducted in human brain

microvascular endothelial cells. Addressing this gap is essential to better understand how okadaic acid and PP2A influence endothelial function, and with implications on BBB function under normal and hyperphosphorylated pathological conditions.

In chapter 4, I demonstrate that okadaic acid alters the proteomic landscape of human brain microvascular endothelial cells by regulating 104 proteins involved in critical biological processes, including cell cycle control, stress response, cytoskeletal dynamics, and metabolism. Key interaction networks were centred on ubiquitin B (UBB) and the catalytic subunit of PP2A (PPP2CA), connecting proteins related to cell adhesion (e.g., VE-cadherin), signalling pathways (e.g., mTOR, CDK1), and membrane trafficking (e.g., Rab1A, Rab11A). Proteomic changes also highlighted upregulation of Alzheimer's disease (AD)-related proteins, including Tau (MAPT), phosphorylated Tau (Tau-pS396), and kinases such as MTOR and MAPK8 (JNK), as well as downregulation of Rab1A, which may contribute to intracellular Tau accumulation. Additional pathways involving neurodegeneration, tight junction integrity, membrane trafficking, and ubiquitin-mediated degradation were enriched, linking PP2A inhibition to BBB dysfunction and neurodegenerative disease mechanisms. Furthermore, this study showed that okadaic acid increased PI3Kδ expression, which is part of the PI3K/AKT/mTOR pathway involved in amyloid precursor protein trafficking and neuroinflammation. Okadaic acid also increased oxysterol binding protein (OSBP), which may affect cholesterol trafficking, though cholesterol metabolism is typically reduced in AD. Rab GTPases were differentially affected: Rab1A decreased while Rab11A increased, with Rab11A implicated in β-secretase recycling and amyloid-β production, although its role in VE-cadherin recycling was not supported within 24 hours. Similarly, Rab5A knockdown did not influence VE-cadherin or PP2A levels, indicating tissue or stimulus-specific regulation. Okadaic acid reduced VE-cadherin via proteasomal degradation, although Rab5A and Rab11A were not directly implicated in this process. Okadaic acid altered expression of cell adhesion molecules, including decreases in VE-cadherin and E-selectin and an increase in PD-L1, suggesting impacts on cell adhesion, inflammation, and immune regulation. Elevated MAPK8 (JNK) and PCNA expression also supported links to Alzheimer's disease pathology through kinase activation and cell cycle dysregulation. Together, these finding reveals that okadaic acid disrupts multiple cellular pathways relevant to neurodegeneration and endothelial barrier dysfunction, primarily through inhibition of PP2A. It highlights mechanistic links between phosphatase inhibition, Tau accumulation, amyloidogenic processes, and VE-cadherin loss. The findings underscore the complex regulation of endothelial integrity by phosphatases and the need for further investigation into long-term effects and other regulatory proteins (e.g., Rab

GTPases) involved in VE-cadherin dynamics. These insights enhance our understanding of how okadaic acid and, by inference, PP2A contribute to Alzheimer ‘s-like pathology and support its use as a tool for probing phosphatase-related mechanisms in neurovascular health.

Previous studies have shown that metformin can reduce Tau phosphorylation at PP2A-dependent sites in both experimental and animal models of Alzheimer’s disease [185, 579, 720, 721]. Moreover, metformin has been shown to activate PP2A in various cell types, including human skeletal muscle cells [471], macrophages [722], primary cortical neurons [723], and in mice [185]. However, whether metformin has a similar effect on PP2A activity in brain microvascular endothelial cells has yet to be determined. In the final chapter, I investigate the impact of metformin on PP2Ac activity and VE-cadherin abundance in human brain microvascular endothelial cells (hCMEC/D3), under normal conditions and in the presence of okadaic acid, which mimics hyperphosphorylated pathophysiological states such as Alzheimer’s disease and cancer.

In this study, metformin, at a concentration of 15 mM (non-toxic to cells), did not modulate PP2Ac activity or its expression at either the protein or mRNA level. These findings are consistent with some previous studies but contrast with others, potentially due to differences in concentration, cell types, and/or experimental duration. Importantly, metformin did not counteract the inhibition of PP2Ac by okadaic acid, suggesting no direct or indirect activation of PP2Ac under the tested conditions. The study also explored the effect of metformin on VE-cadherin, a key adherens junction protein involved in maintaining endothelial integrity. Under physiological conditions, metformin showed a time-dependent, transient decrease in VE-cadherin abundance at early time points (4–8 h), returning to baseline at 24 h. This suggests a non-sustained regulatory effect, differing from prior studies in pathological models where metformin preserved VE-cadherin levels. In the presence of okadaic acid, which reduced VE-cadherin abundance while increasing its mRNA expression, metformin did not generally mitigate this effect. However, a brief attenuation was observed at the 10 h time point only, possibly due to interaction with VEGF signalling pathways. This study showed that metformin does not modulate PP2Ac activity or provide sustained protection against okadaic acid-induced loss of VE-cadherin in human brain endothelial cells. Although a short-term effect was observed at one time point, the transient nature suggests limited therapeutic relevance in targeting VE-cadherin regulation through metformin under these conditions. These findings enhance our understanding of the molecular interactions governing endothelial junction stability and clarify the limitations of metformin in modulating this axis under pathophysiological stress.

In summary, okadaic acid led to a reduction in VE-cadherin levels, an endothelial-specific adhesion molecule critical for preserving the integrity of the endothelial barrier and regulating vascular permeability. This decrease in VE-cadherin was attributed to ubiquitination and subsequent proteasomal degradation, rather than lysosomal degradation, and did not involve RAB5A-mediated internalisation. The loss of VE-cadherin correlated with increased permeability of the BBB. PP2A inhibition not only compromises endothelial integrity but also mimics Alzheimer's disease-like molecular pathology by affecting Tau homeostasis, autophagy, and inflammatory signalling. My thesis provides new insights into how PP2A dysfunction may contribute to neurovascular damage in disease contexts. Beyond VE-cadherin, okadaic acid affected a broad spectrum of proteins. One such protein, Rab11A, a membrane trafficking protein, was shown not to be involved in VE-cadherin recycling, a process crucial for maintaining endothelial barrier function. Efforts to identify therapeutic strategies to counteract VE-cadherin loss or enhance PP2A activity included the use of metformin. However, metformin showed limited effectiveness, as it did not activate PP2A. Moreover, any restoration of VE-cadherin levels appeared to be temporary.

These data establish PP2A as a key regulator of endothelial junction stability and implicate its inhibition in both BBB disruption and AD-related proteomic changes. VE-cadherin emerges as a vulnerable target of PP2A inhibition, and the findings emphasise the need for further studies into phosphatase-regulated pathways in neurovascular health. While metformin showed a limited impact in this model, the results underscore the value of OA as a tool for probing the mechanisms underlying BBB dysfunction in neurodegenerative diseases.

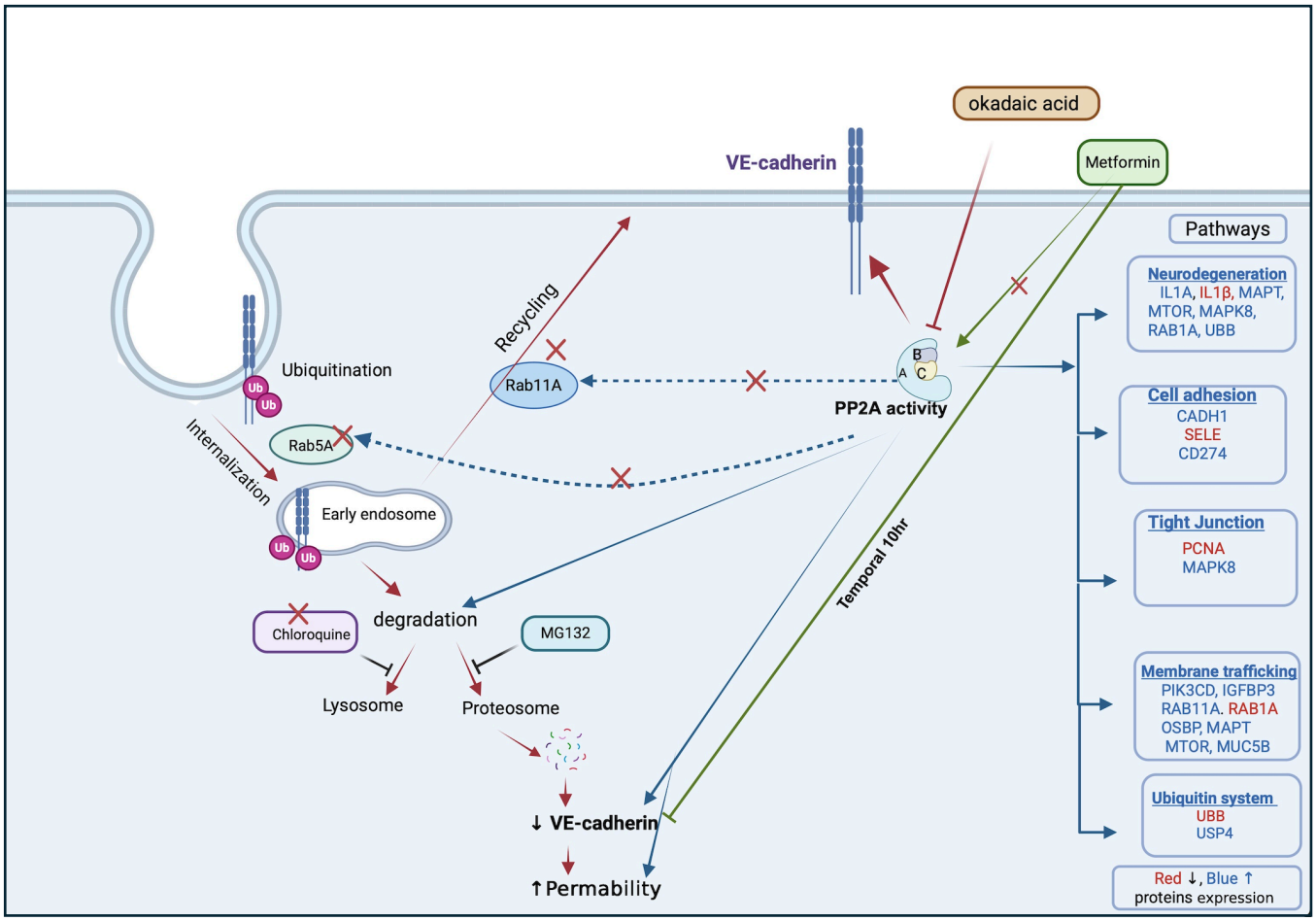


**Figure 6.1: A graphical abstract depicting how pharmacological inhibition of PP2A by okadaic acid modulates endothelial barrier function through alterations in the cellular proteome and VE-cadherin abundance in brain microvascular endothelial cells.**

## 6.2 Future direction

The findings presented in this thesis, which explored the role of protein phosphatase 2A (PP2A) in regulating VE-cadherin dynamics in human cerebral microvascular endothelial cells (hCMEC/D3), have led to several new research questions that merit further investigation.

Firstly, since primary human endothelial cells may respond differently to okadaic acid (OA) compared to immortalised cell lines, it will be important to determine whether OA induces comparable effects in primary endothelial cell lines. Additionally, the downstream effects of OA on key VE-cadherin-associated proteins, particularly p120-catenin and β-catenin, given the critical roles these proteins play in maintaining endothelial barrier integrity and signal transduction, elucidating these mechanisms is essential for understanding how OA influences vascular function. This will be a key focus of future studies. The regulatory role of endogenous PP2A inhibitors, specifically cancerous inhibitor of PP2A (CIP2A) and SET, also warrants further exploration. Their influence on VE-cadherin expression and localisation, as well as their broader impact on BBB integrity, is under investigation and would extend their physiological and pathological relevance in neurological conditions.

Although the current study shows that Rab11A and Rab5A do not mediate the okadaic-acid–induced reduction of VE-cadherin, the precise trafficking mechanism remains unresolved, highlighting the need to identify alternative regulators involved in VE-cadherin internalisation, recycling, and degradation. One candidate of particular interest is FIP2, which has been reported to form a ternary complex with Rab11A and VE-cadherin; future work should therefore examine the role of FIP2 and other potential interacting partners in this pathway. Chapter 3 has already established that okadaic acid reduces VE-cadherin abundance in a concentration-dependent manner without affecting cell viability, promotes its loss from the plasma membrane, enhances its ubiquitination with degradation via the proteasome, and strongly inhibits PP2A activity, suggesting a phosphorylation-driven mechanism. What remains unclear is how PP2A inhibition is linked to VE-cadherin ubiquitination and proteasomal degradation, and which trafficking regulators mediate this response. To address these gaps, future studies should include direct trafficking assays (surface biotinylation or antibody internalisation), investigation of additional Rab GTPases involved in degradative or fast-recycling pathways (e.g., Rab7, Rab4, Rab35), assessment of clathrin- versus caveolin-mediated endocytosis, and analysis of phosphorylation changes in VE-cadherin, β-catenin, and p120-catenin. Together, these experiments will help define the specific trafficking and signalling pathways through which okadaic acid regulates VE-cadherin stability and endothelial barrier integrity.

Concerning metformin, subsequent work should assess its capacity to enhance PP2A activity following immunoprecipitation of the PP2A holoenzyme complex, rather than solely its catalytic subunit, as was done in the current thesis. This will provide more comprehensive insights into how metformin modulates PP2A function. It would also be interesting to investigate whether metformin can modulate the inhibitory effects of the endogenous PP2A inhibitors CIP2A and SET in hCMEC/D3 cells, as this remains to be determined. To investigate this possibility, future studies could assess the impact of metformin after targeted overexpression of CIP2A or SET. This approach would help clarify whether metformin has the potential to restore PP2A activity under conditions where its endogenous inhibitors are elevated

Collectively, these proposed investigations will extend the current understanding of PP2A-mediated regulation of endothelial junctional integrity and may contribute to the development of novel therapeutic strategies targeting the BBB.

# Chapter 7

# References

# References


1. Sweeney, M.D., A.P. Sagare, and B.V. Zlokovic, *Blood-brain barrier breakdown in Alzheimer disease and other neurodegenerative disorders.* Nat Rev Neurol, 2018. **14**(3): p. 133-150.
2. Brightman, M.W. and T.S. Reese, *Junctions between intimately apposed cell membranes in the vertebrate brain.* J Cell Biol, 1969. **40**(3): p. 648-77.
3. Westergaard, E. and M.W. Brightman, *Transport of proteins across normal cerebral arterioles.* J Comp Neurol, 1973. **152**(1): p. 17-44.
4. Tietz, S. and B. Engelhardt, *Brain barriers: Crosstalk between complex tight junctions and adherens junctions.* J Cell Biol, 2015. **209**(4): p. 493-506.
5. Duong, C.N. and D. Vestweber, *Mechanisms Ensuring Endothelial Junction Integrity Beyond VE-Cadherin.* Front Physiol, 2020. **11**: p. 519.
6. Li, F., et al., *Endothelial Smad4 maintains cerebrovascular integrity by activating N-cadherin through cooperation with Notch.* Developmental cell, 2011. **20**(3): p. 291-302.
7. Hatanaka, K., M. Simons, and M. Murakami, *Phosphorylation of VE-cadherin controls endothelial phenotypes via p120-catenin coupling and Rac1 activation.* Am J Physiol Heart Circ Physiol, 2011. **300**(1): p. H162-72.
8. Janssens, V. and J. Goris, *Protein phosphatase 2A: a highly regulated family of serine/threonine phosphatases implicated in cell growth and signalling.* Biochem J, 2001. **353**(Pt 3): p. 417-39.
9. Schuhmacher, D., J.M. Sontag, and E. Sontag, *Protein Phosphatase 2A: More Than a Passenger in the Regulation of Epithelial Cell-Cell Junctions.* Front Cell Dev Biol, 2019. **7**: p. 30.
10. Hawkins, B.T. and T.P. Davis, *The blood-brain barrier/neurovascular unit in health and disease.* Pharmacol Rev, 2005. **57**(2): p. 173-85.
11. Thau, L., V. Reddy, and P. Singh, *Anatomy, Central Nervous System*, in *StatPearls*. 2025, StatPearls Publishing: Treasure Island (FL).
12. Bazira, P.J., *An overview of the nervous system.* Surgery (Oxford), 2021. **39**(8): p. 451-462.
13. Dickens, D., S. Radisch, and M. Pirmohamed, *Drug Transporters at the Blood-Brain Barrier.* Drug Transporters: Vol 1: Role and Importance in Adme and Drug Development, 2016. **54**: p. 151-183.
14. Kadry, H., B. Noorani, and L. Cucullo, *A blood-brain barrier overview on structure, function, impairment, and biomarkers of integrity.* Fluids Barriers CNS, 2020. **17**(1): p. 69.
15. Adam, R. and A.C. Huntelmann, *Edwin Ellen Goldmann (1862-1913).* J Neurol, 2023. **270**(5): p. 2812-2814.
16. Banerjee, S. and M.A. Bhat, *Neuron-glial interactions in blood-brain barrier formation.* Annu Rev Neurosci, 2007. **30**(1): p. 235-58.
17. Ballabh, P., A. Braun, and M. Nedergaard, *The blood-brain barrier: an overview: structure, regulation, and clinical implications.* Neurobiol Dis, 2004. **16**(1): p. 1-13.
18. Stamatovic, S.M., et al., *Junctional proteins of the blood-brain barrier: New insights into function and dysfunction.* Tissue Barriers, 2016. **4**(1): p. e1154641.
19. Zhang, W., et al., *Carbon Dots: A Future Blood-Brain Barrier Penetrating Nanomedicine and Drug Nanocarrier.* Int J Nanomedicine, 2021. **16**: p. 5003-5016.
20. Tajes, M., et al., *The blood-brain barrier: structure, function and therapeutic approaches to cross it.* Mol Membr Biol, 2014. **31**(5): p. 152-67.
21. Wong, A.D., et al., *The blood-brain barrier: an engineering perspective.* Front Neuroeng, 2013. **6**: p. 7.

22. Xiao, G. and L.S. Gan, *Receptor-mediated endocytosis and brain delivery of therapeutic biologics.* Int J Cell Biol, 2013. **2013**: p. 703545.
23. Kovacs, K.B., et al., *Hemorrhagic Transformation of Ischemic Strokes.* Int J Mol Sci, 2023. **24**(18).
24. Coomber, B.L. and P.A. Stewart, *Morphometric analysis of CNS microvascular endothelium.* Microvasc Res, 1985. **30**(1): p. 99-115.
25. Reese, T.S. and M.J. Karnovsky, *Fine structural localization of a blood-brain barrier to exogenous peroxidase.* J Cell Biol, 1967. **34**(1): p. 207-17.
26. Sandoval, K.E. and K.A. Witt, *Blood-brain barrier tight junction permeability and ischemic stroke.* Neurobiol Dis, 2008. **32**(2): p. 200-19.
27. Brown, R.C. and T.P. Davis, *Calcium modulation of adherens and tight junction function: a potential mechanism for blood-brain barrier disruption after stroke.* Stroke, 2002. **33**(6): p. 1706-11.
28. Cheslow, L. and J.I. Alvarez, *Glial-endothelial crosstalk regulates blood-brain barrier function.* Curr Opin Pharmacol, 2016. **26**: p. 39-46.
29. Lien, C.F., et al., *Absence of glial alpha-dystrobrevin causes abnormalities of the blood-brain barrier and progressive brain edema.* J Biol Chem, 2012. **287**(49): p. 41374-85.
30. Kim, Y., J. Park, and Y.K. Choi, *The Role of Astrocytes in the Central Nervous System Focused on BK Channel and Heme Oxygenase Metabolites: A Review.* Antioxidants (Basel), 2019. **8**(5).
31. Ullian, E.M., et al., *Control of synapse number by glia.* Science, 2001. **291**(5504): p. 657-61.
32. Lee, S.W., et al., *SSeCKS regulates angiogenesis and tight junction formation in blood-brain barrier.* Nat Med, 2003. **9**(7): p. 900-6.
33. Volterra, A. and J. Meldolesi, *Astrocytes, from brain glue to communication elements: the revolution continues.* Nat Rev Neurosci, 2005. **6**(8): p. 626-40.
34. Fiacco, T.A., C. Agulhon, and K.D. McCarthy, *Sorting out astrocyte physiology from pharmacology.* Annu Rev Pharmacol Toxicol, 2009. **49**(1): p. 151-74.
35. Freeman, M.R., *Specification and morphogenesis of astrocytes.* Science, 2010. **330**(6005): p. 774-8.
36. Halassa, M.M. and P.G. Haydon, *Integrated brain circuits: astrocytic networks modulate neuronal activity and behavior.* Annu Rev Physiol, 2010. **72**(1): p. 335-55.
37. DeBault, L.E. and P.A. Cancilla, *gamma-Glutamyl transpeptidase in isolated brain endothelial cells: induction by glial cells in vitro.* Science, 1980. **207**(4431): p. 653-5.
38. Janzer, R.C. and M.C. Raff, *Astrocytes induce blood-brain barrier properties in endothelial cells.* Nature, 1987. **325**(6101): p. 253-7.
39. Abbott, N.J., *Astrocyte-endothelial interactions and blood-brain barrier permeability.* J Anat, 2002. **200**(6): p. 629-38.
40. Haseloff, R.F., et al., *In search of the astrocytic factor(s) modulating blood-brain barrier functions in brain capillary endothelial cells in vitro.* Cell Mol Neurobiol, 2005. **25**(1): p. 25-39.
41. Abbott, N.J., L. Ronnback, and E. Hansson, *Astrocyte-endothelial interactions at the blood-brain barrier.* Nat Rev Neurosci, 2006. **7**(1): p. 41-53.
42. Lindahl, P., et al., *Pericyte loss and microaneurysm formation in PDGF-B-deficient mice.* Science, 1997. **277**(5323): p. 242-5.
43. von Tell, D., A. Armulik, and C. Betsholtz, *Pericytes and vascular stability.* Exp Cell Res, 2006. **312**(5): p. 623-9.
44. Balabanov, R. and P. Dore-Duffy, *Role of the CNS microvascular pericyte in the blood-brain barrier.* J Neurosci Res, 1998. **53**(6): p. 637-44.
45. Fisher, M., *Pericyte signaling in the neurovascular unit.* Stroke, 2009. **40**(3 Suppl): p. S13-5.

46. Armulik, A., G. Genove, and C. Betsholtz, *Pericytes: developmental, physiological, and pathological perspectives, problems, and promises.* Dev Cell, 2011. **21**(2): p. 193-215.
47. Bernacki, J., et al., *Physiology and pharmacological role of the blood-brain barrier.* Pharmacol Rep, 2008. **60**(5): p. 600-22.
48. Winkler, E.A., R.D. Bell, and B.V. Zlokovic, *Central nervous system pericytes in health and disease.* Nat Neurosci, 2011. **14**(11): p. 1398-1405.
49. Schlageter, K.E., et al., *Microvessel organization and structure in experimental brain tumors: microvessel populations with distinctive structural and functional properties.* Microvasc Res, 1999. **58**(3): p. 312-28.
50. Zlokovic, B.V., *The blood-brain barrier in health and chronic neurodegenerative disorders.* Neuron, 2008. **57**(2): p. 178-201.
51. Savettieri, G., et al., *Neurons and ECM regulate occludin localization in brain endothelial cells.* Neuroreport, 2000. **11**(5): p. 1081-4.
52. Wolburg, H. and A. Lippoldt, *Tight junctions of the blood-brain barrier: development, composition and regulation.* Vascul Pharmacol, 2002. **38**(6): p. 323-37.
53. Abbott, N.J., et al., *Structure and function of the blood-brain barrier.* Neurobiol Dis, 2010. **37**(1): p. 13-25.
54. Lochhead, J.J., et al., *Structure, Function, and Regulation of the Blood-Brain Barrier Tight Junction in Central Nervous System Disorders.* Front Physiol, 2020. **11**: p. 914.
55. Furuse, M., et al., *Claudin-1 and -2: novel integral membrane proteins localizing at tight junctions with no sequence similarity to occludin.* J Cell Biol, 1998. **141**(7): p. 1539-50.
56. Furuse, M., H. Sasaki, and S. Tsukita, *Manner of interaction of heterogeneous claudin species within and between tight junction strands.* J Cell Biol, 1999. **147**(4): p. 891-903.
57. Ohtsuki, S., et al., *Exogenous expression of claudin-5 induces barrier properties in cultured rat brain capillary endothelial cells.* J Cell Physiol, 2007. **210**(1): p. 81-6.
58. Nitta, T., et al., *Size-selective loosening of the blood-brain barrier in claudin-5-deficient mice.* J Cell Biol, 2003. **161**(3): p. 653-60.
59. Jia, W., et al., *The role of claudin-5 in blood-brain barrier (BBB) and brain metastases (review).* Mol Med Rep, 2014. **9**(3): p. 779-85.
60. Tam, S.J. and R.J. Watts, *Connecting vascular and nervous system development: angiogenesis and the blood-brain barrier.* Annu Rev Neurosci, 2010. **33**(1): p. 379-408.
61. Furuse, M., et al., *Occludin: a novel integral membrane protein localizing at tight junctions.* J Cell Biol, 1993. **123**(6 Pt 2): p. 1777-88.
62. Balda, M.S., et al., *Multiple domains of occludin are involved in the regulation of paracellular permeability.* J Cell Biochem, 2000. **78**(1): p. 85-96.
63. Hirase, T., et al., *Occludin as a possible determinant of tight junction permeability in endothelial cells.* J Cell Sci, 1997. **110 ( Pt 14)**(14): p. 1603-13.
64. Chiba, H., et al., *Transmembrane proteins of tight junctions.* Biochim Biophys Acta, 2008. **1778**(3): p. 588-600.
65. Liu, W.Y., et al., *Tight junction in blood-brain barrier: an overview of structure, regulation, and regulator substances.* CNS Neurosci Ther, 2012. **18**(8): p. 609-15.
66. Gumbiner, B.M., *Regulation of cadherin-mediated adhesion in morphogenesis.* Nat Rev Mol Cell Biol, 2005. **6**(8): p. 622-34.
67. Halbleib, J.M. and W.J. Nelson, *Cadherins in development: cell adhesion, sorting, and tissue morphogenesis.* Genes Dev, 2006. **20**(23): p. 3199-214.
68. Nishimura, T. and M. Takeichi, *Remodeling of the adherens junctions during morphogenesis.* Curr Top Dev Biol, 2009. **89**: p. 33-54.
69. Falk, M.M., *Adherens junctions remain dynamic.* BMC Biol, 2010. **8**: p. 34.

70. Ha, C.H., A.M. Bennett, and Z.G. Jin, *A novel role of vascular endothelial cadherin in modulating c-Src activation and downstream signaling of vascular endothelial growth factor.* J Biol Chem, 2008. **283**(11): p. 7261-70.
71. Ahmed, S.M., et al., *Exocyst dynamics during vesicle tethering and fusion.* Nat Commun, 2018. **9**(1): p. 5140.
72. Gavard, J., *Endothelial permeability and VE-cadherin: a wacky comradeship.* Cell Adh Migr, 2014. **8**(2): p. 158-64.
73. Vestweber, D., *VE-cadherin: the major endothelial adhesion molecule controlling cellular junctions and blood vessel formation.* Arterioscler Thromb Vasc Biol, 2008. **28**(2): p. 223-32.
74. Harris, E.S. and W.J. Nelson, *VE-cadherin: at the front, center, and sides of endothelial cell organization and function.* Curr Opin Cell Biol, 2010. **22**(5): p. 651-8.
75. Carmeliet, P., et al., *Targeted deficiency or cytosolic truncation of the VE-cadherin gene in mice impairs VEGF-mediated endothelial survival and angiogenesis.* Cell, 1999. **98**(2): p. 147-57.
76. Crosby, C.V., et al., *VE-cadherin is not required for the formation of nascent blood vessels but acts to prevent their disassembly.* Blood, 2005. **105**(7): p. 2771-6.
77. Mariner, D.J., et al., *Identification of Src phosphorylation sites in the catenin p120ctn.* J Biol Chem, 2001. **276**(30): p. 28006-13.
78. Reynolds, A.B. and A. Roczniak-Ferguson, *Emerging roles for p120-catenin in cell adhesion and cancer.* Oncogene, 2004. **23**(48): p. 7947-56.
79. Hartsock, A. and W.J. Nelson, *Adherens and tight junctions: structure, function and connections to the actin cytoskeleton.* Biochim Biophys Acta, 2008. **1778**(3): p. 660-9.
80. Perez-Moreno, M., et al., *p120-catenin mediates inflammatory responses in the skin.* Cell, 2006. **124**(3): p. 631-44.
81. Perez-Moreno, M., et al., *Loss of p120 catenin and links to mitotic alterations, inflammation, and skin cancer.* Proc Natl Acad Sci U S A, 2008. **105**(40): p. 15399-404.
82. Xie, Z., et al., *p120-catenin is required for regulating epidermal proliferation, differentiation, and barrier function.* Journal of cellular physiology, 2019. **234**(1): p. 427-432.
83. Xiao, K., et al., *Role of p120-catenin in cadherin trafficking.* Biochim Biophys Acta, 2007. **1773**(1): p. 8-16.
84. Stepniak, E., G.L. Radice, and V. Vasioukhin, *Adhesive and signaling functions of cadherins and catenins in vertebrate development.* Cold Spring Harb Perspect Biol, 2009. **1**(5): p. a002949.
85. Oas, R.G., et al., *p120-Catenin is required for mouse vascular development.* Circ Res, 2010. **106**(5): p. 941-51.
86. Pieters, T., et al., *p120 Catenin-Mediated Stabilization of E-Cadherin Is Essential for Primitive Endoderm Specification.* PLoS Genet, 2016. **12**(8): p. e1006243.
87. Hernandez-Martinez, R., N. Ramkumar, and K.V. Anderson, *p120-catenin regulates WNT signaling and EMT in the mouse embryo.* Proc Natl Acad Sci U S A, 2019. **116**(34): p. 16872-16881.
88. Zhang, Y., et al., *P120-catenin regulates pulmonary fibrosis and TGF-beta induced lung fibroblast differentiation.* Life Sci, 2019. **230**: p. 35-44.
89. Noren, N.K., et al., *p120 catenin regulates the actin cytoskeleton via Rho family GTPases.* J Cell Biol, 2000. **150**(3): p. 567-80.
90. Valenta, T., G. Hausmann, and K. Basler, *The many faces and functions of beta-catenin.* EMBO J, 2012. **31**(12): p. 2714-36.
91. Xing, Y., et al., *Crystal structure of a full-length beta-catenin.* Structure, 2008. **16**(3): p. 478-87.

92. Huber, A.H., W.J. Nelson, and W.I. Weis, *Three-dimensional structure of the armadillo repeat region of beta-catenin.* Cell, 1997. **90**(5): p. 871-82.
93. Fagotto, F., U. Gluck, and B.M. Gumbiner, *Nuclear localization signal-independent and importin/karyopherin-independent nuclear import of beta-catenin.* Curr Biol, 1998. **8**(4): p. 181-90.
94. Yokoya, F., et al., *beta-catenin can be transported into the nucleus in a Ran-unassisted manner.* Mol Biol Cell, 1999. **10**(4): p. 1119-31.
95. Lampugnani, M.G., et al., *The molecular organization of endothelial cell to cell junctions: differential association of plakoglobin, beta-catenin, and alpha-catenin with vascular endothelial cadherin (VE-cadherin).* J Cell Biol, 1995. **129**(1): p. 203-17.
96. Grigoryan, T., et al., *Deciphering the function of canonical Wnt signals in development and disease: conditional loss- and gain-of-function mutations of beta-catenin in mice.* Genes Dev, 2008. **22**(17): p. 2308-41.
97. Huber, A.H. and W.I. Weis, *The structure of the beta-catenin/E-cadherin complex and the molecular basis of diverse ligand recognition by beta-catenin.* Cell, 2001. **105**(3): p. 391-402.
98. Choi, H.J., A.H. Huber, and W.I. Weis, *Thermodynamics of beta-catenin-ligand interactions: the roles of the N- and C-terminal tails in modulating binding affinity.* J Biol Chem, 2006. **281**(2): p. 1027-38.
99. Sampietro, J., et al., *Crystal structure of a beta-catenin/BCL9/Tcf4 complex.* Mol Cell, 2006. **24**(2): p. 293-300.
100. Laksitorini, M.D., et al., *Modulation of Wnt/beta-catenin signaling promotes blood-brain barrier phenotype in cultured brain endothelial cells.* Sci Rep, 2019. **9**(1): p. 19718.
101. Green, K.J., et al., *Intercellular junction assembly, dynamics, and homeostasis.* Cold Spring Harb Perspect Biol, 2010. **2**(2): p. a000125.
102. Harris, T.J. and U. Tepass, *Adherens junctions: from molecules to morphogenesis.* Nat Rev Mol Cell Biol, 2010. **11**(7): p. 502-14.
103. Vestweber, D. and R. Kemler, *Rabbit antiserum against a purified surface glycoprotein decompacts mouse preimplantation embryos and reacts with specific adult tissues.* Exp Cell Res, 1984. **152**(1): p. 169-78.
104. Vestweber, D. and R. Kemler, *Some structural and functional aspects of the cell adhesion molecule uvomorulin.* Cell Differ, 1984. **15**(2-4): p. 269-73.
105. Kobielak, A. and E. Fuchs, *Alpha-catenin: at the junction of intercellular adhesion and actin dynamics.* Nat Rev Mol Cell Biol, 2004. **5**(8): p. 614-25.
106. Pokutta, S. and W.I. Weis, *Structure of the dimerization and beta-catenin-binding region of alpha-catenin.* Mol Cell, 2000. **5**(3): p. 533-43.
107. Kadowaki, T., et al., *E-cadherin and alpha-catenin expression in human esophageal cancer.* Cancer Res, 1994. **54**(1): p. 291-6.
108. Moll, R., et al., *Differential loss of E-cadherin expression in infiltrating ductal and lobular breast carcinomas.* Am J Pathol, 1993. **143**(6): p. 1731-42.
109. Shimazui, T., et al., *Complex cadherin expression in renal cell carcinoma.* Cancer Res, 1996. **56**(14): p. 3234-7.
110. Breen, E., et al., *Poorly differentiated colon carcinoma cell lines deficient in alpha-catenin expression express high levels of surface E-cadherin but lack Ca(2+)-dependent cell-cell adhesion.* Cell Adhes Commun, 1993. **1**(3): p. 239-50.
111. Elgenaidi, I.S. and J.P. Spiers, *Regulation of the phosphoprotein phosphatase 2A system and its modulation during oxidative stress: A potential therapeutic target?* Pharmacol Ther, 2019. **198**: p. 68-89.
112. Thompson, J.J. and C.S. Williams, *Protein Phosphatase 2A in the Regulation of Wnt Signaling, Stem Cells, and Cancer.* Genes (Basel), 2018. **9**(3).

113. Cohen, P.T., et al., *Protein serine/threonine phosphatases; an expanding family.* FEBS Lett, 1990. **268**(2): p. 355-9.
114. Chen, K.C., H.Y. Chen, and C.Y. Chen, *Potential Protein Phosphatase 2A Agents from Traditional Chinese Medicine against Cancer.* Evid Based Complement Alternat Med, 2014. **2014**: p. 436863.
115. Liu, F., Z. Liang, and C.X. Gong, *Hyperphosphorylation of tau and protein phosphatases in Alzheimer disease.* Panminerva Med, 2006. **48**(2): p. 97-108.
116. Baharians, Z. and A.H. Schonthal, *Autoregulation of protein phosphatase type 2A expression.* J Biol Chem, 1998. **273**(30): p. 19019-24.
117. Khew-Goodall, Y. and B.A. Hemmings, *Tissue-specific expression of mRNAs encoding alpha- and beta-catalytic subunits of protein phosphatase 2A.* FEBS Lett, 1988. **238**(2): p. 265-8.
118. Hemmings, B.A., et al., *alpha- and beta-forms of the 65-kDa subunit of protein phosphatase 2A have a similar 39 amino acid repeating structure.* Biochemistry, 1990. **29**(13): p. 3166-73.
119. Zhou, J., et al., *Characterization of the Aalpha and Abeta subunit isoforms of protein phosphatase 2A: differences in expression, subunit interaction, and evolution.* Biochem J, 2003. **369**(Pt 2): p. 387-98.
120. Hendrix, P., et al., *Analysis of subunit isoforms in protein phosphatase 2A holoenzymes from rabbit and Xenopus.* J Biol Chem, 1993. **268**(10): p. 7330-7.
121. Price, N.E. and M.C. Mumby, *Effects of regulatory subunits on the kinetics of protein phosphatase 2A.* Biochemistry, 2000. **39**(37): p. 11312-8.
122. Cho, U.S. and W. Xu, *Crystal structure of a protein phosphatase 2A heterotrimeric holoenzyme.* Nature, 2007. **445**(7123): p. 53-7.
123. Zolnierowicz, S., et al., *Diversity in the regulatory B-subunits of protein phosphatase 2A: identification of a novel isoform highly expressed in brain.* Biochemistry, 1994. **33**(39): p. 11858-67.
124. Strack, S., et al., *Cloning and characterization of B delta, a novel regulatory subunit of protein phosphatase 2A.* FEBS Lett, 1999. **460**(3): p. 462-6.
125. Healy, A.M., et al., *CDC55, a Saccharomyces cerevisiae gene involved in cellular morphogenesis: identification, characterization, and homology to the B subunit of mammalian type 2A protein phosphatase.* Mol Cell Biol, 1991. **11**(11): p. 5767-80.
126. Janssens, V., et al., *Identification and functional analysis of two Ca2+-binding EF-hand motifs in the B"/PR72 subunit of protein phosphatase 2A.* J Biol Chem, 2003. **278**(12): p. 10697-706.
127. Voorhoeve, P.M., et al., *Rapid dephosphorylation of p107 following UV irradiation.* Oncogene, 1999. **18**(3): p. 679-88.
128. Scott, J.I., Q. Deng, and M. Vendrell, *Near-Infrared Fluorescent Probes for the Detection of Cancer-Associated Proteases.* ACS Chem Biol, 2021. **16**(8): p. 1304-1317.
129. Muir, R.K., M. Guerra, and M.M. Bogyo, *Activity-Based Diagnostics: Recent Advances in the Development of Probes for Use with Diverse Detection Modalities.* ACS Chem Biol, 2022. **17**(2): p. 281-291.
130. Zhang, J., et al., *Fluorogenic probes for disease-relevant enzymes.* Chem Soc Rev, 2019. **48**(2): p. 683-722.
131. Cristóbal, I., et al., *Deregulation of the PP2A inhibitor SET shows promising therapeutic implications and determines poor clinical outcome in patients with metastatic colorectal cancer.* Clin Cancer Res, 2015. **21**(2): p. 347-56.
132. Cristóbal, I., et al., *PP2A inhibition is a common event in colorectal cancer and its restoration using FTY720 shows promising therapeutic potential.* Mol Cancer Ther, 2014. **13**(4): p. 938-47.

133. Haesen, D., et al., *Recurrent PPP2R1A Mutations in Uterine Cancer Act through a Dominant-Negative Mechanism to Promote Malignant Cell Growth.* Cancer Res, 2016. **76**(19): p. 5719-5731.
134. Janghorban, M., et al., *Targeting c-MYC by antagonizing PP2A inhibitors in breast cancer.* Proc Natl Acad Sci U S A, 2014. **111**(25): p. 9157-62.
135. Liu, H., et al., *Overexpression of PP2A inhibitor SET oncoprotein is associated with tumor progression and poor prognosis in human non-small cell lung cancer.* Oncotarget, 2015. **6**(17): p. 14913-25.
136. Nobumori, Y., et al., *B56γ tumor-associated mutations provide new mechanisms for B56γ-PP2A tumor suppressor activity.* Mol Cancer Res, 2013. **11**(9): p. 995-1003.
137. Rincón, R., et al., *PP2A inhibition determines poor outcome and doxorubicin resistance in early breast cancer and its activation shows promising therapeutic effects.* Oncotarget, 2015. **6**(6): p. 4299-314.
138. O'Connor, C.M., et al., *Therapeutic targeting of PP2A.* Int J Biochem Cell Biol, 2018. **96**: p. 182-193.
139. Nagao, M., et al., *Protein serine/threonine phosphatases as binding proteins for okadaic acid.* Mutat Res, 1995. **333**(1-2): p. 173-9.
140. Suganuma, M., et al., *Okadaic acid: an additional non-phorbol-12-tetradecanoate-13-acetate-type tumor promoter.* Proc Natl Acad Sci U S A, 1988. **85**(6): p. 1768-71.
141. D'Arcy, B.M., et al., *The Antitumor Drug LB-100 Is a Catalytic Inhibitor of Protein Phosphatase 2A (PPP2CA) and 5 (PPP5C) Coordinating with the Active-Site Catalytic Metals in PPP5C.* Mol Cancer Ther, 2019. **18**(3): p. 556-566.
142. Clark, A.R. and M. Ohlmeyer, *Protein phosphatase 2A as a therapeutic target in inflammation and neurodegeneration.* Pharmacol Ther, 2019. **201**: p. 181-201.
143. Mazhar, S., et al., *Targeting PP2A in cancer: Combination therapies.* Biochim Biophys Acta Mol Cell Res, 2019. **1866**(1): p. 51-63.
144. Martin, L., et al., *Tau protein phosphatases in Alzheimer's disease: the leading role of PP2A.* Ageing Res Rev, 2013. **12**(1): p. 39-49.
145. Seshacharyulu, P., et al., *Phosphatase: PP2A structural importance, regulation and its aberrant expression in cancer.* Cancer Lett, 2013. **335**(1): p. 9-18.
146. Kauko, O., et al., *PP2A inhibition is a druggable MEK inhibitor resistance mechanism in KRAS-mutant lung cancer cells.* Sci Transl Med, 2018. **10**(450).
147. Sontag, E., et al., *Downregulation of protein phosphatase 2A carboxyl methylation and methyltransferase may contribute to Alzheimer disease pathogenesis.* J Neuropathol Exp Neurol, 2004. **63**(10): p. 1080-91.
148. Dodge-Kafka, K.L., et al., *cAMP-stimulated protein phosphatase 2A activity associated with muscle A kinase-anchoring protein (mAKAP) signaling complexes inhibits the phosphorylation and activity of the cAMP-specific phosphodiesterase PDE4D3.* J Biol Chem, 2010. **285**(15): p. 11078-86.
149. DeGrande, S.T., et al., *Molecular mechanisms underlying cardiac protein phosphatase 2A regulation in heart.* J Biol Chem, 2013. **288**(2): p. 1032-46.
150. Takahashi, K., E. Nakajima, and K. Suzuki, *Involvement of protein phosphatase 2A in the maintenance of E-cadherin-mediated cell-cell adhesion through recruitment of IQGAP1.* J Cell Physiol, 2006. **206**(3): p. 814-20.
151. Ogris, E., D.M. Gibson, and D.C. Pallas, *Protein phosphatase 2A subunit assembly: the catalytic subunit carboxy terminus is important for binding cellular B subunit but not polyomavirus middle tumor antigen.* Oncogene, 1997. **15**(8): p. 911-7.
152. Ai, X., et al., *Enhanced activation of p21-activated kinase 1 in heart failure contributes to dephosphorylation of connexin 43.* Cardiovasc Res, 2011. **92**(1): p. 106-14.
153. Farrell, A.S., et al., *Targeting inhibitors of the tumor suppressor PP2A for the treatment of pancreatic cancer.* Mol Cancer Res, 2014. **12**(6): p. 924-39.

154. von Lindern, M., et al., *Can, a putative oncogene associated with myeloid leukemogenesis, may be activated by fusion of its 3' half to different genes: characterization of the set gene.* Mol Cell Biol, 1992. **12**(8): p. 3346-55.
155. Arnaud, L., et al., *Mechanism of inhibition of PP2A activity and abnormal hyperphosphorylation of tau by I2(PP2A)/SET.* FEBS Lett, 2011. **585**(17): p. 2653-9.
156. Li, M., A. Makkinje, and Z. Damuni, *The myeloid leukemia-associated protein SET is a potent inhibitor of protein phosphatase 2A.* Journal of Biological Chemistry, 1996. **271**(19): p. 11059-11062.
157. Pavic, K., et al., *Structural mechanism for inhibition of PP2A-B56alpha and oncogenicity by CIP2A.* Nat Commun, 2023. **14**(1): p. 1143.
158. Soofiyani, S.R., M.S. Hejazi, and B. Baradaran, *The role of CIP2A in cancer: A review and update.* Biomed Pharmacother, 2017. **96**: p. 626-633.
159. Wang, Y., et al., *The novel mechanism of rotenone-induced alpha-synuclein phosphorylation via reduced protein phosphatase 2A activity.* Int J Biochem Cell Biol, 2016. **75**: p. 34-44.
160. Louzao, M.C., et al., *Current Trends and New Challenges in Marine Phycotoxins.* Mar Drugs, 2022. **20**(3): p. 198.
161. Mitsuhashi, S., et al., *Tautomycetin is a novel and specific inhibitor of serine/threonine protein phosphatase type 1, PP1.* Biochem Biophys Res Commun, 2001. **287**(2): p. 328-31.
162. Swingle, M., L. Ni, and R.E. Honkanen, *Small-molecule inhibitors of ser/thr protein phosphatases: specificity, use and common forms of abuse.* Methods Mol Biol, 2007. **365**: p. 23-38.
163. Frydrychowski, V.A., et al., *Importance of the C28-C38 hydrophobic domain of okadaic acid for potent inhibition of protein serine-threonine phosphatases 1 and 2A.* Bioorg Med Chem Lett, 2001. **11**(5): p. 647-9.
164. Cohen, P., C.F. Holmes, and Y. Tsukitani, *Okadaic acid: a new probe for the study of cellular regulation.* Trends Biochem Sci, 1990. **15**(3): p. 98-102.
165. Méndez, J., et al., *Okadaic Acid: More than a Diarrheic Toxin.* 2013.
166. Wang, R., et al., *Okadaic acid inhibits cell multiplication and induces apoptosis in a549 cells, a human lung adenocarcinoma cell line.* Int J Clin Exp Med, 2014. **7**(8): p. 2025-30.
167. Wang, R.J., et al., *Effects of okadaic acid combined with cisplatin on the proliferation and apoptosis of human lung adenocarcinoma A549 cells.* International Journal of Clinical and Experimental Medicine, 2017. **10**(7): p. 10351-10358.
168. Fujiki, H., et al., *The concept of the okadaic acid class of tumor promoters is revived in endogenous protein inhibitors of protein phosphatase 2A, SET and CIP2A, in human cancers.* J Cancer Res Clin Oncol, 2018. **144**(12): p. 2339-2349.
169. McCluskey, A., et al., *Anhydride modified cantharidin analogues: synthesis, inhibition of protein phosphatases 1 and 2A and anticancer activity.* Bioorg Med Chem Lett, 2000. **10**(15): p. 1687-90.
170. Chung, V., et al., *Safety, Tolerability, and Preliminary Activity of LB-100, an Inhibitor of Protein Phosphatase 2A, in Patients with Relapsed Solid Tumors: An Open-Label, Dose Escalation, First-in-Human, Phase I Trial.* Clin Cancer Res, 2017. **23**(13): p. 3277-3284.
171. Lu, J., et al., *Inhibition of serine/threonine phosphatase PP2A enhances cancer chemotherapy by blocking DNA damage induced defense mechanisms.* Proc Natl Acad Sci U S A, 2009. **106**(28): p. 11697-702.
172. Bai, X.L., et al., *Inhibition of protein phosphatase 2A enhances cytotoxicity and accessibility of chemotherapeutic drugs to hepatocellular carcinomas.* Mol Cancer Ther, 2014. **13**(8): p. 2062-72.

173. Di Conza, G., et al., *The mTOR and PP2A Pathways Regulate PHD2 Phosphorylation to Fine-Tune HIF1alpha Levels and Colorectal Cancer Cell Survival under Hypoxia.* Cell Rep, 2017. **18**(7): p. 1699-1712.
174. Chang, K.E., et al., *The protein phosphatase 2A inhibitor LB100 sensitizes ovarian carcinoma cells to cisplatin-mediated cytotoxicity.* Mol Cancer Ther, 2015. **14**(1): p. 90-100.
175. Dias, M.H., et al., *Paradoxical Activation of Oncogenic Signaling as a Cancer Treatment Strategy.* Cancer Discov, 2024. **14**(7): p. 1276-1301.
176. Hong, C.S., et al., *LB100, a small molecule inhibitor of PP2A with potent chemo- and radio-sensitizing potential.* Cancer Biol Ther, 2015. **16**(6): p. 821-33.
177. Mumby, M., *PP2A: unveiling a reluctant tumor suppressor.* Cell, 2007. **130**(1): p. 21-4.
178. Cristobal, I., et al., *PP2A inhibition is a common event in colorectal cancer and its restoration using FTY720 shows promising therapeutic potential.* Mol Cancer Ther, 2014. **13**(4): p. 938-47.
179. Leonard, D., et al., *Selective PP2A Enhancement through Biased Heterotrimer Stabilization.* Cell, 2020. **181**(3): p. 688-701 e16.
180. Kastrinsky, D.B., et al., *Reengineered tricyclic anti-cancer agents.* Bioorg Med Chem, 2015. **23**(19): p. 6528-34.
181. Sangodkar, J., et al., *Activation of tumor suppressor protein PP2A inhibits KRAS-driven tumor growth.* J Clin Invest, 2017. **127**(6): p. 2081-2090.
182. Merisaari, J., et al., *Monotherapy efficacy of blood-brain barrier permeable small molecule reactivators of protein phosphatase 2A in glioblastoma.* Brain Commun, 2020. **2**(1): p. fcaa002.
183. Cong, X.X., et al., *Rab5a activates IRS1 to coordinate IGF-AKT-mTOR signaling and myoblast differentiation during muscle regeneration.* Cell Death Differ, 2020. **27**(8): p. 2344-2362.
184. Tohme, R., et al., *Direct activation of PP2A for the treatment of tyrosine kinase inhibitor-resistant lung adenocarcinoma.* JCI Insight, 2019. **4**(4): p. e125693.
185. Kickstein, E., et al., *Biguanide metformin acts on tau phosphorylation via mTOR/protein phosphatase 2A (PP2A) signaling.* Proc Natl Acad Sci U S A, 2010. **107**(50): p. 21830-5.
186. Asle-Rousta, M., et al., *FTY720 (fingolimod) attenuates beta-amyloid peptide (Abeta42)-induced impairment of spatial learning and memory in rats.* J Mol Neurosci, 2013. **50**(3): p. 524-32.
187. van Eersel, J., et al., *Sodium selenate mitigates tau pathology, neurodegeneration, and functional deficits in Alzheimer's disease models.* Proc Natl Acad Sci U S A, 2010. **107**(31): p. 13888-93.
188. Vitek, M.P., et al., *APOE-mimetic peptides reduce behavioral deficits, plaques and tangles in Alzheimer's disease transgenics.* Neurodegener Dis, 2012. **10**(1-4): p. 122-6.
189. Basurto-Islas, G., et al., *Therapeutic benefits of a component of coffee in a rat model of Alzheimer's disease.* Neurobiol Aging, 2014. **35**(12): p. 2701-2712.
190. Wei, H., et al., *Direct Activation of Protein Phosphatase 2A (PP2A) by Tricyclic Sulfonamides Ameliorates Alzheimer's Disease Pathogenesis in Cell and Animal Models.* Neurotherapeutics, 2020. **17**(3): p. 1087-1103.
191. Montalban, X., et al., *Oral fingolimod (FTY720) in relapsing multiple sclerosis: impact on health-related quality of life in a phase II study.* Mult Scler, 2011. **17**(11): p. 1341-50.
192. Niazy, A.A., et al., *FTY720 Reduces the Biomass of Biofilms in Pseudomonas aeruginosa in a Dose-Dependent Manner.* Antibiotics (Basel), 2024. **13**(7): p. 621.

193. Pippa, R., et al., *Effect of FTY720 on the SET-PP2A complex in acute myeloid leukemia; SET binding drugs have antagonistic activity.* Leukemia, 2014. **28**(9): p. 1915-8.
194. Saddoughi, S.A., et al., *Sphingosine analogue drug FTY720 targets I2PP2A/SET and mediates lung tumour suppression via activation of PP2A-RIPK1-dependent necroptosis.* EMBO Mol Med, 2013. **5**(1): p. 105-21.
195. Chiba, K., *FTY720, a new class of immunomodulator, inhibits lymphocyte egress from secondary lymphoid tissues and thymus by agonistic activity at sphingosine 1-phosphate receptors.* Pharmacol Ther, 2005. **108**(3): p. 308-19.
196. Wang, X., et al., *Dysregulation of protein trafficking in neurodegeneration.* Mol Neurodegener, 2014. **9**: p. 31.
197. Olkkonen, V.M. and E. Ikonen, *When intracellular logistics fails--genetic defects in membrane trafficking.* J Cell Sci, 2006. **119**(Pt 24): p. 5031-45.
198. Gm, C., *The cell: a molecular approach.* Sunderland (MA): Sinauer Associates, 2000: p. 3.
199. Ciechanover, A., *Proteolysis: from the lysosome to ubiquitin and the proteasome.* Nat Rev Mol Cell Biol, 2005. **6**(1): p. 79-87.
200. Tai, H.C. and E.M. Schuman, *Ubiquitin, the proteasome and protein degradation in neuronal function and dysfunction.* Nat Rev Neurosci, 2008. **9**(11): p. 826-38.
201. Wang, X. and J. Robbins, *Proteasomal and lysosomal protein degradation and heart disease.* J Mol Cell Cardiol, 2014. **71**: p. 16-24.
202. Hirohashi, S., *Inactivation of the E-cadherin-mediated cell adhesion system in human cancers.* Am J Pathol, 1998. **153**(2): p. 333-9.
203. Nanes, B.A., et al., *p120-catenin regulates VE-cadherin endocytosis and degradation induced by the Kaposi sarcoma-associated ubiquitin ligase K5.* Mol Biol Cell, 2017. **28**(1): p. 30-40.
204. Veiga, E. and P. Cossart, *Listeria hijacks the clathrin-dependent endocytic machinery to invade mammalian cells.* Nat Cell Biol, 2005. **7**(9): p. 894-900.
205. Ivanov, A.I., A. Nusrat, and C.A. Parkos, *Endocytosis of epithelial apical junctional proteins by a clathrin-mediated pathway into a unique storage compartment.* Mol Biol Cell, 2004. **15**(1): p. 176-88.
206. Doherty, G.J. and H.T. McMahon, *Mechanisms of endocytosis.* Annu Rev Biochem, 2009. **78**(1): p. 857-902.
207. Kaksonen, M. and A. Roux, *Mechanisms of clathrin-mediated endocytosis.* Nat Rev Mol Cell Biol, 2018. **19**(5): p. 313-326.
208. Boulant, S., et al., *Actin dynamics counteract membrane tension during clathrin-mediated endocytosis.* Nat Cell Biol, 2011. **13**(9): p. 1124-31.
209. McMahon, H.T. and E. Boucrot, *Molecular mechanism and physiological functions of clathrin-mediated endocytosis.* Nat Rev Mol Cell Biol, 2011. **12**(8): p. 517-33.
210. Mettlen, M. and G. Danuser, *Imaging and modeling the dynamics of clathrin-mediated endocytosis.* Cold Spring Harb Perspect Biol, 2014. **6**(12): p. a017038.
211. Jaye, S., U.S. Sandau, and J.A. Saugstad, *Clathrin mediated endocytosis in Alzheimer's disease: cell type specific involvement in amyloid beta pathology.* Front Aging Neurosci, 2024. **16**: p. 1378576.
212. Ferreira, A.P.A. and E. Boucrot, *Mechanisms of Carrier Formation during Clathrin-Independent Endocytosis.* Trends Cell Biol, 2018. **28**(3): p. 188-200.
213. Casamento, A. and E. Boucrot, *Molecular mechanism of Fast Endophilin-Mediated Endocytosis.* Biochem J, 2020. **477**(12): p. 2327-2345.
214. Mayor, S. and R.E. Pagano, *Pathways of clathrin-independent endocytosis.* Nat Rev Mol Cell Biol, 2007. **8**(8): p. 603-12.

215. Rennick, J.J., A.P.R. Johnston, and R.G. Parton, *Key principles and methods for studying the endocytosis of biological and nanoparticle therapeutics.* Nat Nanotechnol, 2021. **16**(3): p. 266-276.
216. Hinshaw, J.E., *Dynamin and its role in membrane fission.* Annu Rev Cell Dev Biol, 2000. **16**(1): p. 483-519.
217. Sverdlov, M., A.N. Shajahan, and R.D. Minshall, *Tyrosine phosphorylation-dependence of caveolae-mediated endocytosis.* J Cell Mol Med, 2007. **11**(6): p. 1239-50.
218. Palade, G.E., *An electron microscope study of the mitochondrial structure.* J Histochem Cytochem, 1953. **1**(4): p. 188-211.
219. Parton, R.G. and K. Simons, *The multiple faces of caveolae.* Nat Rev Mol Cell Biol, 2007. **8**(3): p. 185-94.
220. Pilch, P.F. and L. Liu, *Fat caves: caveolae, lipid trafficking and lipid metabolism in adipocytes.* Trends Endocrinol Metab, 2011. **22**(8): p. 318-24.
221. Chow, B.W., et al., *Caveolae in CNS arterioles mediate neurovascular coupling.* Nature, 2020. **579**(7797): p. 106-110.
222. Frank, P.G., S. Pavlides, and M.P. Lisanti, *Caveolae and transcytosis in endothelial cells: role in atherosclerosis.* Cell Tissue Res, 2009. **335**(1): p. 41-7.
223. Parton, R.G. and M.A. del Pozo, *Caveolae as plasma membrane sensors, protectors and organizers.* Nat Rev Mol Cell Biol, 2013. **14**(2): p. 98-112.
224. Chadda, R., et al., *Cholesterol-sensitive Cdc42 activation regulates actin polymerization for endocytosis via the GEEC pathway.* Traffic, 2007. **8**(6): p. 702-17.
225. Kovtun, O., et al., *Cavin family proteins and the assembly of caveolae.* J Cell Sci, 2015. **128**(7): p. 1269-78.
226. Hill, M.M., et al., *PTRF-Cavin, a conserved cytoplasmic protein required for caveola formation and function.* Cell, 2008. **132**(1): p. 113-24.
227. Tillu, V.A., et al., *A variable undecad repeat domain in cavin1 regulates caveola formation and stability.* EMBO Rep, 2018. **19**(9): p. e45775.
228. Tillu, V.A., et al., *Cavin1 intrinsically disordered domains are essential for fuzzy electrostatic interactions and caveola formation.* Nat Commun, 2021. **12**(1): p. 931.
229. Hansen, C.G., et al., *SDPR induces membrane curvature and functions in the formation of caveolae.* Nat Cell Biol, 2009. **11**(7): p. 807-14.
230. McMahon, K.A., et al., *SRBC/cavin-3 is a caveolin adapter protein that regulates caveolae function.* EMBO J, 2009. **28**(8): p. 1001-15.
231. Bastiani, M., et al., *MURC/Cavin-4 and cavin family members form tissue-specific caveolar complexes.* J Cell Biol, 2009. **185**(7): p. 1259-73.
232. Hansen, C.G., G. Howard, and B.J. Nichols, *Pacsin 2 is recruited to caveolae and functions in caveolar biogenesis.* J Cell Sci, 2011. **124**(Pt 16): p. 2777-85.
233. Senju, Y., et al., *Essential role of PACSIN2/syndapin-II in caveolae membrane sculpting.* J Cell Sci, 2011. **124**(Pt 12): p. 2032-40.
234. Moren, B., et al., *EHD2 regulates caveolar dynamics via ATP-driven targeting and oligomerization.* Mol Biol Cell, 2012. **23**(7): p. 1316-29.
235. Stoeber, M., et al., *Oligomers of the ATPase EHD2 confine caveolae to the plasma membrane through association with actin.* EMBO J, 2012. **31**(10): p. 2350-64.
236. Hoernke, M., et al., *EHD2 restrains dynamics of caveolae by an ATP-dependent, membrane-bound, open conformation.* Proc Natl Acad Sci U S A, 2017. **114**(22): p. E4360-E4369.
237. Sonnino, S. and A. Prinetti, *Sphingolipids and membrane environments for caveolin.* FEBS Lett, 2009. **583**(4): p. 597-606.
238. Stan, R.V., *Structure of caveolae.* Biochim Biophys Acta, 2005. **1746**(3): p. 334-48.
239. Goldmann, O. and E. Medina, *Revisiting Pathogen Exploitation of Clathrin-Independent Endocytosis: Mechanisms and Implications.* Cells, 2025. **14**(10): p. 731.

240. Zimnicka, A.M., et al., *Src-dependent phosphorylation of caveolin-1 Tyr-14 promotes swelling and release of caveolae.* Mol Biol Cell, 2016. **27**(13): p. 2090-106.
241. Cao, H., W.E. Courchesne, and C.C. Mastick, *A phosphotyrosine-dependent protein interaction screen reveals a role for phosphorylation of caveolin-1 on tyrosine 14: recruitment of C-terminal Src kinase.* J Biol Chem, 2002. **277**(11): p. 8771-4.
242. Oh, P., D.P. McIntosh, and J.E. Schnitzer, *Dynamin at the neck of caveolae mediates their budding to form transport vesicles by GTP-driven fission from the plasma membrane of endothelium.* J Cell Biol, 1998. **141**(1): p. 101-14.
243. Henley, J.R., et al., *Dynamin-mediated internalization of caveolae.* J Cell Biol, 1998. **141**(1): p. 85-99.
244. Drab, M., et al., *Loss of caveolae, vascular dysfunction, and pulmonary defects in caveolin-1 gene-disrupted mice.* Science, 2001. **293**(5539): p. 2449-52.
245. Zemans, R. and G.P. Downey, *Role of caveolin-1 in regulation of inflammation: different strokes for different folks.* Am J Physiol Lung Cell Mol Physiol, 2008. **294**(2): p. L175-7.
246. Stroupe, C. and A.T. Brunger, *Crystal structures of a Rab protein in its inactive and active conformations.* J Mol Biol, 2000. **304**(4): p. 585-98.
247. Novick, P., C. Field, and R. Schekman, *Identification of 23 complementation groups required for post-translational events in the yeast secretory pathway.* Cell, 1980. **21**(1): p. 205-15.
248. Gallwitz, D., C. Donath, and C. Sander, *A yeast gene encoding a protein homologous to the human c-has/bas proto-oncogene product.* Nature, 1983. **306**(5944): p. 704-7.
249. Touchot, N., P. Chardin, and A. Tavitian, *Four additional members of the ras gene superfamily isolated by an oligonucleotide strategy: molecular cloning of YPT-related cDNAs from a rat brain library.* Proc Natl Acad Sci U S A, 1987. **84**(23): p. 8210-4.
250. Seabra, M.C., E.H. Mules, and A.N. Hume, *Rab GTPases, intracellular traffic and disease.* Trends Mol Med, 2002. **8**(1): p. 23-30.
251. Kaddai, V., Y. Le Marchand-Brustel, and M. Cormont, *Rab proteins in endocytosis and Glut4 trafficking.* Acta Physiol (Oxf), 2008. **192**(1): p. 75-88.
252. Stenmark, H. and V.M. Olkkonen, *The Rab GTPase family.* Genome Biol, 2001. **2**(5): p. REVIEWS3007.
253. Stenmark, H., *Rab GTPases as coordinators of vesicle traffic.* Nat Rev Mol Cell Biol, 2009. **10**(8): p. 513-25.
254. Pereira-Leal, J.B. and M.C. Seabra, *The mammalian Rab family of small GTPases: definition of family and subfamily sequence motifs suggests a mechanism for functional specificity in the Ras superfamily.* J Mol Biol, 2000. **301**(4): p. 1077-87.
255. Moore, I., J. Schell, and K. Palme, *Subclass-specific sequence motifs identified in Rab GTPases.* Trends Biochem Sci, 1995. **20**(1): p. 10-2.
256. Raghavan, S., M.A. Brishti, and M.D. Leo, *Rab GTPases as Modulators of Vascular Function.* Cells, 2022. **11**(19).
257. Itzen, A. and R.S. Goody. *GTPases involved in vesicular trafficking: structures and mechanisms*. in *Seminars in cell & developmental biology*. 2011. Elsevier.
258. Pfeffer, S.R., *Rab GTPase regulation of membrane identity.* Curr Opin Cell Biol, 2013. **25**(4): p. 414-9.
259. Yuan, W. and C. Song, *The Emerging Role of Rab5 in Membrane Receptor Trafficking and Signaling Pathways.* Biochem Res Int, 2020. **2020**(1): p. 4186308.
260. Asaka, M., et al., *Rab5a-mediated localization of claudin-1 is regulated by proteasomes in endothelial cells.* Am J Physiol Cell Physiol, 2011. **300**(1): p. C87-96.
261. Zhao, Z., et al., *Central role for PICALM in amyloid-beta blood-brain barrier transcytosis and clearance.* Nat Neurosci, 2015. **18**(7): p. 978-87.
262. Xu, W., et al., *Dysregulation of Rab5-mediated endocytic pathways in Alzheimer's disease.* Traffic, 2018. **19**(4): p. 253-262.

263. Barbieri, M.A., et al., *Role of rab5 in EGF receptor-mediated signal transduction.* Eur J Cell Biol, 2004. **83**(6): p. 305-14.
264. Barbieri, M.A., et al., *Rab5, an early acting endosomal GTPase, supports in vitro endosome fusion without GTP hydrolysis.* J Biol Chem, 1994. **269**(29): p. 18720-2.
265. Bucci, C., et al., *The small GTPase rab5 functions as a regulatory factor in the early endocytic pathway.* Cell, 1992. **70**(5): p. 715-28.
266. Gorvel, J.P., et al., *rab5 controls early endosome fusion in vitro.* Cell, 1991. **64**(5): p. 915-25.
267. Grbovic, O.M., et al., *Rab5-stimulated up-regulation of the endocytic pathway increases intracellular beta-cleaved amyloid precursor protein carboxyl-terminal fragment levels and Abeta production.* J Biol Chem, 2003. **278**(33): p. 31261-8.
268. Li, G., *Rab5 GTPase and endocytosis.* Biocell, 1996. **20**(3): p. 325-30.
269. Zhang, J., et al., *Structure-based discovery of neoandrographolide as a novel inhibitor of Rab5 to suppress cancer growth.* Comput Struct Biotechnol J, 2020. **18**: p. 3936-3946.
270. Dumas, J.J., et al., *Structural basis of activation and GTP hydrolysis in Rab proteins.* Structure, 1999. **7**(4): p. 413-23.
271. Bucci, C., et al., *Co-operative regulation of endocytosis by three Rab5 isoforms.* FEBS Lett, 1995. **366**(1): p. 65-71.
272. Chiariello, M., C.B. Bruni, and C. Bucci, *The small GTPases Rab5a, Rab5b and Rab5c are differentially phosphorylated in vitro.* FEBS Lett, 1999. **453**(1-2): p. 20-4.
273. Zahraoui, A., et al., *The human Rab genes encode a family of GTP-binding proteins related to yeast YPT1 and SEC4 products involved in secretion.* J Biol Chem, 1989. **264**(21): p. 12394-401.
274. Novick, P. and M. Zerial, *The diversity of Rab proteins in vesicle transport.* Curr Opin Cell Biol, 1997. **9**(4): p. 496-504.
275. Seachrist, J.L., P.H. Anborgh, and S.S.G. Ferguson, *β -adrenergic receptor internalization, endosomal sorting, and plasma membrane recycling are regulated by Rab GTPases.* Journal of Biological Chemistry, 2000. **275**(35): p. 27221-27228.
276. Seachrist, J.L. and S.S. Ferguson, *Regulation of G protein-coupled receptor endocytosis and trafficking by Rab GTPases.* Life Sci, 2003. **74**(2-3): p. 225-35.
277. Stamatovic, S.M., et al., *Relocalization of junctional adhesion molecule A during inflammatory stimulation of brain endothelial cells.* Mol Cell Biol, 2012. **32**(17): p. 3414-27.
278. Coyne, C.B., et al., *Coxsackievirus entry across epithelial tight junctions requires occludin and the small GTPases Rab34 and Rab5.* Cell Host Microbe, 2007. **2**(3): p. 181-92.
279. Miaczynska, M., et al., *APPL proteins link Rab5 to nuclear signal transduction via an endosomal compartment.* Cell, 2004. **116**(3): p. 445-56.
280. Lippe, R., et al., *Functional synergy between Rab5 effector Rabaptin-5 and exchange factor Rabex-5 when physically associated in a complex.* Mol Biol Cell, 2001. **12**(7): p. 2219-28.
281. Vitale, G., et al. *The GDP/GTP cycle of Rab5 in the regulation of endocytotic membrane traffic*. in *Cold Spring Harbor symposia on quantitative biology*. 1995. Cold Spring Harbor Laboratory Press.
282. Torres, V.A. and D.G. Stupack, *Rab5 in the regulation of cell motility and invasion.* Curr Protein Pept Sci, 2011. **12**(1): p. 43-51.
283. Lanzetti, L., *A novel function of Rab5 in mitosis.* Small GTPases, 2012. **3**(3): p. 168-72.
284. Mendoza, P., et al., *Rab5 activation promotes focal adhesion disassembly, migration and invasiveness in tumor cells.* J Cell Sci, 2013. **126**(Pt 17): p. 3835-47.

285. Li, Y., et al., *A novel ER-localized transmembrane protein, EMC6, interacts with RAB5A and regulates cell autophagy.* Autophagy, 2013. **9**(2): p. 150-63.
286. Igarashi, T., et al., *Association of RAB5 overexpression in pancreatic cancer with cancer progression and poor prognosis via E-cadherin suppression.* Oncotarget, 2017. **8**(7): p. 12290-12300.
287. Yang, P.S., et al., *Rab5A is associated with axillary lymph node metastasis in breast cancer patients.* Cancer Sci, 2011. **102**(12): p. 2172-8.
288. McLauchlan, H., et al., *A novel role for Rab5-GDI in ligand sequestration into clathrin-coated pits.* Curr Biol, 1998. **8**(1): p. 34-45.
289. Li, G. and P.D. Stahl, *Structure-function relationship of the small GTPase rab5.* J Biol Chem, 1993. **268**(32): p. 24475-80.
290. Lanzetti, L., et al., *The Eps8 protein coordinates EGF receptor signalling through Rac and trafficking through Rab5.* Nature, 2000. **408**(6810): p. 374-7.
291. Lindsay, A.J. and M.W. McCaffrey, *Rab coupling protein mediated endosomal recycling of N-cadherin influences cell motility.* Oncotarget, 2017. **8**(62): p. 104717-104732.
292. Kelly, E.E., C.P. Horgan, and M.W. McCaffrey, *Rab11 proteins in health and disease.* Biochem Soc Trans, 2012. **40**(6): p. 1360-7.
293. Scapin, S.M., et al., *The crystal structure of the small GTPase Rab11b reveals critical differences relative to the Rab11a isoform.* J Struct Biol, 2006. **154**(3): p. 260-8.
294. Goldenring, J.R., et al., *Rab11 is an apically located small GTP-binding protein in epithelial tissues.* Am J Physiol, 1996. **270**(3 Pt 1): p. G515-25.
295. Goldenring, J.R., et al., *Enrichment of rab11, a small GTP-binding protein, in gastric parietal cells.* Am J Physiol, 1994. **267**(2 Pt 1): p. G187-94.
296. Silvis, M.R., et al., *Rab11b regulates the apical recycling of the cystic fibrosis transmembrane conductance regulator in polarized intestinal epithelial cells.* Mol Biol Cell, 2009. **20**(8): p. 2337-50.
297. Sakurada, K., et al., *Molecular cloning and characterization of a ras p21-like GTP-binding protein (24KG) from rat liver.* Biochem Biophys Res Commun, 1991. **177**(3): p. 1224-32.
298. Lai, F., L. Stubbs, and K. Artzt, *Molecular analysis of mouse Rab11b: a new type of mammalian YPT/Rab protein.* Genomics, 1994. **22**(3): p. 610-6.
299. Ullrich, O., et al., *Rab11 regulates recycling through the pericentriolar recycling endosome.* J Cell Biol, 1996. **135**(4): p. 913-24.
300. Knodler, A., et al., *Coordination of Rab8 and Rab11 in primary ciliogenesis.* Proc Natl Acad Sci U S A, 2010. **107**(14): p. 6346-51.
301. Hobdy-Henderson, K.C., et al., *Dynamics of the apical plasma membrane recycling system during cell division.* Traffic, 2003. **4**(10): p. 681-93.
302. Holubcova, Z., G. Howard, and M. Schuh, *Vesicles modulate an actin network for asymmetric spindle positioning.* Nat Cell Biol, 2013. **15**(8): p. 937-47.
303. Shirane, M. and K.I. Nakayama, *Protrudin induces neurite formation by directional membrane trafficking.* Science, 2006. **314**(5800): p. 818-21.
304. Grosshans, B.L., D. Ortiz, and P. Novick, *Rabs and their effectors: achieving specificity in membrane traffic.* Proc Natl Acad Sci U S A, 2006. **103**(32): p. 11821-7.
305. Zhang, J., et al., *Thirty-one flavors of Drosophila rab proteins.* Genetics, 2007. **176**(2): p. 1307-22.
306. Vernoud, V., et al., *Analysis of the small GTPase gene superfamily of Arabidopsis.* Plant Physiol, 2003. **131**(3): p. 1191-208.
307. Sultana, P. and J. Novotny, *Rab11 and Its Role in Neurodegenerative Diseases.* ASN Neuro, 2022. **14**: p. 17590914221142360.

308. Baetz, N.W. and J.R. Goldenring, *Rab11-family interacting proteins define spatially and temporally distinct regions within the dynamic Rab11a-dependent recycling system.* Mol Biol Cell, 2013. **24**(5): p. 643-58.
309. Takano, T., et al., *LMTK1/AATYK1 is a novel regulator of axonal outgrowth that acts via Rab11 in a Cdk5-dependent manner.* J Neurosci, 2012. **32**(19): p. 6587-99.
310. Casanova, J.E., et al., *Association of Rab25 and Rab11a with the apical recycling system of polarized Madin-Darby canine kidney cells.* Mol Biol Cell, 1999. **10**(1): p. 47-61.
311. Siri, S.O., et al., *Decrease of Rab11 prevents the correct dendritic arborization, synaptic plasticity and spatial memory formation.* Biochim Biophys Acta Mol Cell Res, 2020. **1867**(9): p. 118735.
312. Kawauchi, T., et al., *Rab GTPases-dependent endocytic pathways regulate neuronal migration and maturation through N-cadherin trafficking.* Neuron, 2010. **67**(4): p. 588-602.
313. Ferro, E., C. Bosia, and C.C. Campa, *RAB11-Mediated Trafficking and Human Cancers: An Updated Review.* Biology (Basel), 2021. **10**(1).
314. Nguyen, K., et al., *ST8SIA1 Regulates Tumor Growth and Metastasis in TNBC by Activating the FAK-AKT-mTOR Signaling Pathway.* Mol Cancer Ther, 2018. **17**(12): p. 2689-2701.
315. Kim, D., et al., *Akt/PKB promotes cancer cell invasion via increased motility and metalloproteinase production.* FASEB J, 2001. **15**(11): p. 1953-62.
316. Ramel, D., et al., *Rab11 regulates cell-cell communication during collective cell movements.* Nat Cell Biol, 2013. **15**(3): p. 317-24.
317. Gromov, P. and J.E. Celis, *Rab11a is modified in vivo by isoprenoid geranylgeranyl.* Electrophoresis, 1998. **19**(10): p. 1803-7.
318. Lachance, V., et al., *Regulation of beta2-adrenergic receptor maturation and anterograde trafficking by an interaction with Rab geranylgeranyltransferase: modulation of Rab geranylgeranylation by the receptor.* J Biol Chem, 2011. **286**(47): p. 40802-13.
319. Welz, T., J. Wellbourne-Wood, and E. Kerkhoff, *Orchestration of cell surface proteins by Rab11.* Trends Cell Biol, 2014. **24**(7): p. 407-15.
320. Lachance, V., et al., *Ubiquitylation and activation of a Rab GTPase is promoted by a beta(2)AR-HACE1 complex.* J Cell Sci, 2014. **127**(Pt 1): p. 111-23.
321. Pechlivanis, M. and J. Kuhlmann, *Hydrophobic modifications of Ras proteins by isoprenoid groups and fatty acids--More than just membrane anchoring.* Biochim Biophys Acta, 2006. **1764**(12): p. 1914-31.
322. Solis, G.P., et al., *Reggies/flotillins interact with Rab11a and SNX4 at the tubulovesicular recycling compartment and function in transferrin receptor and E-cadherin trafficking.* Mol Biol Cell, 2013. **24**(17): p. 2689-702.
323. Desclozeaux, M., et al., *Active Rab11 and functional recycling endosome are required for E-cadherin trafficking and lumen formation during epithelial morphogenesis.* Am J Physiol Cell Physiol, 2008. **295**(2): p. C545-56.
324. Yan, Z., et al., *Rab11a Mediates Vascular Endothelial-Cadherin Recycling and Controls Endothelial Barrier Function.* Arterioscler Thromb Vasc Biol, 2016. **36**(2): p. 339-49.
325. Dong, Q., et al., *Rab11a promotes proliferation and invasion through regulation of YAP in non-small cell lung cancer.* Oncotarget, 2017. **8**(17): p. 27800-27811.
326. Porther, N. and M.A. Barbieri, *The role of endocytic Rab GTPases in regulation of growth factor signaling and the migration and invasion of tumor cells.* Small GTPases, 2015. **6**(3): p. 135-44.

327. Zhao, D., B. Wang, and H. Chen, *RAB11A mediates the proliferation and motility of esophageal cancer cells via WNT signaling pathway.* Acta Biochim Pol, 2020. **67**(4): p. 531-538.
328. Chung, Y.C., et al., *Rab11 regulates E-cadherin expression and induces cell transformation in colorectal carcinoma.* BMC Cancer, 2014. **14**: p. 587.
329. Guo, H.J. and P. Tadi, *Biochemistry, ubiquitination.* 2020.
330. Asano, S., et al., *A molecular census of 26 S proteasomes in intact neurons.* Science, 2015. **347**(6220): p. 439-442.
331. Pack, C.G., et al., *Quantitative live-cell imaging reveals spatio-temporal dynamics and cytoplasmic assembly of the 26S proteasome.* Nat Commun, 2014. **5**(1): p. 3396.
332. Choi, W.H., et al., *Aggresomal sequestration and STUB1-mediated ubiquitylation during mammalian proteaphagy of inhibited proteasomes.* Proc Natl Acad Sci U S A, 2020. **117**(32): p. 19190-19200.
333. Tanaka, K. and A. Ichihara, *Half-life of proteasomes (multiprotease complexes) in rat liver.* Biochem Biophys Res Commun, 1989. **159**(3): p. 1309-15.
334. Park, J., J. Cho, and E.J. Song, *Ubiquitin-proteasome system (UPS) as a target for anticancer treatment.* Arch Pharm Res, 2020. **43**(11): p. 1144-1161.
335. Pohl, C. and I. Dikic, *Cellular quality control by the ubiquitin-proteasome system and autophagy.* Science, 2019. **366**(6467): p. 818-822.
336. Kawahata, I. and K. Fukunaga, *Degradation of Tyrosine Hydroxylase by the Ubiquitin-Proteasome System in the Pathogenesis of Parkinson's Disease and Dopa-Responsive Dystonia.* Int J Mol Sci, 2020. **21**(11).
337. Jackson, M.P. and E.W. Hewitt, *Cellular proteostasis: degradation of misfolded proteins by lysosomes.* Essays Biochem, 2016. **60**(2): p. 173-180.
338. Hershko, A. and A. Ciechanover, *The ubiquitin system.* Annu Rev Biochem, 1998. **67**(1): p. 425-79.
339. Eldridge, A.G. and T. O'Brien, *Therapeutic strategies within the ubiquitin proteasome system.* Cell Death Differ, 2010. **17**(1): p. 4-13.
340. Kim, M.N., et al., *Disruption of polyubiquitin gene Ubc leads to attenuated resistance against arsenite-induced toxicity in mouse embryonic fibroblasts.* Biochim Biophys Acta, 2015. **1853**(5): p. 996-1009.
341. Molineaux, S.M., *Molecular pathways: targeting proteasomal protein degradation in cancer.* Clin Cancer Res, 2012. **18**(1): p. 15-20.
342. Tracz, M. and W. Bialek, *Beyond K48 and K63: non-canonical protein ubiquitination.* Cell Mol Biol Lett, 2021. **26**(1): p. 1.
343. King, R.W., et al., *How proteolysis drives the cell cycle.* Science, 1996. **274**(5293): p. 1652-9.
344. Adams, J., *The proteasome: structure, function, and role in the cell.* Cancer Treat Rev, 2003. **29 Suppl 1**: p. 3-9.
345. Tu, Y., et al., *The Ubiquitin Proteasome Pathway (UPP) in the regulation of cell cycle control and DNA damage repair and its implication in tumorigenesis.* Int J Clin Exp Pathol, 2012. **5**(8): p. 726-38.
346. Coux, O., K. Tanaka, and A.L. Goldberg, *Structure and functions of the 20S and 26S proteasomes.* Annu Rev Biochem, 1996. **65**(1): p. 801-47.
347. Baumeister, W., et al., *The proteasome: paradigm of a self-compartmentalizing protease.* Cell, 1998. **92**(3): p. 367-80.
348. Nunes, A.T. and C.M. Annunziata. *Proteasome inhibitors: structure and function*. in *Seminars in oncology*. 2017. Elsevier.
349. Zhang, H.X., et al., *Structural basis of human 20S proteasome biogenesis.* Nature Communications, 2024. **15**(1): p. 8184.
350. Fricker, L.D., *Proteasome Inhibitor Drugs.* Annu Rev Pharmacol Toxicol, 2020. **60**: p. 457-476.

351. Guo, N. and Z. Peng, *MG132, a proteasome inhibitor, induces apoptosis in tumor cells.* Asia Pac J Clin Oncol, 2013. **9**(1): p. 6-11.
352. Kim, Y.M. and H.J. Kim, *Proteasome Inhibitor MG132 is Toxic and Inhibits the Proliferation of Rat Neural Stem Cells but Increases BDNF Expression to Protect Neurons.* Biomolecules, 2020. **10**(11).
353. Sawant, D.A., et al., *Inhibition of VE-cadherin proteasomal degradation attenuates microvascular hyperpermeability.* Microcirculation, 2011. **18**(1): p. 46-55.
354. Willeumier, K., S.M. Pulst, and F.E. Schweizer, *Proteasome inhibition triggers activity-dependent increase in the size of the recycling vesicle pool in cultured hippocampal neurons.* J Neurosci, 2006. **26**(44): p. 11333-41.
355. Meller, R., et al., *Ubiquitin proteasome-mediated synaptic reorganization: a novel mechanism underlying rapid ischemic tolerance.* J Neurosci, 2008. **28**(1): p. 50-9.
356. Lee, C.S., et al., *A proteasomal stress response: pre-treatment with proteasome inhibitors increases proteasome activity and reduces neuronal vulnerability to oxidative injury.* J Neurochem, 2004. **91**(4): p. 996-1006.
357. Lee, H.K., et al., *Proteasome inhibition suppresses Schwann cell dedifferentiation in vitro and in vivo.* Glia, 2009. **57**(16): p. 1825-34.
358. MacInnis, B.L. and R.B. Campenot, *Regulation of Wallerian degeneration and nerve growth factor withdrawal-induced pruning of axons of sympathetic neurons by the proteasome and the MEK/Erk pathway.* Mol Cell Neurosci, 2005. **28**(3): p. 430-9.
359. Zhai, Q., et al., *Involvement of the ubiquitin-proteasome system in the early stages of wallerian degeneration.* Neuron, 2003. **39**(2): p. 217-25.
360. Vincent, P.A., et al., *VE-cadherin: adhesion at arm's length.* Am J Physiol Cell Physiol, 2004. **286**(5): p. C987-97.
361. Costanzi, E., et al., *Structural and Biochemical Analysis of the Dual Inhibition of MG-132 against SARS-CoV-2 Main Protease (Mpro/3CLpro) and Human Cathepsin-L.* Int J Mol Sci, 2021. **22**(21): p. 11779.
362. Stern, S.T., P.P. Adiseshaiah, and R.M. Crist, *Autophagy and lysosomal dysfunction as emerging mechanisms of nanomaterial toxicity.* Part Fibre Toxicol, 2012. **9**: p. 20.
363. Ghavami, S., et al., *Autophagy and apoptosis dysfunction in neurodegenerative disorders.* Prog Neurobiol, 2014. **112**: p. 24-49.
364. Appelqvist, H., et al., *The lysosome: from waste bag to potential therapeutic target.* J Mol Cell Biol, 2013. **5**(4): p. 214-26.
365. Towers, C.G. and A. Thorburn, *Targeting the Lysosome for Cancer Therapy.* Cancer Discov, 2017. **7**(11): p. 1218-1220.
366. Luzio, J.P., P.R. Pryor, and N.A. Bright, *Lysosomes: fusion and function.* Nat Rev Mol Cell Biol, 2007. **8**(8): p. 622-32.
367. Zhao, L., et al., *Targeted protein degradation: mechanisms, strategies and application.* Signal Transduct Target Ther, 2022. **7**(1): p. 113.
368. Xiao, K., et al., *Mechanisms of VE-cadherin processing and degradation in microvascular endothelial cells.* J Biol Chem, 2003. **278**(21): p. 19199-208.
369. Forgac, M., *Vacuolar ATPases: rotary proton pumps in physiology and pathophysiology.* Nat Rev Mol Cell Biol, 2007. **8**(11): p. 917-29.
370. Cui, C.M., et al., *Chloroquine exerts neuroprotection following traumatic brain injury via suppression of inflammation and neuronal autophagic death.* Mol Med Rep, 2015. **12**(2): p. 2323-8.
371. Qin, A., et al., *Is a combination of progesterone and chloroquine more effective than either alone in the treatment of cerebral ischemic injury?* Restor Neurol Neurosci, 2019. **37**(1): p. 1-10.
372. Mauthe, M., et al., *Chloroquine inhibits autophagic flux by decreasing autophagosome-lysosome fusion.* Autophagy, 2018. **14**(8): p. 1435-1455.

373. Al-Bari, M.A., *Chloroquine analogues in drug discovery: new directions of uses, mechanisms of actions and toxic manifestations from malaria to multifarious diseases.* J Antimicrob Chemother, 2015. **70**(6): p. 1608-21.
374. CJ, M., *Matrix metalloproteinases (MMPs) in health and disease: an overview.* Front Biosci, 2006. **11**: p. 1696-1701.
375. Caughlin, S., et al., *Chloroquine Restores Ganglioside Homeostasis and Improves Pathological and Behavioral Outcomes Post-stroke in the Rat.* Mol Neurobiol, 2019. **56**(5): p. 3552-3562.
376. Zhang, Y.P., et al., *Chloroquine pretreatment attenuates ischemia-reperfusion injury in the brain of ob/ob diabetic mice as well as wildtype mice.* Brain Res, 2020. **1726**: p. 146518.
377. Sidibe, A. and B.A. Imhof, *VE-cadherin phosphorylation decides: vascular permeability or diapedesis.* Nat Immunol, 2014. **15**(3): p. 215-7.
378. Orsenigo, F., et al., *Phosphorylation of VE-cadherin is modulated by haemodynamic forces and contributes to the regulation of vascular permeability in vivo.* Nat Commun, 2012. **3**(1): p. 1208.
379. Ozawa, M. and R. Kemler, *Altered cell adhesion activity by pervanadate due to the dissociation of alpha-catenin from the E-cadherin.catenin complex.* J Biol Chem, 1998. **273**(11): p. 6166-70.
380. Chen, X.L., et al., *VEGF-induced vascular permeability is mediated by FAK.* Dev Cell, 2012. **22**(1): p. 146-57.
381. Nottebaum, A.F., et al., *VE-PTP maintains the endothelial barrier via plakoglobin and becomes dissociated from VE-cadherin by leukocytes and by VEGF.* J Exp Med, 2008. **205**(12): p. 2929-45.
382. Esser, S., et al., *Vascular endothelial growth factor induces VE-cadherin tyrosine phosphorylation in endothelial cells.* J Cell Sci, 1998. **111 ( Pt 13)**: p. 1853-65.
383. Andriopoulou, P., et al., *Histamine induces tyrosine phosphorylation of endothelial cell-to-cell adherens junctions.* Arterioscler Thromb Vasc Biol, 1999. **19**(10): p. 2286-97.
384. Shasby, D.M., et al., *Histamine stimulates phosphorylation of adherens junction proteins and alters their link to vimentin.* Am J Physiol Lung Cell Mol Physiol, 2002. **282**(6): p. L1330-8.
385. Potter, M.D., S. Barbero, and D.A. Cheresh, *Tyrosine phosphorylation of VE-cadherin prevents binding of p120- and beta-catenin and maintains the cellular mesenchymal state.* J Biol Chem, 2005. **280**(36): p. 31906-12.
386. Wallez, Y., et al., *Src kinase phosphorylates vascular endothelial-cadherin in response to vascular endothelial growth factor: identification of tyrosine 685 as the unique target site.* Oncogene, 2007. **26**(7): p. 1067-77.
387. Xiao, K., et al., *p120-Catenin regulates clathrin-dependent endocytosis of VE-cadherin.* Mol Biol Cell, 2005. **16**(11): p. 5141-51.
388. Cain, R.J., B. Vanhaesebroeck, and A.J. Ridley, *The PI3K p110alpha isoform regulates endothelial adherens junctions via Pyk2 and Rac1.* J Cell Biol, 2010. **188**(6): p. 863-76.
389. Xiao, K., et al., *Cellular levels of p120 catenin function as a set point for cadherin expression levels in microvascular endothelial cells.* J Cell Biol, 2003. **163**(3): p. 535-45.
390. Gavard, J. and J.S. Gutkind, *VEGF controls endothelial-cell permeability by promoting the beta-arrestin-dependent endocytosis of VE-cadherin.* Nat Cell Biol, 2006. **8**(11): p. 1223-34.
391. Nanes, B.A., et al., *p120-catenin binding masks an endocytic signal conserved in classical cadherins.* J Cell Biol, 2012. **199**(2): p. 365-80.

392. Vandenbroucke St Amant, E., et al., *PKCalpha activation of p120-catenin serine 879 phospho-switch disassembles VE-cadherin junctions and disrupts vascular integrity.* Circ Res, 2012. **111**(6): p. 739-49.
393. Su, W. and A.P. Kowalczyk, *The VE-cadherin cytoplasmic domain undergoes proteolytic processing during endocytosis.* Mol Biol Cell, 2017. **28**(1): p. 76-84.
394. Iyer, S., et al., *VE-cadherin-p120 interaction is required for maintenance of endothelial barrier function.* Am J Physiol Lung Cell Mol Physiol, 2004. **286**(6): p. L1143-53.
395. Oas, R.G., et al., *p120-catenin and beta-catenin differentially regulate cadherin adhesive function.* Mol Biol Cell, 2013. **24**(6): p. 704-14.
396. Le, T.L., et al., *Protein kinase C regulates endocytosis and recycling of E-cadherin.* Am J Physiol Cell Physiol, 2002. **283**(2): p. C489-99.
397. Grimsley-Myers, C.M., et al., *VE-cadherin endocytosis controls vascular integrity and patterning during development.* J Cell Biol, 2020. **219**(5).
398. Hebda, J.K., et al., *The C-terminus region of beta-arrestin1 modulates VE-cadherin expression and endothelial cell permeability.* Cell Commun Signal, 2013. **11**(1): p. 37.
399. Wilkens, M., et al., *Ubiquitination of VE-cadherin regulates inflammation-induced vascular permeability in vivo.* EMBO Rep, 2024. **25**(9): p. 4013-4032.
400. Zhang, Y., et al., *Different contributions of clathrin- and caveolae-mediated endocytosis of vascular endothelial cadherin to lipopolysaccharide-induced vascular hyperpermeability.* PLoS One, 2014. **9**(9): p. e106328.
401. Colas-Algora, N., et al., *Compensatory increase of VE-cadherin expression through ETS1 regulates endothelial barrier function in response to TNFalpha.* Cell Mol Life Sci, 2020. **77**(11): p. 2125-2140.
402. Chichger, H., et al., *Select Rab GTPases Regulate the Pulmonary Endothelium via Endosomal Trafficking of Vascular Endothelial-Cadherin.* Am J Respir Cell Mol Biol, 2016. **54**(6): p. 769-81.
403. Yang, K., et al., *Lactate induces vascular permeability via disruption of VE-cadherin in endothelial cells during sepsis.* Sci Adv, 2022. **8**(17): p. eabm8965.
404. Alexander, J.S., et al., *The role of cadherin endocytosis in endothelial barrier regulation: involvement of protein kinase C and actin-cadherin interactions.* Inflammation, 1998. **22**(4): p. 419-33.
405. Friedrich, E.E., et al., *Endothelial cell Piezo1 mediates pressure-induced lung vascular hyperpermeability via disruption of adherens junctions.* Proc Natl Acad Sci U S A, 2019. **116**(26): p. 12980-12985.
406. Lei, X., et al., *Desacetylvinblastine Monohydrazide Disrupts Tumor Vessels by Promoting VE-cadherin Internalization.* Theranostics, 2018. **8**(2): p. 384-398.
407. Fu, P., et al., *Phospholipase D2 restores endothelial barrier function by promoting PTPN14-mediated VE-cadherin dephosphorylation.* J Biol Chem, 2020. **295**(22): p. 7669-7685.
408. Ushakumari, C.J., et al., *Neutrophil Elastase Increases Vascular Permeability and Leukocyte Transmigration in Cultured Endothelial Cells and Obese Mice.* Cells, 2022. **11**(15).
409. Funamoto, K., et al., *Endothelial monolayer permeability under controlled oxygen tension.* Integr Biol (Camb), 2017. **9**(6): p. 529-538.
410. Benn, A., et al., *VE-cadherin facilitates BMP-induced endothelial cell permeability and signaling.* J Cell Sci, 2016. **129**(1): p. 206-18.
411. Le Guelte, A., et al., *Semaphorin 3A elevates endothelial cell permeability through PP2A inactivation.* J Cell Sci, 2012. **125**(Pt 17): p. 4137-46.
412. Chen, A.Q., et al., *Microglia-derived TNF-alpha mediates endothelial necroptosis aggravating blood brain-barrier disruption after ischemic stroke.* Cell Death Dis, 2019. **10**(7): p. 487.

413. Kowalczyk, A.P. and B.A. Nanes, *Adherens junction turnover: regulating adhesion through cadherin endocytosis, degradation, and recycling.* Subcell Biochem, 2012. **60**: p. 197-222.
414. Hsu, V.W., M. Bai, and J. Li, *Getting active: protein sorting in endocytic recycling.* Nat Rev Mol Cell Biol, 2012. **13**(5): p. 323-8.
415. Giannotta, M., M. Trani, and E. Dejana, *VE-cadherin and endothelial adherens junctions: active guardians of vascular integrity.* Dev Cell, 2013. **26**(5): p. 441-54.
416. Cavallaro, U. and E. Dejana, *Adhesion molecule signalling: not always a sticky business.* Nat Rev Mol Cell Biol, 2011. **12**(3): p. 189-97.
417. Lepore, D.M., L. Martinez-Nunez, and M. Munson, *Exposing the Elusive Exocyst Structure.* Trends Biochem Sci, 2018. **43**(9): p. 714-725.
418. Langevin, J., et al., *Drosophila exocyst components Sec5, Sec6, and Sec15 regulate DE-Cadherin trafficking from recycling endosomes to the plasma membrane.* Dev Cell, 2005. **9**(3): p. 365-76.
419. Xu, B.W., et al., *Effect of p18 on endothelial barrier function by mediating vascular endothelial Rab11a-VE-cadherin recycling.* Biosci Biotechnol Biochem, 2021. **85**(12): p. 2392-2403.
420. Chrifi, I., et al., *CMTM4 regulates angiogenesis by promoting cell surface recycling of VE-cadherin to endothelial adherens junctions.* Angiogenesis, 2019. **22**(1): p. 75-93.
421. Huang, X., et al., *Compromised endothelial Wnt/beta-catenin signaling mediates the blood-brain barrier disruption and leads to neuroinflammation in endotoxemia.* J Neuroinflammation, 2024. **21**(1): p. 265.
422. Yang, Y., et al., *GSTpi regulates VE-cadherin stabilization through promoting S-glutathionylation of Src.* Redox Biol, 2020. **30**: p. 101416.
423. Paulson, D., et al., *IFT20 regulates lymphatic endothelial cell-cell junctions via endocytic trafficking of VE-cadherin.* bioRxiv, 2025: p. 2025.01. 15.631989.
424. Chan, Y.H., et al., *Differential Regulation of LPS-Mediated VE-Cadherin Disruption in Human Endothelial Cells and the Underlying Signaling Pathways: A Mini Review.* Front Cell Dev Biol, 2019. **7**: p. 280.
425. Li, W., et al., *The Role of VE-cadherin in Blood-brain Barrier Integrity Under Central Nervous System Pathological Conditions.* Curr Neuropharmacol, 2018. **16**(9): p. 1375-1384.
426. Chen, T., et al., *Cellular and molecular mechanisms of the blood-brain barrier dysfunction in neurodegenerative diseases.* Fluids Barriers CNS, 2024. **21**(1): p. 60.
427. Dudek, K.A., et al., *Molecular adaptations of the blood-brain barrier promote stress resilience vs. depression.* Proc Natl Acad Sci U S A, 2020. **117**(6): p. 3326-3336.
428. Sweeney, M.D., et al., *The role of brain vasculature in neurodegenerative disorders.* Nat Neurosci, 2018. **21**(10): p. 1318-1331.
429. Menard, C., et al., *Social stress induces neurovascular pathology promoting depression.* Nat Neurosci, 2017. **20**(12): p. 1752-1760.
430. Montagne, A., et al., *Blood-brain barrier breakdown in the aging human hippocampus.* Neuron, 2015. **85**(2): p. 296-302.
431. Hu, H., et al., *MiR-34a Interacts with Cytochrome c and Shapes Stroke Outcomes.* Sci Rep, 2020. **10**(1): p. 3233.
432. Dickstein, D.L., et al., *Abeta peptide immunization restores blood-brain barrier integrity in Alzheimer disease.* FASEB J, 2006. **20**(3): p. 426-33.
433. Buttler, L., et al., *Maintenance of Blood-Brain Barrier Integrity in Hypertension: A Novel Benefit of Exercise Training for Autonomic Control.* Front Physiol, 2017. **8**: p. 1048.
434. Miner, J.J., et al., *The TAM receptor Mertk protects against neuroinvasive viral infection by maintaining blood-brain barrier integrity.* Nat Med, 2015. **21**(12): p. 1464-72.

435. Willis, C.L., et al., *Partial recovery of the damaged rat blood-brain barrier is mediated by adherens junction complexes, extracellular matrix remodeling and macrophage infiltration following focal astrocyte loss.* Neuroscience, 2013. **250**: p. 773-85.
436. Wacker, B.K., et al., *Junctional protein regulation by sphingosine kinase 2 contributes to blood-brain barrier protection in hypoxic preconditioning-induced cerebral ischemic tolerance.* J Cereb Blood Flow Metab, 2012. **32**(6): p. 1014-23.
437. Zhao, Y., et al., *Targeting Vascular Endothelial-Cadherin in Tumor-Associated Blood Vessels Promotes T-cell-Mediated Immunotherapy.* Cancer Res, 2017. **77**(16): p. 4434-4447.
438. Smith, R.O., et al., *Vascular permeability in retinopathy is regulated by VEGFR2 Y949 signaling to VE-cadherin.* Elife, 2020. **9**.
439. Ting, K.K., et al., *Therapeutic regulation of VE-cadherin with a novel oligonucleotide drug for diabetic eye complications using retinopathy mouse models.* Diabetologia, 2019. **62**(2): p. 322-334.
440. Li, J., et al., *Targeting miR-27a/VE-cadherin interactions rescues cerebral cavernous malformations in mice.* PLoS Biol, 2020. **18**(6): p. e3000734.
441. Le Guelte, A., J. Dwyer, and J. Gavard, *Jumping the barrier: VE-cadherin, VEGF and other angiogenic modifiers in cancer.* Biol Cell, 2011. **103**(12): p. 593-605.
442. Chichger, H., et al., *p18, a novel adaptor protein, regulates pulmonary endothelial barrier function via enhanced endocytic recycling of VE-cadherin.* FASEB J, 2015. **29**(3): p. 868-81.
443. Luissint, A.C., et al., *Tight junctions at the blood brain barrier: physiological architecture and disease-associated dysregulation.* Fluids Barriers CNS, 2012. **9**(1): p. 23.
444. Dithmer, S., et al., *The Basic Requirement of Tight Junction Proteins in Blood-Brain Barrier Function and Their Role in Pathologies.* Int J Mol Sci, 2024. **25**(11).
445. Chen, J., et al., *Oxygen-Glucose Deprivation/Reoxygenation Induces Human Brain Microvascular Endothelial Cell Hyperpermeability Via VE-Cadherin Internalization: Roles of RhoA/ROCK2.* J Mol Neurosci, 2019. **69**(1): p. 49-59.
446. Zhang, D., et al., *Netrin-4 promotes VE-cadherin expression in endothelial cells through the NF-kappaB signaling pathway.* Exp Ther Med, 2024. **28**(3): p. 351.
447. Young, J.A., et al., *Regulation of vascular leak and recovery from ischemic injury by general and VE-cadherin-restricted miRNA antagonists of miR-27.* Blood, 2013. **122**(16): p. 2911-9.
448. Salvador, E., S. Shityakov, and C. Forster, *Glucocorticoids and endothelial cell barrier function.* Cell Tissue Res, 2014. **355**(3): p. 597-605.
449. Wang, Z., et al., *FTY720 Protects Against Ischemia-Reperfusion Injury by Preventing the Redistribution of Tight Junction Proteins and Decreases Inflammation in the Subacute Phase in an Experimental Stroke Model.* Transl Stroke Res, 2020. **11**(5): p. 1103-1116.
450. Garcia-Merino, J.A. and A.J. Sanchez, *[Basic mechanisms of action of fingolimod in relation to multiple sclerosis].* Rev Neurol, 2012. **55**(1): p. 31-7.
451. Di Menna, L., et al., *Fingolimod protects cultured cortical neurons against excitotoxic death.* Pharmacol Res, 2013. **67**(1): p. 1-9.
452. Brinkmann, V., et al., *Fingolimod (FTY720): discovery and development of an oral drug to treat multiple sclerosis.* Nat Rev Drug Discov, 2010. **9**(11): p. 883-97.
453. Wang, L., et al., *FTY720-induced human pulmonary endothelial barrier enhancement is mediated by c-Abl.* Eur Respir J, 2011. **38**(1): p. 78-88.
454. Sarai, K., et al., *Endothelial barrier protection by FTY720 under hyperglycemic condition: involvement of focal adhesion kinase, small GTPases, and adherens junction proteins.* Am J Physiol Cell Physiol, 2009. **297**(4): p. C945-54.

455. Oggungwan, K., et al., *FTY720 restores endothelial cell permeability induced by malaria sera.* Sci Rep, 2018. **8**(1): p. 10959.
456. Li, J., et al., *Development of Novel Therapeutics Targeting the Blood-Brain Barrier: From Barrier to Carrier.* Adv Sci (Weinh), 2021. **8**(16): p. e2101090.
457. Sontag, J.M. and E. Sontag, *Protein phosphatase 2A dysfunction in Alzheimer's disease.* Front Mol Neurosci, 2014. **7**: p. 16.
458. Nunbhakdi-Craig, V., et al., *Protein phosphatase 2A associates with and regulates atypical PKC and the epithelial tight junction complex.* J Cell Biol, 2002. **158**(5): p. 967-78.
459. Elias, B.C., et al., *Phosphorylation of Tyr-398 and Tyr-402 in occludin prevents its interaction with ZO-1 and destabilizes its assembly at the tight junctions.* J Biol Chem, 2009. **284**(3): p. 1559-69.
460. Hanawa, S., A. Mitsuhashi, and M. Shozu, *Antitumor effects of metformin via indirect inhibition of protein phosphatase 2A in patients with endometrial cancer.* PLoS One, 2018. **13**(2): p. e0192759.
461. Martin-Montalvo, A., et al., *Metformin improves healthspan and lifespan in mice.* Nat Commun, 2013. **4**(1): p. 2192.
462. Bailey, C.J. and C. Day, *Traditional plant medicines as treatments for diabetes.* Diabetes Care, 1989. **12**(8): p. 553-64.
463. Pernicova, I. and M. Korbonits, *Metformin--mode of action and clinical implications for diabetes and cancer.* Nat Rev Endocrinol, 2014. **10**(3): p. 143-56.
464. Xenos, D., P. Mecocci, and V. Boccardi, *A blast from the past: To tame time with metformin.* Mech Ageing Dev, 2022. **208**: p. 111743.
465. Bailey, C.J., *Biguanides and NIDDM.* Diabetes Care, 1992. **15**(6): p. 755-72.
466. Owen, M.R., E. Doran, and A.P. Halestrap, *Evidence that metformin exerts its anti-diabetic effects through inhibition of complex 1 of the mitochondrial respiratory chain.* Biochem J, 2000. **348 Pt 3**(Pt 3): p. 607-14.
467. Li, N., T. Zhou, and E. Fei, *Actions of Metformin in the Brain: A New Perspective of Metformin Treatments in Related Neurological Disorders.* Int J Mol Sci, 2022. **23**(15): p. 8281.
468. Sanati, M., et al., *Mechanistic insight into the role of metformin in Alzheimer's disease.* Life Sci, 2022. **291**: p. 120299.
469. Paudel, Y.N., et al., *Emerging neuroprotective effect of metformin in Parkinson's disease: A molecular crosstalk.* Pharmacol Res, 2020. **152**: p. 104593.
470. Arnoux, I., et al., *Metformin reverses early cortical network dysfunction and behavior changes in Huntington's disease.* Elife, 2018. **7**: p. e38744.
471. Mestareehi, A., et al., *Metformin Increases Protein Phosphatase 2A Activity in Primary Human Skeletal Muscle Cells Derived from Lean Healthy Participants.* J Diabetes Res, 2021. **2021**: p. 9979234.
472. Kruczkowska, W., et al., *Overview of Metformin and Neurodegeneration: A Comprehensive Review.* Pharmaceuticals (Basel), 2025. **18**(4).
473. Dutta, S., et al., *Metformin: A Review of Potential Mechanism and Therapeutic Utility Beyond Diabetes.* Drug Des Devel Ther, 2023. **17**: p. 1907-1932.
474. Jiralerspong, S., et al., *Metformin and pathologic complete responses to neoadjuvant chemotherapy in diabetic patients with breast cancer.* J Clin Oncol, 2009. **27**(20): p. 3297-302.
475. Cheng, M., et al., *Understanding the action mechanisms of metformin in the gastrointestinal tract.* Front Pharmacol, 2024. **15**: p. 1347047.
476. Vasamsetti, S.B., et al., *Metformin inhibits monocyte-to-macrophage differentiation via AMPK-mediated inhibition of STAT3 activation: potential role in atherosclerosis.* Diabetes, 2015. **64**(6): p. 2028-41.

477. Cameron, A.R., et al., *Anti-Inflammatory Effects of Metformin Irrespective of Diabetes Status.* Circ Res, 2016. **119**(5): p. 652-65.
478. Bannister, C.A., et al., *Can people with type 2 diabetes live longer than those without? A comparison of mortality in people initiated with metformin or sulphonylurea monotherapy and matched, non-diabetic controls.* Diabetes, Obesity and Metabolism, 2014. **16**(11): p. 1165-1173.
479. Kalender, A., et al., *Metformin, independent of AMPK, inhibits mTORC1 in a rag GTPase-dependent manner.* Cell Metab, 2010. **11**(5): p. 390-401.
480. Cui, W., et al., *Novel targets and therapies of metformin in dementia: old drug, new insights.* Front Pharmacol, 2024. **15**: p. 1415740.
481. Poor, S.R., et al., *Metformin a Potential Pharmacological Strategy in Late Onset Alzheimer's Disease Treatment.* Pharmaceuticals (Basel), 2021. **14**(9).
482. Sanchis, A., et al., *Metformin treatment reduces motor and neuropsychiatric phenotypes in the zQ175 mouse model of Huntington disease.* Exp Mol Med, 2019. **51**(6): p. 1-16.
483. Loan, A., et al., *Promising use of metformin in treating neurological disorders: biomarker-guided therapies.* Neural Regen Res, 2024. **19**(5): p. 1045-1055.
484. Kciuk, M., et al., *Alzheimer's Disease as Type 3 Diabetes: Understanding the Link and Implications.* Int J Mol Sci, 2024. **25**(22).
485. Capes-Davis, A., *Cell line detective work: basic principles and molecular applications.* Advances in Molecular Pathology, 2018. **1**(1): p. 229-238.
486. Stepanenko, A.A. and V.M. Kavsan, *Immortalization and malignant transformation of eukaryotic cells.* Tsitol Genet, 2012. **46**(2): p. 36-75.
487. Sachs, L. and D. Medina, *In vitro transformation of normal cells by polyoma virus.* Nature, 1961. **189**(4763): p. 457-8.
488. Berwald, Y. and L. Sachs, *In Vitro Cell Transformation with Chemical Carcinogens.* Nature, 1963. **200**(4912): p. 1182-4.
489. Wolbank, S., et al., *Immortalized Human Amnion- and Adipose-Derived Mesenchymal Stem Cells: Maintenance of Differentiation and Immunomodulatory Characteristics.* Tissue Engineering Part A, 2009. **15**(7): p. 1843-1854.
490. Irfan Maqsood, M., et al., *Immortality of cell lines: challenges and advantages of establishment.* Cell biology international, 2013. **37**(10): p. 1038-1045.
491. Okamoto, T., et al., *Clonal heterogeneity in differentiation potential of immortalized human mesenchymal stem cells.* Biochem Biophys Res Commun, 2002. **295**(2): p. 354-61.
492. Kaur, G. and J.M. Dufour, *Cell lines: Valuable tools or useless artifacts*. 2012, Taylor & Francis. p. 1-5.
493. Voloshin, N., et al., *Practical Use of Immortalized Cells in Medicine: Current Advances and Future Perspectives.* Int J Mol Sci, 2023. **24**(16): p. 12716.
494. Weksler, B., I.A. Romero, and P.O. Couraud, *The hCMEC/D3 cell line as a model of the human blood brain barrier.* Fluids Barriers CNS, 2013. **10**(1): p. 16.
495. Roux, F., et al., *Regulation of gamma-glutamyl transpeptidase and alkaline phosphatase activities in immortalized rat brain microvessel endothelial cells.* J Cell Physiol, 1994. **159**(1): p. 101-13.
496. Greenwood, J., et al., *SV40 large T immortalised cell lines of the rat blood-brain and blood-retinal barriers retain their phenotypic and immunological characteristics.* J Neuroimmunol, 1996. **71**(1-2): p. 51-63.
497. Weksler, B.B., et al., *Blood-brain barrier-specific properties of a human adult brain endothelial cell line.* FASEB J, 2005. **19**(13): p. 1872-4.
498. Coureuil, M., et al., *Meningococcal type IV pili recruit the polarity complex to cross the brain endothelium.* Science, 2009. **325**(5936): p. 83-7.

499. Cucullo, L., et al., *Immortalized human brain endothelial cells and flow-based vascular modeling: a marriage of convenience for rational neurovascular studies.* J Cereb Blood Flow Metab, 2008. **28**(2): p. 312-28.
500. Dauchy, S., et al., *Expression and transcriptional regulation of ABC transporters and cytochromes P450 in hCMEC/D3 human cerebral microvascular endothelial cells.* Biochem Pharmacol, 2009. **77**(5): p. 897-909.
501. Forster, C., et al., *Differential effects of hydrocortisone and TNFalpha on tight junction proteins in an in vitro model of the human blood-brain barrier.* J Physiol, 2008. **586**(7): p. 1937-49.
502. Gu, X., et al., *Brain and retinal vascular endothelial cells with extended life span established by ectopic expression of telomerase.* Invest Ophthalmol Vis Sci, 2003. **44**(7): p. 3219-25.
503. Huang, W., et al., *PPARalpha and PPARgamma attenuate HIV-induced dysregulation of tight junction proteins by modulations of matrix metalloproteinase and proteasome activities.* FASEB J, 2009. **23**(5): p. 1596-606.
504. Tai, L.M., et al., *Polarized P-glycoprotein expression by the immortalised human brain endothelial cell line, hCMEC/D3, restricts apical-to-basolateral permeability to rhodamine 123.* Brain Res, 2009. **1292**: p. 14-24.
505. Edgell, C.J., C.C. McDonald, and J.B. Graham, *Permanent cell line expressing human factor VIII-related antigen established by hybridization.* Proc Natl Acad Sci U S A, 1983. **80**(12): p. 3734-7.
506. Lieber, M., et al., *A continuous tumor-cell line from a human lung carcinoma with properties of type II alveolar epithelial cells.* Int J Cancer, 1976. **17**(1): p. 62-70.
507. Binz, R.L. and R. Pathak, *G-Banding and Molecular Cytogenetics Detect Novel Translocations and Cryptic Aberrations in Human Immortal Endothelial Cells.* Int J Mol Sci, 2024. **25**(14): p. 7941.
508. Rabiet, M.J., et al., *Thrombin-induced increase in endothelial permeability is associated with changes in cell-to-cell junction organization.* Arterioscler Thromb Vasc Biol, 1996. **16**(3): p. 488-96.
509. Pei-Yuan, Z., et al., *Overexpression of Axl reverses endothelial cells dysfunction in high glucose and hypoxia.* J Cell Biochem, 2019. **120**(7): p. 11831-11841.
510. Abdelgawad, I.Y., et al., *EA.hy926 Cells and HUVECs Share Similar Senescence Phenotypes but Respond Differently to the Senolytic Drug ABT-263.* Cells, 2022. **11**(13): p. 1992.
511. Montesano, R., et al., *Increased proteolytic activity is responsible for the aberrant morphogenetic behavior of endothelial cells expressing the middle T oncogene.* Cell, 1990. **62**(3): p. 435-45.
512. Brown, R.C., A.P. Morris, and R.G. O'Neil, *Tight junction protein expression and barrier properties of immortalized mouse brain microvessel endothelial cells.* Brain Res, 2007. **1130**(1): p. 17-30.
513. Liu, J., et al., *Matrix metalloproteinase-2-mediated occludin degradation and caveolin-1-mediated claudin-5 redistribution contribute to blood-brain barrier damage in early ischemic stroke stage.* J Neurosci, 2012. **32**(9): p. 3044-57.
514. Sandal, P., et al., *Protein phosphatase 2A - structure, function and role in neurodevelopmental disorders.* J Cell Sci, 2021. **134**(13): p. jcs248187.
515. McCole, D.F., *Phosphatase regulation of intercellular junctions.* Tissue Barriers, 2013. **1**(5): p. e26713.
516. Wuerger, L.T.D., et al., *Proteomic analysis of hepatic effects of okadaic acid in HepaRG human liver cells.* EXCLI J, 2023. **22**: p. 1135-1145.
517. Wuerger, L.T.D., et al., *A multi-omics approach to elucidate okadaic acid-induced changes in human HepaRG hepatocarcinoma cells.* Arch Toxicol, 2024. **98**(9): p. 2919-2935.

518. Oliveira, J.M., et al., *Toward Neuroproteomics in Biological Psychiatry: A Systems Approach Unravels Okadaic Acid-Induced Alterations in the Neuronal Phosphoproteome.* OMICS, 2017. **21**(9): p. 550-563.
519. Shen, D., et al., *Metformin Preserves VE-Cadherin in Choroid Plexus and Attenuates Hydrocephalus via VEGF/VEGFR2/p-Src in an Intraventricular Hemorrhage Rat Model.* Int J Mol Sci, 2022. **23**(15): p. 8552.
520. Pardridge, W.M., *Molecular biology of the blood-brain barrier.* Mol Biotechnol, 2005. **30**(1): p. 57-70.
521. Broman, M.T., et al., *Cdc42 regulates adherens junction stability and endothelial permeability by inducing alpha-catenin interaction with the vascular endothelial cadherin complex.* Circ Res, 2006. **98**(1): p. 73-80.
522. Montero-Balaguer, M., et al., *Stable vascular connections and remodeling require full expression of VE-cadherin in zebrafish embryos.* PLoS One, 2009. **4**(6): p. e5772.
523. Gavard, J., *Endothelial permeability and VE-cadherin: a wacky comradeship.* Cell Adh Migr, 2013. **7**(6): p. 455-61.
524. Le, T.L., A.S. Yap, and J.L. Stow, *Recycling of E-cadherin: a potential mechanism for regulating cadherin dynamics.* J Cell Biol, 1999. **146**(1): p. 219-32.
525. Arima, S., et al., *Angiogenic morphogenesis driven by dynamic and heterogeneous collective endothelial cell movement.* Development, 2011. **138**(21): p. 4763-76.
526. Bentley, K., et al., *The role of differential VE-cadherin dynamics in cell rearrangement during angiogenesis.* Nat Cell Biol, 2014. **16**(4): p. 309-21.
527. Neto, F., et al., *YAP and TAZ regulate adherens junction dynamics and endothelial cell distribution during vascular development.* Elife, 2018. **7**.
528. Aicher, B., et al., *Cellular redistribution of protein tyrosine phosphatases LAR and PTPsigma by inducible proteolytic processing.* J Cell Biol, 1997. **138**(3): p. 681-96.
529. Curry, F.R. and R.H. Adamson, *Vascular permeability modulation at the cell, microvessel, or whole organ level: towards closing gaps in our knowledge.* Cardiovasc Res, 2010. **87**(2): p. 218-29.
530. Dejana, E., E. Tournier-Lasserve, and B.M. Weinstein, *The control of vascular integrity by endothelial cell junctions: molecular basis and pathological implications.* Dev Cell, 2009. **16**(2): p. 209-21.
531. Komarova, Y. and A.B. Malik, *Regulation of endothelial permeability via paracellular and transcellular transport pathways.* Annu Rev Physiol, 2010. **72**(1): p. 463-93.
532. Spring, K., et al., *Tyrosine phosphorylation of DEP-1/CD148 as a mechanism controlling Src kinase activation, endothelial cell permeability, invasion, and capillary formation.* Blood, 2012. **120**(13): p. 2745-56.
533. Timmerman, I., P.L. Hordijk, and J.D. van Buul, *Phosphorylation at endothelial cell–cell junctions: Implications for VE-cadherin function.* Cell Health and Cytoskeleton, 2010: p. 23-31.
534. Johnson, H., S. Narayan, and A.K. Sharma, *Altering phosphorylation in cancer through PP2A modifiers.* Cancer Cell Int, 2024. **24**(1): p. 11.
535. Aune, T. and M. Yndestad, *Diarrhetic shellfish poisoning*. 1993, Academic Press: London, UK. p. 87-104.
536. Munday, R., *Is protein phosphatase inhibition responsible for the toxic effects of okadaic Acid in animals?* Toxins (Basel), 2013. **5**(2): p. 267-85.
537. Zhang, Z. and J.W. Simpkins, *An okadaic acid-induced model of tauopathy and cognitive deficiency.* Brain Res, 2010. **1359**: p. 233-46.
538. Bialojan, C. and A. Takai, *Inhibitory effect of a marine-sponge toxin, okadaic acid, on protein phosphatases. Specificity and kinetics.* Biochem J, 1988. **256**(1): p. 283-90.
539. Arendt, T., et al., *In vivo phosphorylation in the rat basal nucleus induces PHF-like and APP immunoreactivity.* Neuroreport, 1994. **5**(11): p. 1397-400.

540. Mudher, A.K. and V.H. Perry, *Using okadaic acid as a tool for the in vivo induction of hyperphosphorylated tau.* Neuroscience, 1998. **85**(4): p. 1329-32.
541. Blum, M.S., et al., *Cytoskeletal rearrangement mediates human microvascular endothelial tight junction modulation by cytokines.* Am J Physiol, 1997. **273**(1 Pt 2): p. H286-94.
542. Simonovic, I., et al., *Enteropathogenic Escherichia coli dephosphorylates and dissociates occludin from intestinal epithelial tight junctions.* Cell Microbiol, 2000. **2**(4): p. 305-15.
543. Gong, Q., C. Huntsman, and D. Ma, *Clathrin-independent internalization and recycling.* J Cell Mol Med, 2008. **12**(1): p. 126-44.
544. Archie, S.R., A. Al Shoyaib, and L. Cucullo, *Blood-Brain Barrier Dysfunction in CNS Disorders and Putative Therapeutic Targets: An Overview.* Pharmaceutics, 2021. **13**(11): p. 1779.
545. Kamat, P.K., et al., *A study on neuroinflammatory marker in brain areas of okadaic acid (ICV) induced memory impaired rats.* Life Sci, 2012. **90**(19-20): p. 713-20.
546. Takai, A., et al., *Inhibition of specific binding of okadaic acid to protein phosphatase 2A by microcystin-LR, calyculin-A and tautomycin: method of analysis of interactions of tight-binding ligands with target protein.* Biochem J, 1995. **306 ( Pt 3)**(Pt 3): p. 657-65.
547. Louzao, M.C., M.R. Vieytes, and L.M. Botana, *Effect of okadaic acid on glucose regulation.* Mini Rev Med Chem, 2005. **5**(2): p. 207-15.
548. Ghasemi, M., et al., *The MTT Assay: Utility, Limitations, Pitfalls, and Interpretation in Bulk and Single-Cell Analysis.* Int J Mol Sci, 2021. **22**(23).
549. Tsao, C.C., et al., *Mitochondrial protein phosphatase 2A regulates cell death induced by simulated ischemia in kidney NRK-52E cells.* Cell Cycle, 2007. **6**(19): p. 2377-85.
550. Moskot, M., et al., *The Role of Dimethyl Sulfoxide (DMSO) in Gene Expression Modulation and Glycosaminoglycan Metabolism in Lysosomal Storage Disorders on an Example of Mucopolysaccharidosis.* Int J Mol Sci, 2019. **20**(2).
551. Malaguti, C. and G.P. Rossini, *Recovery of cellular E-cadherin precedes replenishment of estrogen receptor and estrogen-dependent proliferation of breast cancer cells rescued from a death stimulus.* J Cell Physiol, 2002. **192**(2): p. 171-81.
552. Maheshwari, S., et al., *Discovery of a Novel Small-Molecule Inhibitor that Targets PP2A-beta-Catenin Signaling and Restricts Tumor Growth and Metastasis.* Mol Cancer Ther, 2017. **16**(9): p. 1791-1805.
553. Edfors, F., et al., *Gene-specific correlation of RNA and protein levels in human cells and tissues.* Mol Syst Biol, 2016. **12**(10): p. 883.
554. Liu, W., et al., *MicroRNA-27b functions as a new inhibitor of ovarian cancer-mediated vasculogenic mimicry through suppression of VE-cadherin expression.* Rna, 2017. **23**(7): p. 1019-1027.
555. Rubiolo, J.A., et al., *Okadaic acid and dinophysis toxin 2 have differential toxicological effects in hepatic cell lines inducing cell cycle arrest, at G0/G1 or G2/M with aberrant mitosis depending on the cell line.* Arch Toxicol, 2011. **85**(12): p. 1541-50.
556. Valdiglesias, V., et al., *Okadaic acid induces morphological changes, apoptosis and cell cycle alterations in different human cell types.* J Environ Monit, 2011. **13**(6): p. 1831-40.
557. Beckers, C.M., et al., *Nuclear targeting of beta-catenin and p120ctn during thrombin-induced endothelial barrier dysfunction.* Cardiovasc Res, 2008. **79**(4): p. 679-88.
558. Magnaudeix, A., et al., *PP2A blockade inhibits autophagy and causes intraneuronal accumulation of ubiquitinated proteins.* Neurobiol Aging, 2013. **34**(3): p. 770-90.

559. Ward, M.P. and J.P. Spiers, *Protein phosphatase 2A regulation of markers of extracellular matrix remodelling in hepatocellular carcinoma cells: functional consequences for tumour invasion.* Br J Pharmacol, 2017. **174**(10): p. 1116-1130.
560. Kasa, A., et al., *Protein phosphatase 2A activity is required for functional adherent junctions in endothelial cells.* Microvasc Res, 2013. **89**: p. 86-94.
561. Beckers, C.M., et al., *Nuclear targeting of beta-catenin and p120ctn during thrombin-induced endothelial barrier dysfunction.* Cardiovasc Res, 2008. **79**(4): p. 679-88.
562. Tiruppathi, C., et al., *Ubiquitin ligase CHFR mediated degradation of VE-cadherin through ubiquitylation disrupts endothelial adherens junctions.* Nat Commun, 2023. **14**(1): p. 6582.
563. Bik, E., et al., *Chloroquine-Induced Accumulation of Autophagosomes and Lipids in the Endothelium.* Int J Mol Sci, 2021. **22**(5).
564. Redmann, M., et al., *Inhibition of autophagy with bafilomycin and chloroquine decreases mitochondrial quality and bioenergetic function in primary neurons.* Redox Biol, 2017. **11**: p. 73-81.
565. Klionsky, D.J., et al., *Guidelines for the use and interpretation of assays for monitoring autophagy (4th edition)(1).* Autophagy, 2021. **17**(1): p. 1-382.
566. Ramakrishna, S., Y.H. Kim, and H. Kim, *Stability of zinc finger nuclease protein is enhanced by the proteasome inhibitor MG132.* PLoS One, 2013. **8**(1): p. e54282.
567. Lee, D.H. and A.L. Goldberg, *Proteasome inhibitors: valuable new tools for cell biologists.* Trends Cell Biol, 1998. **8**(10): p. 397-403.
568. Tsubuki, S., et al., *Differential inhibition of calpain and proteasome activities by peptidyl aldehydes of di-leucine and tri-leucine.* J Biochem, 1996. **119**(3): p. 572-6.
569. Park, W.H. and S.H. Kim, *MG132, a proteasome inhibitor, induces human pulmonary fibroblast cell death via increasing ROS levels and GSH depletion.* Oncol Rep, 2012. **27**(4): p. 1284-91.
570. Jin, F., et al., *Proteasome inhibitor MG132 suppresses pancreatic ductal adenocarcinoma-cell migration by increasing ESE3 expression.* Oncol Lett, 2020. **19**(1): p. 858-868.
571. Gong, Y., et al., *Nuclear export signal of androgen receptor (NESAR) regulation of androgen receptor level in human prostate cell lines via ubiquitination and proteasome-dependent degradation.* Endocrinology, 2012. **153**(12): p. 5716-25.
572. Diwan, A.H., et al., *Inhibition of serine-threonine protein phosphatases decreases barrier function of rat pulmonary microvascular endothelial cells.* J Cell Physiol, 1997. **171**(3): p. 259-70.
573. Palmiotti, C.A., et al., *In vitro cerebrovascular modeling in the 21st century: current and prospective technologies.* Pharm Res, 2014. **31**(12): p. 3229-50.
574. Banks, W.A., *From blood-brain barrier to blood-brain interface: new opportunities for CNS drug delivery.* Nat Rev Drug Discov, 2016. **15**(4): p. 275-92.
575. Gory-Faure, S., et al., *Role of vascular endothelial-cadherin in vascular morphogenesis.* Development, 1999. **126**(10): p. 2093-102.
576. Gaengel, K., et al., *The sphingosine-1-phosphate receptor S1PR1 restricts sprouting angiogenesis by regulating the interplay between VE-cadherin and VEGFR2.* Dev Cell, 2012. **23**(3): p. 587-99.
577. Brock, T., et al., *The Influence of VE-Cadherin on Adhesion and Incorporation of Breast Cancer Cells into Vascular Endothelium.* Int J Mol Sci, 2021. **22**(11).
578. Kadoglou, N.P.E., et al., *Exercise training inhibits atherosclerosis progression and reduces VE-cadherin levels within atherosclerotic plaques in hypercholesterolemic mice.* Biochem Biophys Res Commun, 2022. **623**: p. 39-43.
579. Ting, K.K., et al., *Vascular senescence and leak are features of the early breakdown of the blood-brain barrier in Alzheimer's disease models.* Geroscience, 2023. **45**(6): p. 3307-3331.

580. Maxfield, F.R. and T.E. McGraw, *Endocytic recycling.* Nat Rev Mol Cell Biol, 2004. **5**(2): p. 121-32.
581. Bhuin, T. and J.K. Roy, *Rab proteins: the key regulators of intracellular vesicle transport.* Exp Cell Res, 2014. **328**(1): p. 1-19.
582. Wandinger-Ness, A. and M. Zerial, *Rab proteins and the compartmentalization of the endosomal system.* Cold Spring Harb Perspect Biol, 2014. **6**(11): p. a022616.
583. Sharma, K., et al., *Ultradeep human phosphoproteome reveals a distinct regulatory nature of Tyr and Ser/Thr-based signaling.* Cell Rep, 2014. **8**(5): p. 1583-94.
584. Thomas, D.M., C. Kannabiran, and D. Balasubramanian, *Identification of Key Genes and Pathways in Persistent Hyperplastic Primary Vitreous of the Eye Using Bioinformatic Analysis.* Front Med (Lausanne), 2021. **8**: p. 690594.
585. Ge, S.X., D. Jung, and R. Yao, *ShinyGO: a graphical gene-set enrichment tool for animals and plants.* Bioinformatics, 2020. **36**(8): p. 2628-2629.
586. Searl, T., et al., *Pathway Enrichment Analysis of Microarray Data Fom Human Penis of Diabetic and Peyronie's Patients, in Comparison With Diabetic Rat Erectile Dysfunction Models.* J Sex Med, 2022. **19**(1): p. 37-53.
587. Wang, J., et al., *Quantitative proteomic analysis of okadaic acid treated mouse small intestines reveals differentially expressed proteins involved in diarrhetic shellfish poisoning.* J Proteomics, 2012. **75**(7): p. 2038-52.
588. Wang, J., L. Lin, and D.Z. Wang, *Quantitative proteomic analysis reveals novel insights into hepatic toxicity in mice exposed chronically to okadaic acid.* Science of the Total Environment, 2021. **775**.
589. Sala, G.L., et al., *Proteomic analysis reveals multiple patterns of response in cells exposed to a toxin mixture.* Chem Res Toxicol, 2009. **22**(6): p. 1077-85.
590. Opsahl, J.A., et al., *Identification of dynamic changes in proteins associated with the cellular cytoskeleton after exposure to okadaic acid.* Mar Drugs, 2013. **11**(6): p. 1763-82.
591. Arif, M., et al., *Tau pathology involves protein phosphatase 2A in parkinsonism-dementia of Guam.* Proc Natl Acad Sci U S A, 2014. **111**(3): p. 1144-9.
592. Grundke-Iqbal, I., et al., *Abnormal phosphorylation of the microtubule-associated protein tau (tau) in Alzheimer cytoskeletal pathology.* Proc Natl Acad Sci U S A, 1986. **83**(13): p. 4913-7.
593. Medeiros, R., D. Baglietto-Vargas, and F.M. LaFerla, *The role of tau in Alzheimer's disease and related disorders.* CNS Neurosci Ther, 2011. **17**(5): p. 514-24.
594. Moore, K.B.E., T.J. Hung, and J.S. Fortin, *Hyperphosphorylated tau (p-tau) and drug discovery in the context of Alzheimer's disease and related tauopathies.* Drug Discov Today, 2023. **28**(3): p. 103487.
595. Harris, K.A., et al., *Okadaic acid induces hyperphosphorylated forms of tau protein in human brain slices.* Ann Neurol, 1993. **33**(1): p. 77-87.
596. Liu, F., et al., *Contributions of protein phosphatases PP1, PP2A, PP2B and PP5 to the regulation of tau phosphorylation.* Eur J Neurosci, 2005. **22**(8): p. 1942-50.
597. Gong, C.X., et al., *Phosphatase activity toward abnormally phosphorylated tau: decrease in Alzheimer disease brain.* J Neurochem, 1995. **65**(2): p. 732-8.
598. Sontag, E., et al., *Altered expression levels of the protein phosphatase 2A ABalphaC enzyme are associated with Alzheimer disease pathology.* J Neuropathol Exp Neurol, 2004. **63**(4): p. 287-301.
599. Park, H.J., et al., *Dysregulation of protein phosphatase 2A in parkinson disease and dementia with lewy bodies.* Ann Clin Transl Neurol, 2016. **3**(10): p. 769-780.
600. Strang, K.H., T.E. Golde, and B.I. Giasson, *MAPT mutations, tauopathy, and mechanisms of neurodegeneration.* Lab Invest, 2019. **99**(7): p. 912-928.
601. Mohamed, N.V., A. Desjardins, and N. Leclerc, *Tau secretion is correlated to an increase of Golgi dynamics.* PLoS One, 2017. **12**(5): p. e0178288.

602. Querfurth, H. and H.K. Lee, *Mammalian/mechanistic target of rapamycin (mTOR) complexes in neurodegeneration.* Mol Neurodegener, 2021. **16**(1): p. 44.
603. Guglielmotto, M., et al., *Abeta1-42 monomers or oligomers have different effects on autophagy and apoptosis.* Autophagy, 2014. **10**(10): p. 1827-43.
604. Glass, C.K., et al., *Mechanisms underlying inflammation in neurodegeneration.* Cell, 2010. **140**(6): p. 918-34.
605. Erickson, M.A., M.L. Wilson, and W.A. Banks, *In vitro modeling of blood-brain barrier and interface functions in neuroimmune communication.* Fluids Barriers CNS, 2020. **17**(1): p. 26.
606. Mrak, R.E. and W.S. Griffin, *Interleukin-1, neuroinflammation, and Alzheimer's disease.* Neurobiol Aging, 2001. **22**(6): p. 903-8.
607. Donnelly, R.J., et al., *Interleukin-1 stimulates the beta-amyloid precursor protein promoter.* Cell Mol Neurobiol, 1990. **10**(4): p. 485-95.
608. Ng, A., et al., *IL-1beta, IL-6, TNF- alpha and CRP in Elderly Patients with Depression or Alzheimer's disease: Systematic Review and Meta-Analysis.* Sci Rep, 2018. **8**(1): p. 12050.
609. Tachida, Y., et al., *Interleukin-1 beta up-regulates TACE to enhance alpha-cleavage of APP in neurons: resulting decrease in Abeta production.* J Neurochem, 2008. **104**(5): p. 1387-93.
610. Tyler, S.J., et al., *alpha- and beta-secretase: profound changes in Alzheimer's disease.* Biochem Biophys Res Commun, 2002. **299**(3): p. 373-6.
611. Cras, P., et al., *Senile plaque neurites in Alzheimer disease accumulate amyloid precursor protein.* Proc Natl Acad Sci U S A, 1991. **88**(17): p. 7552-6.
612. Keller, J.N., K.B. Hanni, and W.R. Markesbery, *Impaired proteasome function in Alzheimer's disease.* J Neurochem, 2000. **75**(1): p. 436-9.
613. Thibaudeau, T.A., R.T. Anderson, and D.M. Smith, *A common mechanism of proteasome impairment by neurodegenerative disease-associated oligomers.* Nat Commun, 2018. **9**(1): p. 1097.
614. van Leeuwen, F.W., et al., *Frameshift mutants of beta amyloid precursor protein and ubiquitin-B in Alzheimer's and Down patients.* Science, 1998. **279**(5348): p. 242-7.
615. Maniv, I., et al., *Altered ubiquitin signaling induces Alzheimer's disease-like hallmarks in a three-dimensional human neural cell culture model.* Nat Commun, 2023. **14**(1): p. 5922.
616. Chen, X. and D. Petranovic, *Role of frameshift ubiquitin B protein in Alzheimer's disease.* Wiley Interdiscip Rev Syst Biol Med, 2016. **8**(4): p. 300-13.
617. Zhang, M., et al., *Overexpression of ubiquitin carboxyl-terminal hydrolase L1 (UCHL1) delays Alzheimer's progression in vivo.* Sci Rep, 2014. **4**: p. 7298.
618. Rossi, G. and F. Tagliavini, *Frontotemporal lobar degeneration: old knowledge and new insight into the pathogenetic mechanisms of tau mutations.* Front Aging Neurosci, 2015. **7**: p. 192.
619. Seelaar, H., et al., *Clinical, genetic and pathological heterogeneity of frontotemporal dementia: a review.* J Neurol Neurosurg Psychiatry, 2011. **82**(5): p. 476-86.
620. Goedert, M., et al., *Multiple isoforms of human microtubule-associated protein tau: sequences and localization in neurofibrillary tangles of Alzheimer's disease.* Neuron, 1989. **3**(4): p. 519-26.
621. Hartmann, C., et al., *MAPT Mutations V337M and N297K Alter Organelle Trafficking in Frontotemporal Dementia Patient-Specific Motor Neurons.* Biomedicines, 2024. **12**(3).
622. Wren, M.C., et al., *Frontotemporal dementia-associated N279K tau mutant disrupts subcellular vesicle trafficking and induces cellular stress in iPSC-derived neural stem cells.* Mol Neurodegener, 2015. **10**: p. 46.

623. Nelson, M.P., et al., *Autophagy-lysosome pathway associated neuropathology and axonal degeneration in the brains of alpha-galactosidase A-deficient mice.* Acta Neuropathol Commun, 2014. **2**: p. 20.
624. Naseri, N. and M.R. Mofid, *Role of IGFBP-3 in Human Diseases Relying on Different Cell Signaling Pathways.* Adv Biomed Res, 2025. **14**: p. 15.
625. Rensink, A.A., et al., *Expression of the cytokine leukemia inhibitory factor and pro-apoptotic insulin-like growth factor binding protein-3 in Alzheimer's disease.* Acta Neuropathol, 2002. **104**(5): p. 525-33.
626. Titone, R., M. Zhu, and D.M. Robertson, *Insulin mediates de novo nuclear accumulation of the IGF-1/insulin Hybrid Receptor in corneal epithelial cells.* Sci Rep, 2018. **8**(1): p. 4378.
627. Glaviano, A., et al., *PI3K/AKT/mTOR signaling transduction pathway and targeted therapies in cancer.* Mol Cancer, 2023. **22**(1): p. 138.
628. Martinez-Marmol, R., et al., *p110delta PI3-Kinase Inhibition Perturbs APP and TNFalpha Trafficking, Reduces Plaque Burden, Dampens Neuroinflammation, and Prevents Cognitive Decline in an Alzheimer's Disease Mouse Model.* J Neurosci, 2019. **39**(40): p. 7976-7991.
629. Low, P.C., et al., *Phosphoinositide 3-kinase delta regulates membrane fission of Golgi carriers for selective cytokine secretion.* J Cell Biol, 2010. **190**(6): p. 1053-65.
630. Zwaenepoel, O., et al., *Functional CSF-1 receptors are located at the nuclear envelope and activated via the p110delta isoform of PI 3-kinase.* FASEB J, 2012. **26**(2): p. 691-706.
631. Joshi, S., et al., *Altered Mucins (MUC) trafficking in benign and malignant conditions.* Oncotarget, 2014. **5**(17): p. 7272-84.
632. Ridgway, N.D., et al., *Differential effects of sphingomyelin hydrolysis and cholesterol transport on oxysterol-binding protein phosphorylation and Golgi localization.* J Biol Chem, 1998. **273**(47): p. 31621-8.
633. Lim, C.Y., et al., *ER-lysosome contacts enable cholesterol sensing by mTORC1 and drive aberrant growth signalling in Niemann-Pick type C.* Nat Cell Biol, 2019. **21**(10): p. 1206-1218.
634. Kovacs, D., et al., *Lipid exchange at ER-trans-Golgi contact sites governs polarized cargo sorting.* J Cell Biol, 2024. **223**(1).
635. Yang, X., et al., *New insight into the role of altered brain cholesterol metabolism in the pathogenesis of AD: A unifying cholesterol hypothesis and new therapeutic approach for AD.* Brain Res Bull, 2025. **224**: p. 111321.
636. Braun, N.A., et al., *Intracellular trafficking of recycling apolipoprotein E in Chinese hamster ovary cells.* J Lipid Res, 2006. **47**(6): p. 1176-86.
637. Zhang, X., et al., *Role of Rab GTPases in Alzheimer's Disease.* ACS Chem Neurosci, 2019. **10**(2): p. 828-838.
638. Jin, M., et al., *Rab1a and multiple other Rab proteins are associated with the transcytotic pathway in rat liver.* J Biol Chem, 1996. **271**(47): p. 30105-13.
639. Komano, H., et al., *A new functional screening system for identification of regulators for the generation of amyloid beta-protein.* J Biol Chem, 2002. **277**(42): p. 39627-33.
640. Li, Z., et al., *Rab1A knockdown represses proliferation and promotes apoptosis in gastric cancer cells by inhibition of mTOR/p70S6K pathway.* Arch Biochem Biophys, 2020. **685**: p. 108352.
641. Yang, X.Z., et al., *Rab1 in cell signaling, cancer and other diseases.* Oncogene, 2016. **35**(44): p. 5699-5704.
642. Ren, B., et al., *RAB1A regulates glioma cellular proliferation and invasion via the mTOR signaling pathway and epithelial-mesenchymal transition.* Future Oncol, 2021. **17**(24): p. 3203-3216.

643. Mukhopadhyay, A., J.A. Quiroz, and A.W. Wolkoff, *Rab1a regulates sorting of early endocytic vesicles.* Am J Physiol Gastrointest Liver Physiol, 2014. **306**(5): p. G412-24.
644. Udayar, V., et al., *A paired RNAi and RabGAP overexpression screen identifies Rab11 as a regulator of beta-amyloid production.* Cell Rep, 2013. **5**(6): p. 1536-51.
645. Momenbeitollahi, N., T. Cloet, and H. Li, *Pushing the detection limits: strategies towards highly sensitive optical-based protein detection.* Anal Bioanal Chem, 2021. **413**(24): p. 5995-6011.
646. Guatimosim, C., et al., *Okadaic acid disrupts synaptic vesicle trafficking in a ribbon-type synapse.* J Neurochem, 2002. **82**(5): p. 1047-57.
647. Schnatwinkel, C., et al., *The Rab5 effector Rabankyrin-5 regulates and coordinates different endocytic mechanisms.* PLoS Biol, 2004. **2**(9): p. E261.
648. Lagendijk, A.K. and B.M. Hogan, *VE-cadherin in vascular development: a coordinator of cell signaling and tissue morphogenesis.* Curr Top Dev Biol, 2015. **112**: p. 325-52.
649. Wennstrom, M. and H.M. Nielsen, *Cell adhesion molecules in Alzheimer's disease.* Degener Neurol Neuromuscul Dis, 2012. **2**: p. 65-77.
650. Elangbam, C.S., C.W. Qualls, Jr., and R.R. Dahlgren, *Cell adhesion molecules--update.* Vet Pathol, 1997. **34**(1): p. 61-73.
651. Tarawneh, R., et al., *Vascular endothelial-cadherin as a marker of endothelial injury in preclinical Alzheimer disease.* Ann Clin Transl Neurol, 2022. **9**(12): p. 1926-1940.
652. Yoshida, M., et al., *Phosphorylation of the cytoplasmic domain of E-selectin is regulated during leukocyte-endothelial adhesion.* J Immunol, 1998. **161**(2): p. 933-41.
653. Bevilacqua, M.P., et al., *Endothelial-leukocyte adhesion molecules in human disease.* Annu Rev Med, 1994. **45**: p. 361-78.
654. Milstone, D.S., et al., *Mice lacking E-selectin show normal numbers of rolling leukocytes but reduced leukocyte stable arrest on cytokine-activated microvascular endothelium.* Microcirculation, 1998. **5**(2-3): p. 153-71.
655. Yoshida, M., et al., *Leukocyte adhesion to vascular endothelium induces E-selectin linkage to the actin cytoskeleton.* J Cell Biol, 1996. **133**(2): p. 445-55.
656. Cha, J.H., et al., *Mechanisms Controlling PD-L1 Expression in Cancer.* Mol Cell, 2019. **76**(3): p. 359-370.
657. Zhou, Y.J., et al., *PD-L1: expression regulation.* Blood Sci, 2023. **5**(2): p. 77-91.
658. Sharpe, A.H., et al., *The function of programmed cell death 1 and its ligands in regulating autoimmunity and infection.* Nat Immunol, 2007. **8**(3): p. 239-45.
659. Coelho, M.A., et al., *Oncogenic RAS Signaling Promotes Tumor Immunoresistance by Stabilizing PD-L1 mRNA.* Immunity, 2017. **47**(6): p. 1083-1099 e6.
660. Dietrich, J., et al., *The marine biotoxin okadaic acid affects intestinal tight junction proteins in human intestinal cells.* Toxicol In Vitro, 2019. **58**: p. 150-160.
661. Barr, R.K. and M.A. Bogoyevitch, *The c-Jun N-terminal protein kinase family of mitogen-activated protein kinases (JNK MAPKs).* Int J Biochem Cell Biol, 2001. **33**(11): p. 1047-63.
662. Pei, J.J., et al., *Okadaic-acid-induced inhibition of protein phosphatase 2A produces activation of mitogen-activated protein kinases ERK1/2, MEK1/2, and p70 S6, similar to that in Alzheimer's disease.* Am J Pathol, 2003. **163**(3): p. 845-58.
663. Shoji, M., et al., *JNK activation is associated with intracellular beta-amyloid accumulation.* Brain Res Mol Brain Res, 2000. **85**(1-2): p. 221-33.
664. Zhu, X., et al., *JKK1, an upstream activator of JNK/SAPK, is activated in Alzheimer's disease.* J Neurochem, 2003. **85**(1): p. 87-93.
665. Kamat, P.K., et al., *Molecular and cellular mechanism of okadaic acid (OKA)-induced neurotoxicity: a novel tool for Alzheimer's disease therapeutic application.* Mol Neurobiol, 2014. **50**(3): p. 852-65.

666. Ferrer, I. and R. Blanco, *N-myc and c-myc expression in Alzheimer disease, Huntington disease and Parkinson disease.* Brain Res Mol Brain Res, 2000. **77**(2): p. 270-6.
667. Pei, J.J., et al., *Localization of active forms of C-jun kinase (JNK) and p38 kinase in Alzheimer's disease brains at different stages of neurofibrillary degeneration.* J Alzheimers Dis, 2001. **3**(1): p. 41-48.
668. Correa, S.A. and K.L. Eales, *The Role of p38 MAPK and Its Substrates in Neuronal Plasticity and Neurodegenerative Disease.* J Signal Transduct, 2012. **2012**: p. 649079.
669. Kelman, Z., *PCNA: structure, functions and interactions.* Oncogene, 1997. **14**(6): p. 629-40.
670. Hoglinger, G.U., et al., *The pRb/E2F cell-cycle pathway mediates cell death in Parkinson's disease.* Proc Natl Acad Sci U S A, 2007. **104**(9): p. 3585-90.
671. Wharton, S.B., et al., *Expression of Ki67, PCNA and the chromosome replication licensing protein Mcm2 in glial cells of the ageing human hippocampus increases with the burden of Alzheimer-type pathology.* Neurosci Lett, 2005. **383**(1-2): p. 33-8.
672. Busser, J., D.S. Geldmacher, and K. Herrup, *Ectopic cell cycle proteins predict the sites of neuronal cell death in Alzheimer's disease brain.* J Neurosci, 1998. **18**(8): p. 2801-7.
673. Hoozemans, J.J., et al., *Cyclin D1 and cyclin E are co-localized with cyclo-oxygenase 2 (COX-2) in pyramidal neurons in Alzheimer disease temporal cortex.* J Neuropathol Exp Neurol, 2002. **61**(8): p. 678-88.
674. Nagy, Z., *Cell cycle regulatory failure in neurones: causes and consequences.* Neurobiol Aging, 2000. **21**(6): p. 761-9.
675. Nagy, Z., M.M. Esiri, and A.D. Smith, *Expression of cell division markers in the hippocampus in Alzheimer's disease and other neurodegenerative conditions.* Acta Neuropathol, 1997. **93**(3): p. 294-300.
676. Smith, M.Z., Z. Nagy, and M.M. Esiri, *Cell cycle-related protein expression in vascular dementia and Alzheimer's disease.* Neurosci Lett, 1999. **271**(1): p. 45-8.
677. Yang, Y., E.J. Mufson, and K. Herrup, *Neuronal cell death is preceded by cell cycle events at all stages of Alzheimer's disease.* J Neurosci, 2003. **23**(7): p. 2557-63.
678. Daneman, R., *The blood-brain barrier in health and disease.* Ann Neurol, 2012. **72**(5): p. 648-72.
679. Gong, C.X., et al., *Phosphoprotein phosphatase activities in Alzheimer disease brain.* J Neurochem, 1993. **61**(3): p. 921-7.
680. Mondal, P., et al., *Protein Phosphatase 2A Activation for the Treatment of Alzheimer Disease-Promises and Challenges.* International Journal of Pharmaceutical Investigation, 2023. **13**(4): p. 711-720.
681. Lu, R., et al., *Genomic characterisation and epidemiology of 2019 novel coronavirus: implications for virus origins and receptor binding.* Lancet, 2020. **395**(10224): p. 565-574.
682. Farr, S.A., et al., *Metformin Improves Learning and Memory in the SAMP8 Mouse Model of Alzheimer's Disease.* J Alzheimers Dis, 2019. **68**(4): p. 1699-1710.
683. De Felice, F.G. and S.T. Ferreira, *Inflammation, defective insulin signaling, and mitochondrial dysfunction as common molecular denominators connecting type 2 diabetes to Alzheimer disease.* Diabetes, 2014. **63**(7): p. 2262-72.
684. Ansari, S.A. and B.S. Emerald, *The Role of Insulin Resistance and Protein O-GlcNAcylation in Neurodegeneration.* Front Neurosci, 2019. **13**: p. 473.
685. Zhao, B., et al., *Effects of metformin treatment on glioma-induced brain edema.* Am J Transl Res, 2016. **8**(8): p. 3351-63.
686. Alonso Adel, C., et al., *Promotion of hyperphosphorylation by frontotemporal dementia tau mutations.* J Biol Chem, 2004. **279**(33): p. 34873-81.

687. An, D., et al., *Metformin influences cardiomyocyte cell death by pathways that are dependent and independent of caspase-3.* Diabetologia, 2006. **49**(9): p. 2174-84.
688. Nair, V., et al., *Metformin inhibits pancreatic cancer cell and tumor growth and downregulates Sp transcription factors.* Carcinogenesis, 2013. **34**(12): p. 2870-9.
689. Zhao, S., et al., *Metformin Attenuates Tau Pathology in Tau-Seeded PS19 Mice.* Neurotherapeutics, 2023. **20**(2): p. 452-463.
690. Du, M.R., et al., *Exploring the Pharmacological Potential of Metformin for Neurodegenerative Diseases.* Front Aging Neurosci, 2022. **14**: p. 838173.
691. Zhang, L., et al., *Metformin reduced NLRP3 inflammasome activity in Ox-LDL stimulated macrophages through adenosine monophosphate activated protein kinase and protein phosphatase 2A.* Eur J Pharmacol, 2019. **852**: p. 99-106.
692. Ismail Hassan, F., et al., *Metformin Attenuates Brain Injury by Inhibiting Inflammation and Regulating Tight Junction Proteins in Septic Rats.* Cell J, 2020. **22**(Suppl 1): p. 29-37.
693. Erices, R., et al., *Metformin, at concentrations corresponding to the treatment of diabetes, potentiates the cytotoxic effects of carboplatin in cultures of ovarian cancer cells.* Reprod Sci, 2013. **20**(12): p. 1433-46.
694. Bond, N.L.S., et al., *Low-Dose Metformin Treatment Reduces In Vitro Growth of the LL/2 Non-small Cell Lung Cancer Cell Line.* Biomedicines, 2022. **11**(1): p. 65.
695. Lalau, J.D., A.S. Lemaire-Hurtel, and C. Lacroix, *Establishment of a database of metformin plasma concentrations and erythrocyte levels in normal and emergency situations.* Clin Drug Investig, 2011. **31**(6): p. 435-8.
696. Deepa, S.S., et al., *APPL1 mediates adiponectin-induced LKB1 cytosolic localization through the PP2A-PKCzeta signaling pathway.* Mol Endocrinol, 2011. **25**(10): p. 1773-85.
697. Zhou, X., et al., *Metformin Inhibit Lung Cancer Cell Growth and Invasion in Vitro as Well as Tumor Formation in Vivo Partially by Activating PP2A.* Med Sci Monit, 2019. **25**: p. 836-846.
698. Auger, C., et al., *Metformin prevents the pathological browning of subcutaneous white adipose tissue.* Mol Metab, 2019. **29**: p. 12-23.
699. Kawashima, I. and K. Kirito, *Metformin inhibits JAK2V617F activity in MPN cells by activating AMPK and PP2A complexes containing the B56alpha subunit.* Exp Hematol, 2016. **44**(12): p. 1156-1165 e4.
700. Cheng, G. and L. Li, *High-glucose-induced apoptosis, ROS production and pro-inflammatory response in cardiomyocytes is attenuated by metformin treatment via PP2A activation.* J Biosci, 2020. **45**.
701. Joseph, B.K., et al., *Inhibition of AMP Kinase by the Protein Phosphatase 2A Heterotrimer, PP2APpp2r2d.* J Biol Chem, 2015. **290**(17): p. 10588-98.
702. Gan, T., et al., *Okadaic Acid Inhibits Protein Phosphatases to Suppress Spermatogonial Cell Proliferation.* Biology Bulletin, 2022. **49**(Suppl 2): p. S12-S19.
703. Park, M.J., et al., *Metformin Augments Anti-Inflammatory and Chondroprotective Properties of Mesenchymal Stem Cells in Experimental Osteoarthritis.* J Immunol, 2019. **203**(1): p. 127-136.
704. Amable, G., et al., *Metformin inhibition of colorectal cancer cell migration is associated with rebuilt adherens junctions and FAK downregulation.* J Cell Physiol, 2020. **235**(11): p. 8334-8344.
705. Takata, F., et al., *Metformin induces up-regulation of blood-brain barrier functions by activating AMP-activated protein kinase in rat brain microvascular endothelial cells.* Biochem Biophys Res Commun, 2013. **433**(4): p. 586-90.
706. Kalsi, K.K., et al., *Metformin attenuates the effect of Staphylococcus aureus on airway tight junctions by increasing PKC ζ-mediated phosphorylation of occludin.* Journal of cellular and molecular medicine, 2019. **23**(1): p. 317-327.

707. Chen, L., et al., *Activating AMPK to Restore Tight Junction Assembly in Intestinal Epithelium and to Attenuate Experimental Colitis by Metformin.* Front Pharmacol, 2018. **9**: p. 761.
708. Wu, W., et al., *Metformin Protects against LPS-Induced Intestinal Barrier Dysfunction by Activating AMPK Pathway.* Mol Pharm, 2018. **15**(8): p. 3272-3284.
709. Milczarek, G.J., et al., *Okadaic acid mediates p53 hyperphosphorylation and growth arrest in cells with wild-type p53 but increases aberrant mitoses in cells with non-functional p53.* Carcinogenesis, 1999. **20**(6): p. 1043-8.
710. Greenbaum, D., et al., *Comparing protein abundance and mRNA expression levels on a genomic scale.* Genome Biol, 2003. **4**(9): p. 117.
711. Beyer, A., et al., *Post-transcriptional expression regulation in the yeast Saccharomyces cerevisiae on a genomic scale.* Mol Cell Proteomics, 2004. **3**(11): p. 1083-92.
712. Qiu, Z.H., M.S. de Carvalho, and C.C. Leslie, *Regulation of phospholipase A2 activation by phosphorylation in mouse peritoneal macrophages.* J Biol Chem, 1993. **268**(32): p. 24506-13.
713. Kim, I.S., et al., *Selective inhibition of collagen synthesis by okadaic acid in cultured human fibroblasts.* Biochem Biophys Res Commun, 1994. **199**(1): p. 177-82.
714. Kuhl, T., et al., *Collagen VII Half-Life at the Dermal-Epidermal Junction Zone: Implications for Mechanisms and Therapy of Genodermatoses.* J Invest Dermatol, 2016. **136**(6): p. 1116-1123.
715. Bell, J.D. and R.L. Biltonen, *Activation of phospholipase A2 on lipid bilayers.* Methods Enzymol, 1991. **197**: p. 249-58.
716. Wakiya, K. and M. Shibuya, *Okadaic acid stimulates the expression of vascular endothelial growth factor gene.* Biochem Biophys Res Commun, 1999. **265**(2): p. 584-8.
717. Schuhmacher, D., J.M. Sontag, and E. Sontag, *A Novel Role of PP2A Methylation in the Regulation of Tight Junction Assembly and Integrity.* Front Cell Dev Biol, 2022. **10**: p. 911279.
718. Dorfel, M.J. and O. Huber, *Modulation of tight junction structure and function by kinases and phosphatases targeting occludin.* J Biomed Biotechnol, 2012. **2012**(1): p. 807356.
719. Sheth, P., et al., *Protein phosphatase 2A plays a role in hydrogen peroxide-induced disruption of tight junctions in Caco-2 cell monolayers.* Biochem J, 2009. **421**(1): p. 59-70.
720. Moreira, P.I., *Metformin in the diabetic brain: friend or foe?* Ann Transl Med, 2014. **2**(6): p. 54.
721. Chen, Y., et al., *Metformin attenuates plaque-associated tau pathology and reduces amyloid-beta burden in APP/PS1 mice.* Alzheimers Res Ther, 2021. **13**(1): p. 40.
722. Feng, X., et al., *Metformin, Macrophage Dysfunction and Atherosclerosis.* Front Immunol, 2021. **12**: p. 682853.
723. Ali, M., et al., *VEGF signalling causes stalls in brain capillaries and reduces cerebral blood flow in Alzheimer's mice.* Brain, 2022. **145**(4): p. 1449-1463.